DOE/NASA/0289-1
NASA CR-175007
PSD FCR-6848

Advanced On-Site Power Plant Development Technology Program

1984 Annual Report

United Technologies Corporation
Power Systems Division
Fuel Cell Operations
South Windsor, Connecticut

June 1985

Prepared for
National Aeronautics and Space Administration
Lewis Research Center
Cleveland, Ohio 44135
Under Contract DEN3-289

for
U.S. Department of Energy
Office of Fossil Energy
Morgantown Energy Technology Center
Under Interagency Agreement DE-A1-21-80ET17088

DOE/NASA/0289-1
NASA CR-175007
PSD FCR-6848

Advanced On-Site Power Plant Development Technology Program

1984 Annual Report

United Technologies Corporation
Power Systems Division
Fuel Cell Operations

June 1985

Prepared for
National Aeronautics and Space Administration
Lewis Research Center
Cleveland, Ohio 44135
Under Contract DEN3-289

for
U.S. Department of Energy
Morgantown Energy Technology Center
Under Interagency Agreement DE-A1-21-80ET17088

CONTENTS

LIST OF ILLUSTRATIONS

LIST OF ILLUSTRATIONS (CONT'D)

LIST OF ILLUSTRATIONS (CONT'D)

LIST OF ILLUSTRATIONS (CONT'D)

LIST OF ILLUSTRATIONS (CONT'D)

LIST OF ILLUSTRATIONS (CONT'D)

LIST OF ILLUSTRATIONS (CONT'D)

LIST OF TABLES

LIST OF TABLES (CONT'D)

LIST OF TABLES (CONT'D)

EXECUTIVE SUMMARY

The Department of Energy On-Site Fuel Cell Technology program under NASA Contract DEN3-289 is one of three efforts aimed at building the technological foundation necessary for commercial development of on-site fuel cell power plants. The 40-kW fuel cell power plant field test project is aimed at demonstrating the fuel cell's capabilities and identifying deficiencies that must be corrected in order for commercial units to become practical. A complementary technology development effort by the Gas Research Institute establishes new technology feasibility and defines power plant and major component designs.

This program concentrates on developing and demonstrating the technologies of the three major components and associated critical heat exchangers. Subscale and full-scale hardware is used. The effort is planned to conclude with a demonstration of full-scale (200-kW power plant site) major components in a Verification Test Article.

The effort during this second reporting period involved development of full-scale hardware for the cell stack, reformer, inverter, and critical heat exchangers, and preliminary definition of Verification Test Article plans.

The cell stack activity during this second report period included completion of a 7200-hour test on the first development short stack. Several features to reduce cost and increase the time between maintenance activities were successfully demonstrated and introduced for the first time in this stack. These include a lower cost, higher performance cooler, a cell configuration change that reduces electrolyte loss by 50% (cathode exit condensation zone), and lower cost alternatives for the cell end plates and manifolds. The stack was also used for the successful evaluation of an electrolyte addition approach. Electrodes made with a lower cost electrode fabrication process suffered performance loss as a result of the electrolyte addition process and a diagnostic teardown; improvements are being sought for future stacks.

Further improvements to the cell stack are being developed. The most important is a configuration change which increases cell performance to the program goal or higher, and increases electrolyte storage capability by 150%. This feature and other new features were incorporated into a second short stack, which began test at the end of the report period.

In the fuel processor area, improved catalysts for each function were tested in a catalyst train at simulated power plant conditions for 2000 hours. Performance was stable and met predictions. The hydrodesulfurizer catalyst reduces cost and provides a wider operating envelope, eliminating the need for a number of controls.

Burner tests and water table tests were utilized to select an up-fired burner configuration as the approach for the development reformer. A 200-kW scale development reformer with fewer long tubes (made possible by the new reformer catalyst) and a single up-fired industrial burner were fabricated and prepared for test at the end of the report period.

Inverter activity focused on fabrication of a 200-kW scale brassboard inverter. This inverter incorporates a new switching (commutating) circuit, which provides lower losses and reduced parts count. The control logic used in the brassboard inverter is more sophisticated than required in commercial use in order to provide diagnostics to facilitate the development process. By the end of the report period, the brassboard inverter circuit performance had been shown to agree with analytical simulations. The overall inverter efficiency agreed with predictions at high power levels, but was several percentage points lower at low power levels. This discrepancy was being investigated at the end of the report period.

The effort also includes improvement of three important heat exchangers. During the previous report period, an improved heat exchanger for the acid condenser was tested successfully except for excess cooling at low power. During this report period, a revised configuration was defined that eliminates this problem. Four candidate approaches for the reformer burner air-preheater have been identified.

One candidate, a ripple plate unit, has been tested successfully; a formed plate unit has been fabricated and is ready for test. A phenolic coated heat exchanger has been selected for the condenser. This unit will be designed and tested in the next report period.

The DOE/NASA focus for the program end point is a test of full-scale components in a system test referred to as the Verification Test Article. This test vehicle was defined to include a cell stack, reformer, and water recovery/treatment/cooling system. Test of a subscale stack and water treatment system will begin in the next report period. The objective of the test is to demonstrate improvement on the water system maintenance period and to investigate water system issues. The full-scale Verification Test Article will be fabricated and tested in 1986 and 1987.

TASK 1

CELL TECHNOLOGY

TASK 1 - CELL TECHNOLOGY

Subtask 1.1 - Electrode Catalyst Evaluation

Objective

The objective of this task is to evaluate by means of subscale cell tests catalysts and electrodes which have shown sufficient promise to be selected for development and scale-up trials.

Summary

The electrode performance improvement activity involves testing of laboratory scale (2" by 2") single cells incorporating new catalyst layers and configurations developed in other programs. For the first part of the program this testing involved improved catalysts. During this period, performance improvements were demonstrated, but the higher performance levels were not retained beyond approximately 7000 hours of operation. One of the cells that was started early in the program, however, has operated for nearly two years with stable performance. The ability to scale up catalyst processing from laboratory scale to development program scale lots has been demonstrated.

Nine subscale cells were endurance tested during 1984. These tests provided information on the long-term behavior of shop-made HYCAN anodes and GSB-18/26 cathodes at the operating conditions of an on-site power plant. A new matrix, substrate, and cell configuration were also evaluated relative to the On-Site performance development goal. The status of subscale cells is presented in Table 1-1.

Table 1-1. Status of Subscale Cells at 12/15/84

Build No.	Cathode	Purpose	Cell Voltages: Max.	11-15-84	Total Time (Hours)	Status
3638	GSB-18B	Long-term endurance	0.660	0.618	16,720	Continues
3700	GSB-18	Eval. stack electrodes	0.650	(0.625)	(7,400)	Terminated
3739	GSB-18	Compare shop-	0.658	0.633	10,945	Tests
3771	GSB-18	made versions	0.667	0.637	9,413	Continue
3751	GSB-26	of "18" and	0.654	0.631	10,296	
3772	GSB-26	"26" cathodes	0.657	(0.629)	(8,550)	Terminated
3861	GSB-18	Dry mix anode	0.667	(0.574)	(1,649)	Terminated
3864	GSB-18	Low-cost ribbed substrates	0.671	0.656	3,105	Continues
3890	GSB-18	Configuration "B"	0.670	0.666	1,557	Continues

Cell voltages are at 200 ASF/400°F on RL-1 (140°F dew point) and dry air at 80% H_2 and 50% O_2 utilizations.

Highlights

- A subscale cell with a HYCAN anode and a GSB-18 cathode is 30 mV below the performance development goal (at 200 ASF) after 17,000 hours of operation at on-site conditions.

- Portions of full-size electrodes incorporating shop-made batches of catalyst are within 20 mV of the performance goal after 10,000 hours of operation at on-site conditions in subscale cells.

- The latest subscale cells, incorporating an improved matrix, are exceeding the On-Site performance goal.

Discussion

Long-Term Endurance Test

It was decided to continue running Cell 3638 to determine the long-term decay rate of the GSB-18/HYCAN electrode combination. Over the past year, from 9000 to 17,000 hours load time, the cell has been run at 200 ASF/400°F. Diagnostic tests were performed at 10,000 hours and the cell was shut down for three weeks in August. Additions of electrolyte have been made periodically to replenish acid lost through evaporation. The complete performance history of the cell from startup to 17,000 hours is shown in Figure 1-1. Cell voltage at 17,000 hours is 0.618V/200 ASF--30 mV below the On-Site development goal and 10 mV lower than it was at 9,000 hours.

Cell 3638 has suffered an overall loss in performance of 40 mV during its life, from a peak voltage of 0.658V/200 ASF at 1,000 hours to 0.618V/200 ASF at 17,000 hours. Most of this loss was associated with specific events such as diagnostic tests and shutdowns. Development work to improve the ability of cells to tolerate off-design operating conditions has continued in the laboratory.

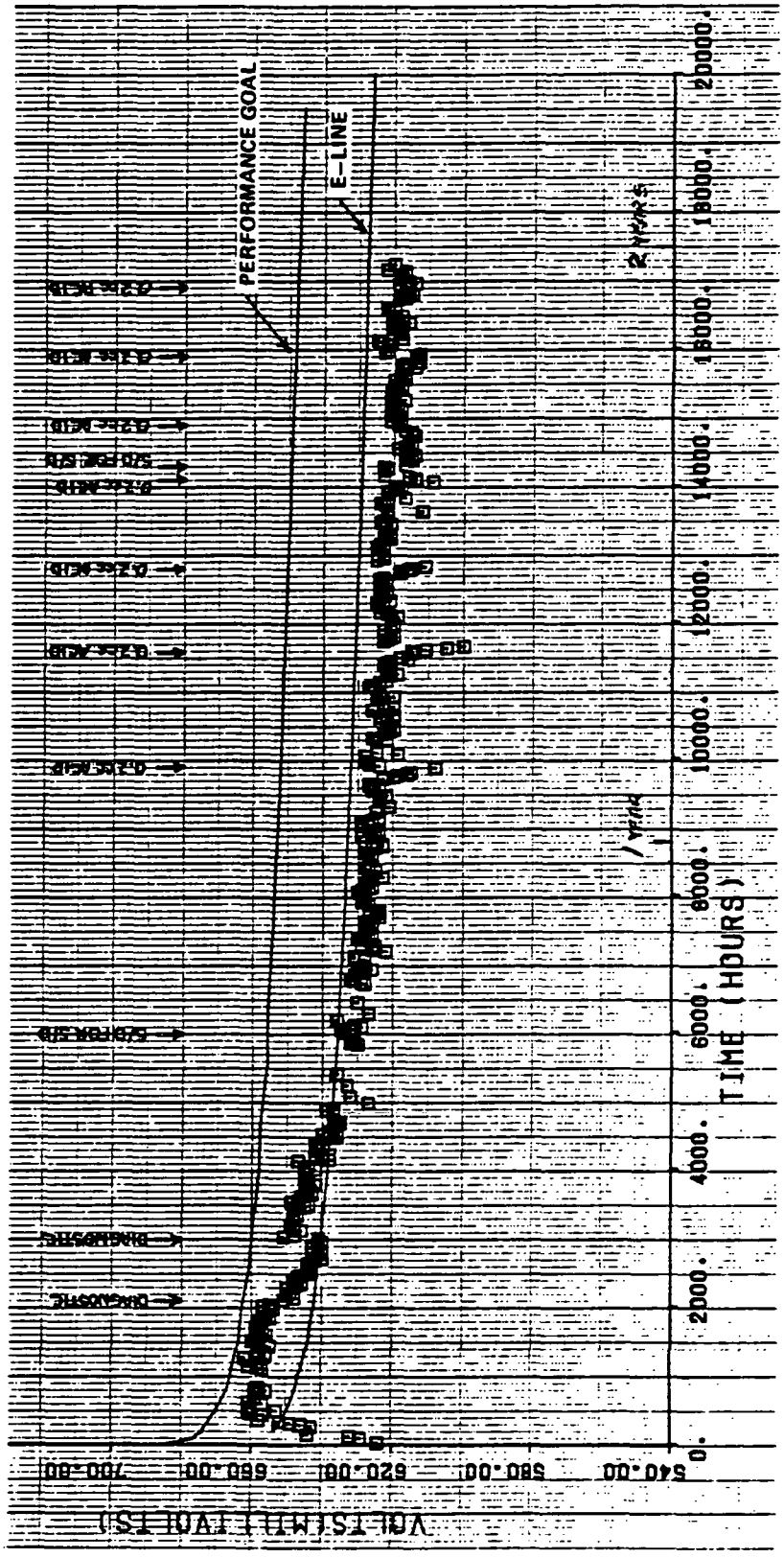

Figure 1-1. Performance History of Cell 3638
Lab-Made GSB-18B Cathode

Evaluation of Shop-Made Catalysts and Electrodes

The technology for the preparation of GSB-18 catalyst and electrodes transitioned from laboratory shop process scale development in 1983. Following scale-up trials, an advanced technology 30-cell stack with 3.2-ft² active area was fabricated, assembled, and tested.

Prior to starting up the stack, pieces cut from 3.2-ft² electrodes were built into 2-inch by 2-inch cells to obtain a preview of stack performance. One of these cells, Build 3700, was finally shut down in April 1984 after completing 7400 hours of operation. The performance versus time is shown in Figure 1-2. Although the performance level of cell 3700 was lower than that of 3638, it was stable and closely matched the average performance of the cells in the 30-cell stack. An abrupt decrease in voltage at 6660 hours was recovered by addition of electrolyte. The cell was shut down at 7400 hours.

In September-October 1983, kilogram-size batches of GSB-18 and GSB-26 catalysts were prepared and fabricated into 2.2-ft² electrodes. Pieces cut from the full-scale cathodes were paired with portions cut from full-scale HYCAN anodes, and these electrodes were assembled into subscale cells for testing on the endurance bench at the operating conditions listed in Table 1-2.

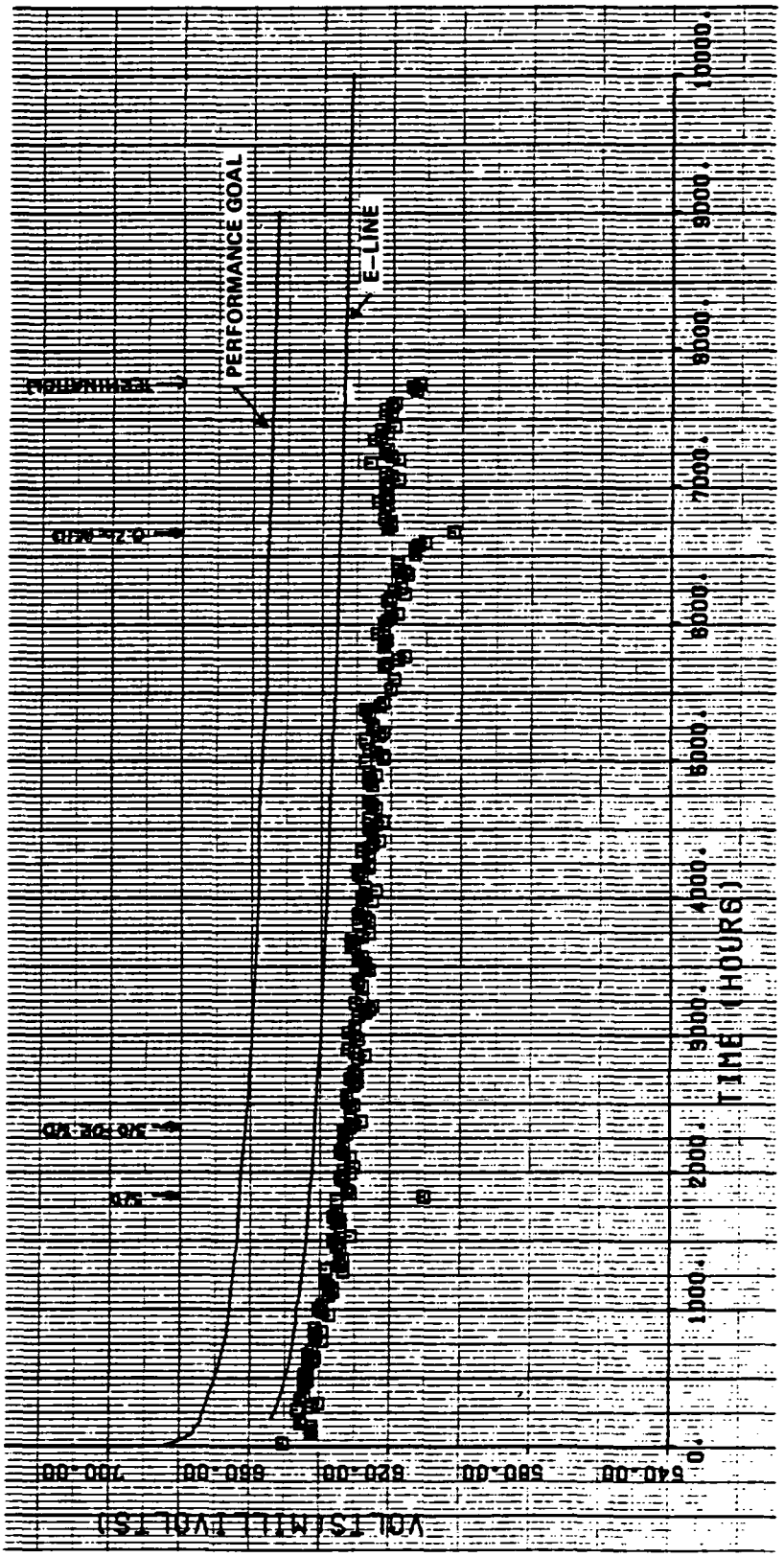

Figure 1-2. Performance History of Cell 3700
Shop-Made GSB-18 Cathode

Table 1-2. Test Conditions for Subscale Cells

Pressure:	Atmospheric
Temperature:	400°F
Fuel:	"RL1" (70% H_2, 1% CO, 29% CO_2, dry basis)
Dew Point of Fuel:	140°F
Utilization of H_2:	80%
Oxidant:	Air
Utilization of O_2:	50%
Current Density:	200 ASF

Performance data is quoted at these conditions unless noted otherwise.

Table 1-3 identifies the type of cathode that was in the individual subscale cells and also records the maximum voltages obtained. The performance histories of the cells are shown in Figures 1-3 through 1-9.

Table 1-3. Cells Used to Compare the Performances of GSB-18 and GSB-26 Shop-Made Cathodes

Build #	Cathode	Max. Cell Voltage (at 200 ASF)
3739	GSB-18	0.658
3771	GSB-18	0.667
3751	GSB-26	0.654
3772	GSB-26	0.657

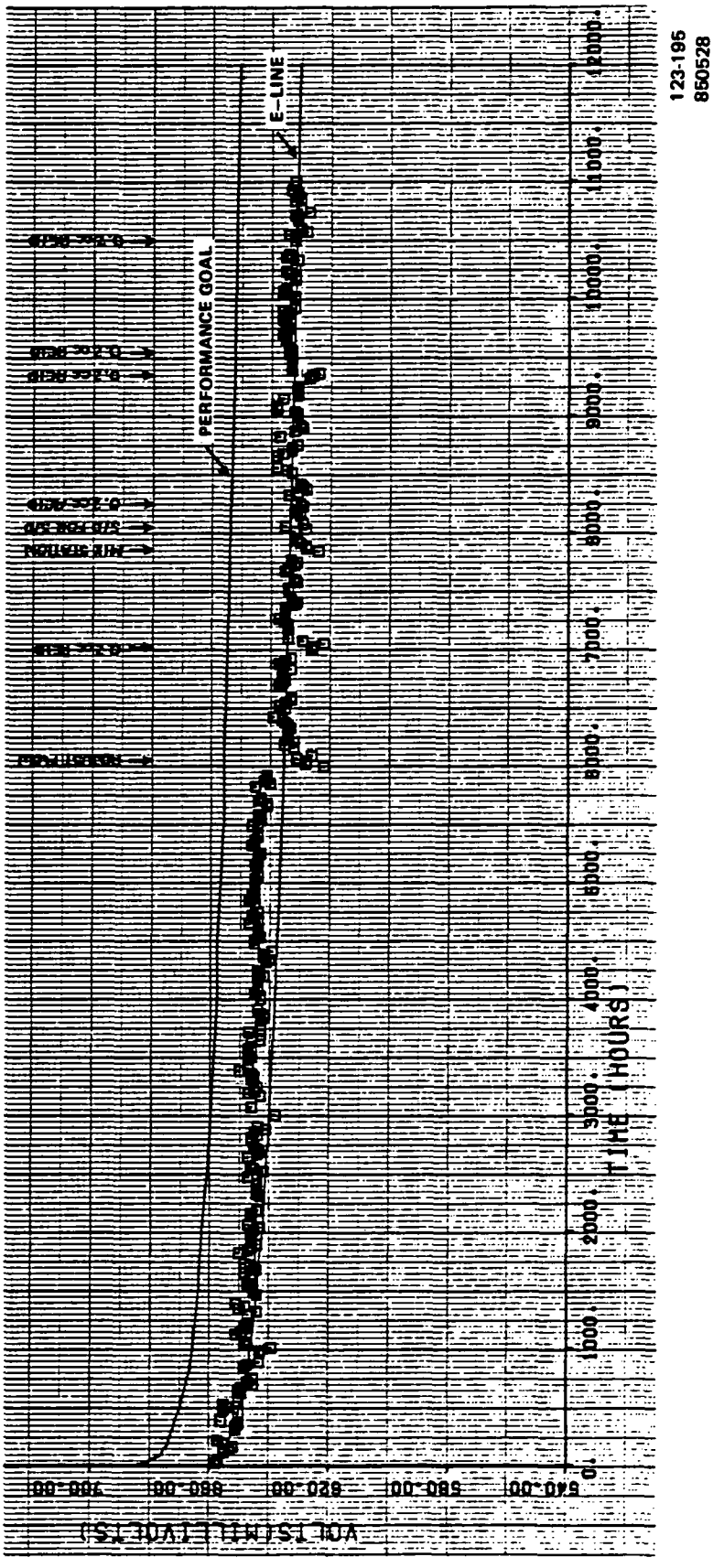

Figure 1-3. Performance History of Cell 3739
Shop-Made GSB-18 Cathode

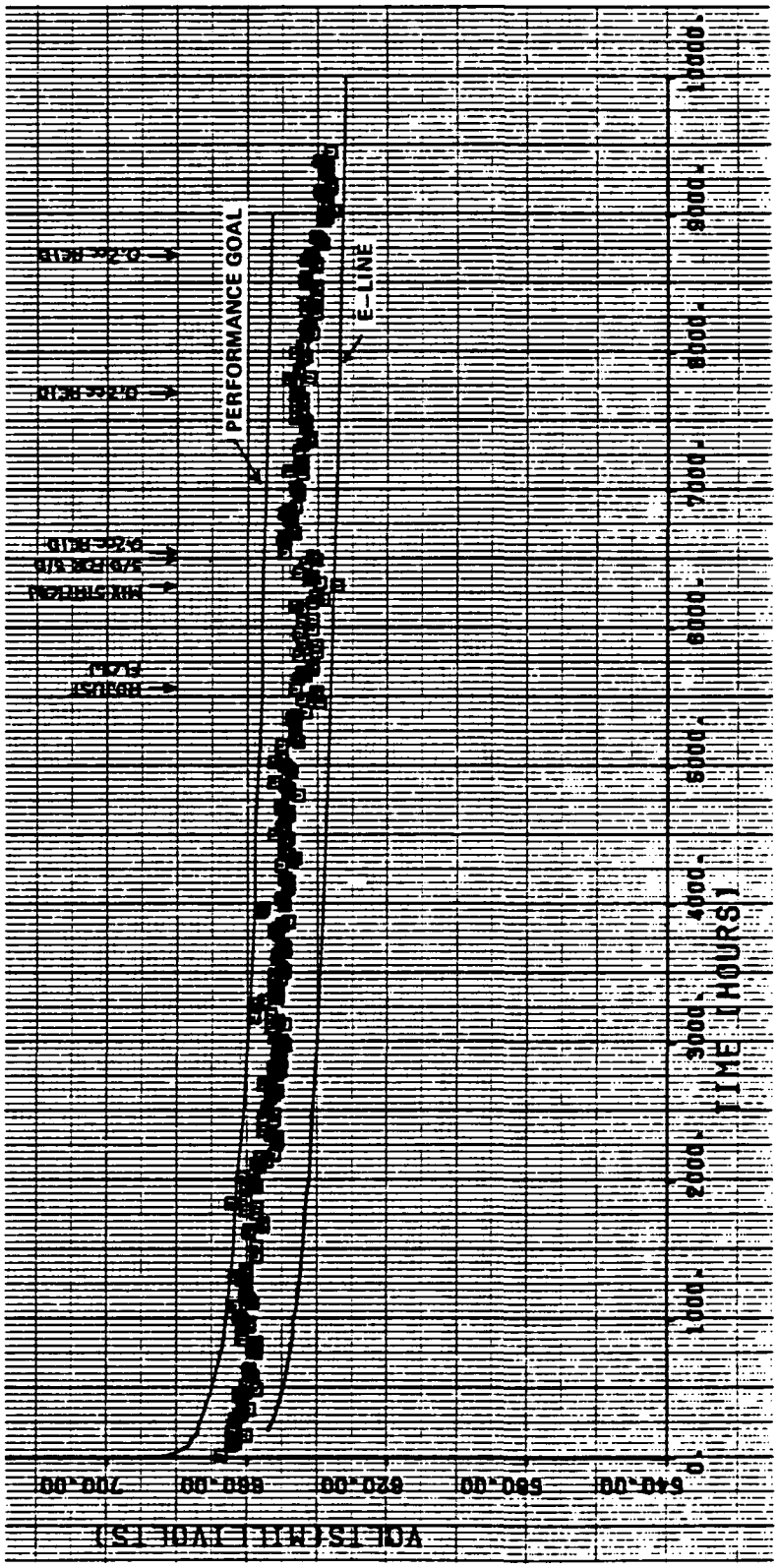

Figure 1-4. Performance History of Cell 3771
Shop-Made GSB-18 Cathode

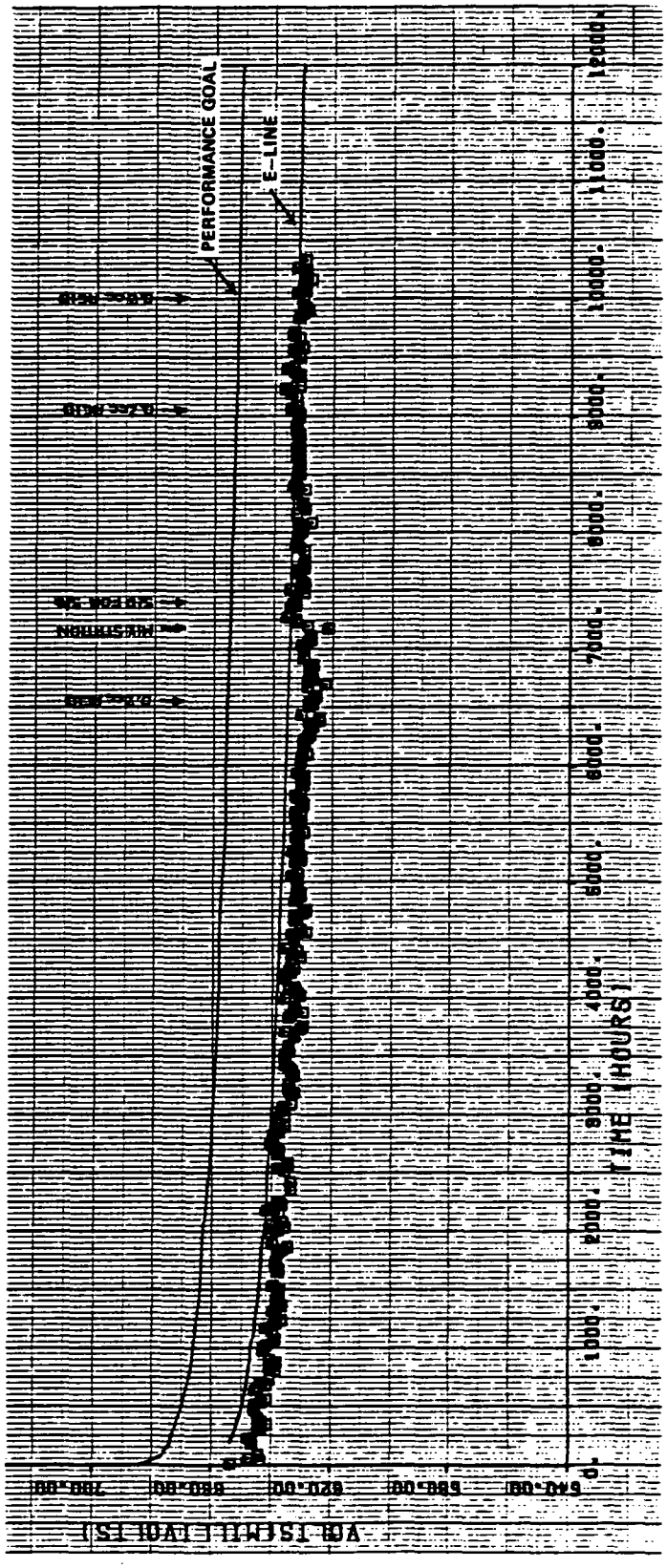

Figure 1-5. Performance History of Cell 3751
Shop-Made GSB-26 Cathode

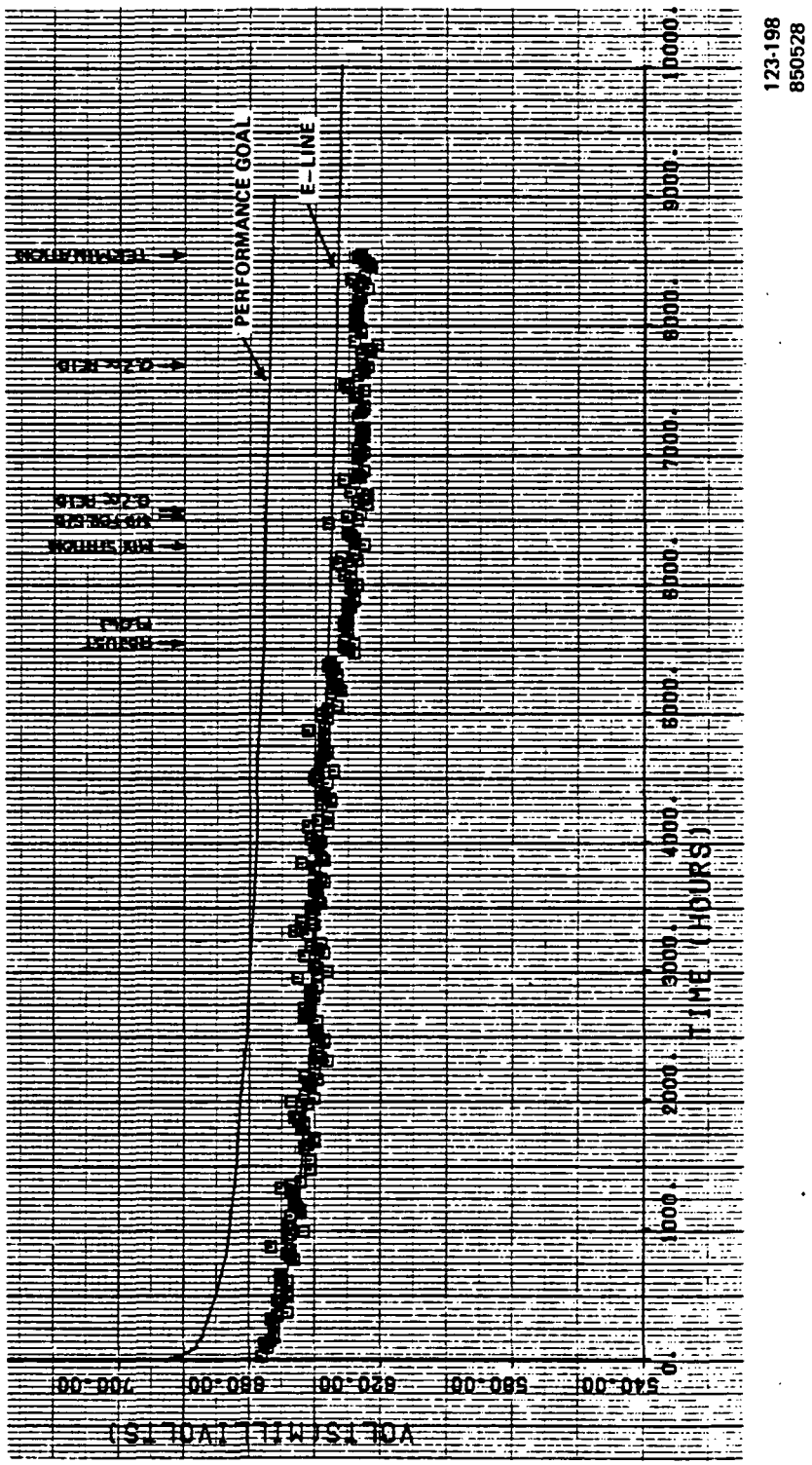

Figure 1-6. Performance History of Cell 3772
Shop-Made GSB-26 Cathode

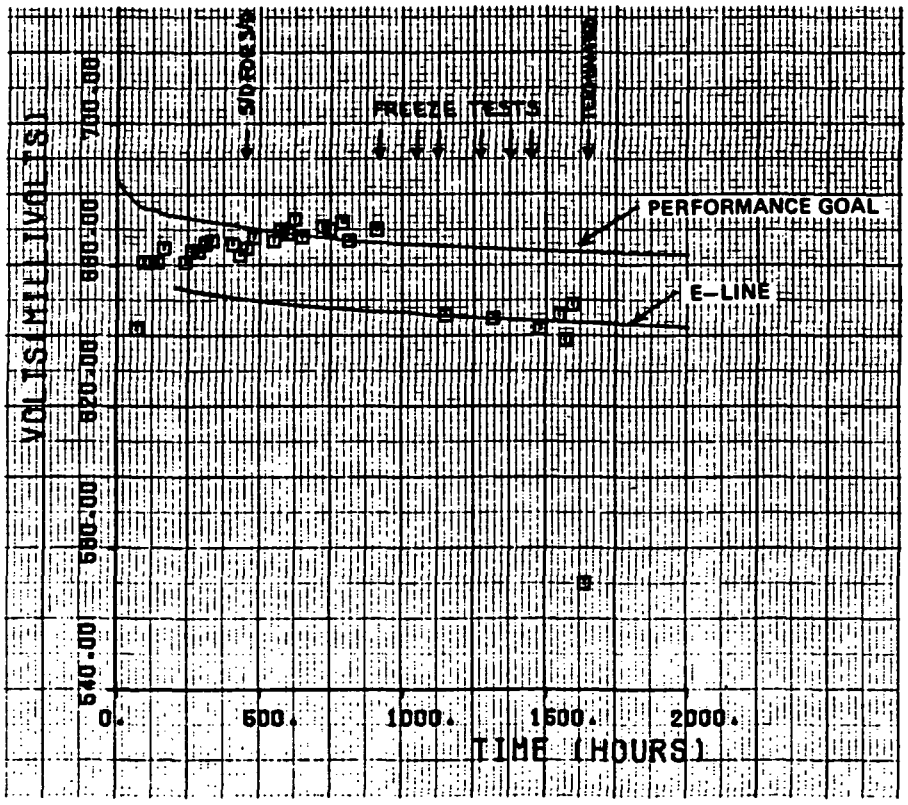

123-199
850528

Figure 1-7. Performance History of Cell 3861

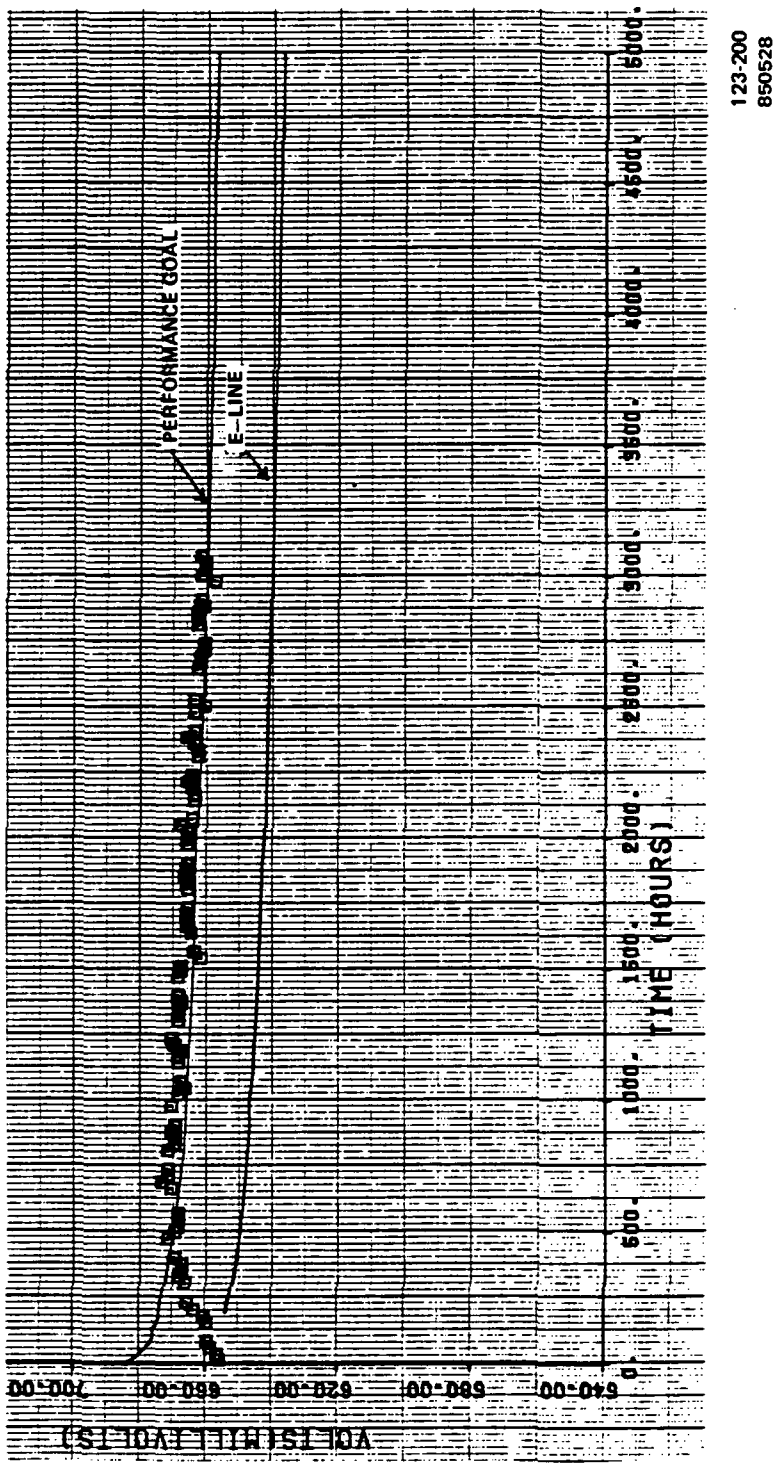

Figure 1-8. Performance History of Cell 3864

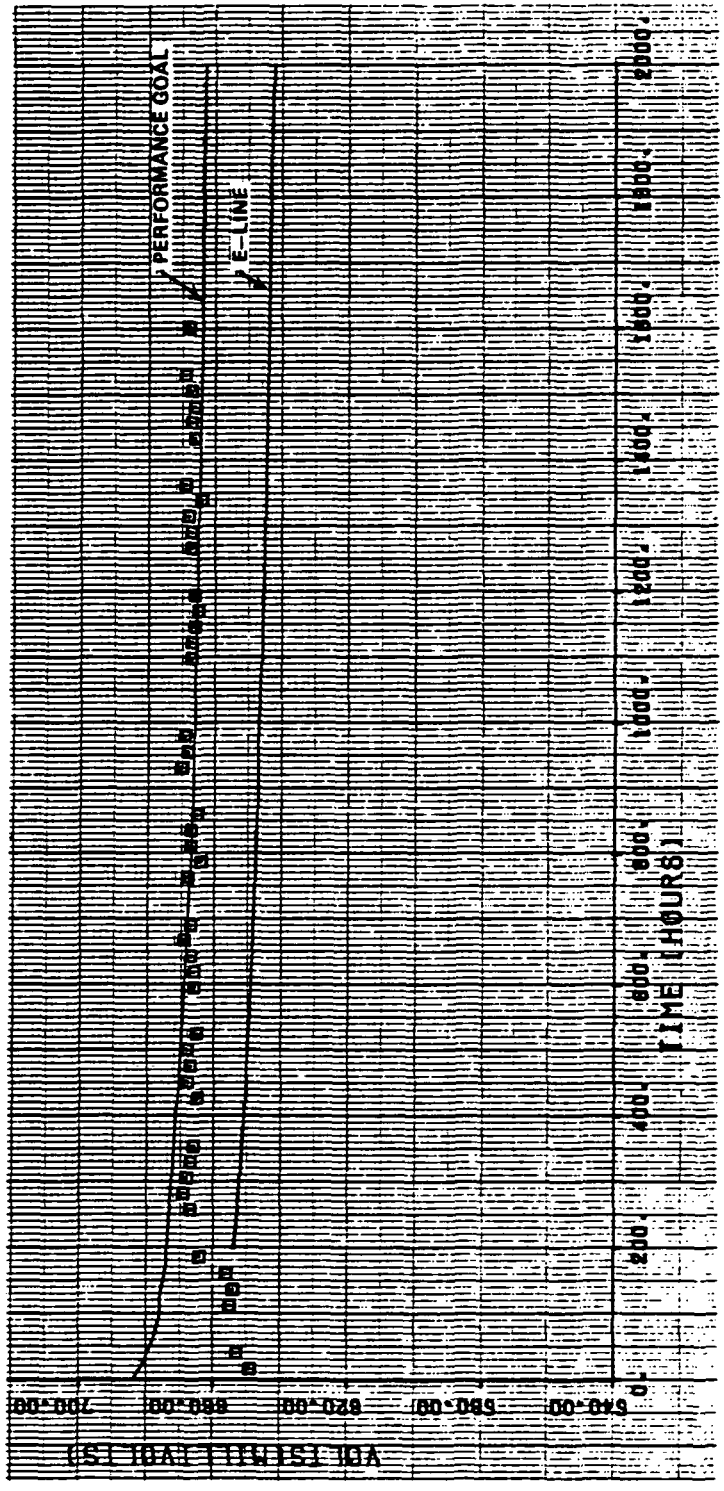

Figure 1-9. Performance History of Cell 3890

Apart from diagnostic tests following start-up, the cells were run at 200 ASF without interference other than flow adjustments to ensure that the proper utilizations of the reactants were being maintained. At load times beyond 6500 hours, electrolyte was added periodically to replenish acid lost by evaporation. All four cells (especially 3739 and 3771 with the GSB-18 cathodes) performed better than the cells run in the 30-cell stack (Figures 1-3 and 1-4). None, however, attained the performance development goal of E + 20 mV. The lowest performer, Build 3772, was terminated after 8600 hours; the other three cells were continued to establish long-term decay rates.

New Components and Configurations

During 1984, work was done on all components to improve life and reduce cost of the cell stack. Areas covered were matrix material, electrode substrate development, and cell design. The following is a summary of the results obtained from this effort.

Matrix "B" - All of the subscale cells discussed in the previous sections contained silicon carbide matrices. A new matrix formulation (Matrix "B") which gave an appreciably lower cell iR was evaluated. This resulted in an increase in cell performance of 10-12 mV at 200 ASF.

To establish the long-term reliability of Matrix "B", all of the following subscale cells were built with this matrix.

Anode Development - Anodes in the 30-cell stack showed some decay, symptomatic of flooding. A more hydrophobic dry mix anode was prepared in the shop and was tested in Cell 3861 versus a shop-made GSB-18 cathode. After 900 hours at 200 ASF, the cell was running above the On-Site development goal.

To determine the stability of the anode, the cell was subjected to a series of seven electrolyte solidification cycles, which involve shutting the cell down and storing it for three days at -25°F. The new anode's tolerance to "freezing" was equal to that of the normal HYCAN anode.

Substrate Development - A variety of substrates either made from low-cost materials or having improved physical properties have been developed during the past year (see parallel Task 2.1). The most notable of these is the low-cost, ribbed substrate made from alternate carbon fiber "D".

Pieces from both a HYCAN anode and a GSB-18 cathode made in the shop from this ribbed substrate were assembled into a subscale cell for evaluation on the endurance bench at on-site operating conditions. This cell, Build 3864, also contains Matrix "B".

Cell 3864 has now run for over 3000 hours at 400 °F/200 ASF and has shown exceptional performance and stability -- matching the On-Site performance development goal. The performance history is shown in Figure 1-8. This test will be continued.

Configuration "B" - In addition to evaluating the new matrix formulation, testing of a new cell configuration has also been started. The first cell incorporating both Matrix "B" and Configuration "B" (3890) has completed 1600 hours at on-site operating conditions. It contains a HYCAN anode catalyst layer and a GSB-18 cathode catalyst layer, both made in the laboratory.

This cell, which is being run without diagnostic tests other than hydrogen and oxygen gains, is running very stably at a performance level above the On-Site development goal. The test continues.

A more detailed discussion of the development of Configuration "B" is presented in Subtask 2.1.

Plans for 1985

Shop-made fuel cell electrodes will be evaluated at on-site conditions in subscale cells to support the cell stack test program.

TASK 2

CELL STACK DEVELOPMENT

TASK 2 - CELL STACK DEVELOPMENT

Subtask 2.1 - Electrode Substrate Technology

Objectives

The objectives of this task are to develop lower cost substrate and related repeat component materials, and to increase the acid storage capability without compromising performance or cost.

Summary

The electrode substrate represents a major portion of the material in the cell. During the past year, substrates with lower cost materials have been fabricated with acceptable properties; scale-up will be the next step.

Two approaches to develop low-cost substrates from low-cost materials were evaluated in this program. The first approach was development of commercially formed substrate precursors. The second approach was development of a low-cost substrate material defined under prior UTC funding. Substrate samples formed with the UTC defined material exhibit significantly improved thermal and electrical conductivity in comparison to the best commercially formed substrates. The electrode performance of these lower cost substrates was also shown to be equivalent to the standard substrate material currently in use in the 40-kW power plant.

Scale-up of the new low-cost substrate material has begun. This effort includes defining raw material processing requirements and costs, plus fabrication of full size electrode substrates to define forming and processing requirements for the new material. In addition, an effort to improve the cell stack maintenance situation was explored, which involved modifying the cell to permit increase electrolyte storage in

the cell stack. Initial efforts to achieve increased storage involved the development of dual porosity substrates. These efforts were partially successful, resulting in a 50% increase in time between refills. Effort on dual porosity substrates was terminated, however, when the new cell configuration referred to as Configuration "B" showed the potential for a 150% increase in time between electrolyte refills.

Dual porosity and Configuration "B" cells were evaluated to increase electrolyte storage and extend operating life. Dual porosity substrates had been shown to have improved electrolyte storage capacity, in comparison to standard ribbed substrates in earlier programs. The dual porosity configuration evaluated in this program was shown to be superior to the original composition in 2-inch by 2-inch cell tests by comparing performance stability as a function of electrolyte fill levels. The performance of second generation dual porosity substrates was stable at the 40% fill level, which projects to a 50% increase in operating time compared to the baseline substrate used in the 40-kW power plant.

Cell configuration "B" was evaluated as a second approach to increase electrolyte storage. The performance stability of this configuration was demonstrated in 2-inch by 2-inch cell tests. Initial performance averaged E-line + 30 mV at the baseline fill conditions at 30% fill and remained near E-line + 20 mV at 50% fill. This projects to a 150% increase in time between acid refill intervals when compared to the baseline configuration. In view of the benefits derived from the Configuration "B" cell, components were fabricated for the second short stack and are being evaluated and reported in Subtask 2.4.

Highlights

- Performance of substrates formed from low-cost materials was equivalent to that obtained with 40-kW substrates.
- The improved dual porosity substrate extends baseline refill interval by 50%.

- Configuration "B" cells perform at E-line + 20 mV while increasing the refill interval by 150%.

- Full size Configuration "B" cell components were fabricated for test in the second short stack.

Discussion

Low-Cost Substrate Materials

The program to form substrates from commercially formed precursor materials was based on combining low-cost raw materials with conventional commercial forming processes to achieve low costs. This precursor material must then be heat-treated to produce a finished substrate. The activity began in 1983 and was continued during the past year. Initially, laboratory scale handsheet samples provided by several commercial material processors were evaluated and compared. The supplier's ability to optimize materials and provide processing flexibility was also evaluated and a primary vendor was selected for scale-up activities. The effort to improve material properties was conducted on the handsheet scale with the other suppliers.

The scale-up of commercially formed substrate structures was begun by attempting to reproduce a candidate composition on full size production equipment. The material was produced on a 60-inch wide machine and the quantities produced were sufficient to estimate processing and material costs. The definition of preliminary processing variables was completed in 1983 and the resultant stock was identified as first generation material. Delamination and edge cracking occurred when this material was heat-treated, which indicated significant binder maldistribution. Substrate precursor sheets with improved binder distribution were produced during the past year and are identified as second generation material.

The second generation material contained a different resin system formulated to prevent resin maldistribution. Carbonizing of the second generation material also resulted in a high proportion of cracked sheets. No delamination or edge cracks

were apparent, indicating that the binder was uniformly distributed as intended. The shape and extent of the cracks suggested the likelihood of variable shrinkage rates due to thermal gradients during the heat-treat process.

A carbonizing trial was undertaken to reduce the cracking using a modified heat treat cycle. For comparison, both first and second generation substrate structures were included and instrumented to measure the thermal gradients from edge to center in a part and from top to bottom in the stack of parts. The run was stopped at two points to examine the parts for cracks or shrinkage. All of the second generation precursor sheets survived carbonization without cracks. Within the stack, parts near the middle of the stack lagged the farthest behind the oven and retort temperatures. Also, the center of each part was found to lag the oven temperature more than the edge of the part. These edge to center differentials were consistently greater in the first generation sheets than in the second generation sheets, as shown in Figure 2-1.

After completion of the experimental carbonizing trial, a full stack of second generation sheets was carbonized using the modified cycle. Again the stack was instrumented to measure thermal gradients. All of the second generation precursor sheets survived carbonization in excellent condition. The edge to center differentials recorded for this run were comparable to those documented in the experimental carbonizing trial.

The full sized sheets were then graphitized. Of the 38 parts graphitized, 29 were in satisfactory condition with the balance showing one or two cracks starting at the center of an edge. These parts experienced a 25% linear shrinkage and 55% thickness shrinkage as a result of being heat-treated.

The commercially formed substrate precursors consistently yielded high mechanical strength and low thermal and electrical conductivity relative to the 40-kW substrates, as shown in Table 2-1. Experiments to improve these properties were conducted on the handsheet and pilot plant scale with several suppliers. Parameters investigated in these experiments included fiber length, resin content, substrate basis weight, fillers, and alternative precursors.

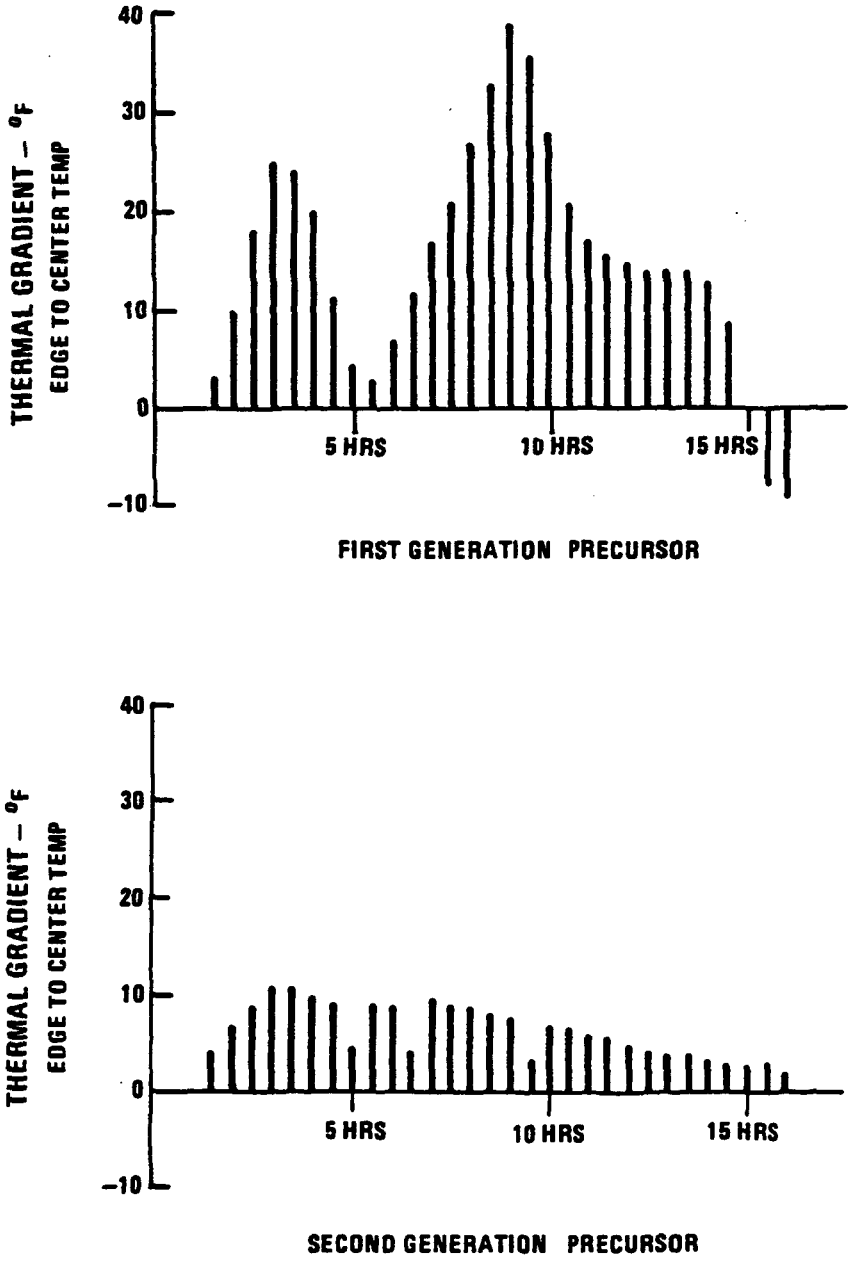

Figure 2-1. Edge to Center Temperature Differential During Experimental Carbonization

Table 2-1. Substrate Property Comparison

Substrate	iR (mV/Mil/100ASF) x 10^{-2}	Thermal Conductivity (Btu/Hr/Ft/°F)	Flex Strength (psi)
Commercially Formed Substrate	2.30	0.8	930
40-kW Substrate	0.50	4.0	450

Commercially formed substrates containing fillers to improve thermal and electrical conductivity were evaluated. Handsheets were formed with a range of filler levels and the material heat treated. The thermal and electrical properties were measured and found to be similar to the control without a filler. The data in Table 2-2 indicate that the filler was not effective in improving the thermal and electrical conductivities.

Table 2-2. Filler Materials

Property	Control Substrate (No Filler)	Experimental Substrate (Filler Added)
Bulk Density, g/cc	0.48	0.50
Thermal Conductivity (Btu/Hr-Ft°F)	0.61	0.68
iR @ 100 ASF, 100 psi (x 10-2 mV/mil)	2.4	2.2

The result of efforts to evaluate the effect of fiber length on the electrical resistance of the low-cost substrate precursor are shown in Table 2-3. Parts were made with three different fiber lengths. The data indicate that the fiber length has little impact on substrate electrical conductivity.

Table 2-3. Fiber Length
iR (mV/mil x 10^{-2} @ 100 ASF, 100 psi)

Graphitized Density of Sample (g/cc)	Relative Fiber Length		
	Long	Medium	Short
0.28	2.1	2.0	1.8
0.37	2.5	2.7	2.3
0.47	-	2.8	-
0.70	-	3.8	-
0.76	-	3.8	-

The effect of increased resin content on iR is shown in Table 2-4. Relative comparisons show that resin content does not significantly affect the iR of the low-cost substrate.

Table 2-4. Increased Resin Content
iR (mV/mil x 10^{-2} @ 100 ASF, 100 psi)

Approximate Graphitized Density of Sample (g/cc)	Fiber to Resin Ratio	
	1/1	2/1
.30	2.0	2.1
.40	2.5	2.7
.50	2.6	2.9
.55	2.7	-

Many additional handsheets and pilot samples using alternative low-cost precursors were also evaluated during the past year. As reported, the materials consistently exhibited significantly lower thermal and electrical properties than the standard substrate. The performance of full size electrodes fabricated from the low-cost precursor substrates was also significantly below the standard substrate in 2-inch by 2-inch cell tests (Figure 2-2). The low performance was due to the high substrate electrical resistance and poor diffusion characteristics. Development of this material was, therefore, discontinued.

UTC-funded efforts to develop a low-cost substrate material have produced an alternative to the commercially formed substrate precursors. This third generation material is made by adding the fiber into a substrate by a process similar to that used to form 40-kW substrates. Substrate handsheets were formed with the new material. Properties are shown in Table 2-5 in comparison to the 40-kW substrate.

Table 2-5. Substrate Property Comparison

Substrate	iR (mV/mil x 10^{-2})	Thermal Conductivity (Btu/Hr-Ft/°F)	Flex Strength (psi)	Flex Modulus (psi x 10^{-6})
Third Generation	0.60	2.7	1,274	0.22
40-kW	0.50	4.0	400	0.12

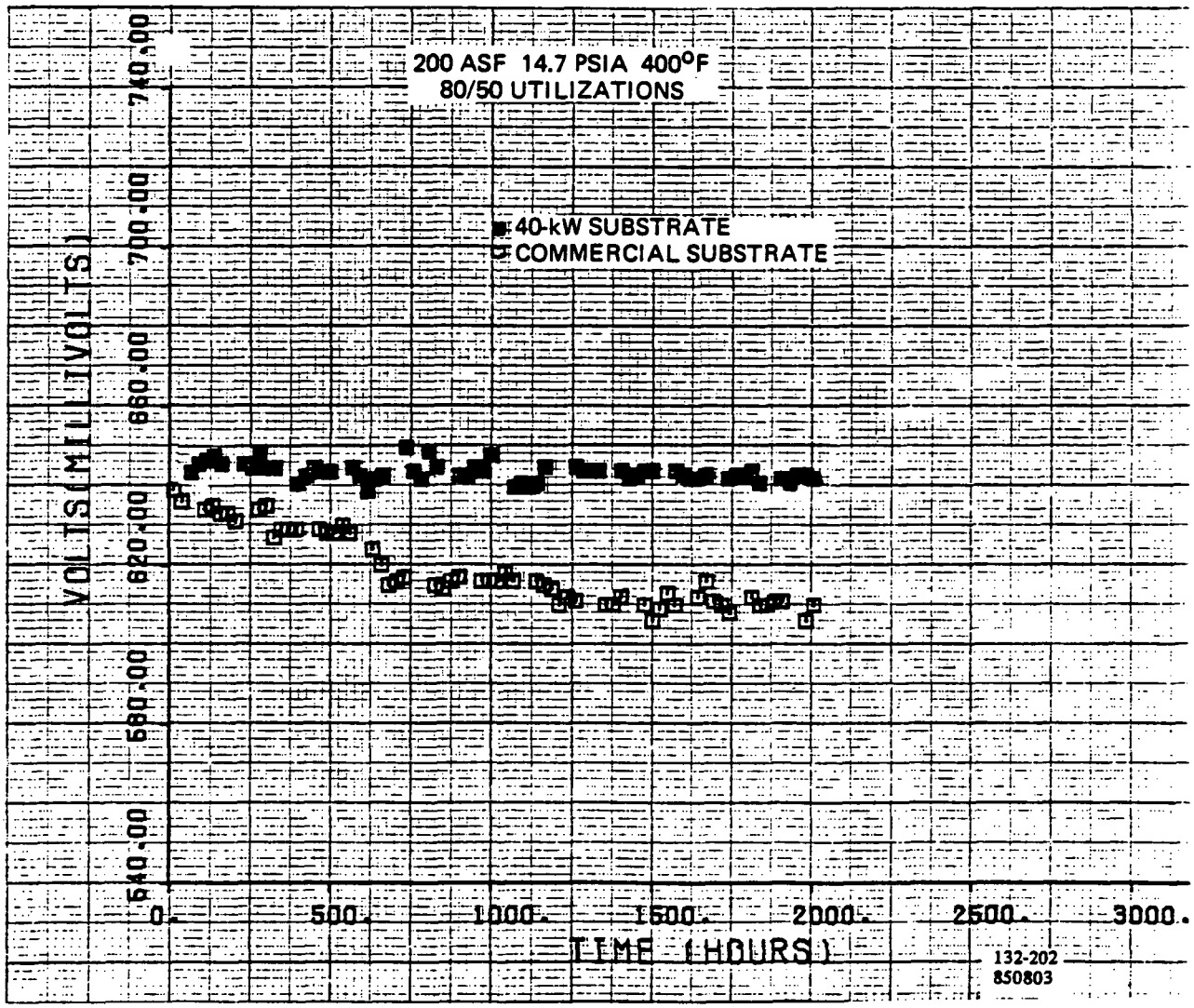

Figure 2-2. Substrate Performance Comparison

The diffusion characteristics of this substrate material were measured as a function of electrolyte fill levels. These tests indicated acceptable diffusion, as shown in Figure 2-3. A 2-inch by 2-inch cell was tested with this material and, at the standard electrolyte fill of 30%, the cell performance exceeds the On-Site goal of E + 20 mV with acceptable cathode and anode limiting current densities. Performance of cell 3864 is shown in Figure 2-4 in comparison to E-line + 20 mV.

Scale-up of the low-cost material was initiated; an initial batch of five hundred pounds of material was produced for evaluation. This quantity is sufficient for a full-scale forming trial. The initial tests to verify compatibility with existing equipment forming parameters were conducted with a subscale forming equipment and were successful. Full sized substrates will be formed to establish the physical properties and handling characteristics.

Increased Electrolyte Storage

Two approaches to increase electrolyte storage and extend cell operating life were evaluated in this program. They were the dual porosity substrates and the Configuration "B" cell. The initial activity was directed toward continuing development of the dual porosity substrate. Testing confirmed that the dual porosity substrate outperformed conventional ribbed substrates at high electrolyte fill levels, but the gains were less than anticipated. Testing of the Configuration "B" cell showed it to be less sensitive to electrolyte fill than either the conventional or dual porosity cell. The Configuration "B" cell performed acceptably at a 50% electrolyte fill. This results in a 150% increase in the refill interval.

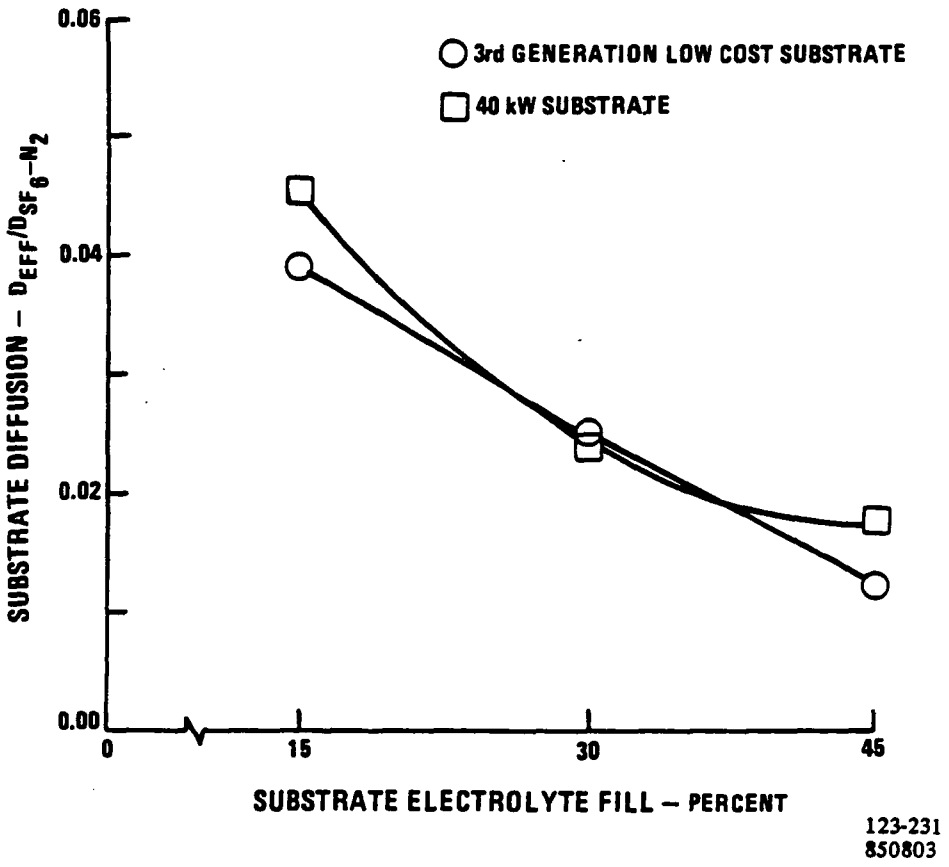

Figure 2-3. Effective Gas Diffusion vs. Electrolyte Fill

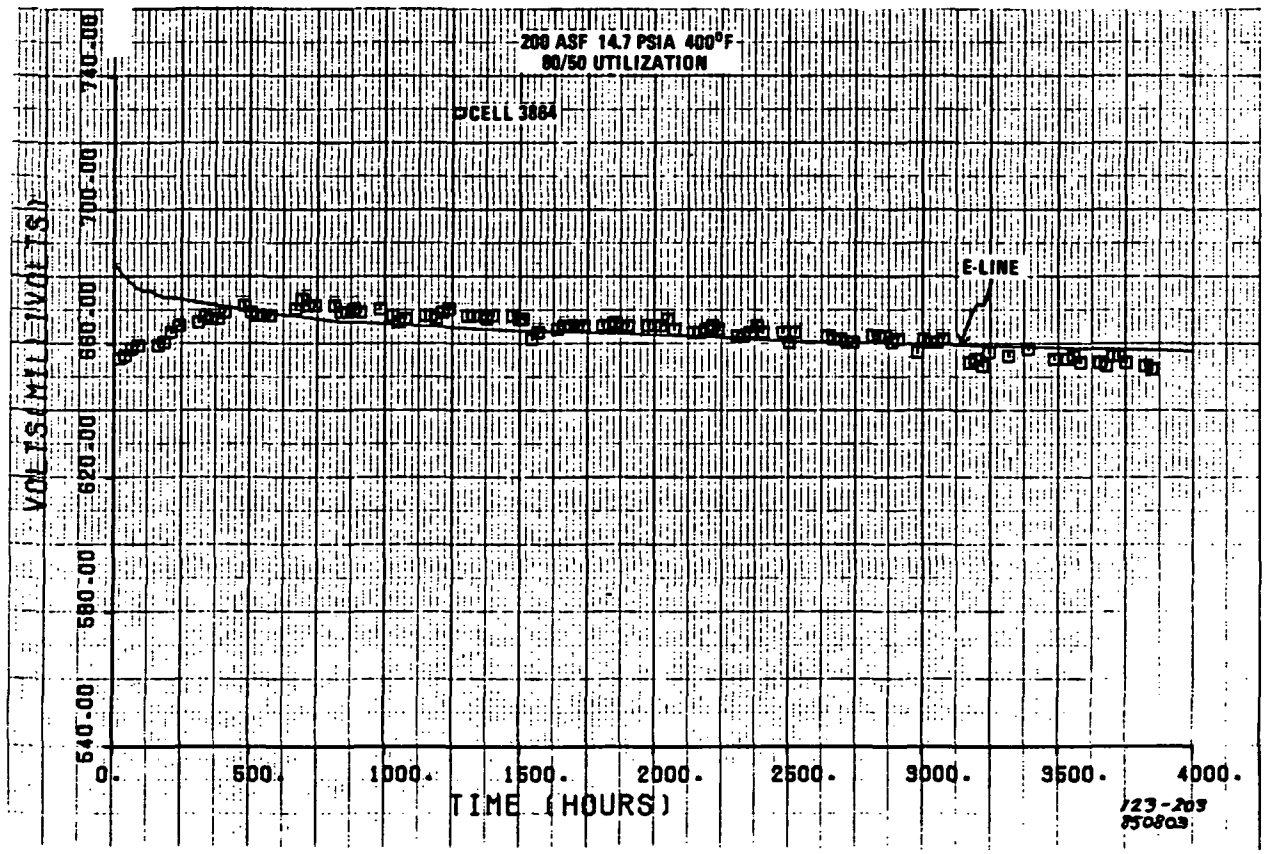

Figure 2-4. Voltage vs. Time - Cell 3864

Earlier work had demonstrated the feasibility of constructing ribbed substrates with variable porosities adjusted to increase electrolyte storage in the ribs and increase diffusivity in the web or gas transport layer. A second generation dual porosity substrate with an advanced rib composition designed for additional electrolyte storage was evaluated in this phase of the program.

Substrate handsheets were formed with the advanced rib composition, as well as first generation dual porosity and standard substrates for comparison. Electrodes fabricated from these substrates were tested in 2-inch by 2-inch cells to determine performance as a function of electrolyte content. Since all web layers were nominally identical, performance stability at increasing electrolyte levels would serve to indicate the rib structure's ability to store the excess electrolyte and maintain high diffusion levels in the web.

The standard substrate cell with uniform porosity was tested satisfactorily at the baseline acid fill level of 30%, but would not operate after the first acid fill increment of 5%, which raised the total fill. The performance of the two second generation dual porosity cells are shown in comparison to the first generation cell in Figure 2-5. As expected, both types of dual porosity cells outperformed the standard substrate with uniform porosity. The second generation dual porosity substrate also outperformed the first generation substrate structure. The second generation dual porosity cells did not perform acceptably as the electrolyte fill was increased to 45%. The performance of both second generation dual porosity cells was about 12 mV above E-line at the 40% fill level. This fill level projects to a 50% increase in the time between acid refill intervals compared to the current 30% fill of conventional ribbed substrate cells.

The acid content of the anode and cathode from the three dual porosity cells was determined by post-test analysis in Table 2-6. The percent electrolyte fill was calculated to account for acid in the matrix and catalyst layers. This data shows a significant electrolyte maldistribution between anode and cathode.

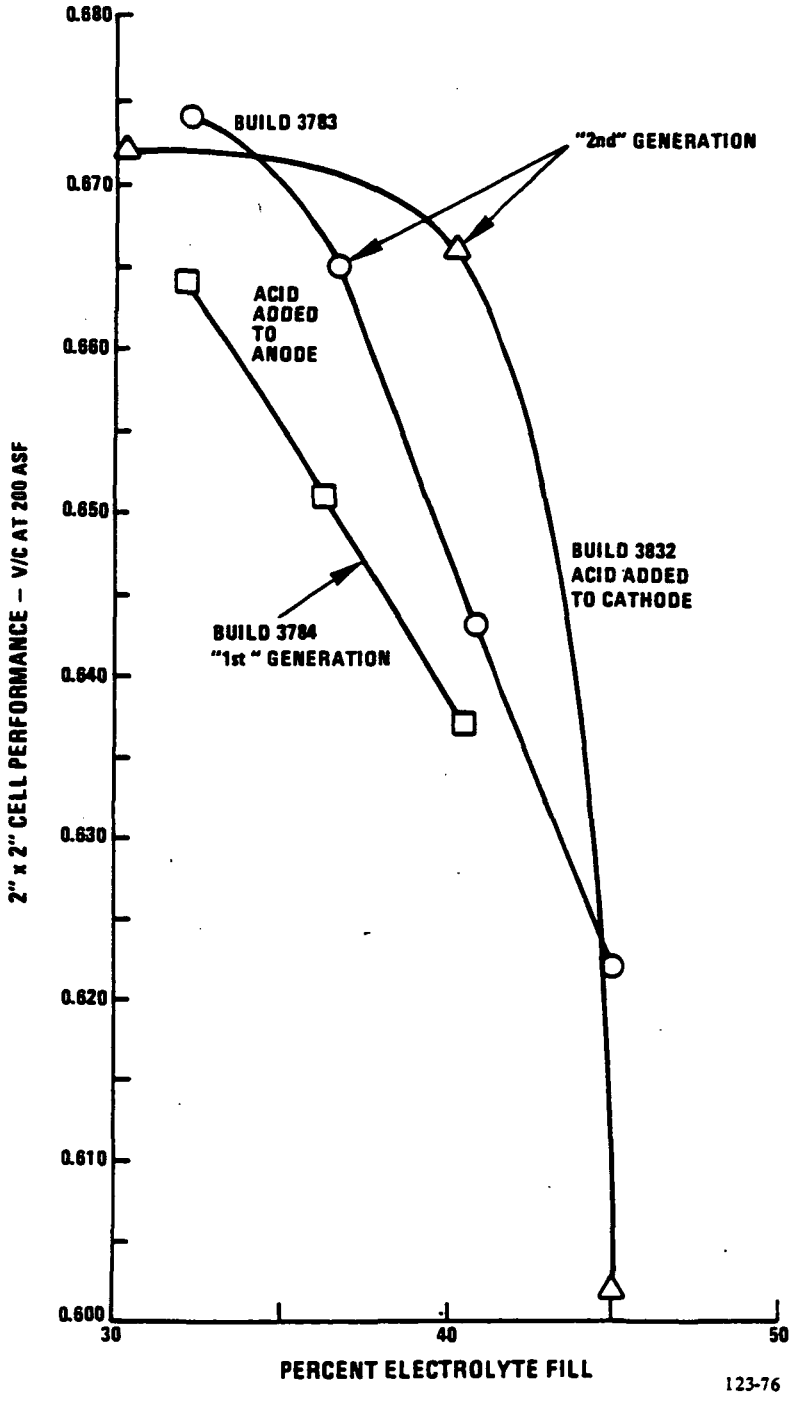

Figure 2-5. Dual Porosity Substrate 2-Inch by 2-Inch Cell Performance vs. Percent Electrolyte Fill

Table 2-6. Electrolyte Distribution

Build #	Description	Percent Electrolyte Fill		
		Average	Anode	Cathode
3784	1st generation acid added to anode	45%	65%	28%
3783	2nd generation acid added to anode	50%	68%	19%
3832	2nd generation acid added to cathode	45%	63%	16%

Diffusion measurements as a function of electrolyte fill were also completed on the second generation dual porosity substrates. Figure 2-6 shows that dual porosity substrates have higher diffusion coefficients at equivalent fills than the single porosity substrates. The diffusion measurements are in agreement with subscale cell testing.

These tests show the performance of the dual porosity substrates to be less sensitive to electrolyte content than the conventional substrates, but the sensitivity to percent electrolyte fill is still greater than expected. Post-test analysis also shows a significant electrolyte maldistribution between anode and cathode. The dual porosity substrate development effort was discontinued because improvements in acid storage were not as great as desired and an attractive alternative had been identified.

UTC funded the conceptual development of an alternative cell configuration with high electrolyte storage capability. The alternate cell configuration was designated Configuration "B" and was described to NASA in a proprietary briefing at UTC. In addition to improved performance characteristics, the configuration facilitated the use of low-cost materials. The development of processes to fabricate these components in scale was supported by the parallel GRI On-Site Technology Program, and full size repeat part components were fabricated for test in the second NASA on-site short stack.

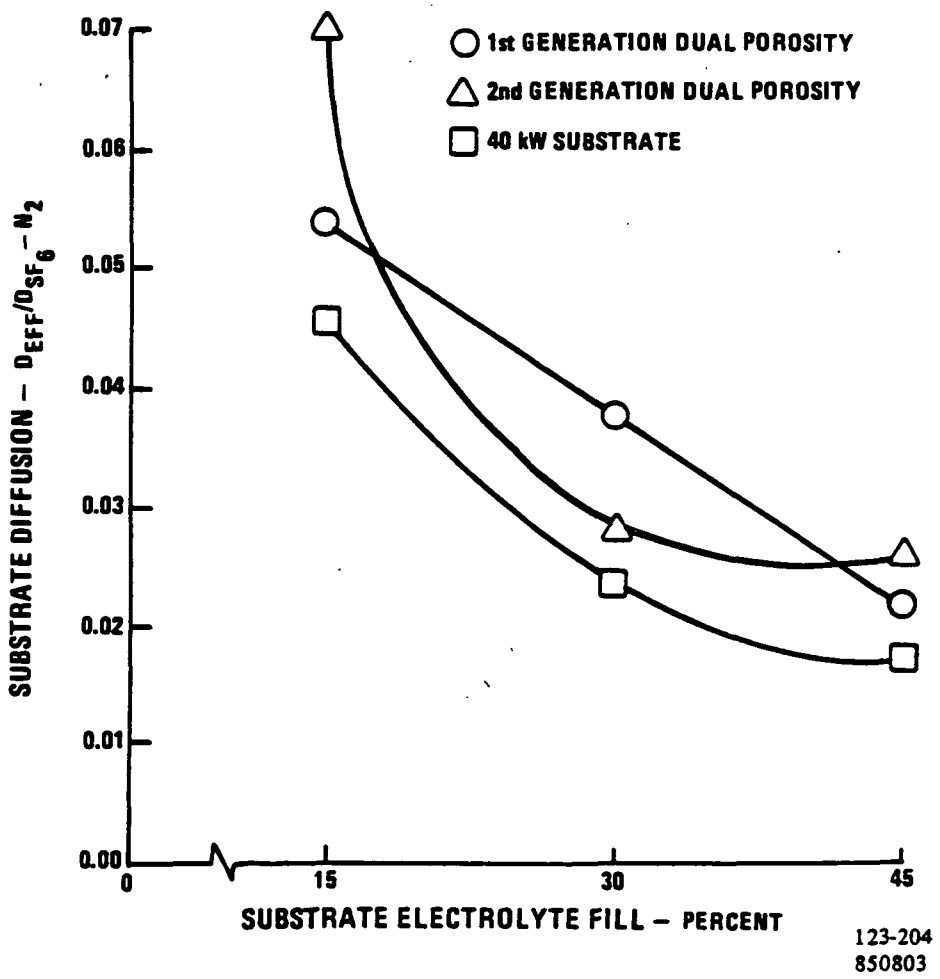

Figure 2-6. Effective Diffusion Coefficient vs. Percent Electrolyte Fill

Development tests had shown that the alternative cell configuration offered significant electrolyte storage increases using lower cost materials without penalty to cell thermal performance or electrical output. Two subscale cells were fabricated from components of the second short stack for testing to determine performance as a function of electrolyte content. The test program was identical to that employed in evaluating dual porosity substrate structures, but the results were exceedingly better. Fill levels have exceeded 50% without significant performance penalty and will be continued. Performance of both cells is about 20 mV above E-line at the 50% fill level, which projects to a 150% increase in time between refill interval when compared to the baseline fill.

Development activity to optimize material selection for reduced cost and additional gains in electrolyte storage is being continued.

Subtask 2.2 - Cooler Technology

Objectives

The objectives of this task are to reduce cooler cost by improving thermal conductivity and reducing assembly costs, and to verify reliability by documenting resistance to acid side/water side corrosion.

Summary

The cooler is also a major cell stack cost element. An improved cooler configuration, the encapsulated serpentine cooler, was introduced at the beginning of the program based on its development in the GRI program. This cooler provides lower cost (per cooler), fewer coolers per stack, less vulnerability to corrosion, and increases the cooling system maintenance interval.

Totally encapsulated, single-element serpentine 3/8-inch diameter copper coolers were successfully tested in the first short stack. After 5200 hours there was no acid penetration into the coolers and no measurable coolant side erosion-corrosion. Encapsulated coolers were fabricated for the second short stack with 7/16-inch diameter stainless steel serpentine arrays, and component testing showed no measurable erosion-corrosion after 3000 hours with coolant velocities twice that of design. Testing shows thick walled Teflon® dielectric connector hoses meet power plant life requirements. Reinforced thin walled Teflon hoses are being evaluated to determine if they provide increased reliability and reduced cost. Higher conductivity cooler holders are being evaluated. New subscale and full-scale heat transfer rigs were constructed to measure cooler thermal performance.

Highlights

- The encapsulated cooler concept was successfully demonstrated in short stack testing.
- No coolant side corrosion occurred in short stack and component tests.
- Larger diameter stainless steel serpentine coolers are now being used in encapsulated coolers.
- Dielectric coolant hoses meet power plant life requirements at 200 kW design conditions.

Discussion

Development of the encapsulated cooler concept continued. Cooler holder material and configuration changes aimed at improving thermal performance were developed and evaluated in subscale and full-scale heat transfer rigs. Cooler reliability was evaluated by analyzing used coolers from the first short stack for signs of corrosion by phosphoric acid or the coolant, by running erosion-corrosion tests at accelerated conditions, and by establishing the long-term burst strength of the dielectric connector hoses.

Post-Test Evaluation of Encapsulated Coolers

The three encapsulated cooler assemblies from the 30-cell stack were evaluated after approximately 5200 hours of total hot time. Radiographs of the three assemblies taken before and after stack testing showed no changes in the copper arrays. One cooler assembly was disassembled to verify the condition of the copper cooler array. There was no acid corrosion of the copper array and no acid present in the holders. This indicates the encapsulation concept was effective in preventing acid penetration.

The cooler array was examined metallographically for evidence of erosion-corrosion. Cross sections showed the tube wall thickness to be unchanged from the inlet to the exit of the array, indicating no significant erosion-corrosion had occurred.

The other two encapsulated coolers in the 30-cell stack remained on test in the second build of the rig and accumulated a total of 8389 hours of operation. These coolers will be analyzed when the stack is disassembled.

Heat Transfer Rigs

Subscale Rig

A subscale heat transfer rig has been designed and constructed to provide a convenient means of screening candidate cooler materials and configurations before committing to testing in the full size heat transfer rig. This rig is also used to measure the thermal conductivity of cell components. The subscale rig has a 6-inch by 6-inch planform area and utilizes a 3/8-inch diameter serpentine array with a pitch of 1.5 inches. All candidate coolers are fabricated to fit this array, allowing results to be measured against a standard. The basic operating principal of the subscale heat transfer rig is identical to the full size rig. The data collection and reduction process for the subscale heat transfer rig has been computerized to provide rapid readout of cooler performance. The subscale heat transfer rig is shown in Figure 2-7.

Initially, a cooler assembly of the type used in the first 30-cell stack was tested in the subscale heat transfer rig to establish a baseline for comparison. This assembly consisted of a copper array with a fibrous cooler holder. The same type of cooler was tested with a stainless steel array to provide an additional baseline. The thermal resistance data of these coolers are shown in Table 2-7. Results are in agreement with the full size heat transfer rig. Additional testing was conducted to support the cooler and design activity.

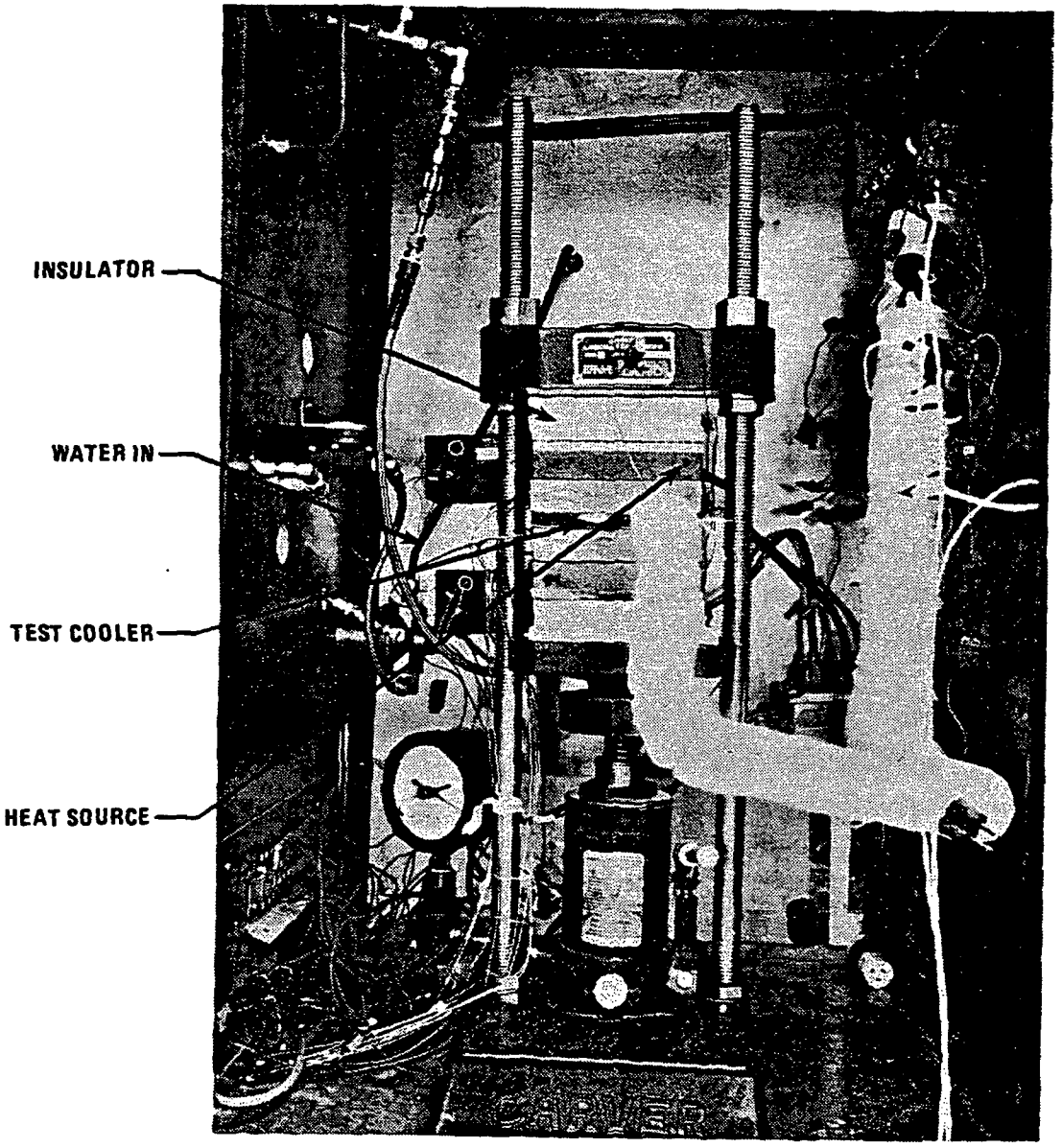

Figure 2-7. Subscale Heat Transfer Rig WCN 11013

Table 2-7. Baseline Tests - Subscale Heat Transfer Rig

Cooler Holder	Cooler Tube	Thermal Resistance Hr-Ft² °F/Btu	Comments
Fiber A	Copper	0.0082	Baseline
Fiber A	Stainless Steel	0.0091	Baseline

Full-Scale Rig

An additional heat transfer rig was constructed to test coolers of 27-inch by 27-inch planform size that are being developed for the 200-kW cell stack. The rig consists of a test cart containing an electrical heater control system that will simulate the heat flux in a cell stack, and a cooler assembly representative of the cooler arrangement found in a cell stack. A schematic of the rig is shown in Figure 2-8.

The first test of a 27-inch by 27-inch cooler was conducted using a test cooler of the same design as the encapsulated cooler used in the 30-cell short stack. Figures 2-9 and 2-10 show the new heat transfer rig with the test cooler installed. The measured thermal resistance of the cooler was 0.0095 hr ft²°F/Btu. This agrees with the results obtained for a similar cooler tested earlier in the 20-inch by 20-inch heat transfer rig. Additional testing was conducted to support the cooler development and design activity.

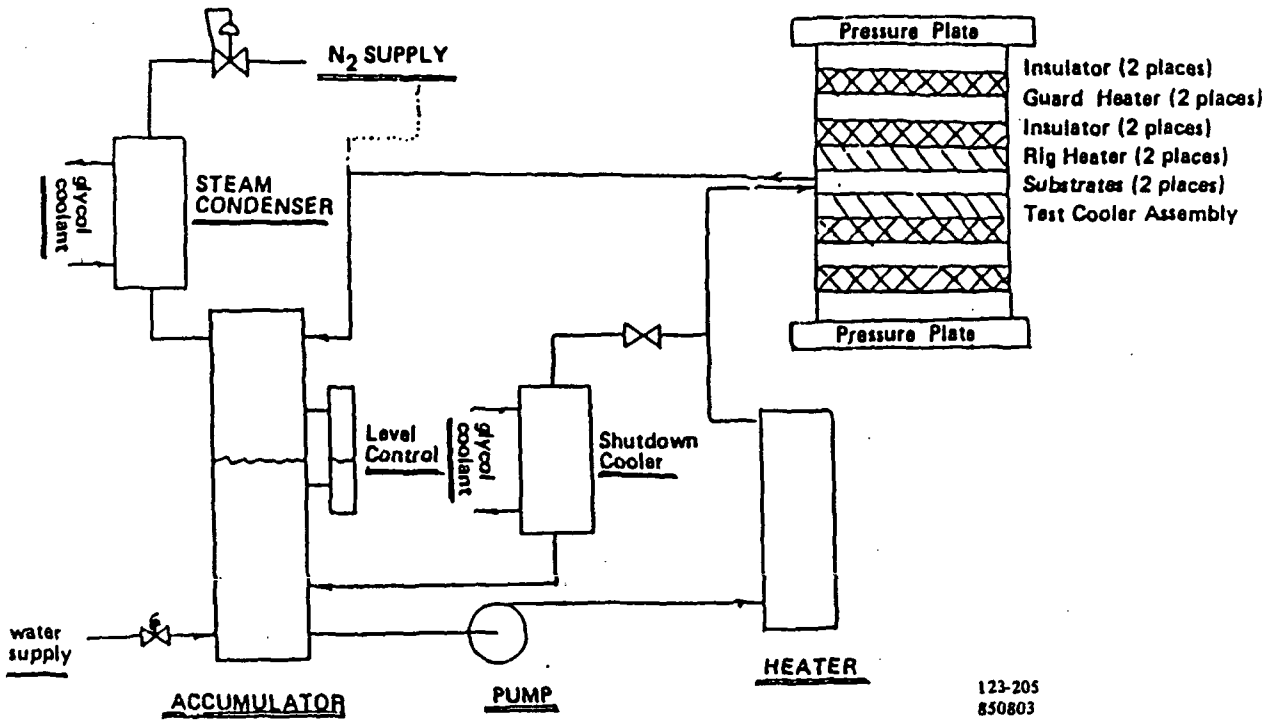

Figure 2-8. Heat Transfer Rig Schematic, 27-Inch by 27-Inch Cooler Planform

WCN 12034-6

Figure 2-9. Heat Transfer Test Rig for 27-Inch by 27-Inch Planform Coolers

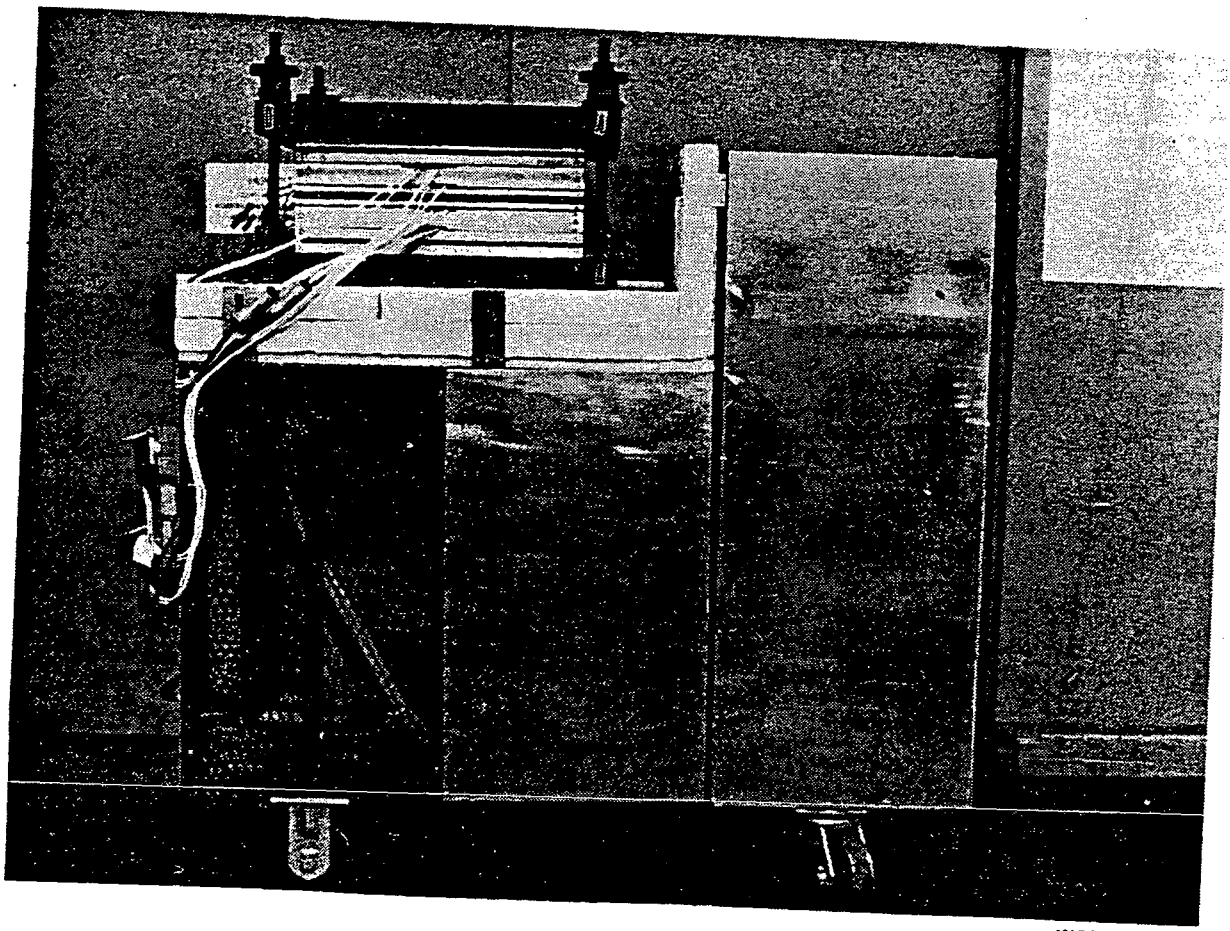

WCN 12034-7

Figure 2-10. Heat Transfer Test Rig for 27-Inch by 27-Inch Planform Coolers

Cooler Holder Development

Alternative cooler holders are being investigated to improve thermal performance and reduce cost. Evaluation of cooler holders includes fabrication trials, testing in subscale and full-scale heat transfer rigs, and determination of projected cost. Two alternative cooler holders were evaluated and a third was identified for evaluation in 1985.

Solid Graphite Holder - Subscale heat transfer tests were conducted to evaluate a solid graphite cooler holder as a means of obtaining higher cooler thermal conductivity (Table 2-8). For the case of zero nominal clearance between the tube and holder, the thermal resistance is slightly lower than the baseline. When the tube-to-holder clearance is 2.5 mils nominal, the thermal resistance is considerably higher. The results indicated that thermal caulks would be required to accommodate the tube to holder clearances that would be required with the incompressible holder to result in practical manufacturing tolerances.

Two commercially available thermal caulks were evaluated. Solid cooler holders with a tube to holder clearance of 2-3 mils were used in conjunction with the thermal caulks. These results are included in Table 2-8.

Testing showed that modifying the thermal caulks produced only a slight reduction in thermal resistance. It is concluded that a solid graphite holder does not provide a significant performance improvement or cost advantage over the baseline holder. No further activity is planned with the solid graphite holder.

Table 2-8. Subscale Heat Transfer Rig Test Results

Cooler Holder	Cooler Tube	Tube to Holder Fit	Caulk Thermal	Thermal Resistance (Hr Ft^2 °F/BTU)
Graphite Fiber	Stainless Steel	Interference	None	0.0091 (Baseline)
Solid	Stainless Steel	Zero nominal clearance	None	0.0081
Solid	Stainless Steel	2-3 mil clearance	None	0.0365
Solid	Stainless Steel	2-3 mil clearance	Commercial Type A	0.0093
Solid	Stainless Steel	2-3 mil clearance	Commercial Type B	0.0112
Solid	Stainless Steel	2-3 mil clearance	Type A with 9% Graphite	0.0083
Solid	Stainless Steel	2-3 mil clearance	Type A with 20% Graphite	0.0089

Metallic Cooler Holder - Two types of metal cooler holders were evaluated to obtain higher holder thermal conductivity. Subscale 6-inch by 6-inch and full-scale 3.7 ft^2 metal cooler holders of the first type were fabricated initially. Heat transfer testing in both the subscale and full-scale rigs indicated that cooler thermal resistance was unexpectedly high and exceeded the conventional holder (Table 2-9). The high thermal resistance was determined to be the result of poor tube to holder contact at the operating temperature, which is due to the difference in thermal expansion between the holder material and cooler material.

A second type of metal cooler holder was identified. Subscale cooler holders were fabricated and tested in the subscale heat transfer rig. The results are shown in Table 2-9. The second type of metal holder is shown to have a thermal resistance about 15% lower than the conventional fiber holder. Full-scale 3.7 ft^2 cooler

holders were then fabricated using the new permanent tooling. A 3.7 ft² encapsulated cooler with the second type of metal holder is being fabricated for testing in the heat transfer rig.

Table 2-9. Subscale Heat Transfer Rig Test Results

Cooler Holder	Cooler Tube	Relative Thermal Resistance
Graphite Fiber	Stainless Steel	1.00
Metal - First Type	Stainless Steel	1.52
Metal - Second Type	Stainless Steel	0.85

Development of a more conductive and lower cost cooler holder is being conducted in the parallel Electric Utility Technology and Development Program, DOE Contract DE-AC01-83FE60338. Initial subscale heat transfer test results indicate cooler thermal resistance is reduced 30% with this holder. Full-scale 3.7 ft² holders are being fabricated and will be tested in the full-scale heat transfer rig in early 1985.

Erosion-Corrosion

Testing is being conducted to evaluate erosion-corrosion of the single-element serpentine cooler array. The 20-inch by 20-inch heat transfer rig is being used for erosion-corrosion testing. This rig was redesigned to produce higher coolant velocities, and a feedwater treatment system and polishing loop were added to control coolant conditions. The following conditions are maintained during testing:

- The steam exit velocity is held at about 55 ft/sec.
- The pH is controlled to a neutral level and at a conductivity below 1.0 μmho by the ion-exchange beds.

- The coolant oxygen content is maintained between 30 and 500 PPB by the feedwater treatment system.

- The water inlet is held at controlled potential with respect to the cooler tube array. The potential is set to control the shunt current through the coolant hose connections at 50 μamps. This simulates full size cell stack conditions and permits evaluation of corrosion rates and electrophoretic deposition rates in the coolant manifold.

Build 1 - In the first build of the erosion-corrosion rig a stainless steel serpentine cooler and a stainless steel inlet manifold were tested for 3144 hours to evaluate erosion-corrosion under a high coolant oxygen level. The coolant oxygen content was in the desired range, 400-600 PPB, during the first 1900 hours and then decreased to 30-40 PPB over the last 1200 hours. The test conditions and coolant properties are shown in Table 2-10. No significant changes in pressure drop or thermal profile occurred during the 3144 hours of testing (Figures 2-11 through 2-13).

The stainless steel serpentine cooler array was removed from the cooler assembly for the post-test evaluation. Radiographs showed no significant change in wall thickness of the array. Metallographic cross sections showed the wall thickness to be unchanged from the inlet to exit of the array. These results indicate no measurable erosion-corrosion occurred during this test.

A metallographic cross section of the inlet tube on the manifold showed there was no significant change in the diameter and no measurable corrosion at the tip of the tube. A deposit (average thickness of about 0.001 inch) was present on the wall of the tube. Elemental analysis showed the material to be primarily copper and iron. The source of the copper is components in the feedwater treatment module and the coolant cart.

TABLE 2-10. EROSION-CORROSION RIG - BUILD 1

Test Conditions	Time Averaged Values Beginning of Test 25 - 50 Hours	 3038 - 3061 Hours
Coolant Flow Rate, pph	165	165
Steam Exit Velocity, FPS	60	60
Coolant - Inlet Temperature, °F	338	343
- Exit Temperature, °F	354	354
- Inlet Pressure, psig	128.6	126.5
- Delta P Across Cooler, PSID	6.7	6.2
Heat Input to Cooler, Watts	5940	5730
Temperature - Top of Cooler, °F	391 ave.	387 ave.
- Bottom of Cooler, °F	390 ave.	388 ave.

Coolant Properties	270 Hours	1321 Hours	1935 - 2111 Hours	2498 Hours	2978 - 2999 Hours
Oxygen Content (PPB)	600	400	40	30	30
pH	8.15	-	7.8	7.99	7.6
Conductivity (umho)	1.3	0.85	0.38	0.7	0.45
Turbidity (NTU)	0.5	-	0.25	3.1	3.3

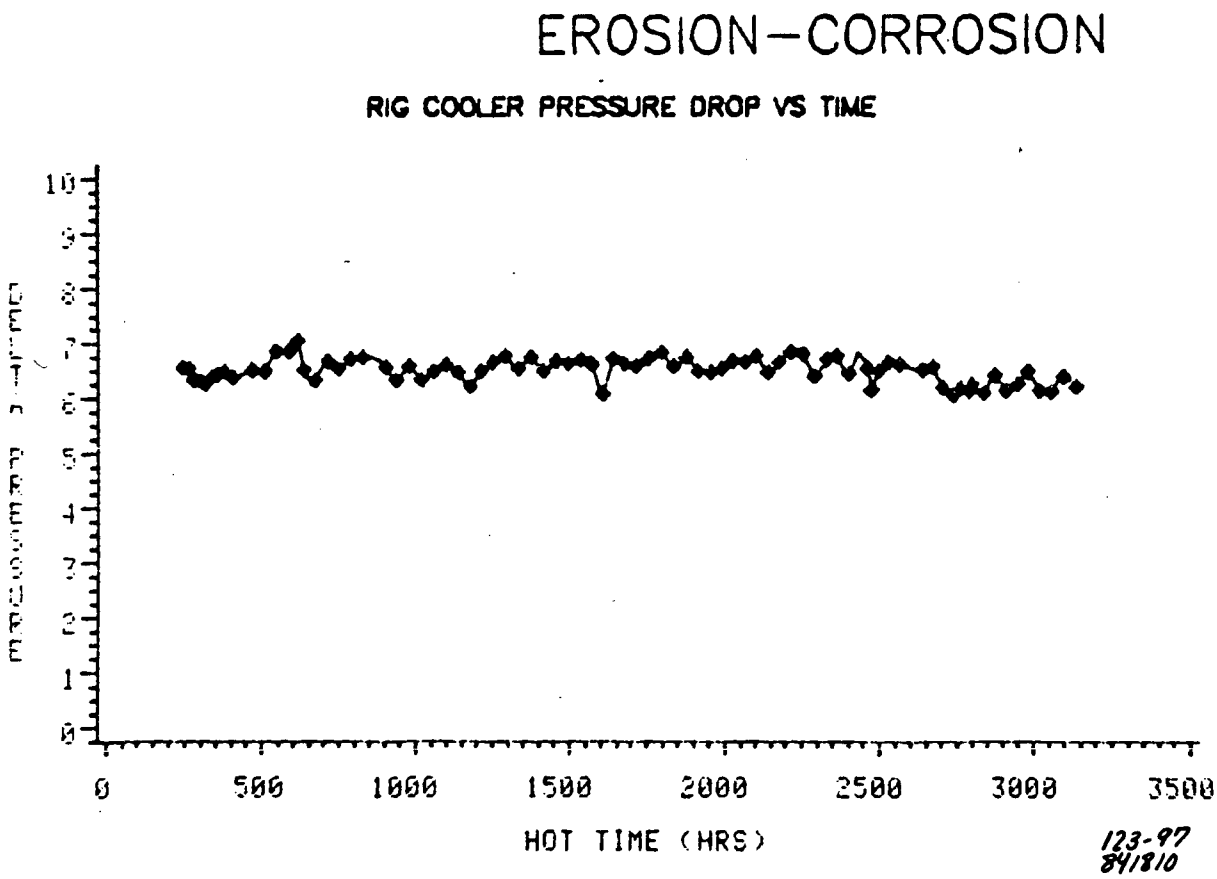

Figure 2-11. Erosion-Corrosion Rig Cooler Pressure Drop vs. Time

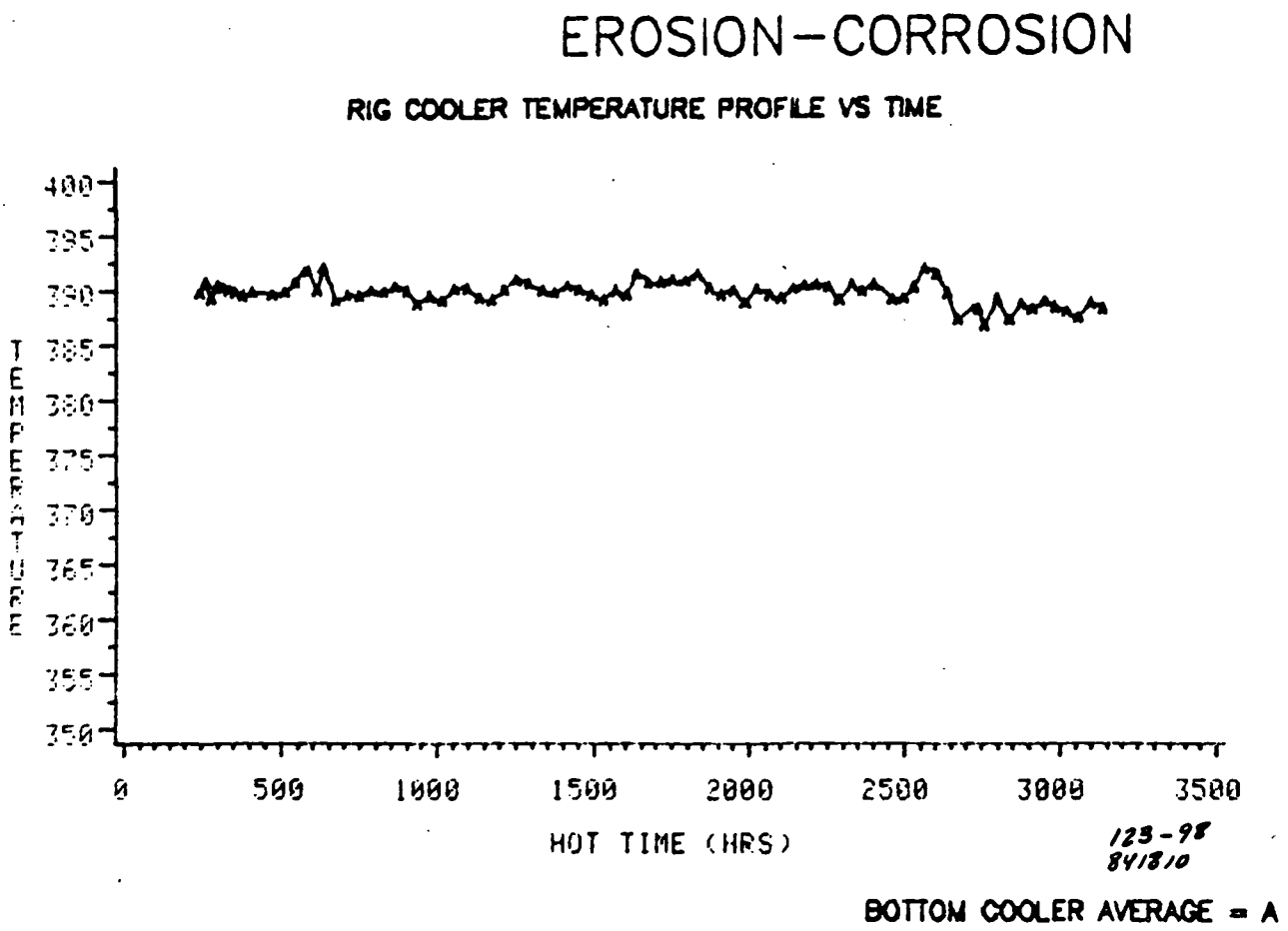

Figure 2-12. Erosion-Corrosion Rig Cooler Temperature Profile vs. Time

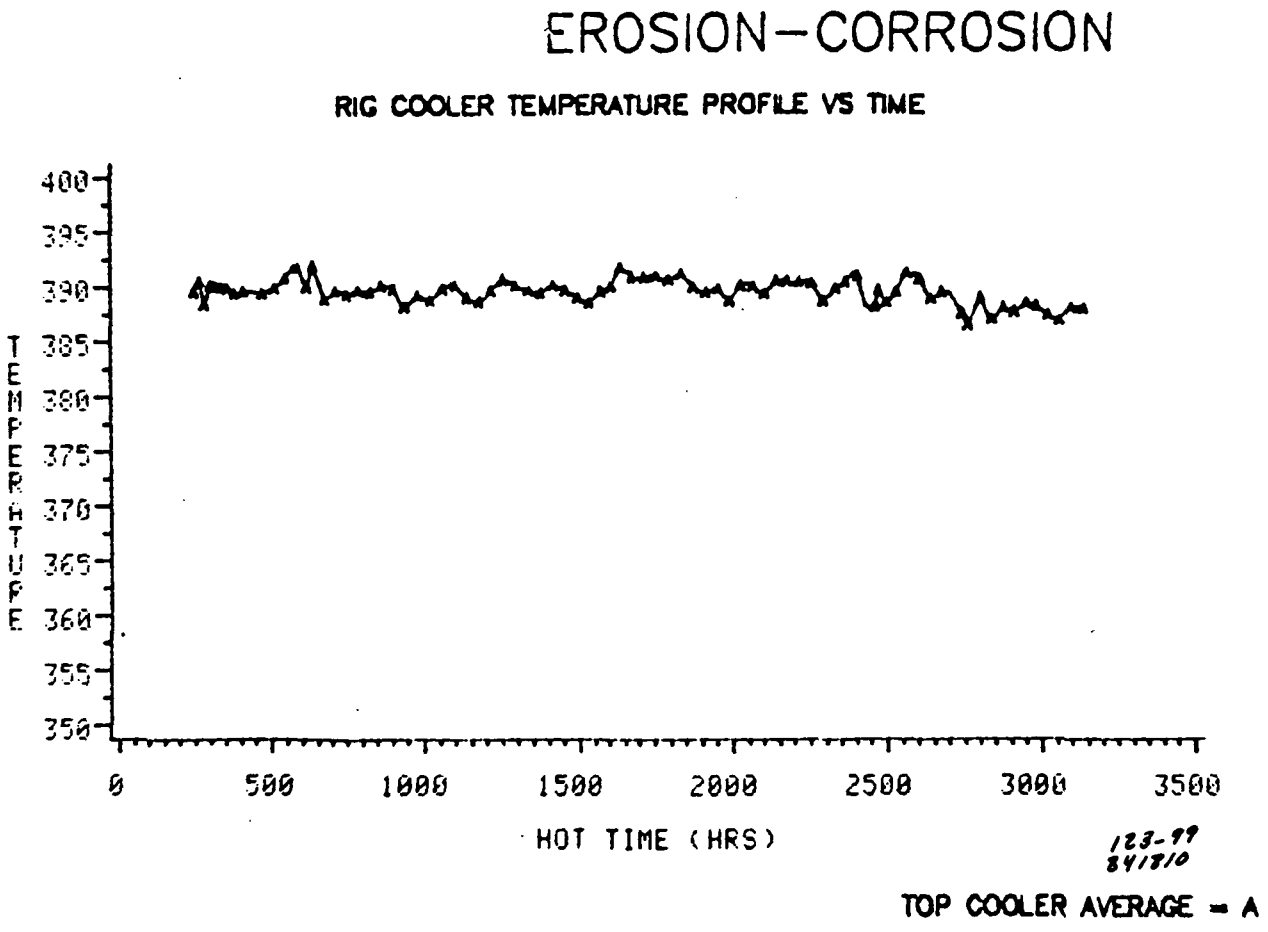

Figure 2-13. Erosion-Corrosion Rig Cooler Temperature Profile vs. Time

Build 2 - Testing of the second build of the erosion-corrosion rig is in progress to evaluate a stainless steel cooler and coolant inlet manifold under low coolant oxygen levels. Approximately 2400 hours of test time have been accumulated. The test conditions and coolant properties are shown in Table 2-11. Testing will be continued to at least 3000 hours.

Tests will be conducted in 1985 to evaluate erosion-corrosion of serpentine cooler arrays fabricated from lower cost stainless steel tubing. The lower cost tubing is welded, versus welded and drawn, and has a thinner wall. This tubing reduces the cost of the serpentine array by 40-50%.

TABLE 2-11. EROSION-CORROSION RIG
BUILD II

Test Conditions	Time Averaged Values			
	91 - 115 Hours	1121 - 1145 Hours	1754 - 1777 Hours	2314 - 2337 Hours
Coolant Flow Rate, PPH	165	165	165	165
Steam Exit Velocity, FPS	47	45	54	54
Coolant - Inlet Temperature, °F	342	340	348	349
- Exit Temperature, °F	355	353	355	356
- Inlet Pressure, PSIG	122.6	125.2	128.9	130.3
- ΔP Across Cooler, PSID	5.4	4.5	5.8	5.9
Heat Input to Cooler, Watts	5288	5084	5552	5616
Temperature - Top of Cooler, °F	387 ave.	380 ave.	388 ave.	387 ave.
- Bottom of Cooler, °F	393 ave.	390 ave.	387 ave.	395 ave.

Coolant Properties	605 Hours	1064 Hours	1414 Hours	2346 Hours
Oxygen Content (PPB)	60	30	30	40
pH	7.6	7.6	7.0	6.8
Conductivity (μmho)	0.25	0.61	0.44	0.60
Turbidity (NTU)	6.3	6.3	3.1	-

Dielectric Coolant Hoses

Thick Wall Teflon® Hoses

A test program was conducted to characterize the long-term burst strength of the dielectric connector hoses used to connect the coolers to the coolant manifold. Testing was conducted at temperatures of 350, 375, and 400°F. The hoses were 3/8-inch diameter Teflon® with a 0.150 inch wall thickness. This is the size required for the 3/8-inch diameter serpentine coolers that were used when the test program was initiated in late 1983. The tests were conducted using the procedure in ASTM-D-2837 for evaluating thermoplastic hose material. Testing was conducted under subcontract by a testing laboratory familiar with this procedure.

The hoses that were tested at 350°F and 375°F reached the planned 10,000 hours. None of the 400°F hoses reached 10,000 hours because of a temperature override in the test environment. This affected eight hoses that had reached 6300 to 7300 hours at the time of the overtemperature.

The failed hoses from the 10,000 hour test program were categorized with respect to type of failure. The types of failure include leakage between the clamped hose and tube, short axial splits about 1/8-inch long, and burst failures that resulted in axial splitting. Table 2-12 shows the breakdown of these failures for each test temperature.

Table 2-12. Failure Summary for Teflon® Dielectric Hoses

Type of Failure	Number of Failures 350°F	375°F	400°F
Leakage at Clamp	6	2	0
Short Axial Split	3	7	7
Burst - Axial Split	10	13	15
(Non-Failures)	6	11	8*

*Testing discontinued because of overtemperature

Figures 2-14 through 2-16 show failure pressure as a function of time for the three test temperatures. Failure type is noted.

Failures caused by leakage between the hose and tube were due to surface oxidation of the copper tubes. This is shown in the cross sectional photomicrograph, Figure 2-17. Stainless steel is now being used for the serpentine cooler arrays instead of copper; therefore, the oxidation problem is limited to this test program.

Hoses that failed because of short axial splits were analyzed by the supplier. The results indicate these failures are caused by foreign material inclusions or processing defects. Figure 2-18 shows a failed hose with a short axial split. The feasibility of conducting a non-destructive quality control test such as a radiograph to identify defects in the hoses will be investigated.

The balance of the hoses failed by bursting, which is the expected failure mechanism. A typical burst failure is shown in Figure 2-19.

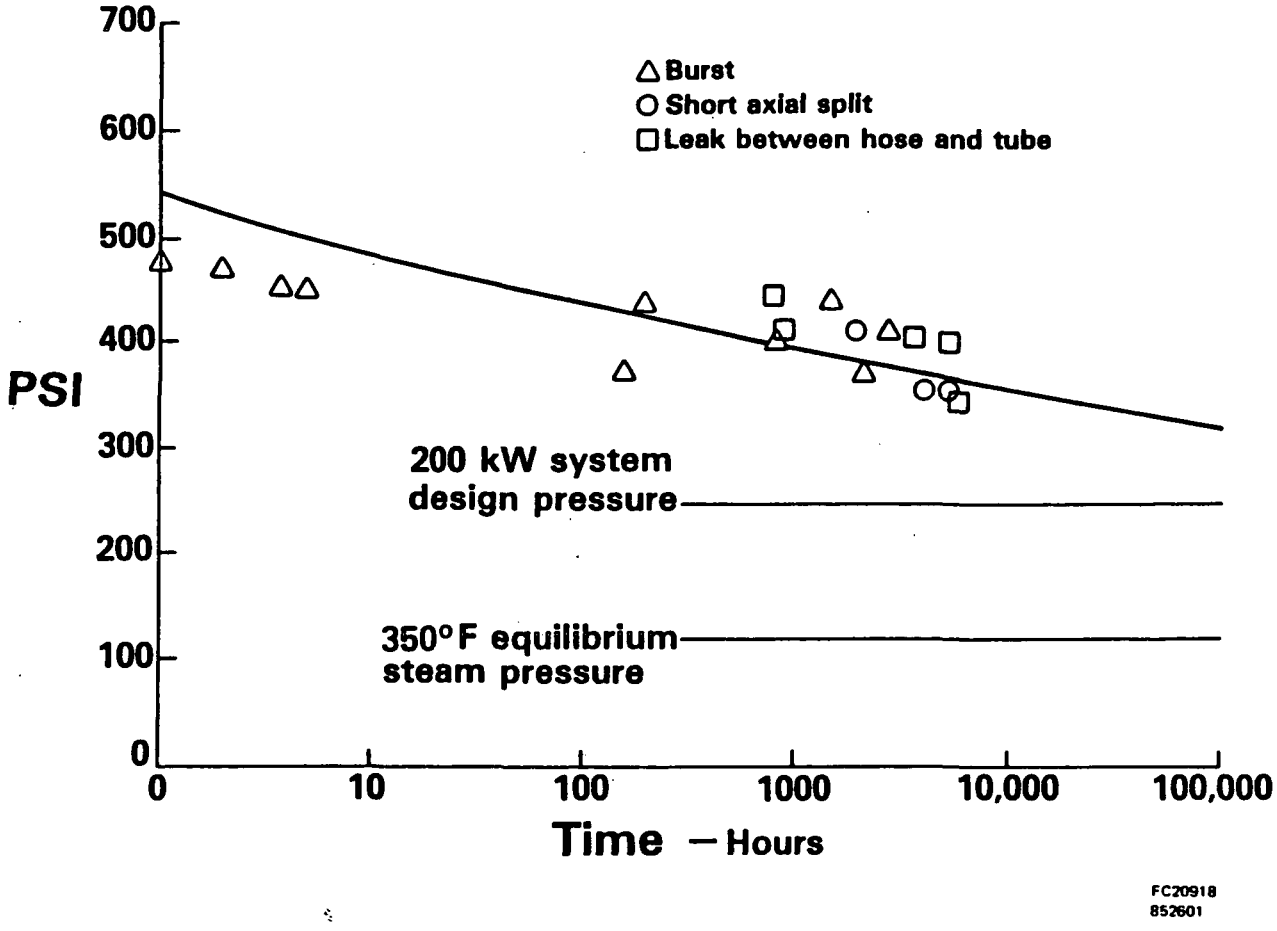

Figure 2-14. Failure Pressure vs. Time - 350°F

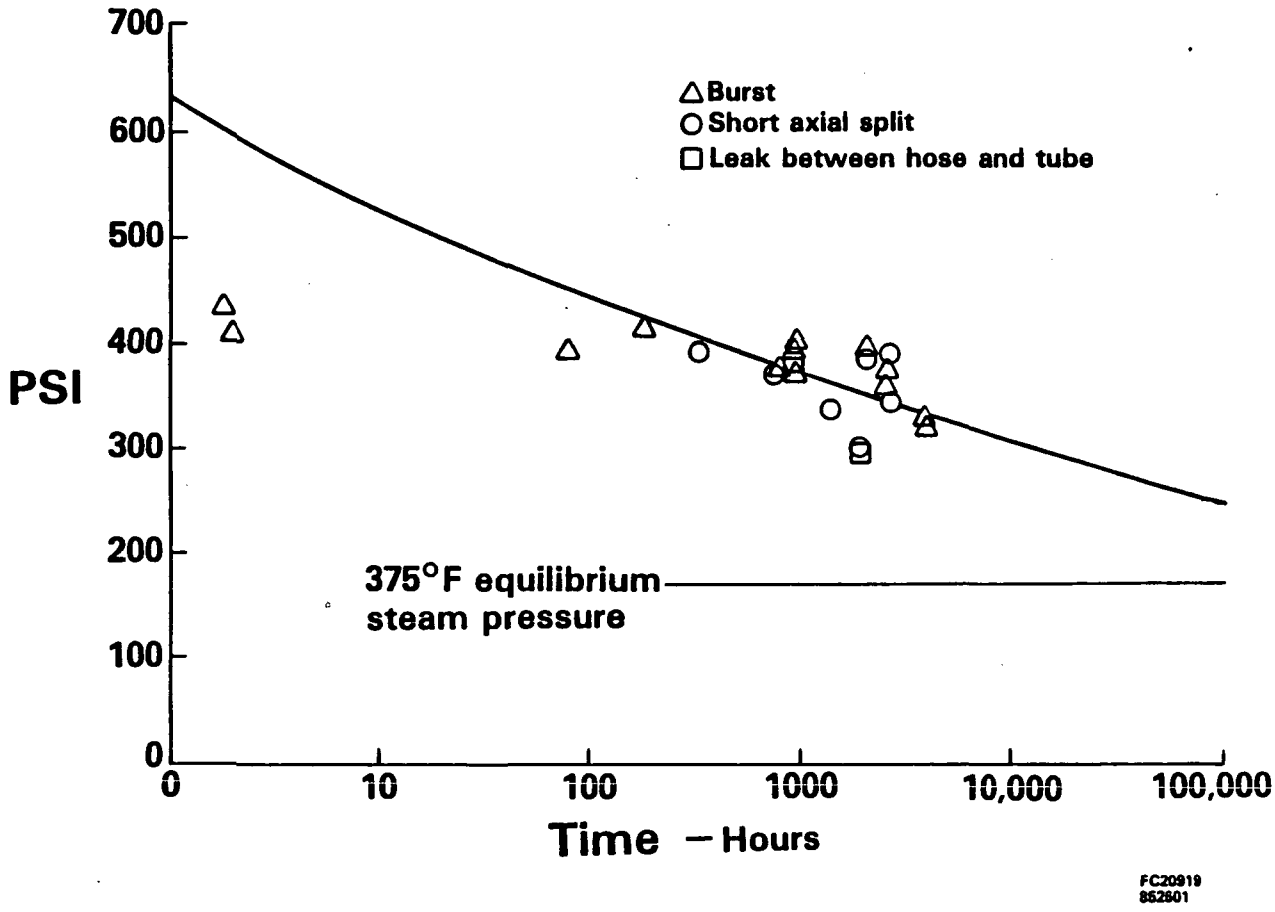

Figure 2-15. Failure Pressure vs. Time - 375°F

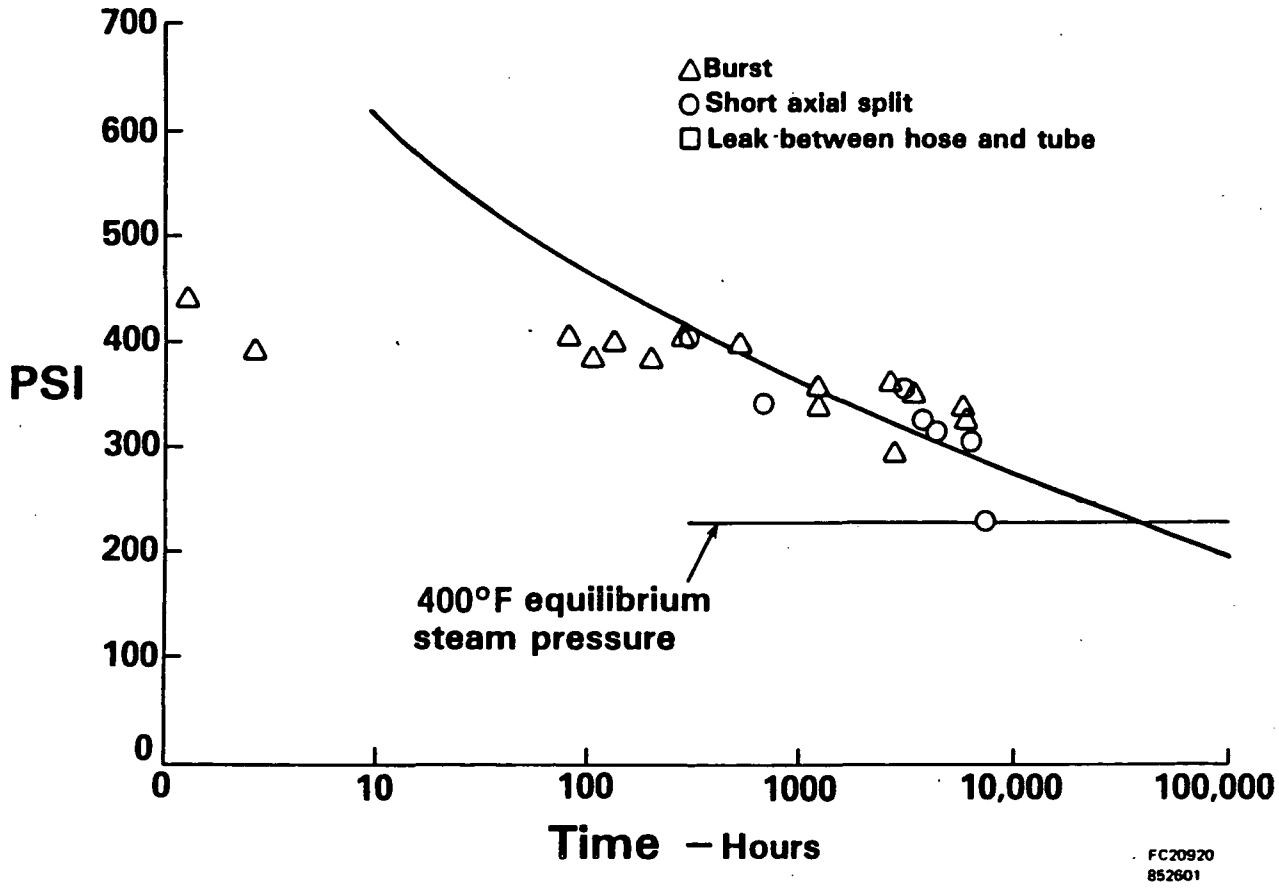

Figure 2-16. Failure Pressure vs. Time - 400°F

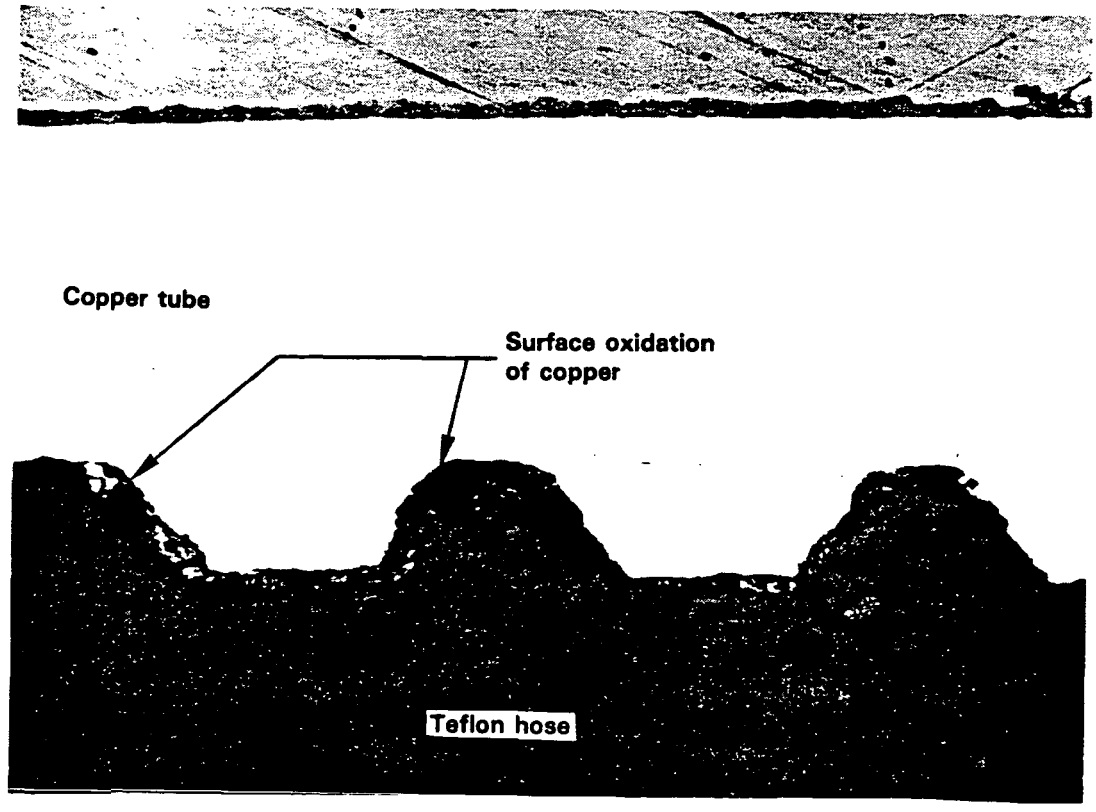

FC20923
852601

Figure 2-17. Cross Sectional Photomicrograph of Hose Assembly with Surface Oxidation of Copper Tube

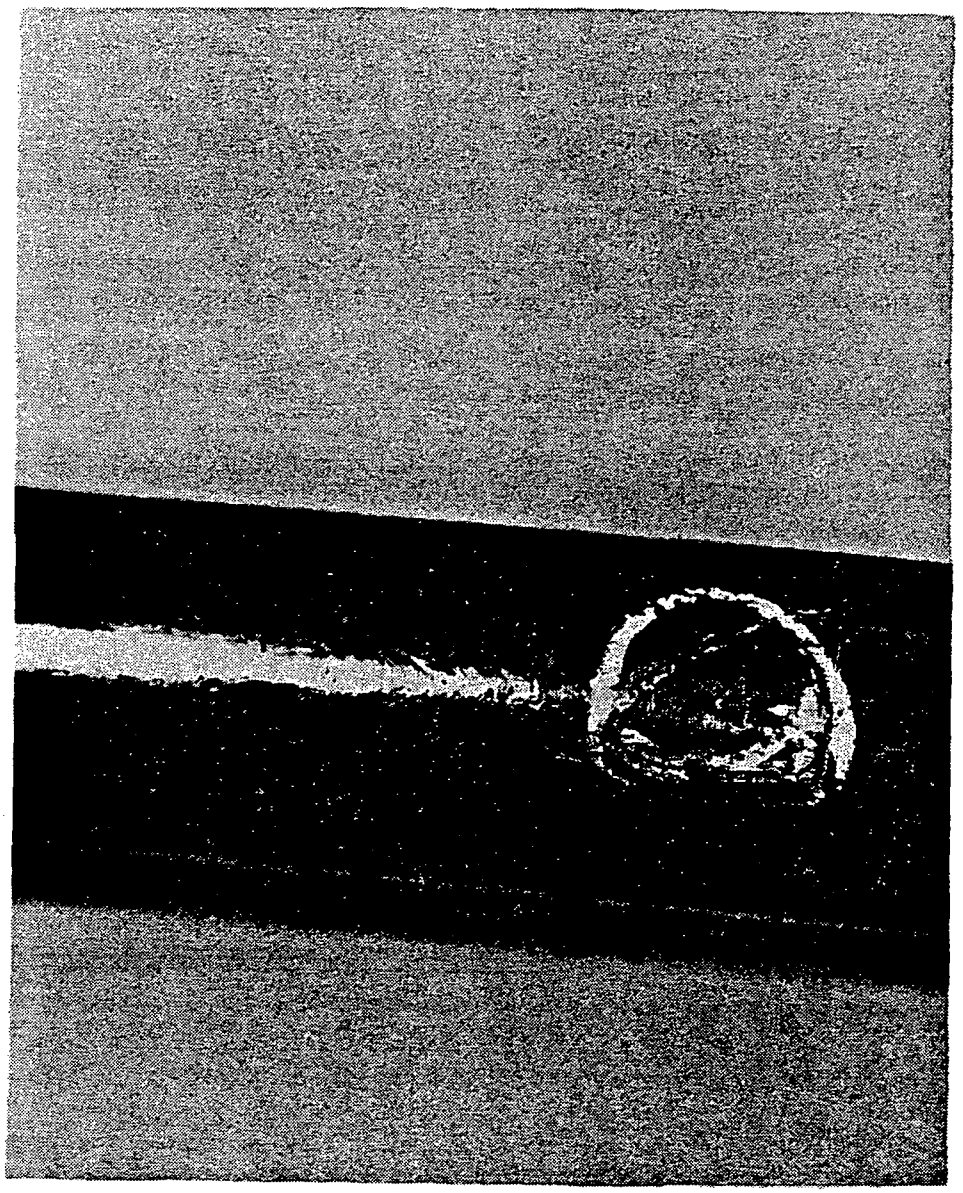

WCN 11079

Figure 2-18. Failure Due to Short Axial Split

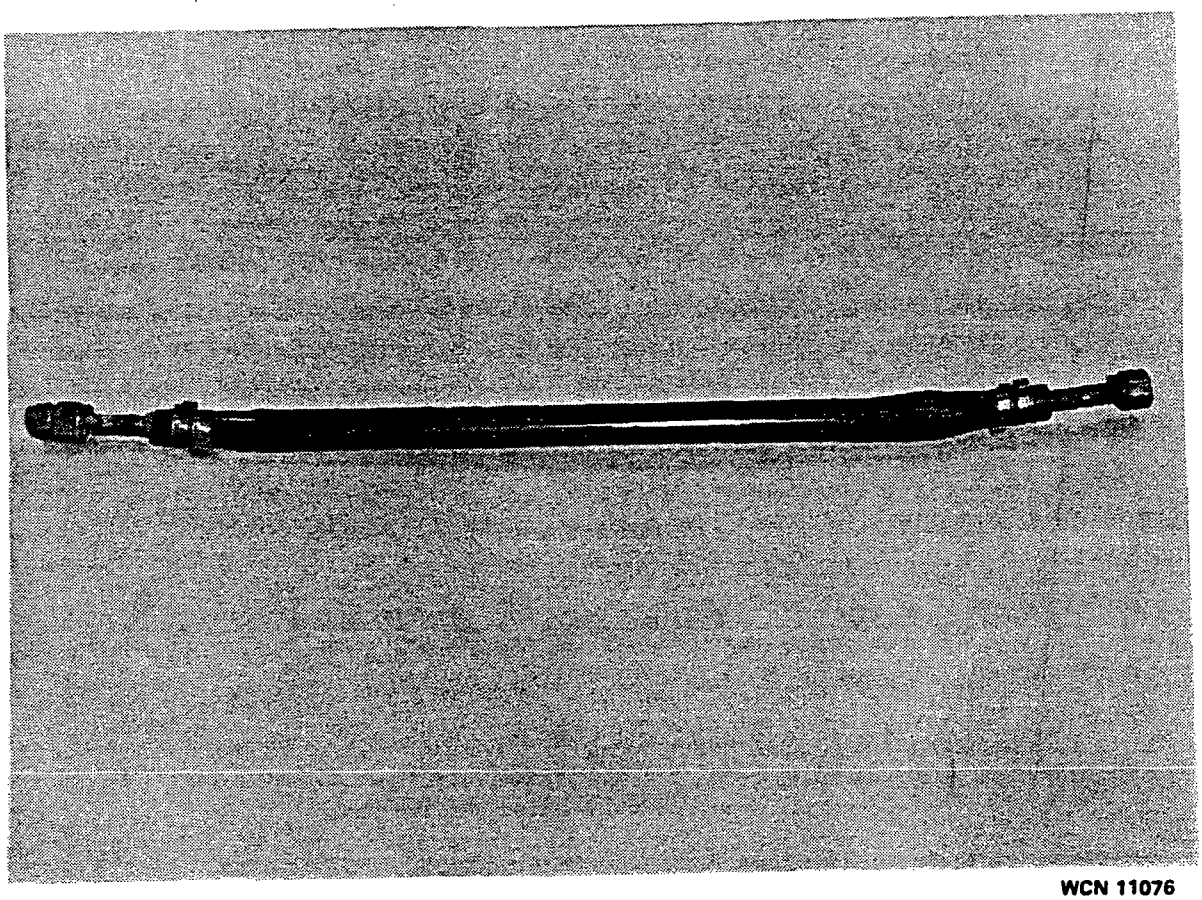

WCN 11076

Figure 2-19. Burst Failure

Approximately 80% of burst and short axial split failures initiated or occurred near either end of the hose. This is attributed to reduced wall thickness at the ends. The hoses were drilled out at the ends to increase the inside diameter slightly to match the size of the tube.

A statistical analysis was conducted to determine the maximum acceptable operating temperature of the hoses for a 40,000-hour power plant life. These results, shown in Table 2-13, were determined from log-log regression analyses. It is concluded that the hose configuration tested is acceptable for use up to 350°F, which is the current design temperature for the 200-kW power plant. The hose configuration has an unacceptably high probability of failure at 375 and 400°F. The lower confidence limit (LCL) ratios for the 375 and 400°F tests are below the ASTM requirement of 0.085 due to scatter in the data.

Table 2-13. Statistical Analysis of Dielectric Hose Test Results

Temperature	100,000 Hour Pressure (1)	100,000 Hour Lower Confidence Level (LCL) (2)	LCL Ratio (3)	Probability of Failure in 40 k Hours
350°F	327.3 psig	275.9 psig	0.843	0.035% (at 120 psig)
375°F	256.8 psig	178.8 psig	0.696	0.91% (at 169 psig)
400°F	210.7 psig	150.8 psig	0.716	44.1% (at 232 psig)

Note: (1) Pressure at which 50% of samples fail in 100,000 hours.
(2) Pressure at which 2.5% of samples fail in 100,000 hours.
(3) LCL/100,000 hour pressure (0.85 is required).

It should be noted that these results are for the particular hose configuration tested and are not an accurate indication of the capability of the Teflon® hose material itself.

Reinforced Hoses

Activity was initiated to evaluate a thin walled Teflon® hose with woven reinforcement. This type of hose has higher pressure capability and costs less than the thick walled Teflon® hose.

Testing has shown that the present connector clamp design used on the thick walled Teflon® hose is not adequate for the reinforced thin walled Teflon® hose. Four 7/16-inch diameter reinforced hoses were tested at 300 psi and 375°F. After 75 hours of testing, one of the samples experienced failure at the connector clamp. This indicated that a new clamp design is required. The supplier of the reinforced hose has initiated development of swaged clamp, which is expected to be available in early 1985. A test program will then be conducted to characterize the long-term burst strength of the reinforced hose.

Coolers for the Second Short Stack

Coolers were fabricated for the second short stack. These coolers are of the conventional encapsulated design and have a 27-inch by 27-inch planform. The serpentine cooler arrays are 7/16-inch diameter stainless steel. The electrical resistance of the completed cooler assemblies measured 4-6 mV/100 ASF at 30 psi.

The dielectric hoses for the second short stack are 7/16-inch diameter Teflon® with a 0.186 inch wall thickness. The short-term burst pressure of this type of hose was determined to be a minimum of 450 psi at 350°F. This is at least three times the operating pressure of the second short stack.

Subtask 2.3 - Non-Repeat Component Technology

Objective

The objective of this task is to extend stack operating intervals by developing a method for periodically adding electrolyte to a cell stack. An additional objective is to develop an improved initial electrolyte fill procedure based on this electrolyte addition method.

Summary

Electrolyte loss over tens of thousands of hours will require electrolyte additions to the cells. An electrolyte addition approach practical for field use was conducted late in the previous report period in a non-operational full height stack. Results of this analysis showed this addition approach was successful. Subsequently, the electrolyte addition approach was successfully tested on a short stack of full-area cells.

The first acid refill trial was conducted on a 40-kW stack containing 270 cells. The acid spray approach was used. The cells to be filled or refilled were dry or contained 10, 20, and 30% full reservoirs. This trial confirmed that the acid spray refill approach was acceptable, that there was no sensitivity to cell position within the stack, that the initial fill level had an insignificant effect on the final fill level, that there were no problems with shunt currents, and that the intracell distribution was acceptable.

A survey of nozzle and spray system manufacturers was conducted and a commercially available spray nozzle was selected. This nozzle is compatible with the fuel cell environment and was characterized for flow rate and pressure relationship. A portable acid spray cart was constructed. This cart consisted of a 100 gallon tank, pumps, a filter, and plumbing connected to a spray nozzle manifold. This spray system was successfully used for the second acid refill trial on a 40-kW stack.

The 30-cell stack being tested in Subtask 2.4 was refilled using this acid spray approach. The stack has operated for 6100 hours prior to the refill and was essentially unchanged as a result of the spray refill procedure.

The second acid refill trial was conducted on a 40-kW stack containing 240 cells. Eight different cell configurations were present in this stack to evaluate the fill level, the orientation of the gas channels through which the acid was added, and the effect of acid fill tabs. The stack was successfully spray filled and was disassembled. Analysis of the acid inventory data is in progress.

Highlights

- The first acid spray refill trial was conducted on a non-operational 40-kW stack containing 270 cells.
- Hardware was defined and constructed for an acid spray refill system.
- An acid spray refill test was successfully conducted on an operational short stack.
- The second acid spray refill trial was conducted on a non-operational 40-kW stack containing 240 cells.

Discussion

The first acid refill trial was conducted on a used 40-kW stack containing 270 cells. This stack was assembled with 90 new cells, located in 6-cell substacks throughout the entire stack. The new cells were filled with varying amounts of acid: dry, 10, 20, and 30% full reservoirs. The refill test involved spraying the entire face of one side of the stack until all cells including the gas channels were full of acid and acid was cascading uniformly down the opposite side of the stack. The acid in the stack was then conditioned, the stack was disassembled, and acid inventory data was obtained on each of the 90 new cells.

The following observations were made in this acid refill test:

- o There is no sensitivity of acid refill volume to cell position in the stack.
- o The initial acid fill level has an insignificant effect on the final refill volume.
- o Acid is absorbed into the cells once the spray has stopped. There is insufficient acid on the face of the stack to support shunt currents.
- o Intracell acid distribution was acceptable. The data indicated, however, that the refill procedure should be modified slightly to improve acid distribution within the cell.

A photograph of the stack and the acid refill cart used in this refill trial is presented in Figure 2-20.

Figure 2-21 presents the acid volume after refill versus cell position within the stack. This data indicates that there is no correlation between acid volume and cell position within the stack.

Intracell acid distribution was measured on the 90 new cells. This data is presented in Table 2-14 and indicates that the cell fills were at the desired level, and that full cells do not overfill.

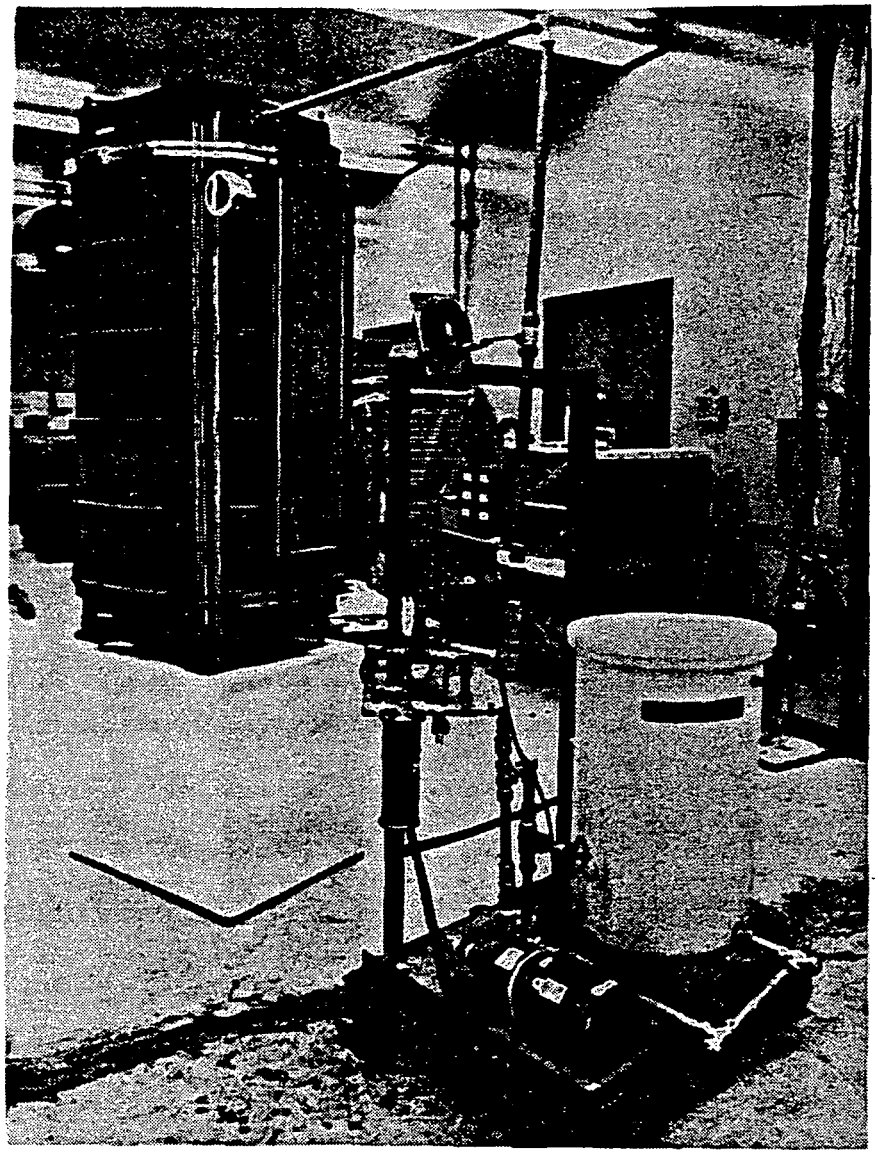

WCN 10844

Figure 2-20. Stack and the Acid Refill Cart

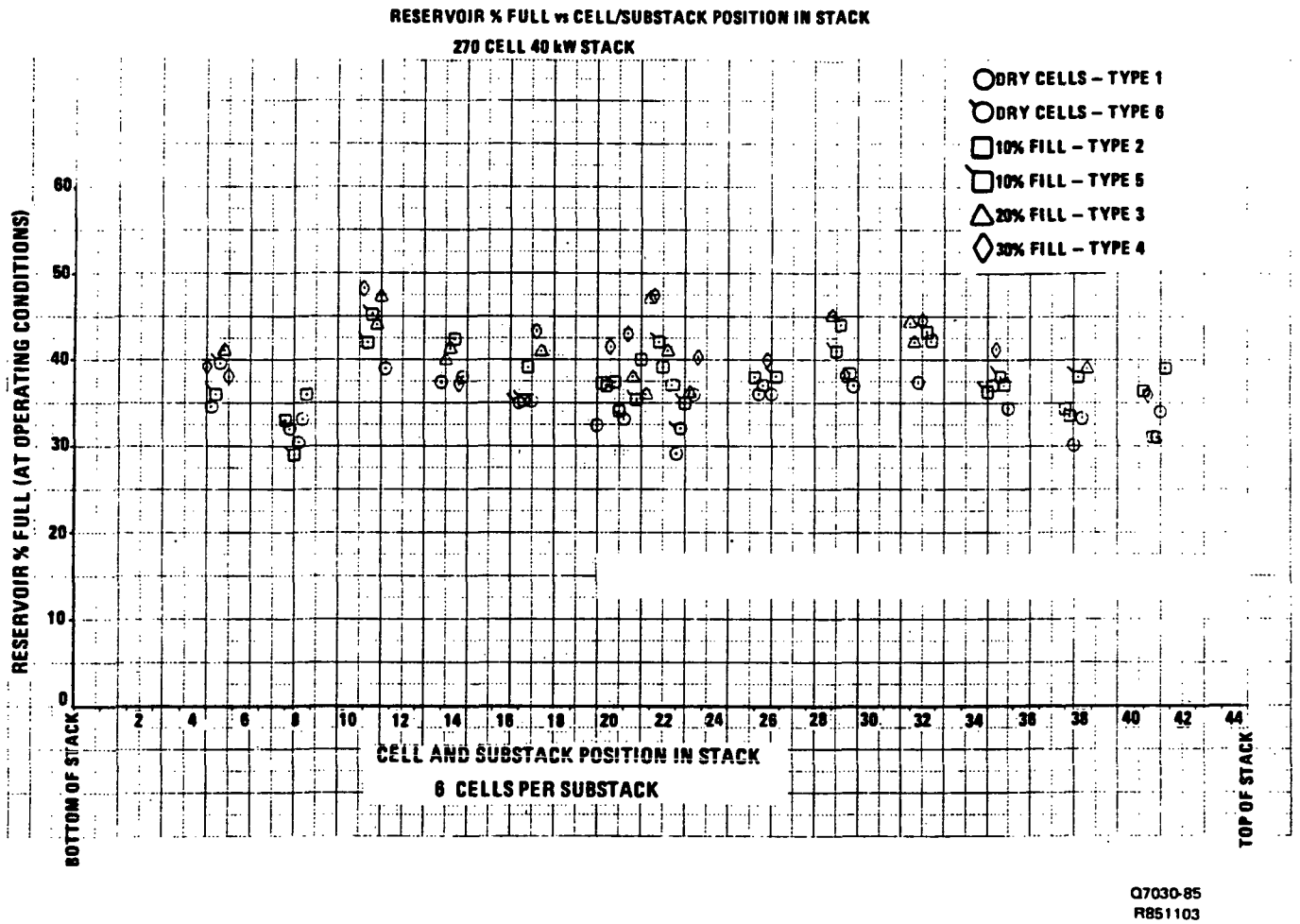

Figure 2-21. Acid Spray Refill Results

Table 2-14. Acid Spray Refill Approach Data Summary
(270-Cell 40-kW Stack)

Initial Fill (Reservoir % Full)	Final Fill (Reservoir % Full)				
	Total Cell	Anode	Cathode	Cell Type	Number of Cells
Dry	34	36	33	40-kW	19
10	37	42	34	40-kW	22
20	41	45	39	40-kW	15
30	41	47	37	40-kW	14
Dry	34	36	33	Condensate Zone	5
10	39	42	34	Condensate Zone	15

A survey of nozzle and spray system manufacturers was conducted. The objective was to select a commercially available spray nozzle that will be compatible with the fuel cell environment and will provide an acid spray pattern for refilling each cell in an assembled stack. The nozzles that were selected for evaluation were made of Teflon®, operate at low pressures and low flows, are compatible with 1/4 and 3/8-inch plumbing, and are in some cases of non-clogging design.

The results of these nozzle evaluations lead to the selection of a solid cone spray. The flow characteristics of this type of nozzle are given in Figures 2-22 and 2-23. Figure 2-22 presents the acid flow rate versus pressure, and Figure 2-23 presents the uniformity of the spray pattern. These acid spray nozzles were used to refill the 30-cell stack being tested in Subtask 2.4 (Figure 2-24).

These nozzles were also installed in a manifold and were used in the second acid refill trial on a 40-kW stack. Figure 2-25 shows the portable acid spray cart that was used along with the spray manifold for the refill trial on this stack.

A second acid spray refill trial was conducted on a full size stack. The stack is non-operational and contains 240 cells of the 40-kW configuration. The cells in this stack included the following configurations.

- 30% full acid reservoirs
- 10 to 15% full acid reservoirs
- Dry cell packages
- Cells with acid fill tabs on separator plates
- Cells with acid fill tabs on substrates
- Cells with gas channels being filled on top (cathode up)

The configuration of this stack, giving the number of cells and the location of the different cell configurations, is given in Figure 2-26.

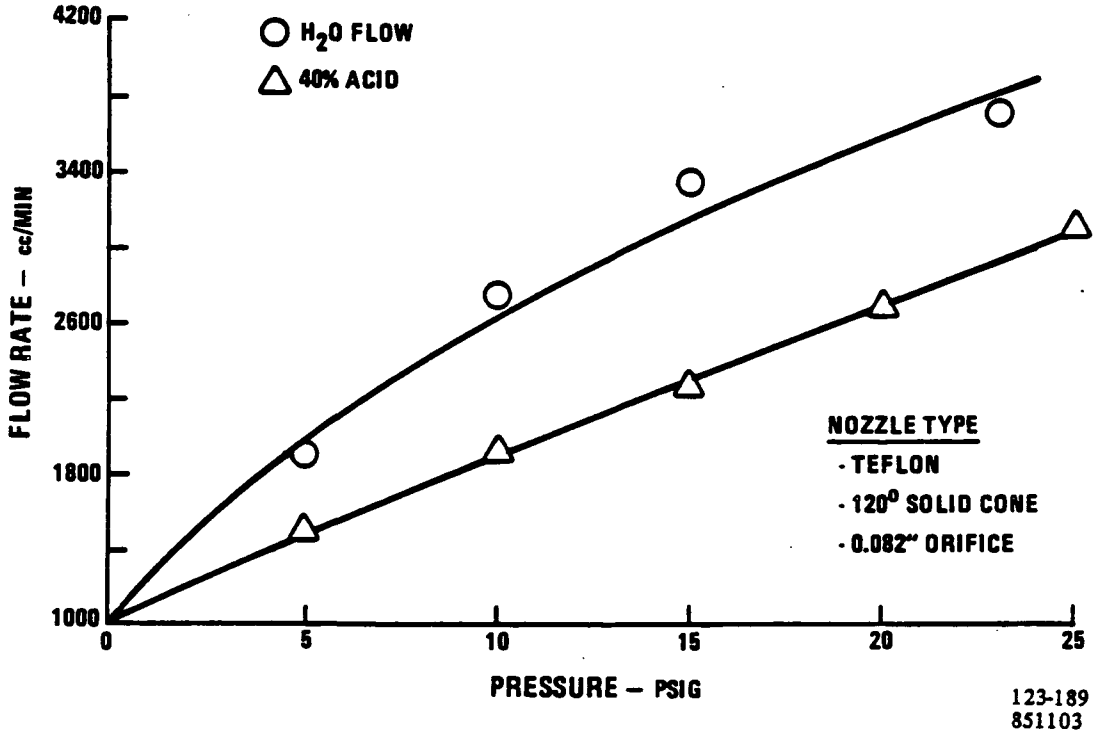

Figure 2-22. Acid Spray Refill Nozzle Characterization Test Flow Rate vs. Pressure

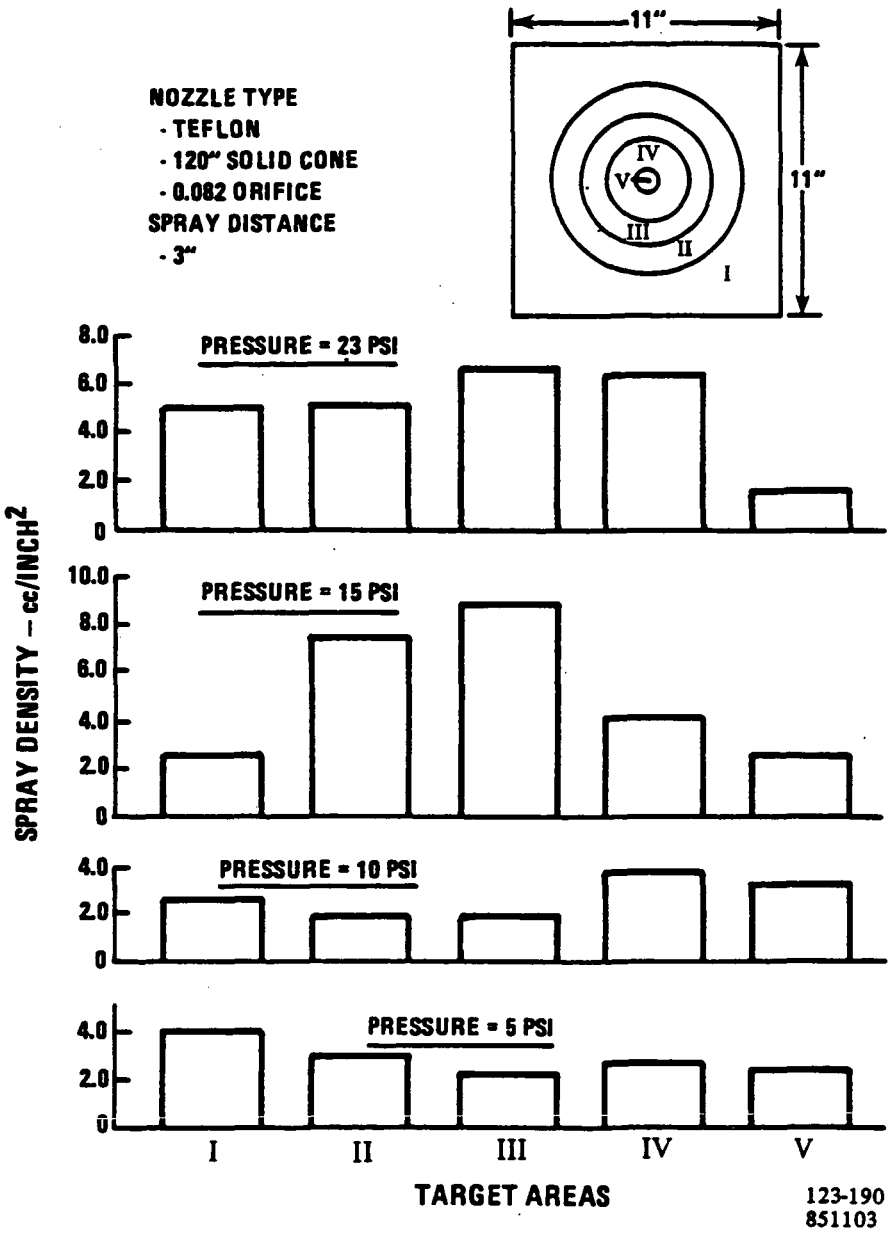

Figure 2-23. Acid Spray Refill Spray Distribution Test

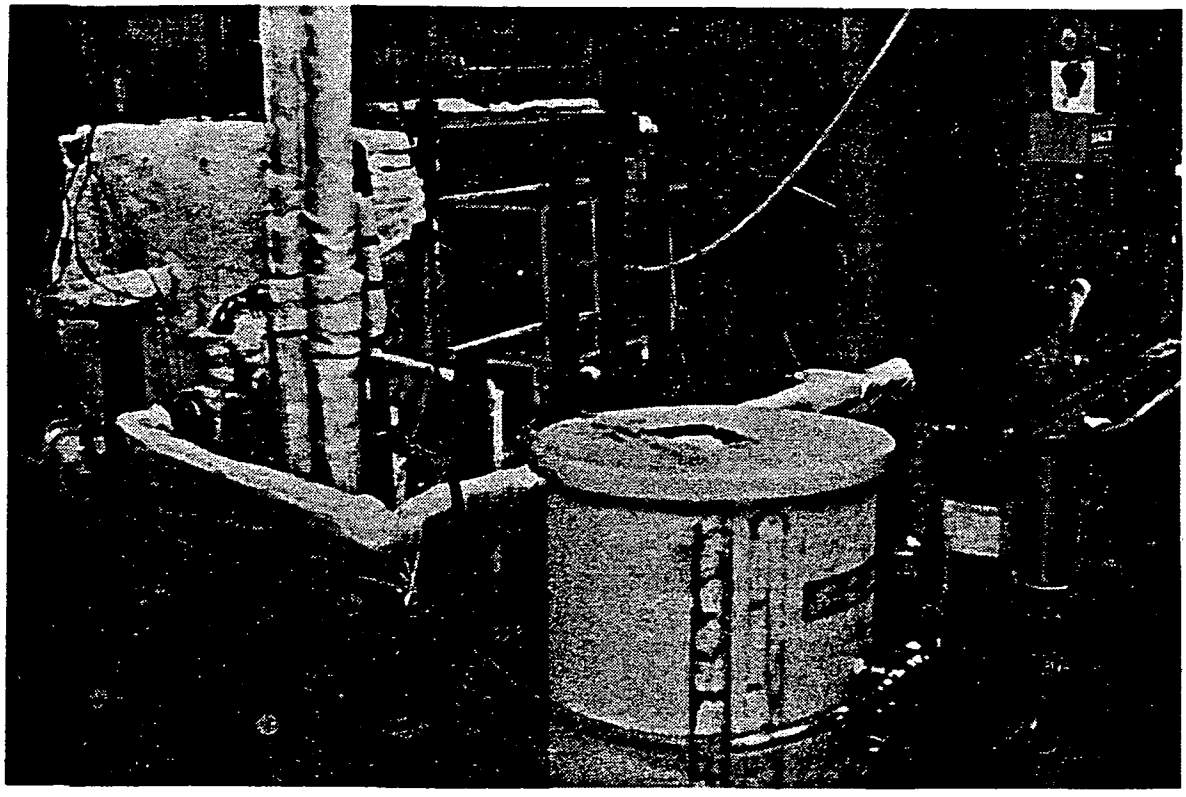

WCN 12027-10

Figure 2-24. 30-Cell Stack with Acid Spray Refill Cart

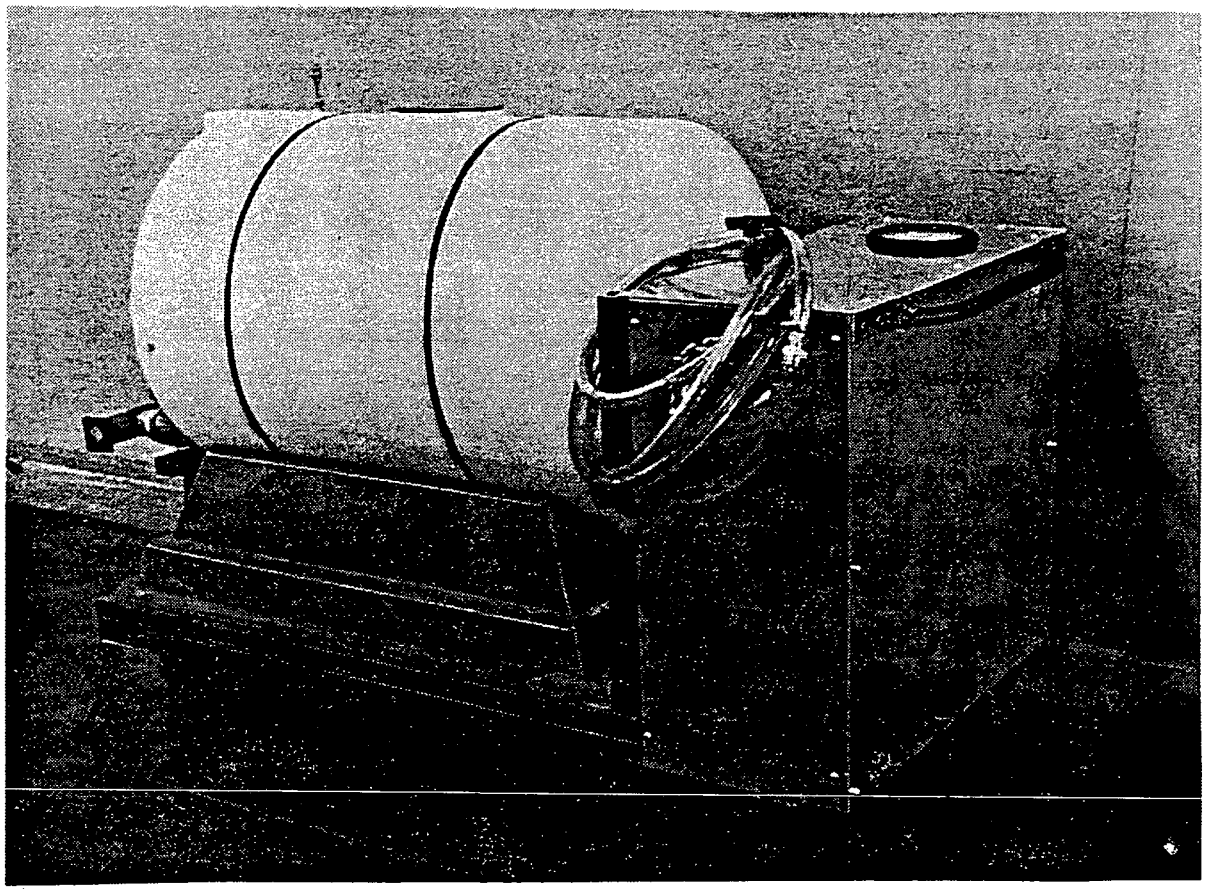

WCN 13013-10

Figure 2-25. Portable Acid Spray Refill Cart

FILE NAME:
STCK6S1A

STACKING CONFIGURATION
ACID SPRAY REFILL TRIAL NO. 2
240 CELL 40 KW STACK

SUBSTACK TYPES:

1 -- NO TABS
2 -- SEPARATOR TABS
3 -- SUBSTRATE TABS

CELL TYPES:

A -- 91 CELLS, END OF LIFE, CHANNELS UP

B -- 33 CELLS, BEGINNING OF LIFE, CHANNELS UP

C -- 38 CELLS, INITIAL FILL CHANNELS UP

D -- 44 CELLS, END OF LIFE CHANNELS DOWN

E -- 12 CELLS, BEGINNING OF LIFE, CHANNELS DOWN

F -- 22 CELLS, INITIAL FILL CHANNELS DOWN

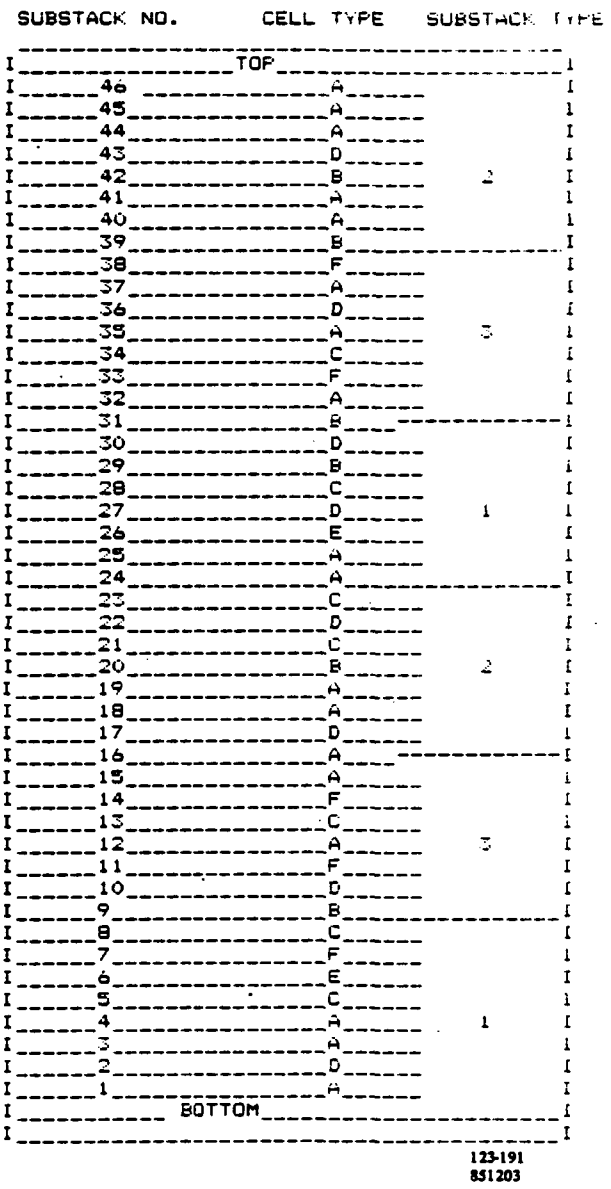

Figure 2-26. Cell Stacking Configuration
Acid Spray Fill Rig

The stack was sprayed with acid for four hours. After a two-hour spray period the stack was allowed to drain for one hour and then the spraying continued for two more hours. The stack was initially sprayed with 32% H_3PO_4, and during the spray period the concentration of acid in the spray cart increased, as shown in Figure 2-23. The acid transfer between the stack and spray cart is given in Table 2-15.

Table 2-15. Second Acid Spray Refill Trial on 40-kW Stack

	Acid in Cart		Acid in Stack	
	Weight $\%H_3PO_4$ (kg 100% H_3PO_4)		Weight $\%H_3PO_4$ (kg 100% H_3PO_4)	
o Start	105.3	33	103.1	47
o Finish	35.1	37	117.5	TBD

The stack has been disassembled and the acid inventory of each cell has been measured. This data is now being analyzed.

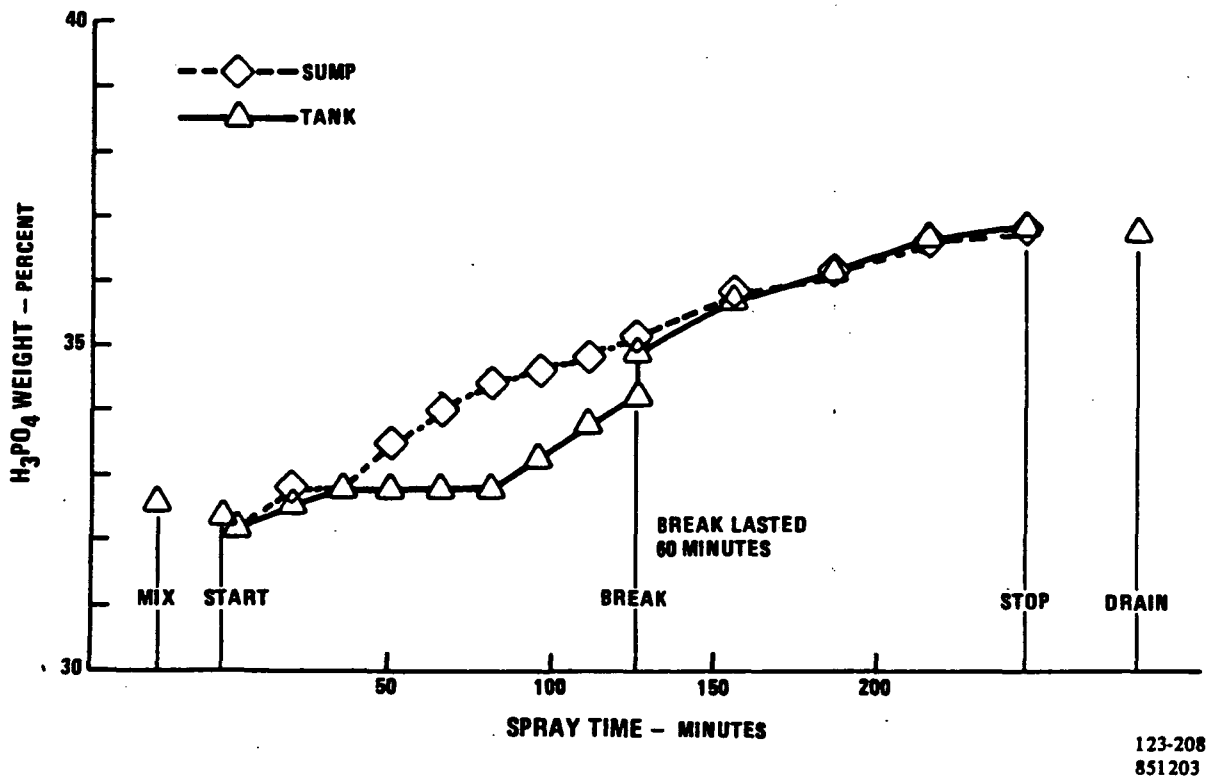

Figure 2-27. Acid Concentration vs. Time

Subtask 2.4 - Cell Stack Testing

Objective

The objective of this task is to evaluate the operational capabilities of stack components developed in other tasks. Included in this are evaluation of new design configurations, compatibility of new materials, and performance and decay characteristics of advanced catalysts.

Summary

The cell stack components that are demonstrated successfully in subscale cells and rig tests are scaled up for test in short stacks of full area cells. The first cell stack tested in this program incorporated a number of improvements developed in this program and the complementary GRI program. The second cell stack was placed on test at the end of the report period. The key feature of this stack is a new cell configuration referred to as Configuration "B". The stack was operating properly at the end of the report period.

Two short stacks were assembled and tested under this subtask in 1984. The first stack was assembled and the test program was completed. The second stack was assembled and the test program was initiated.

The first short stack contains components with advanced features that were developed in this program and in parallel programs. This stack contains 30 cells and was tested for 5228 hours. At this point the test program was voluntarily interrupted and a post-test inspection of all stack components was conducted. The stack was then reassembled and returned to test. After 6100 hours of operation the test program was again interrupted and the stack was refilled with acid using the acid spray approach. The endurance test program was then continued, the test being terminated after a total operating time of 7125 hours was accumulated, including 22 thermal cycles. A final post-test inspection is now being conducted on this stack.

The second short stack also contains components with advanced features that were developed in parallel programs. This stack contains 32 cells and has just started its test program; it has accumulated approximately 100 hours of operation.

Highlights

- Over 5000 hours of short stack operation was demonstrated at a performance level within 10 mV of E-line.
- The short stack was disassembled after 5000 hours of operation, inspected, and reassembled for additional testing.
- An acid spray refill test was conducted on this stack after 6000 hours of operation.
- Post-test inspection of the short stack is being conducted after 7200 hours of operation.
- A second short stack was assembled and testing was initiated.

Discussion

The first short stack contains the following special features:

- Thirty cells with GSB-18 cathode catalyst and HYCAN anode catalyst (both dry mix and wet mix anode and cathode formulations)
- Encapsulated serpentine coolers, ten cells per cooler
- Acid condensation zone
- New end plate and current collector configuration
- Low-cost matrix material

The endurance test program was conducted at 14.7 psia reactant pressures and at 400°F average cell temperature. The cell operating conditions are 200 ASF, 80% fuel utilization, 60% air utilization, and 148°F fuel dew point.

Diagnostic tests were conducted during the life of this stack. Diagnostics were conducted at 5000 hours prior to the teardown inspection. At 5500 hours the diagnostic tests reflect the effects of the post-test inspection and rebuild. At 6100 hours the diagnostics reflect the effects of the acid spray refill. These diagnostic tests included the following:

- Performance calibration
- Individual cell performance at design conditions
- Average cell performance history
- Reactant gas utilization sensitivity
- Anode and cathode performance
- Effective thermal resistance of stack
- Cell package and cooler assembly electrical resistance
- Reactant gas crossover leakage

Cell performance is presented in Figures 2-28 and 2-29, and cell performance history is presented in Figure 2-30. This data shows that the average performance of all cells remained within 10 mV of the E-line goal until the post-test inspection and rebuild. The performance then decreased approximately 20 mV, but improved during the next 200 hours of operation. The average cell performance was not changed by the acid refill. Figure 2-30 indicates that the cells with dry mix anode catalyst formulation were more sensitive to the post-test inspection and the acid refill test. The cells with wet mix anode catalyst formulation improved with test time after the rebuild and were within a few millivolts of the E-line goal at the end of the test.

The fuel and air utilization effect on cell performance is presented in Figure 2-31.

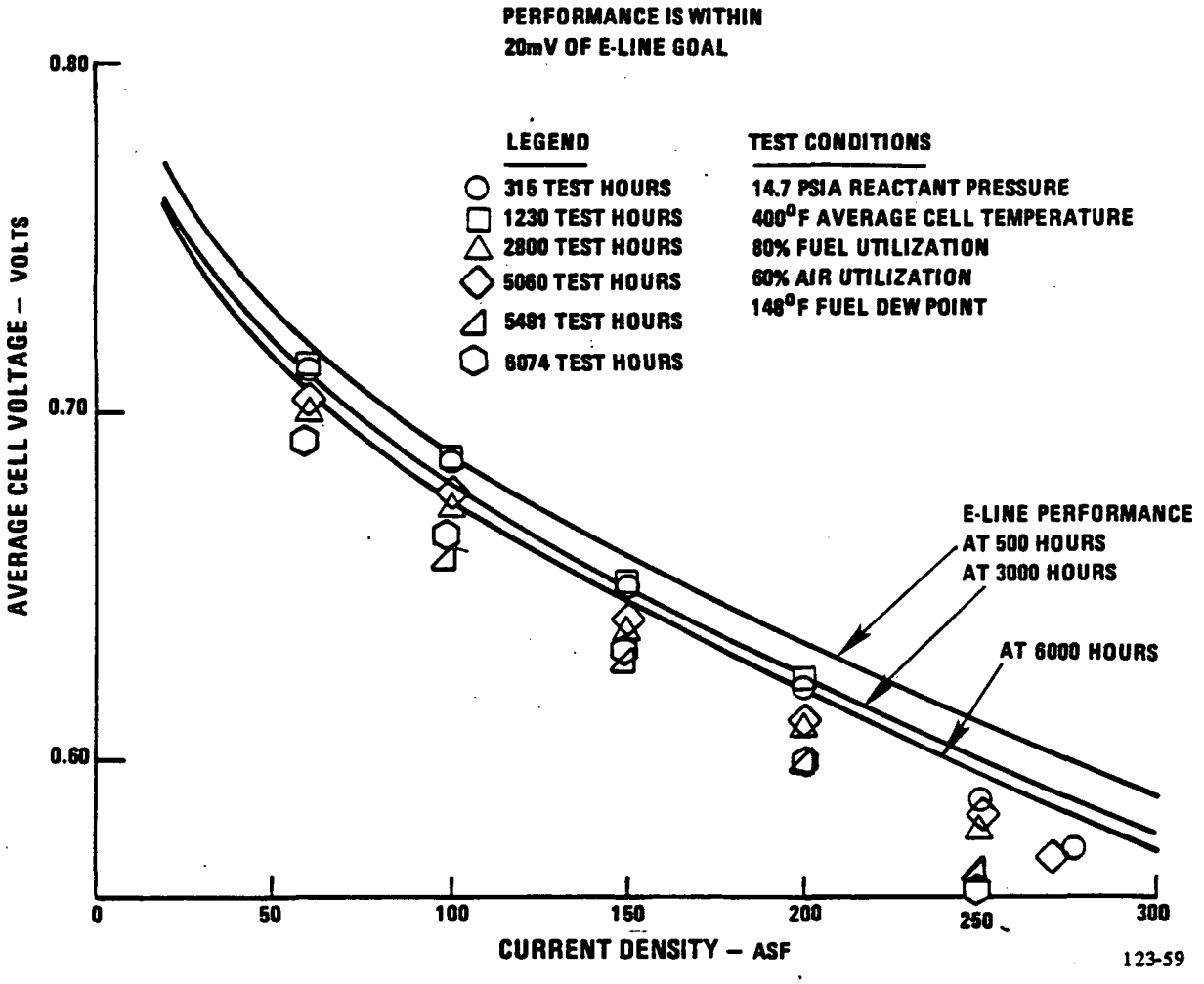

Figure 2-28. Average Cell Voltage vs. Current Density

C-2

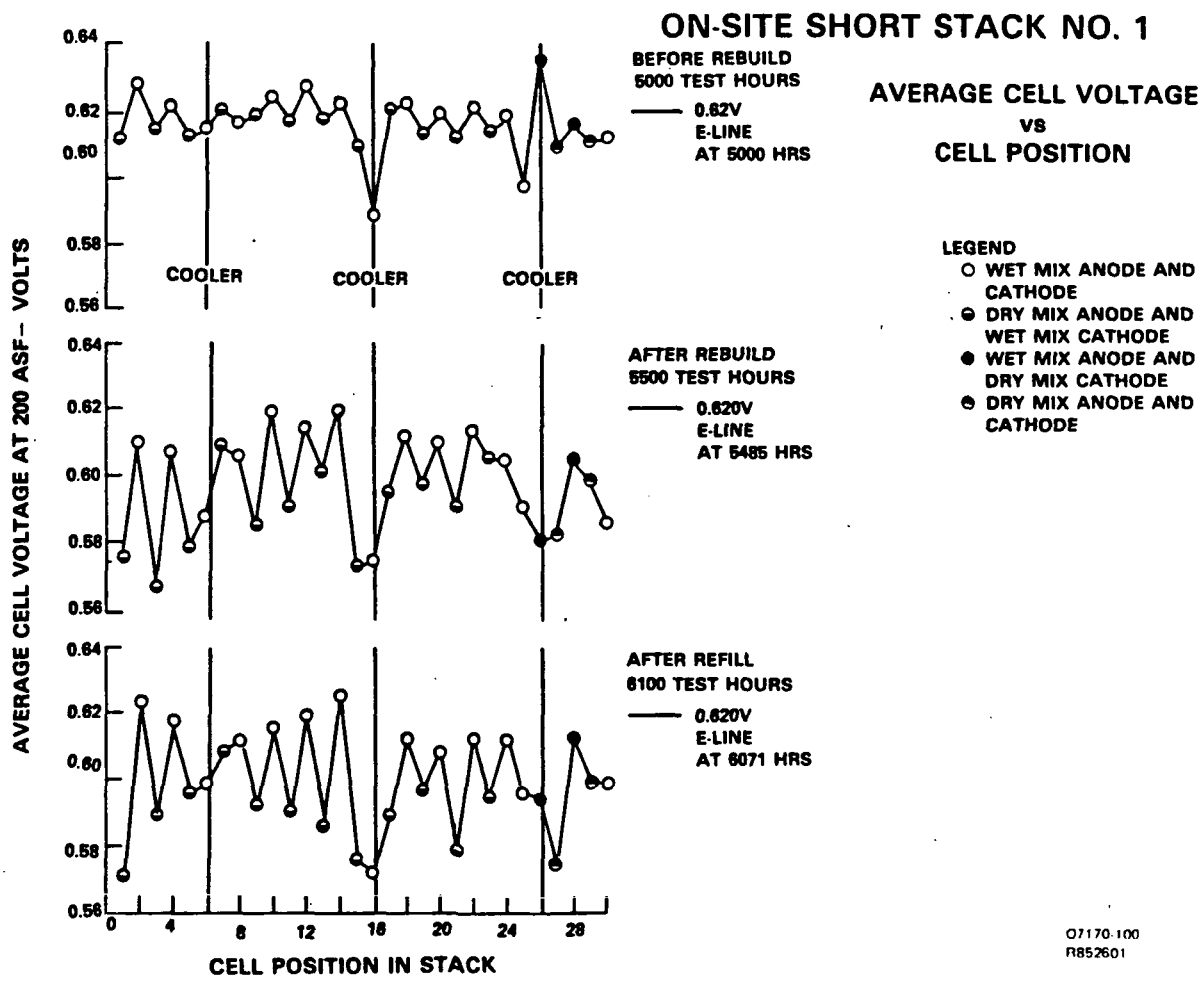

Figure 2-29. Average Cell Voltage vs. Cell Position

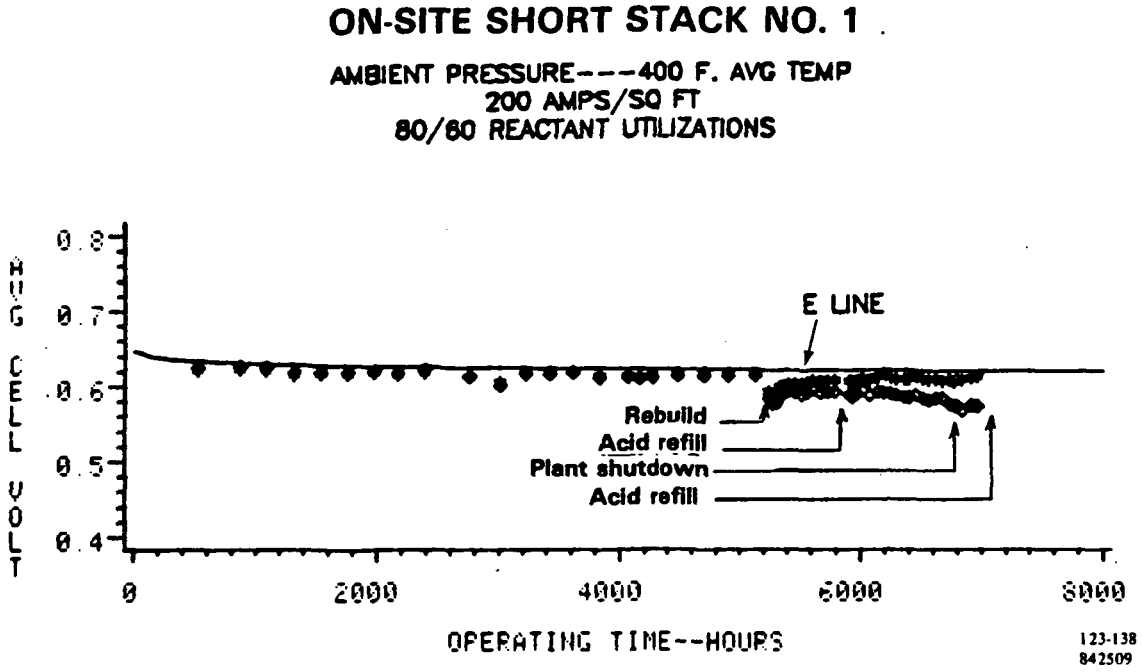

Figure 2-30. Standard Anode Performance vs. Operating Time
Dry Mix Anode Performance vs. Operating Time for Short Stack 1

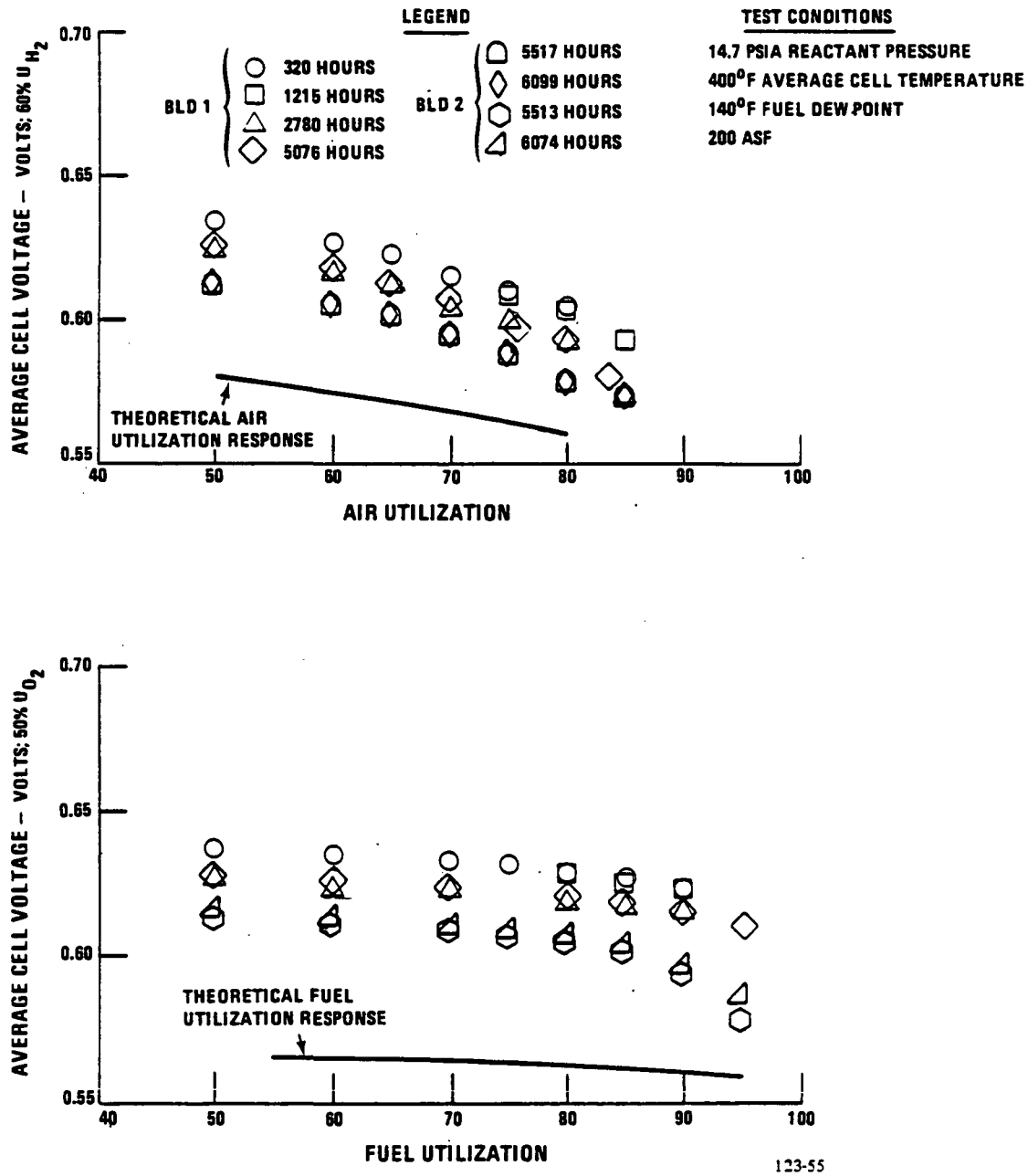

Figure 2-31. Reactant Gas Utilization vs. Average Cell Voltage

The anode and cathode performance gain for operating on pure hydrogen and oxygen is presented in Figure 2-32. The hydrogen gain has increased after the rebuild and after the acid refill.

The stack effective thermal resistance is presented in Figure 2-33. The stack thermal profile data is presented in Figure 2-34.

The cell package electrical resistance is presented in Figure 2-35. The average iR for cell packages with separator plates is 11.9 mV per 100 ASF. The cell packages with cooler assemblies are 13.3 mV per 100 ASF higher resistance.

The reactant gas leakage is presented in Figure 2-36. The data reports the leakage in each cell package measured as a change in open circuit voltage for a change in the reactant gas cross-pressure. The total measured reactant gas leakage after the rebuild was 0.1% of the fuel flow at design power (Figure 2-37).

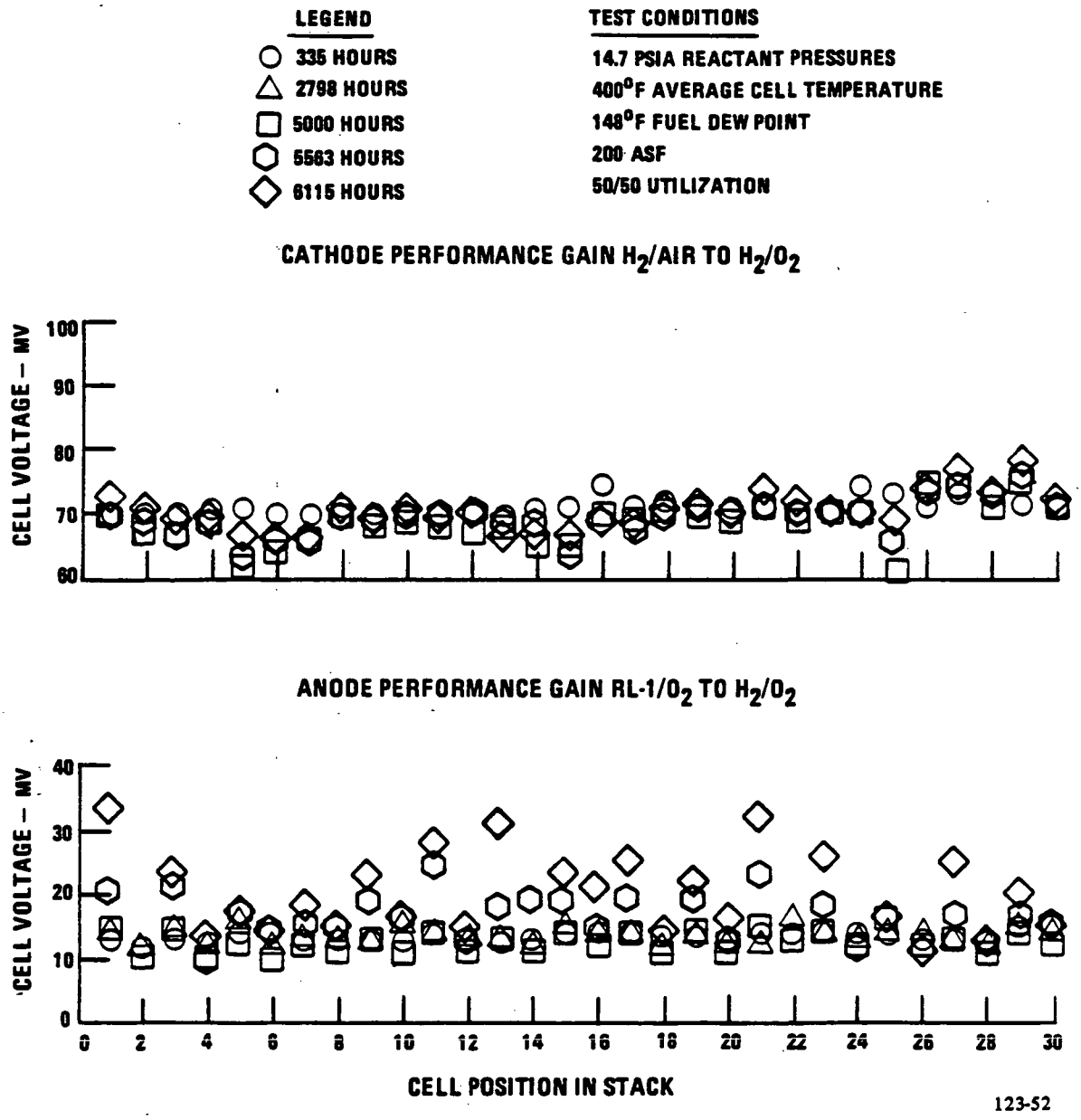

Figure 2-32. Anode and Cathode Performance Gain for Pure Reactant

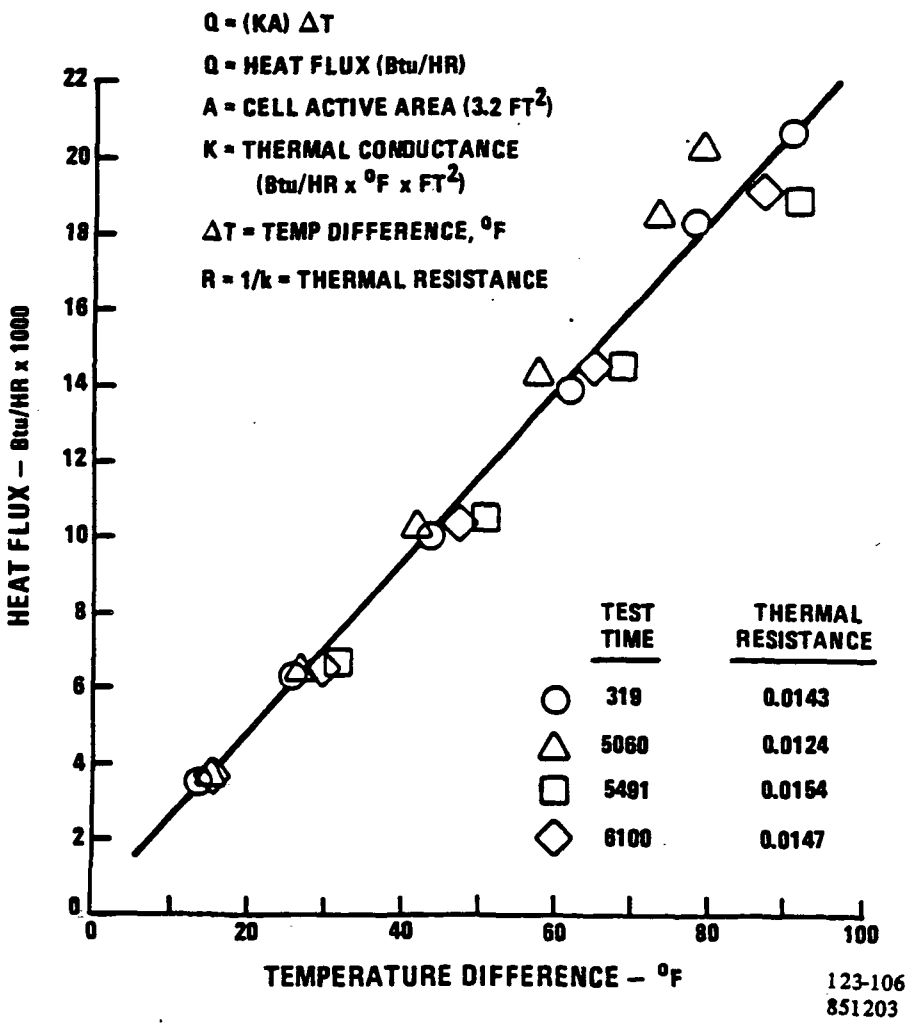

Figure 2-33. Stack Thermal Resistance

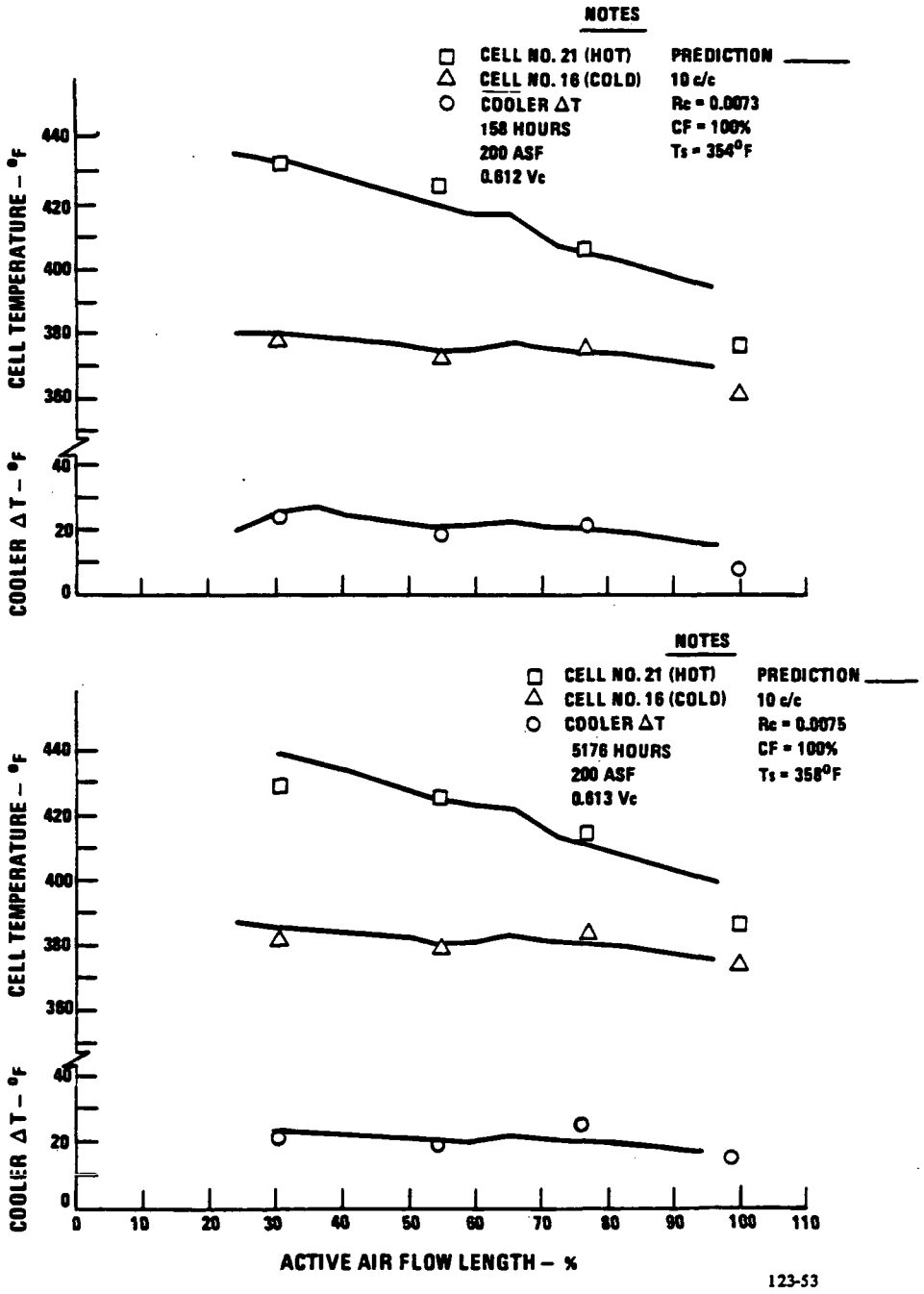

Figure 2-34. Heat Transfer Data

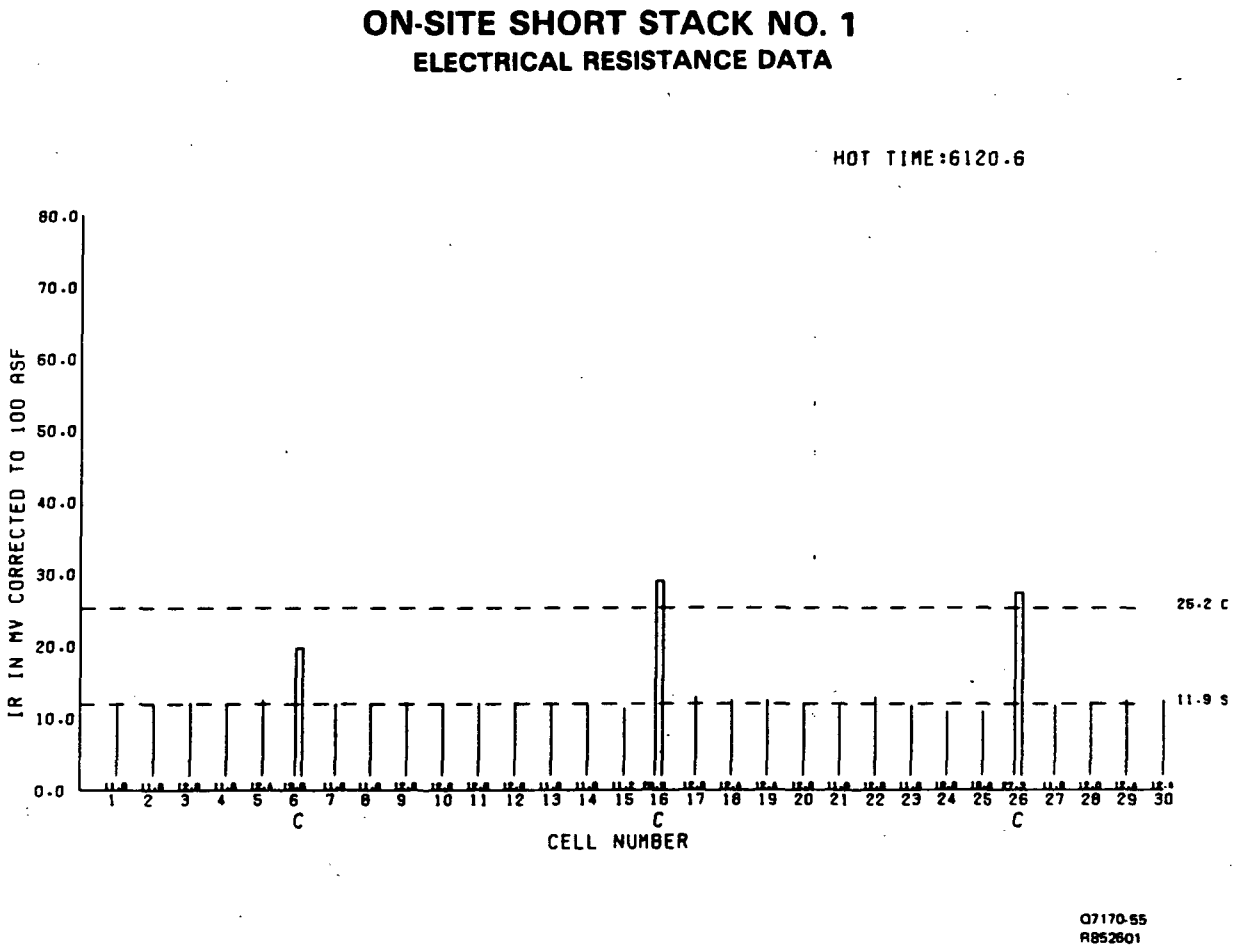

Figure 2-35. Electrical Resistance Data

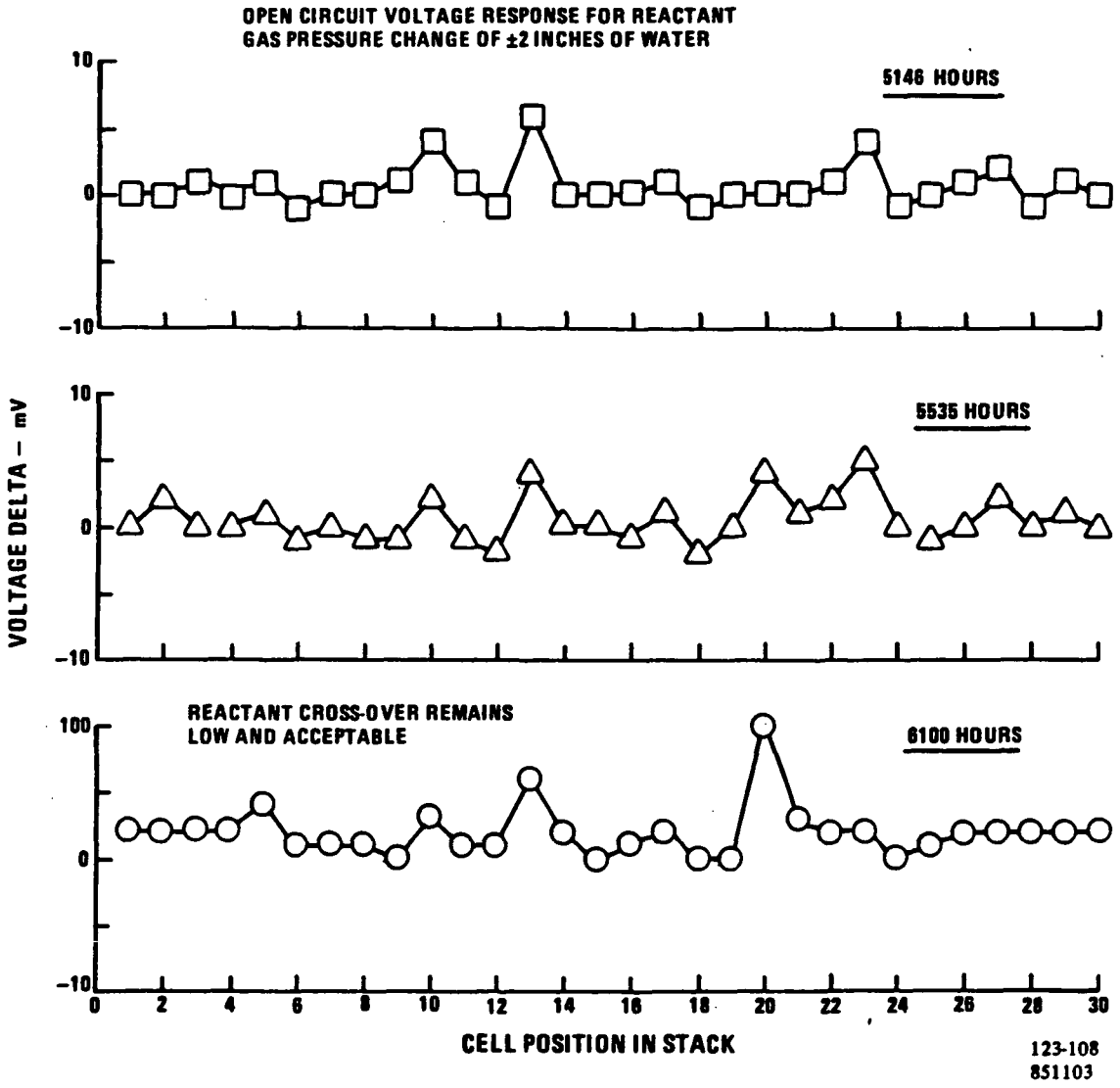

Figure 2-36. Reactant Gas Cross-Leakage Test

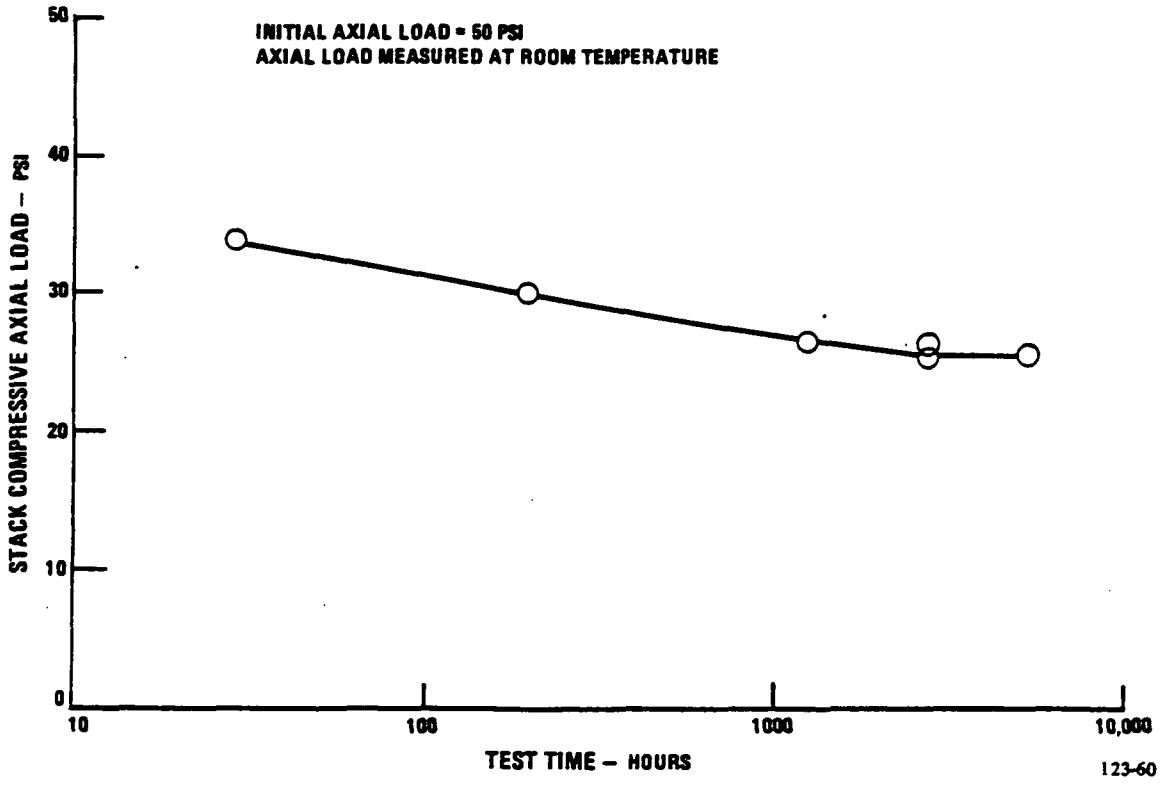

Figure 2-37. Axial Load vs. Test Time

The post-test inspection of all stack components that was conducted after the stack had completed 5228 hours of operation resulted in the following observations:

- The general condition of all stack components was excellent.
- There was no evidence of deterioration in the cell packages.
- Acid inventory data indicated that the cells were uniformly filled.
- The cell package acid loss data is in good agreement with the predicted acid loss.
- The acid condensation zone doubles the time between acid refill intervals.
- The cooler assemblies were in excellent condition, indicating that the acid-proofing concept used in these cooler assemblies was effective.
- There was no restriction of coolant flow, and the only deposits found were small and were located at the water inlet of the top cooler in the stack.
- The protective coatings in the reactant manifolds were defect-free and in excellent condition. The fuel in/out and air exit manifolds were carbon steel with a PPS coating. The fuel turn and air in manifolds were carbon steel with a PFA coating. There was a small area of delamination in one corner of the fuel turn manifold.
- The reactant crossover at one inch of water cross-pressure was low at 0.4 percent of the fuel flow at design power.

The air exit manifold installed on this stack after the rebuild was a reinforced plastic manifold. The other reactant gas manifolds are carbon steel with various plastic protective coatings. The endurance test of this stack will evaluate the acceptability of these materials.

The stack was reassembled with the original 30 cells. The separator plates were changed to plates with a different heat treatment. One cooler was disassembled for inspection and was replaced with a new cooler assembly.

The final post-test inspection of all components in this stack is in progress.

The second short stack contains the following special features:

- o 32 cells with GSB-18 cathode catalyst and HYCAN anode catalyst (both dry and wet mix anode and cathode catalyst formulations)
- o Configuration "B" cell package with 3.7 sq. ft. active area and square planform
- o Impregnated edge seals on cell packages
- o Reduced matrix thickness
- o Totally encapsulated cooler assemblies with eight cells per cooler, five coolers per stack
- o Reactant manifolds with PFS and PPS protective coatings and strap/spring retention system
- o Integrated end plate, pressure plate, and power takeoff

The endurance test is being conducted at 14.7 psia reactant pressures and 400°F average cell temperature. The cell operating conditions are 300 ASF, 80% fuel utilization, 60% air utilization, and 148°F fuel dew point.

The test program has just been initiated and approximately 100 hours of operation has been accumulated. Stack operation is at the expected level for this test time. The endurance test program on this stack is continuing.

TASK 3
POWER PROCESSOR DEVELOPMENT

TASK 3 - POWER PROCESSOR DEVELOPMENT

Subtask 3.1 - Define Inverter Technology

Objective

The objectives of this subtask were to establish the preliminary design of the main power processor control unit, procure a main control for utilization in the 200-kW brassboard inverter test program, and identify and select any advanced semiconductors to be evaluated in the brassboard inverter.

Summary

At the beginning of 1984, a brassboard inverter had been fabricated (Subtask 3.2) and its bridge control logic was under construction (Subtask 3.1). This inverter was a two-bridge design that used asymmetrical silicon controlled rectifiers (ASCR's) as its switching elements. To verify the brassboard inverter technology, final assembly of the bridges and their control units had to be completed and a main control unit had to be designed, built, tested, and installed in the two-bridge inverter system. The main control unit was required to run the inverters in parallel with the utility line.

The logic selected for the On-Site brassboard inverter is based on the multimegawatt inverter design, developed in another UTC program sponsored by DOE. This logic is more sophisticated than required for on-site application and has a mechanical arrangement well-suited to this development stage of the On-Site inverter.

At the beginning of this period, the controls being built for the two bridges in the brassboard inverter were sufficient to operate the inverter power poles, but did not contain the logic necessary to operate the inverters connected to the utility grid. A main logic was required to provide real and reactive power control, utility line related protection, and synchronization with the utility line.

The inverters built at the beginning of this period utilized ASCR power semiconductors as their power switching elements; these devices were the presently available near-term technology. Future versions of these inverters may use more advanced power semiconductors for greater efficiency. Part of the effort under Subtask 3.1 was to identify and select any advanced semiconductors to be evaluated in the brassboard inverter.

A two-bridge ASCR brassboard inverter was obtained with a separate control for each bridge to enhance checkout and technology verification while a separate main control was being built. The main control would provide sequencing, power regulation, and utility line related protection for subsequent on-line testing. The physical separation of bridge controls and main controls was not an optimum approach, so an additional conceptual design study was done to show how the hardware for the bridges and main controls could be combined into one package.

The brassboard main control unit selection was narrowed to two choices: (1) use of a laboratory constructed breadboard version, or (2) procurement of a second set of the hardware designed for multi-megawatt converters under DOE contract DE-AC01-79ET29079. The second choice (DOE hardware) was selected because the design was already available and had more sophisticated control, protection, and diagnostic functions, which enhanced the brassboard inverter test capability.

The advanced semiconductor evaluation task effort determined that the ASCR was the best choice for the near term baseline system and that verifying the ASCR in the brassboard inverter test program would also verify that design technology if either silicon controlled rectifiers (SCR's) or reverse conducting thyristors (RCT's) were used in the final system.

Another type of advanced semiconductor, the gate turnoff thyristor (GTO), was established as a candidate for future systems. This device is capable of being turned off with a signal to its gate input rather than requiring the separate communication circuit used by other thyristors. Further studies of GTO's, however, indicated that specific designs for low voltage systems such as the on-site fuel cell

were not receiving market impetus; therefore, optimization could not be anticipated. It was decided not to incorporate advanced device testing in the brassboard inverter. Further study of advanced inverter systems was carried out in the companion GRI On-Site Program.

Highlights

- Preliminary definition of main control unit was completed.
- Brassboard inverter main control unit for brassboard test was identified.
- Conceptual approach to simplified combination of main and bridge controls was established.
- Advanced semiconductor selection was narrowed to include only gate controlled devices -- ASCR brassboard design inclusive of SCR's and RCT's for technology considerations.
- A consultant study confirmed the use of the brassboard ASCR to be well within device capability.

Discussion

The version of the main inverter control unit that was selected for brassboard testing is shown in block diagram form in Figure 3-1. This selection was made earlier than originally planned to insure that hardware would be available as required, and to use this activity to identify a low-cost advanced design for the main control. Two approaches for obtaining a main control unit brassboard testing were evaluated:

1) A laboratory constructed breadboard version with the basic control functions but limited protection and no diagnostic features.

2) Procurement of a second set of the hardware designed for multimegawatt converters (under DOE Contract DE-AC01-79ET29079) that provide more sophisticated control and protection functions than required and also contain a sophisticated level of diagnostics.

The evaluation showed that the actual costs were not significantly different, but that two significant advantages were offered in the multimegawatt design: it provided excellent hardware and software flexibility (necessary to evaluate the control concepts required for the on-site power processor), and its diagnostics would greatly simplify the checkout and evaluation process.

The simplified (baseline) inverter control unit consists of a cabinet that contains both a circuit board chassis with all of the circuit boards installed and a local panel. Table 3-1 shows a comparison of brassboard components and simplified baseline components, Table 3-2 is a list of the simplified baseline components and Figure 3-2 is a block diagram of the simplified baseline control unit configuration.

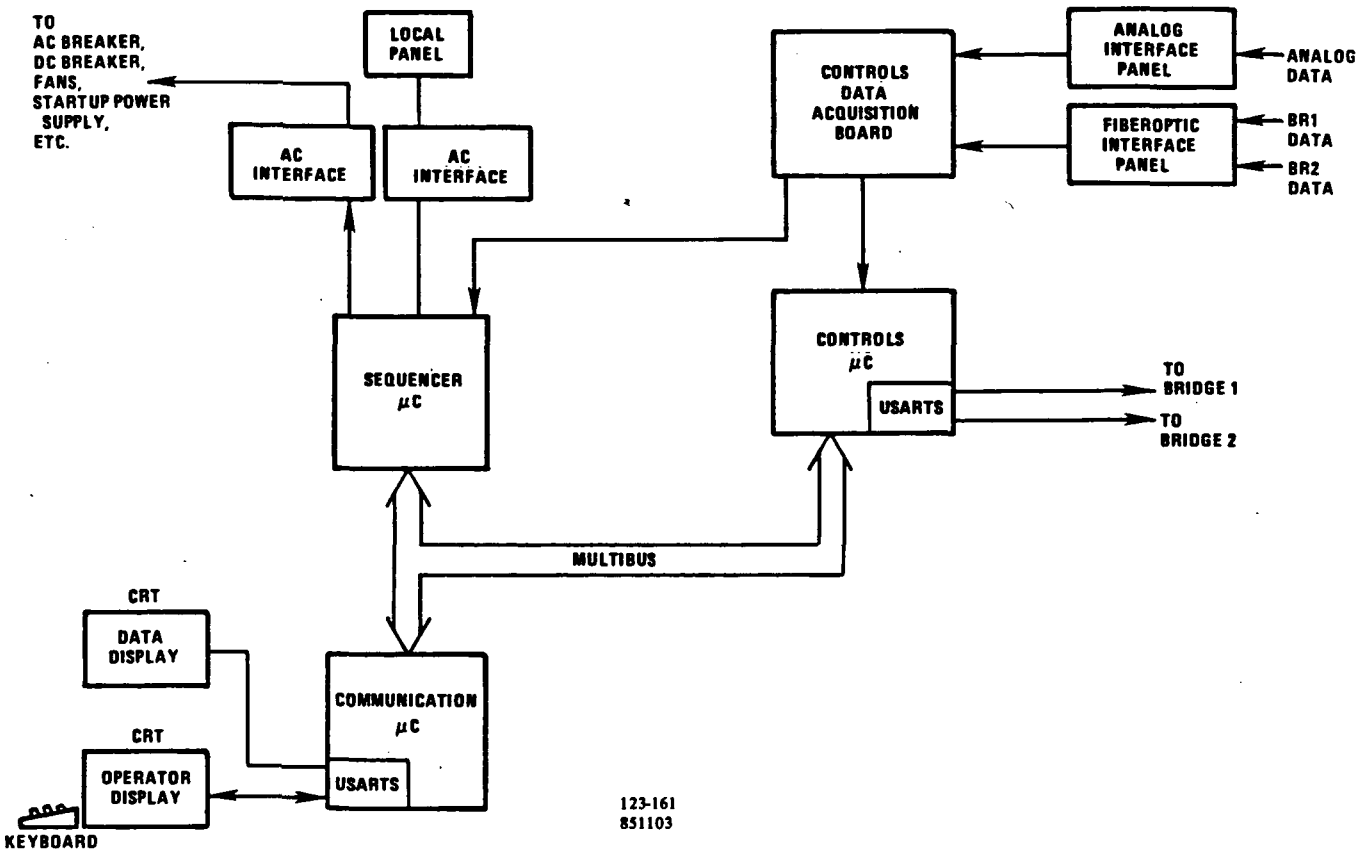

Figure 3-1. Brassboard Main Control Unit Block Diagram

Table 3-1. Simplified Baseline Inverter Control Unit Comparison to Brassboard

	Brassboard	Baseline
Circuit Boards		
Total	10	8
Custom	5	5
Off-the-Shelf	5	3
Interface Panels	11	5
Chassis	3	1
Power Supply Assembly	3	1
Cabinet	3	1

Table 3-2. Hardware for Simplified Baseline Inverter Control Unit

1	Controls Microprocessor Board
1	Main Interface Panel
1	Controls Data Acquisition Board
1	Local Control Panel
1	AC Interface Panel
1	Bridge Hardware Interface
1	Bridge Optocoupled Interface
2	Bridge Singal Conditioner Board
2	Bridge Interface Board
2	Bridge Waveform Generator Board
2	Gate Interface Panel
1	Logic Card Cage
1	Power Supply Assembly
1	Cabinet

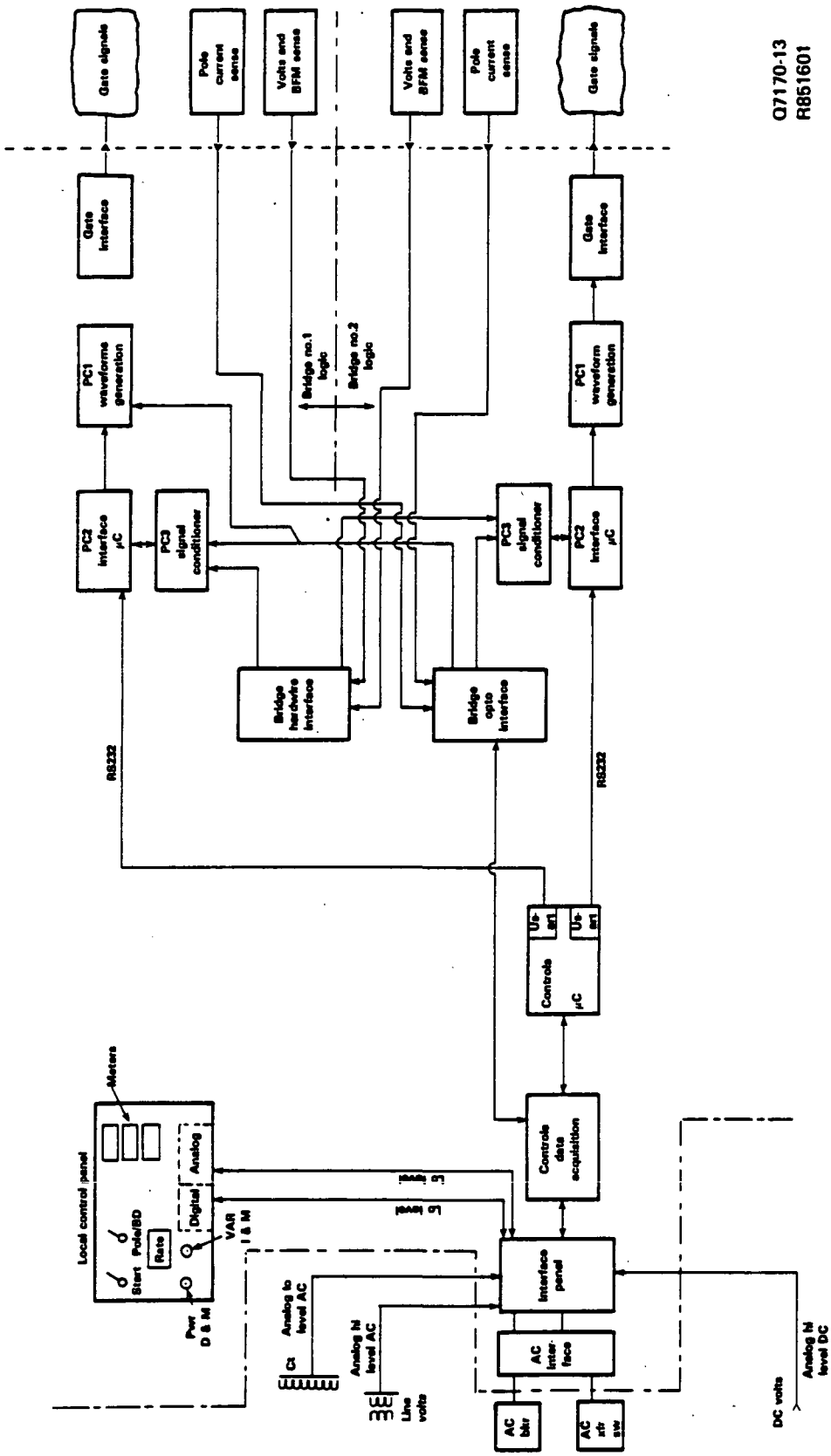

Figure 3-2. Block Diagram - Simplified Baseline Logic

The effort to select advanced semiconductors for evaluation in the brassboard inverter resulted in the following conclusions:

- For the near term baseline system, ASCR's are the best selection in terms of cost and performance.

- Evaluation of the brassboard inverter with its present ASCR's will verify the design technology applicable to SCR's, RCT's, or any generic device that requires a commutation circuit; that technology being an inverter bridge with individual commutation operating at low voltage, high current, and high switching frequencies.

- For future systems, gate controlled devices offer the greatest potential benefits for evolving a single-bridge, high frequency design with commutation circuits either eliminated or significantly reduced in size.

Advanced semiconductor evaluations were also conducted, including a small consultant study that evaluated the ASCR's used in the 200-kW brassboard inverter in both the main switch and commutation switch positions. Table 3-3 summarizes the study results.

Table 3-3. Summary of Semiconductor Evaluation

Parameter		Main ASCR	Comm. ASCR
Peak Current -	Normal Operation	710 A (8.33 ms P.W.)	1800 A (40μs.)
	Overload (5-Sec.)	1500 A (8.33 ms P.W.)	2250 A (40μs.)
	Short-Circuit (5-Sec.)	2250 A (8.33 ms P.W.)	3375 A (40μs.)
Power Loss -	Normal Operation	336 W	211 W
	Overload	930 W	273 W
	Short-Circuit	1500 W	663 W
Junction Temp-	Normal Operation	105°C	94°C
	Overload	155°C	101°C
	Short-Circuit	185°C	145°C
Life Expectancy - Normal Operation		800 years	310 years
Life Reduction - Overload		Negligible	< 42 hours
(for each 5-sec. short-circuit occurrence)		Negligible	42 hours
Heatsinking			
Max. Allowable RO Case → Air		0.11° C/W	0.10° C/W
Actual (per NWL meas.)		0.05° C/W	0.07° C/W

The brassboard main control unit delivered to the inverter for test is a fully featured unit that has demonstrated its capability in inverter operation under Subtask 3.2. This design is excellent for brassboard test because of its capabilities, but is overqualified for an optimized commercial inverter. Follow-up work will include simplification of this brassboard control design.

The simplified baseline control concept is a "near term" approach, intended as a modification of the existing brassboard control. Further simplifications can be made if the near term constraint is eliminated. Follow-up studies should evaluate simplification or elimination of functions, advanced logic technologies, combination of control functions, and design optimization where practical. The brassboard controls should be modified to test these new approaches where possible. Activity for the remainder of this program phase will concentrate on defining a low-cost advanced design tailored to on-site requirements.

Additional control studies should evaluate approaches to improve control reliability, including evaluation of the design in terms of component stress and component tolerance.

Subtask 3.2 - Verify Inverter Technology

Objective

The objective of this subtask is to test the brassboard power processor from the initial subsystem/component level through on-line system operation, including evaluation of inverter control logic and alternative semiconductors.

Summary

The brassboard inverter being developed and tested in this program is a two bridge design. At the beginning of this report period, fabrication of the inverter bridges was completed.

Initial evaluation of the inverter included hybrid (digital-analog) simulation of the bridge operation followed by testing of the actual bridge hardware.

This subtask established a test program that fully evaluated the inverter technology. Existing UTC computer programs were utilized to predict performance results and compare them with actual performance. Initial testing was at the component/powerpole level with a separate bench evaluation of the control logic. The control logic and bridges were then integrated and the system tested in an on-line configuration. Alternative advanced semiconductor testing was not incorporated as a result of the Subtask 3.1 studies.

This subtask produced the test plan, a summary of test results, a comparison of the test results to the analysis results, and an overall summary of the ability of the inverter technology to perform as required. Further definition of the activities in this subtask were:

- The test plan for the brassboard technology verification activity took the brassboard hardware through the entire checkout process including a static evaluation of the mechanical and electrical design, individual pole and bridge dynamic testing, and on-line system testing.

- Computer analysis provided analytical predictions of pole and bridge dynamics, system control response, and generated harmonics.

- Bridge testing began with a static evaluation that measured critical inductive, capacitive, and resistive circuit elements. In addition, bridges were inspected for any construction flaws. Finally, a dc voltage was applied to the input to measure voltage withstand and static leakage.

- After static evaluation, dynamic tests were conducted on individual powerpoles to measure critical parameters such as main and auxiliary commutation circuit operation.

- The bridge control logic was then integrated with the bridges such that evaluation of bridge dynamics, overall bridge protection schemes, and switching patterns could be performed.

- In addition to system on-line operation, some testing was performed under abnormal conditions to verify protection functions.

Highlights

- Brassboard bridges static checks confirm that hardware was built to design.
- Dynamic pole and bridge test results agree with analytical predictions.
- Bridge and main logic bench testing was completed.
- Brassboard system line is paralleled in automatic mode.
- Line parallel operation characterization generally meets design requirements for stability, efficiency, power quality, and protection.
- Previously identified deficiencies (efficiency, waveform pattern transition, harmonics) being evaluated.

Discussion

The Brassboard Inverter Test Plan sequence of events are discussed below.

Brassboard Bridge Static Checks

The brassboard inverter bridges and controls underwent the static evaluation portion of the test plan. The wiring and circuitry verifications and circuit element measurements resulted in minor corrections:

- The connection between the main ASCR's and antiparallel diodes was corrected.

- The connection between the auxiliary commutation capacitor and auxiliary commutation diode/ASCR was revised.

- The connection between the auxiliary commutation diode and auxiliary commutation SCR was corrected.

- Bridge 2, Pole B commutation diode had a low static resistance reading.

- Bridge 2, Pole B had a connection in the loss of fan protection circuit missing.

- All six poles in both bridges had two 5 ohm resistors in parallel instead of two 10 ohm resistors in parallel for the semiconductor snubber circuits.

- The UTC hybrid analog/digital simulator was programmed for analyzing the dynamic operation of a powerpole.

- The bridge control units for the 200-kW brassboard inverter were checked out for conformance to print and operation of subassemblies.

Bridge Static Voltage Testing

Static voltage tests to 350 volts dc resulted in a per bridge total of 470 milliamps static current drain, as compared to a calculated value of 475 milliamps and a measurement by the manufacturer of 440 milliamps.

Bridge Dynamic Pole Testing and Analytic Comparison

The individual 200-kW brassboard powerpole tests were completed. Figures 3-3 through 3-10 provide a summary comparison of the test data versus the results of powerpole modeling on UTC's hybrid digital/analog simulator.

The results are in close agreement. Close agreement has also been found between the test results and design calculations. Discussion of Figures 3-3 through 3-10 follows:

Figures 3-3 and 3-4 - Commutation Circuit Current

A model of the inverter powerpole commutation circuit was tested in the hybrid computer simulator and its current was compared to actual circuit current during a commutation interval. Both the amplitude and pulse duration of the actual commutation current agreed with the predictions of the model. This result confirmed the circuit design. Figures 3-3 and 3-4 show the circuit's performance at two different dc input voltage levels.

Figures 3-5 and 3-6 - Commutation Capacitor Voltage

The model of the inverter powerpole commutation circuit described above was tested as before, but this time the simulated commutation capacitor voltage during a commutation interval was compared to an actual commutation. Both Figures 3-5 and 3-6 showed close agreement between predicted commutation capacitor voltage and actual voltage.

Figures 3-7 through 3-10 - Main Switch ASCR Voltage

A model of the inverter powerpole circuit was tested in the hybrid simulator and voltages of the two powerpole main thyristors (upper (+) and lower (-) devices) were observed during thyristor turn-on and turn-off at several dc input voltage levels. These simulations of thyristor voltage were compared to actual thyristor voltages during a switching interval. There was close agreement between predicted and actual switching voltages, which confirmed the main powerpole design.

Hybrid Computer Simulation

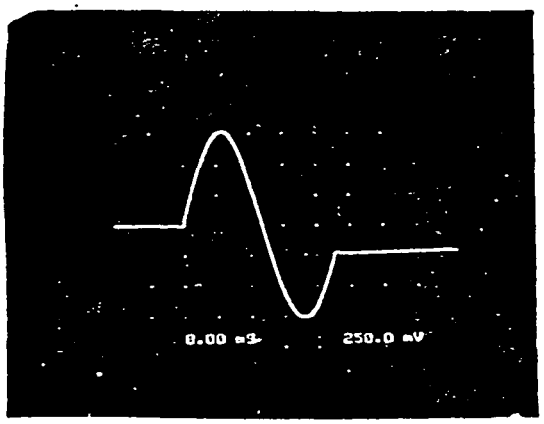

I=500 A/Div, T=16 μs/Div

$I_{P(1st\ pulse)}$=1550A
$T_{P(1st\ pulse)}$38.5 μs
$I_{P(2nd\ pulse)}$=1500A
$T_{P(1st\ pulse)}$=38.5 μs

Range for
12 Switch
Assemblies

$I_{P(1st)}$=1460-1520A
$T_{P(1st)}$=39.0=40.5 μs
$I_{P(2nd)}$=1260-1375A
$T_{P(2nd)}$=38.0-40.0 μs

Mean

$I_{P(2nd)}$=1347A
$T_{P(2nd)}$=39.9μs

Pole 1A Comm Current and Voltage

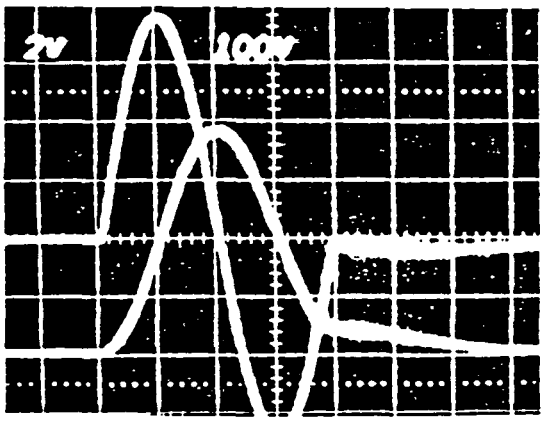

123-163
850528

I=400 A/Div, T=20 μs/Div

$I_{P(1st)}$=1520A
$T_{P(1st)}$=40.0μs
$I_{P(2nd)}$=1360A
$T_{P(2nd)}$=39.5 μs

Figure 3-3. On-Site Brassboard Inverter Pole Data - Commutation Circuit Current at 190 Vdc

Hybrid Computer Simulation

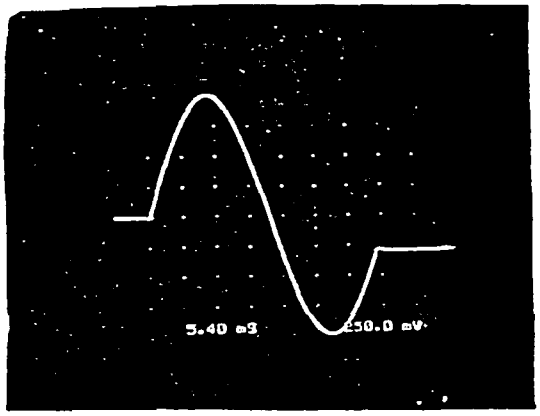

I=500 A/Div, T=10.8 μs/Div

$I_{P(1st\ pulse)}$=2000A

$T_{P(1st\ pulse)}$38.6 μs

$I_{P(2nd\ pulse)}$=1948A

$T_{P(1st\ pulse)}$=38.6 μs

Range for
12 Switch
Assemblies

$I_{P(1st)}$=1960-2100A

$T_{P(1st)}$=39.0=40.5 μs

$I_{P(2nd)}$=1800-1900A

$T_{P(2nd)}$=38.0-40.0 μs

Mean

$I_{P(2nd)}$=1825A

$T_{P(2nd)}$=39.25μs

Pole 1A Comm Current and Voltage

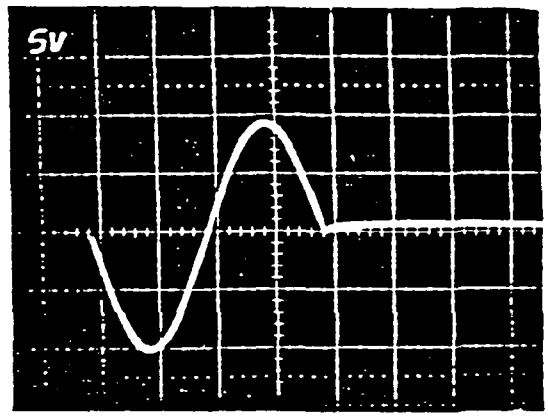

I=1000 A/Div, T=40 μs/Div

$I_{P(1st)}$=2000A

$T_{P(1st)}$=40.0μs

$I_{P(2nd)}$=1900A

$T_{P(2nd)}$=40.0 μs

123-164
850528

Figure 3-4. Commutation Circuit Current at 250 Vdc

Hybrid Computer Simulation

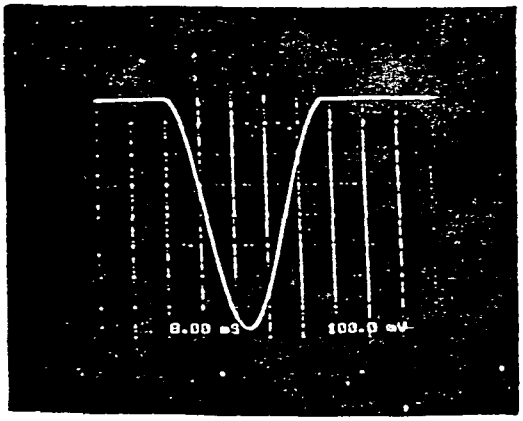

V=50 V/Div, T=16 μs/Div

$V_{peak\text{-}to\text{-}peak}$=380 volts

Pole 1A Comm Cap Voltage

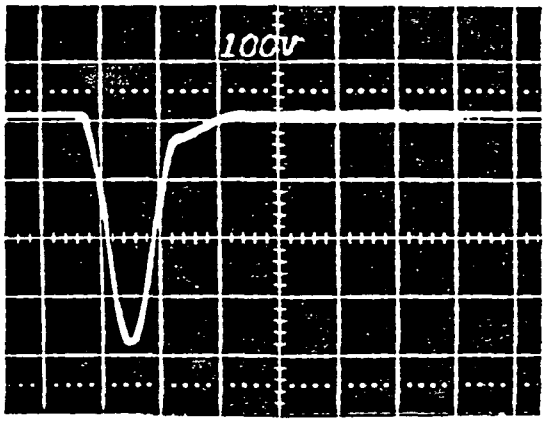

123-165
850528

V=100 V/Div, T=50 μs/Div

$V_{peak\text{-}to\text{-}peak}$=380 volts

Range for
12 Switch
Assemblies

$V_{p\text{-}p}$=370-390 volts

Mean

$V_{p\text{-}p}$=380 volts

Figure 3-5. Commutation Capacitor Voltage at 190 Vdc

Hybrid Computer Simulation

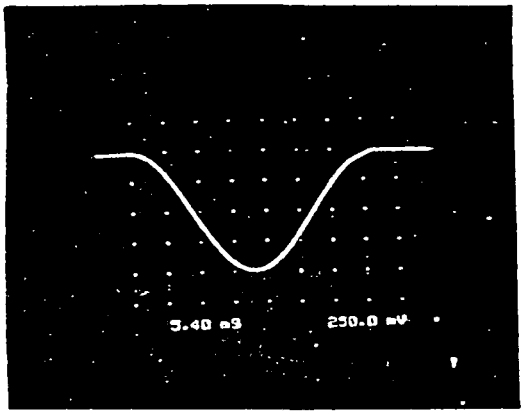

V=125 V/Div, T=10.8 μs/Div

$V_{peak\text{-}to\text{-}peak}$=500 volts

Pole 1A Comm Cap Voltage

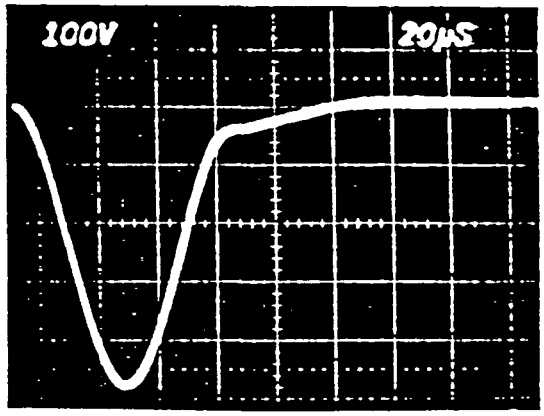

123-166
850528

V=100 V/Div, T=20 μs/Div

$V_{peak\text{-}to\text{-}peak}$=485 volts

Range for
12 Switch
Assemblies

$V_{p\text{-}p}$=485-510 volts

Mean

$V_{p\text{-}p}$=497 volts

Figure 3-6. Commutation Capacitor Voltage at 250 Vdc

Hybrid Computer Simulation

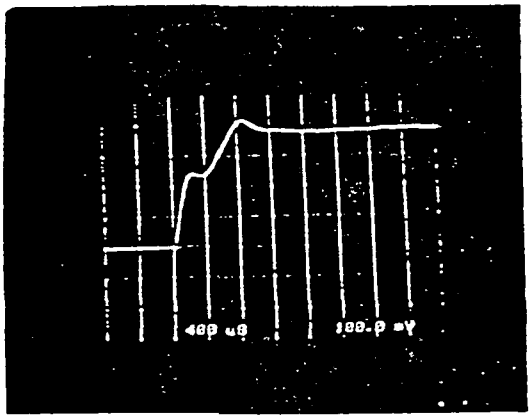

V=50 V/Div, T=800 ns/Div
10-90% dv/dt=130V/μs

Pole 1A Upper Main ASCR

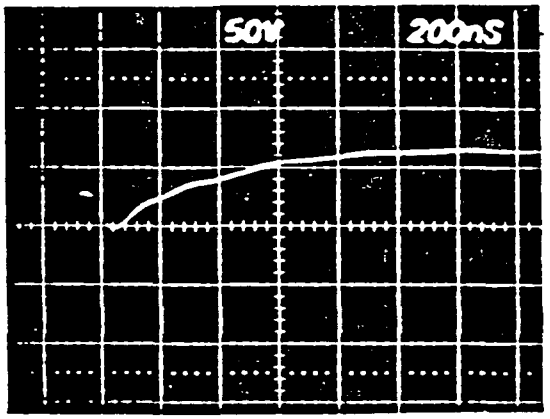

123-167
850528

V=50 V/Div, T=200 ns/Div
10-90% dv/dt=250 V/μs

Range for
12 Switch
Assemblies

10-90% dv/dt=95-250v/μ

Mean

10-90% dv/dt=155v/μs

Figure 3-7. Main Switch ASCR Turn-Off Voltage at 190 Vdc

Hybrid Computer Simulation

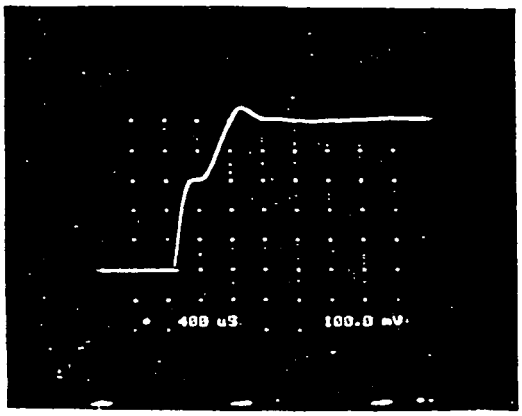

V=50 V/Div, .T=800 ns/Div
10-90% dv/dt=180V/μs

Pole 1A Lower Main ASCR

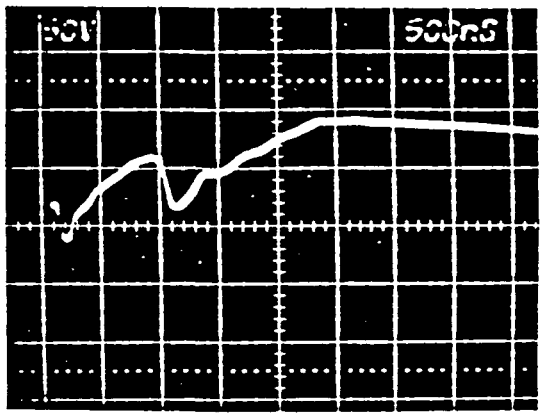

V=50 V/Div, T=500 ns/Div
10-90% dv/dt=210 V/μs

123-168
850528

Range for
12 Switch
Assemblies

10-90% dv/dt=70-315v/μ

Mean

10-90% dv/dt=199v/μs

Figure 3-8. Main Switch ASCR Turn-Off Voltage at 250 Vdc

Hybrid Computer Simulation

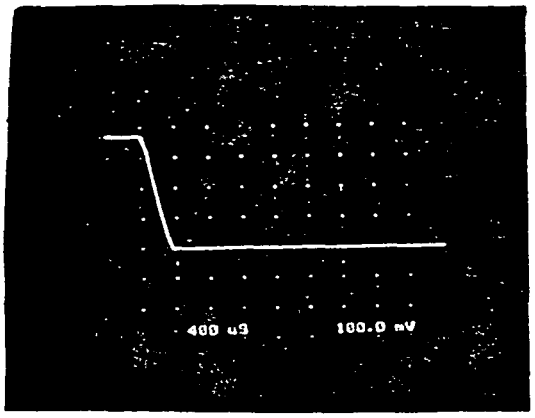

V=50 V/Div, T=800 ns/Div
10-90% dv/dt=700ns

Pole 1A Upper Main ASCR

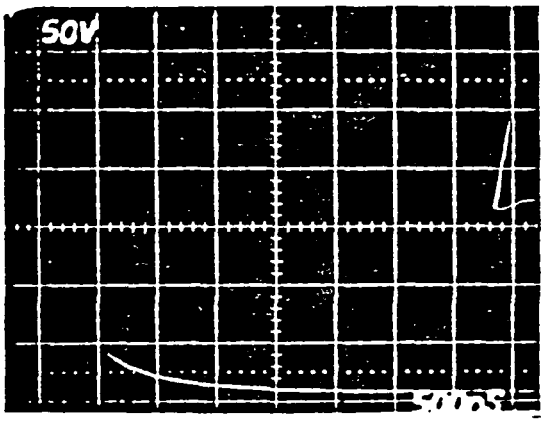

123-169
850528

V=50 V/Div, T=500 ns/Div
10-90% dv/dt=900ns

Range for
12 Switch
Assemblies

10-90% dv/dt=700-1500ns

Mean

T= 1.0µs

Figure 3-9. Main Switch ASCR Turn-Off Voltage at 190 Vdc

Hybrid Computer Simulation

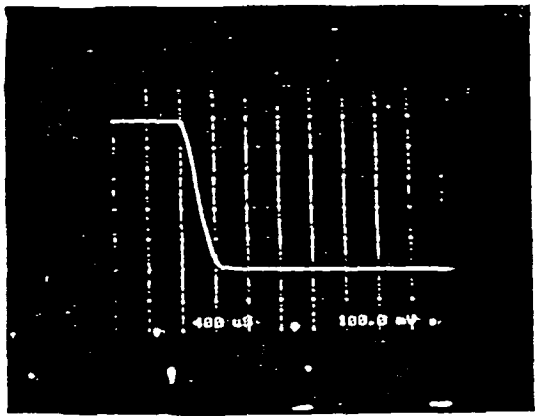

123-170
850528

V=50 V/Div, T=800 ns/Div
10-90% dv/dt=800ns

Pole 1A Upper Main ASCR

(No Photo Available)

10-90% T=1.0 µs

Range for
12 Switch
Assemblies

10-90% dv/dt=900-1500ns

Mean

T= 1.0µs

Figure 3-10. Main Switch Turn-Off Voltage at 250 Vdc

In addition, the dynamic characteristics of the auxiliary commutation circuitry were determined, with operation within 10% of predicted. Figure 3-11 depicts typical dynamic data taken with a digital storage scope. The auxiliary commutation circuitry is designed for limited duty cycle operation, which requires use of storage instruments.

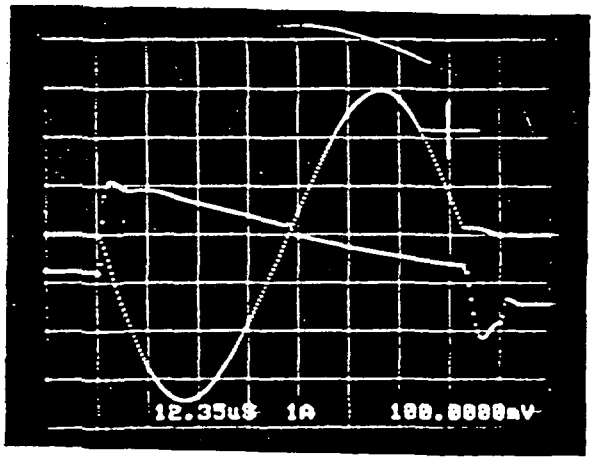

Aux. Comm. Current (Lower) 100 A/Div.

IP_1 = 340A TP_1 = 12,35 x 3.8 = 47.7 µs

IP_2 = 300A TP_2 = 12.35 x 3.6 = 45 µs

Voltage Across Q6 10 V/Div

Vdc = 190 Volts Vc5 = 225 Volts

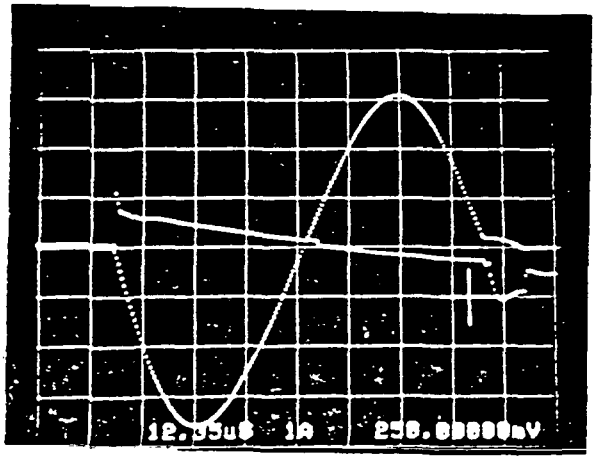

Aux. Comm. Current (Lower) 200 A/Div.

IP_1 = 800A TP_1 = 12.35 x 3.75 = 47 µs

IP_2 = 610A TP_2 = 12.35 x 3.6 = 45 µs

Aux. Comm. Voltage Q6 25 V/Div.

123-173
850528

Figure 3-11. Typical Auxiliary Commutation Circuit Data

Control Unit Bench Tests

The bridge control unit was procured from vendors, bench tested, delivered to the bridges, and installed.

System Integration

The 200-kW inverter bridge and main control units were integrated with the brass-board bridges and isolated operation was verified. In addition, power wiring was installed from the 200-kW test dc power supply to the bridge inputs and from the bridge outputs to the system output transformers. Current transformers, switchgear, and the ac utility line tees were completed and pre-line-parallel checkout was completed.

Control Logic Integration Tests

The bridge and main control units were verified as being correctly wired, then the thyristor gate signal circuitry design was verified by operating the control and observing the gate signals. Tables 3-4 through 3-7 show gate drive circuit data. The critical parameters for the gating signal to a thyristor are shown. They are peak gate current (I peak), rate of change of current (di/dt), reverse current, and pulse width. All of the data on Tables 3-4 through 3-7 are in agreement with calculated design values and will correctly operate the thyristors. Figure 3-12 shows typical oscilloscope pictures of the thyristor gate signals from which the data in Tables 3-4 through 3-7 was derived.

Table 3-4. Bridge 1 Gate Drive Data (Short Circuit Test)

Bridge	Pole	Device	Ipeak	di/dt	Reverse Current	Pulse Width On/Off	Comments
#1	A Upper	Main	1.8A	1.6A/µs	0.45A	12.7µs/3.35µs	Short
	A Lower	Main	1.9A	1.7A/µs	0.75A	12.2µs/3.8µs	Circuit
	A Upper	Comm	2.0A	1.52A/µs	0.5A	40µs	Test
	A Lower	Comm	1.9A	1.7A/µs	20 mA	40µs	
	Aux Upper		1.96A	1.47A/µs		36.8µs	
	Aux Lower		1.98A	1.47A/µs		39.6µs	
	B Lower	Main	1.8A	1.46A/µs	0.3A	12.75µs/3.25µs	
	B Upper	Main	1.9A	1.47A/µs	0.55A	12.7µs/3.35µs	
	B Upper	Comm	1.95A	1.48A/µs	0.5A	39.55µs	
	B Lower	Comm	1.95A	1.55A/µs	0.65A	39.4µs	
	Aux Upper		1.94A	1.49A/µs		36.6µs	
	Aux Lower		1.92A	1.47A/µs	0.13A	39.4µs	
	C Upper	Main	1.9A	1.55A/µs	0.45A	12.7µs/3.3µs	
	C Lower	Main	1.8A	1.49A/µs	0.35A	12.75µs/3.3µs	
	C Upper	Comm	2.0A	1.58A/µs	0.5A	39.5µs	
	C Lower	Comm	1.95A	1.55A/µs	0.7A	39.5µs	
	Aux Upper		1.97A	1.51A/µs		36.7µs	
	Aux Lower		1.94A	1.52A/µs		39.45µs	

Table 3-5. Bridge 1 Gate Drive Data (Actual ASCR Current)

Bridge	Pole	Device	Ipeak	di/dt	Reverse Current	Pulse Width On/Off	Comments
#1	A Upper	Main	1.2A	0.93A/µs	0.15A/ 0.45A	12.75µs/3.25µs	Device Test
	A Lower	Main	1.3A	0.992A/µs	0.3A	12.65µs/3.35µs	
	A Upper	Comm	1.4A	1.08A/µs	0.25A	39.5µs	
	A Lower	Comm	1.35A	1.05A/µs	0.35A	39.5µs	
	A Upper	Aux	1.2A	0.9A/µs		36.65µs	
	A Lower	Aux	1.35A	1.03A/µs		39.45µs	
	B Lower	Main	1.45A	1.1A/µs	0.25	12.7µs/3.35µs	
	B Upper	Main	1.4A	1.04A/µs	0.3A	12.7µs/3.25µs	
	B Upper	Comm	1.2A	0.96A/µs	0.2A	39.5µs	
	B Lower	Comm	1.3A	1.02A/µs	0.3A	39.5µs	
	B Upper	Aux	1.06A	0.85A/µs		36.5µs	
	B Lower	Aux	1.2A	0.93A/µs		39.5µs	
	C Upper	Main	1.45A	1.2A/µs	0.3A	12.7µs/3.3µs	
	C Lower	Main	1.35A	1.06A/µs	0.2A	12.75µs/3.3µs	
	C Upper	Comm	1.4A	1.12A/µs	0.2A	39.5µs	
	C Lower	Comm	1.3A	1.06A/µs	0.3A	39.5µs	
	C Upper	Aux	1.49A	1.2A/µs		36.7µs	
	C Lower	Aux	1.44A	1.07A/µs		39.6µs	

Table 3-6. Bridge 2 Gate Drive Data (Short Circuit Test)

Bridge	Pole	Device	Ipeak	di/dt	Reverse Current	Pulse Width On/Off	Comments
#2	A Upper	Main	1.91A	1.48A/µs	0.7A	12.75µs/3.2µs	Changed
			1.68A	1.32A/µs			Transformer
	A Lower	Main	1.68A	1.55A/µs	0.65A	12.6µs/3.4µs	Short Test
	A Upper	Comm	1.94A	1.52A/µs	0.7A	39.5µs	
	A Lower	Comm	1.97A	1.54A/µs	0.45A	39.55µs	
	A Upper	Aux	1.92A	1.48A/µs		36.95µs	
	A Lower	Aux	1.9A	1.52A/µs		39.45µs	
	B Upper	Main	1.92A	1.46A/µs	0.5A	12.7µs/3.3µs	
	B Lower	Main	1.94A	1.46A/µs	0.35A	12.75µs/3.25µs	
	B Upper	Comm	1.95A	1.47A/µs	0.5A	39.6µs	
	B Lower	Comm	1.97A	1.52A/µs	0.5A	39.7µs	
	B Upper	Aux	1.94A	1.47A/µs		36.8µs	
	B Lower	Aux	1.92A	1.45A/µs		39.65µs	
	C Upper	Main	1.94A	1.46A/µs	0.6A	12.65µs/3.35µs	
	C Lower	Main	1.95A	1.44A/µs	0.55A	12.7µs/3.3µs	
	C Upper	Comm	1.95A	1.5A/µs	0.5A	39.5µs	
	C Lower	Comm	1.92A	1.46A/µs	0.4A	39.6µs	
	C Upper	Aux	1.88A	1.46A/µs		36.75µs	
	C Lower	Aux	1.92A	1.42A/µs		39.5µs	

Table 3-7. Bridge 2 Gate Drive Data (Actual ASCR Current)

Bridge	Pole	Device	Ipeak	di/dt	Reverse Current	Pulse Width On/Off	Comments
#2	A Upper	Main	1.21A 0.72A	1.02A/µs 0.68A/µs	0.45A	12.45µs/3.5µs	Changed Transformer
	A Lower	Main	1.22A	0.99A/µs	0.25A	12.7µs/3.4µs	Device Test
	A Upper	Comm	1.23A	1.02A/µs	0.5A	39.45µs	
	A Lower	Comm	1.38A	1.08A/µs	0.3A	39.5µs	
	A Upper	Aux	1.41A	1.1A/µs		36.75µs	
	A Lower	Aux	1.39A	1.1A/µs		39.45µs	
	B Upper	Main	1.22A	0.93A/µs	0.4A	12.7µs/3.3µs	
	B Lower	Main	1.31A	0.94µs	0.3A	12.9µs/3.2µs	
	B Upper	Comm	1.23A	0.94A/µs	0.25A	39.6µs	
	B Lower	Comm	1.39A	1.06A/µs	0.25A	39.7µs	
	B Upper	Aux	1.33A	1.01A/µs		36.9µs	
	B Lower	Aux	1.264A	0.976A/µs		39.7µs	
	C Upper	Main	1.39A	1.02A/µs	0.4A	12.8µs/3.3µs	
	C Lower	Main	1.18A	0.91A/µs	0.5A	12.8µs/3.2µs	
	C Upper	Comm	1.25A	0.98A/µs	0.25A	39.6µs	
	C Lower	Comm	1.25A	0.96A/µs	0.5A	39.5µs	
	C Upper	Aux	1.31A	1.06A/µs		36.7µs	
	C Lower	Aux	1.17A	0.93A/µs		39.5µs	

Upper Main

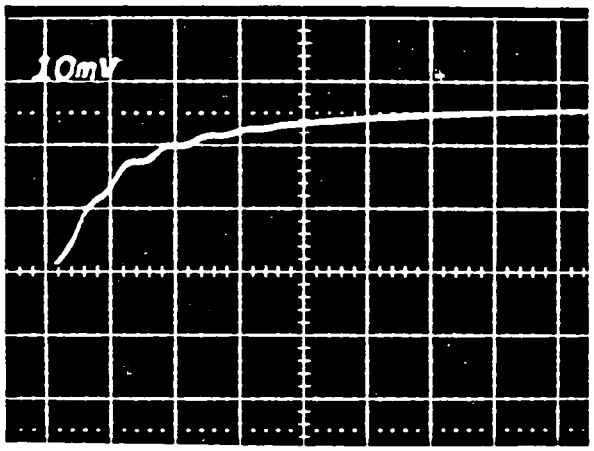

Vert. - 5Δ di/dt = 0.95Δ/μsec, 10%-90%

Upper Main

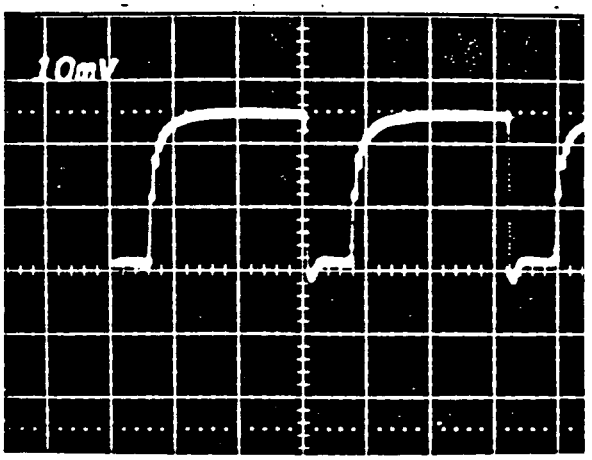

Horz. - 5 μsec/div. Turn On/Turn Off Sequence

Upper Comm.

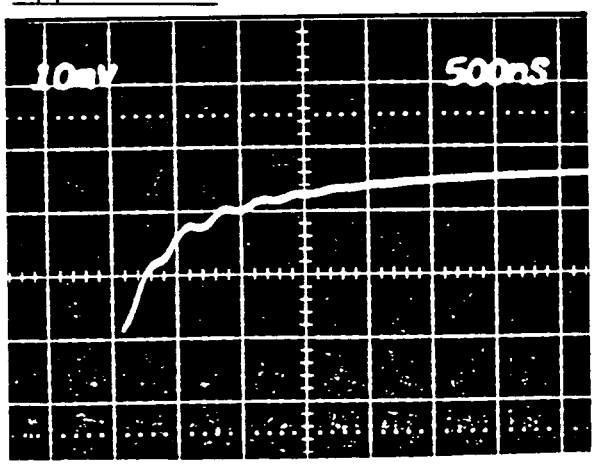

Vert. - 5Δ div. di/dt = 1.00 Δ/μs 10%-90%

Upper Comm.

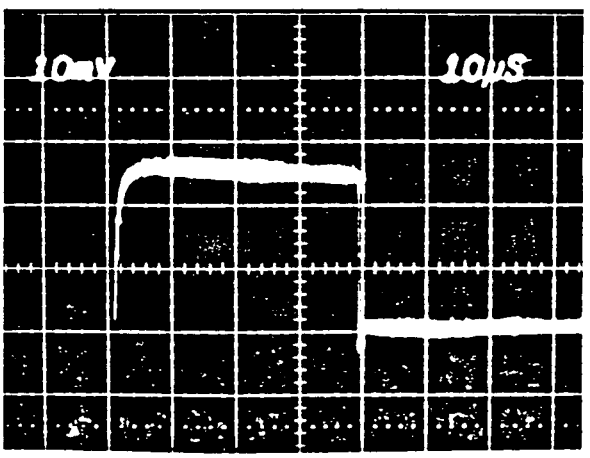

Turn On/Turn Off Sequence

123-171
850528

Figure 3-12. Typical Gate Drive Oscilloscope Data

Dynamic Isolated Testing

Once operation of the thyristor gating signals was confirmed, each powerpole was operated individually (at no load but at high dc input voltage) with the new controls. Multiple powerpoles were operated simultaneously, then on the entire bridge, and finally on two bridges. The objective of this testing was to observe powerpole operating parameters and confirm that operation of multiple poles did not cause dynamic anomalies through interaction between the poles. Interaction anomalies that can occur are circuit resonance on the dc input bus or oscillating currents between bridges. A summary of the dynamic test data is given in Table 3-8. No anomalies were observed due to interaction between poles or bridges.

Various anomalies were encountered and resolved during the dynamic tests and checkout of the two bridge system with main and bridge controls. One example is shown in Figure 3-13, which shows an output from a programmable logic analyzer that was utilized to characterize instability in the inverter waveform switching patterns. The figure shows that the inverter waveform synchronizing circuitry was stable 15% of the time, but shifted by more than 21 microseconds 15% of the time. Once this problem had been identified, it was resolved by a minor circuit modification to the phase lock loop circuit.

Table 3-8. 200-kW On-Site Brassboard Inverter

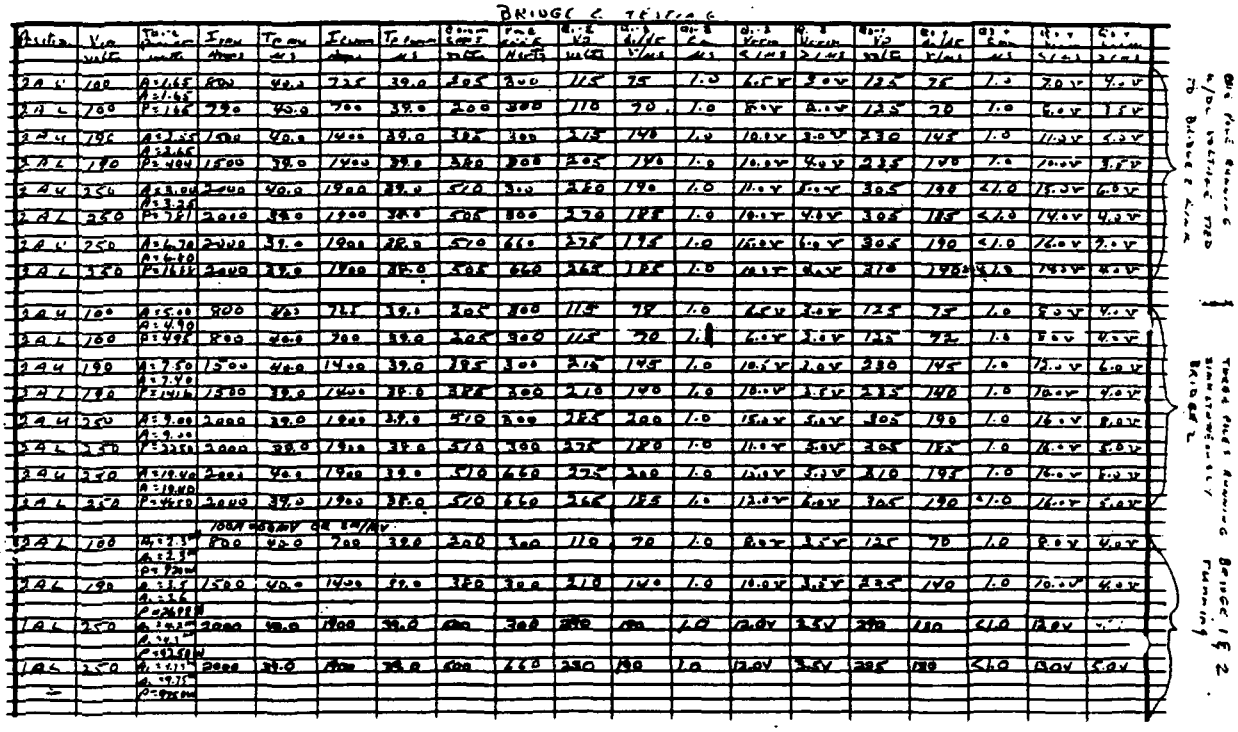

Histogram of PLL Bridge #1-PC1-U26-1 with Line Sync.

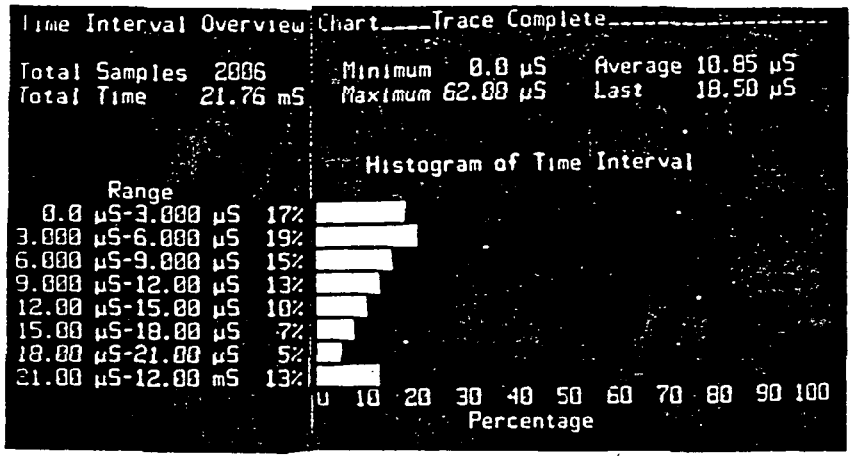

Histogram of PLL Bridge #2-PC1-U26-1 with Line Sync.

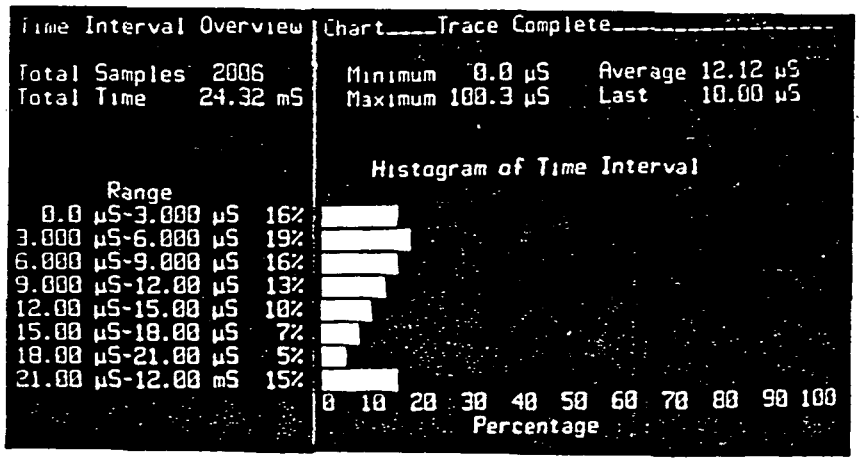

Figure 3-13. Histograms of PLL Bridges

123-172
850528

Line Parallel Preparation

Final preparations for line paralleling the 200-kW brassboard inverter were completed. The correct operation of the output transformer was verified. Its input (primary) and output (secondary) voltages were measured with the secondary side of the transformer connected to the utility line (Table 3-9). Secondary currents were also measured, which represent transformer magnetizing current. Magnetizing kilovoltamperes (kVA) was then calculated; it is also shown in Table 3-9. Next, transformer phasing was checked, as shown in Figure 3-14. This chart recorder data shows the phase relationship of transformer primary to secondary connections and confirms the proper phase relationship of inverter input to the transformer and utility line output.

In addition to the output transformer, a line variac was installed in the test setup, along with a transfer switch to allow the utility line interface voltage levels to be varied for test purposes. Figure 3-15 depicts the variac wiring arrangement. The input to the variac comes from the inverter and the output is connected to the utility line.

Table 3-9. 200 kVA Brassboard Output Transformer Test Results

Output transformer secondary energized from 480 Vac line with primaries disconnected.

Secondary Voltage (RMS)

VAN = 269.3 v	VAB = 466.5 v
VBN = 268.0 v	VBC = 462.6 v
VCN = 267.3 v	VCA = 464.5 v

Primary Voltage RMS

WYE Connections

VAN = 67 v	VAB = 130 v
VBN = 71 v	VBC = 130 v
VCN = 83 v	VCA = 130 v

Delta Connections

VAN = 52 v	VAB = 130 v
VBN = 87 v	VBC = 130 v
VCN = 89 v	VCA = 130 v

Secondary Current RMS

I_A = 188 ma x 60 = 11.3 amps I_B = 194.1 x 60 = 11.6 amps I_C = 176.4 ma x 6 = 10.6 amps

Voltages on 8 Channel Recorder

Secondary	VAN, VBN, VCN
Primary	VAB1, VAB2

- o Steady State
- o Transient

Magnetizing KVA = 3 Vcc i_c = 9.0 KVA

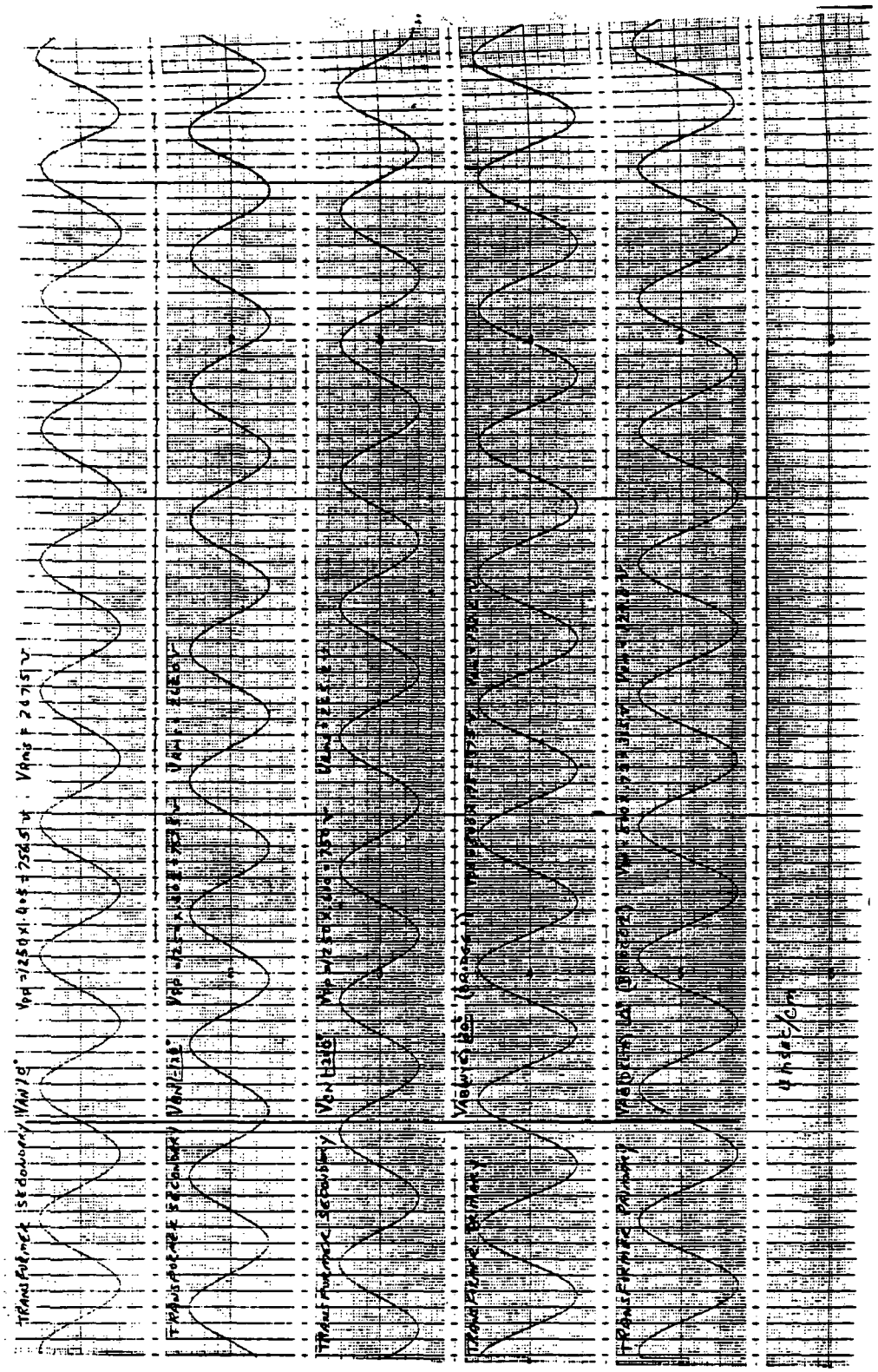

Figure 3-14. Phasing for 200 kVA Output Transformer

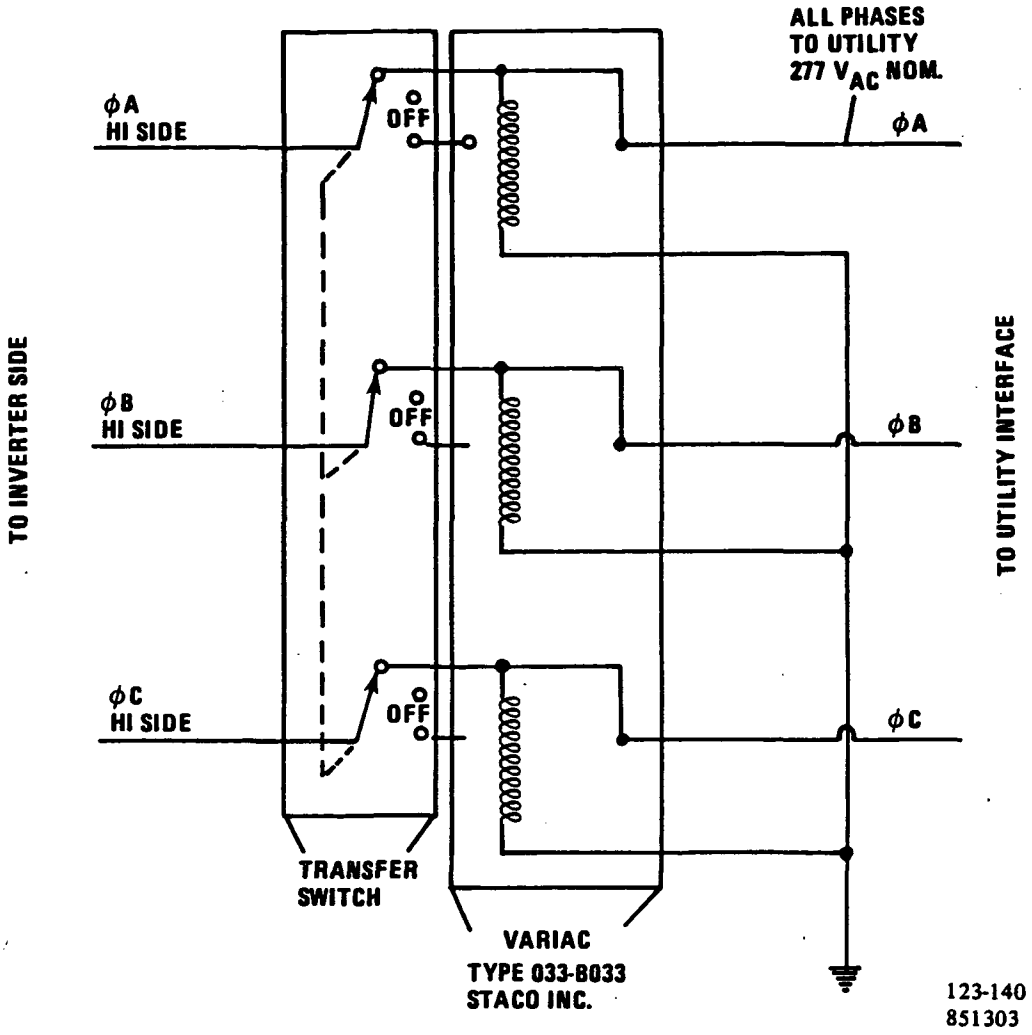

Figure 3-15. 200-kW Brassboard Inverter Test Variac Installation

Other line parallel preparations were completed:

- All of the different pulse width modulated switching patterns that the inverter produces at various operating conditions were evaluated.
- The control for limiting dc circulating current in the ac output was confirmed to be operational.
- Real and reactive power controls were verified.
- Protection set levels were verified to be as desired.
- Test instrumentation was installed to observe line parallel operation.
- Controls analog data acquisition calibrations were verified.

Initial Line Parallel Testing

The brassboard inverter automatic sequence to line parallel operation was successfully verified. Once the inverter was operating in parallel with the utility line, dynamic running currents and voltages were observed. Figures 3-16, 3-17, and 3-18 show oscillograph recordings of inverter three-phase output load at 50 kilowatts, 75 kilowatts, and 100 kilowatts, respectively. Table 3-10 provides a summary of the data for the steady state load points that have been run to this stage of testing.

During this period's brassboard functional checkout efforts, several problems and anomalies were identified and resolved. Table 3-11 summarizes the problems and anomalies. Of particular significance were the resolution of unstable operation (items 6 and 8 in Table 3-11) and the blown fuse (item 7). The unstable operation described in item 6 was due to instability of the synchronizing circuits, which synchronize the inverter output with the utility line. The synchronizing circuit was unstable because of harmonic distortion in the utility line signal used for synchronization. The problem was resolved by adding an active filter network to the utility line synchronizing signal, which removed the harmonic distortion. The unstable operation described in item 8 was due to incorrect waveform patterns at one operating point. The waveform patterns are stored in the memory of a waveform generator microcomputer, so correcting the waveform was simply a matter of correcting the data in memory. The item 7 blown fuse was caused by an incorrect thyristor gate drive signal, attributed to a hardware problem. Fixing the hardware problem corrected the gate drive signal.

ORIGINAL PAGE IS
OF POOR QUALITY

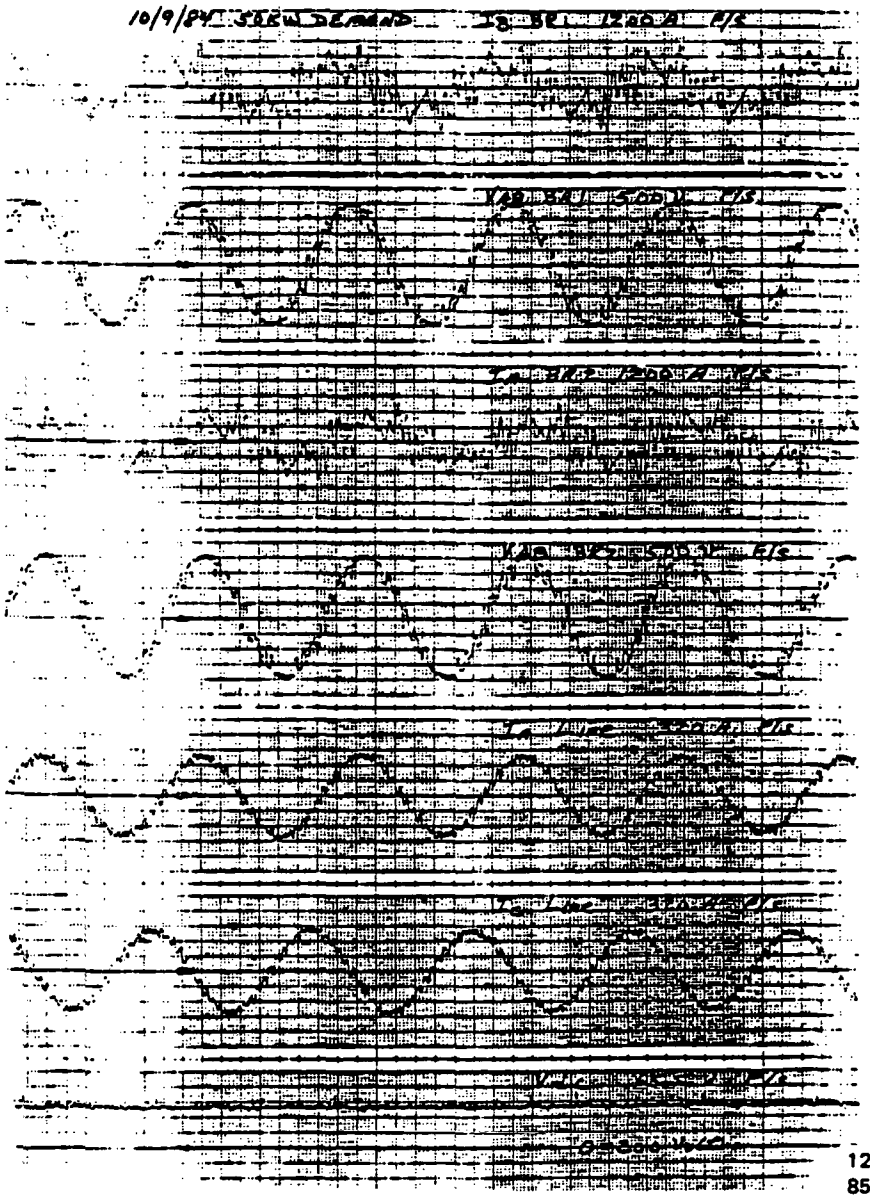

Figure 3-16. Brassboard Inverter at 50-kW Load

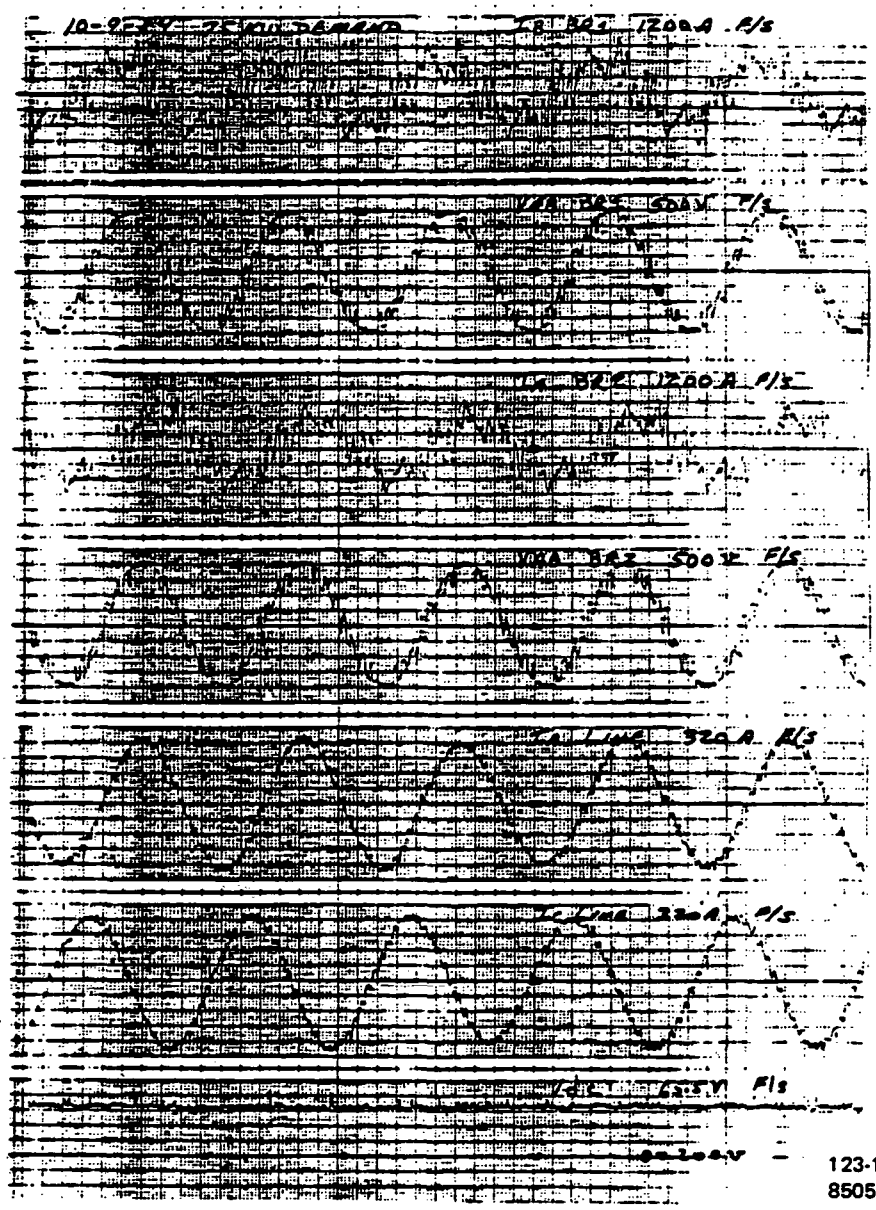

Figure 3-17. Brassboard Inverter at 75-kW Load

ORIGINAL PAGE IS
OF POOR QUALITY

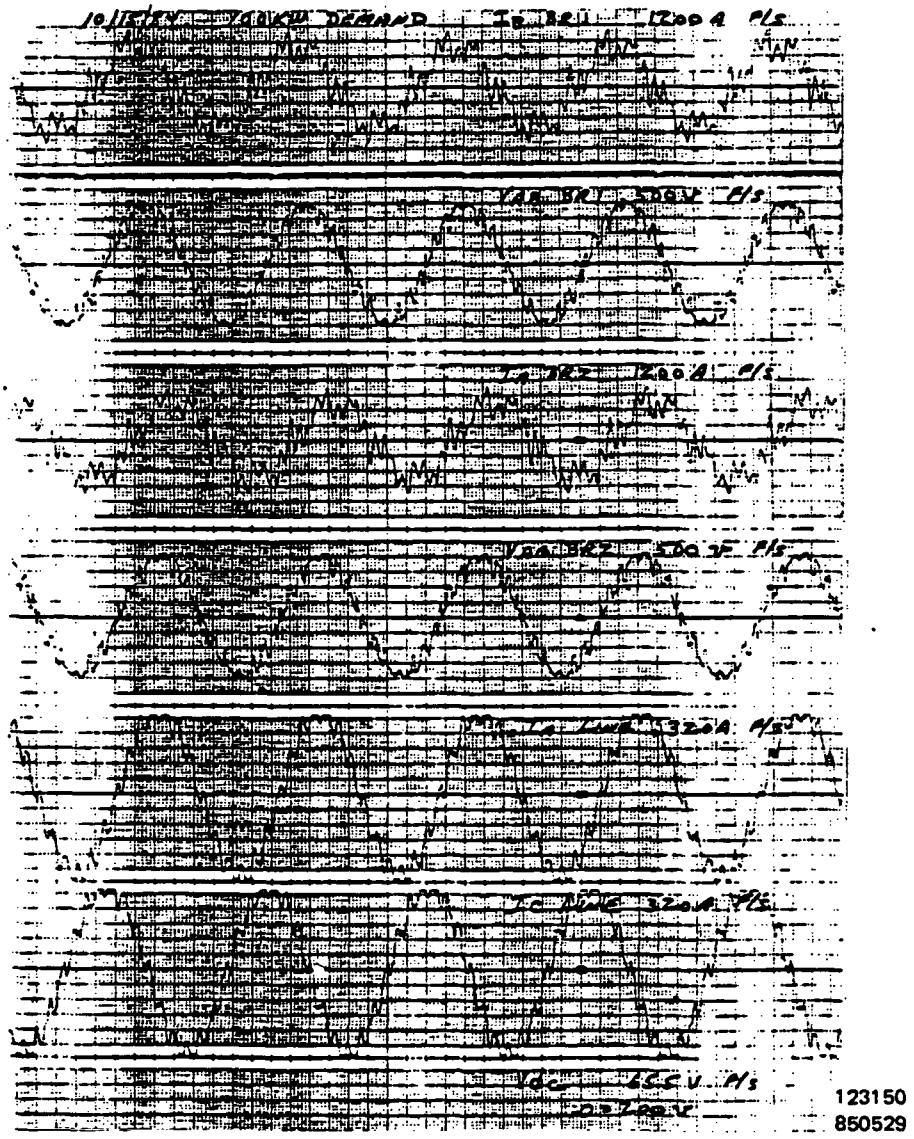

Figure 3-18. Brassboard Inverter at 100-kW Load

TABLE 3-10. 200-kW ON-SITE BRASSBOARD INVERTER LINE PARALLEL TEST DATA

Date	kW Demand	Vdc	Idc × 24	Pin*	VAN	VBN	VCN	IA × 60	IB × 60	IC × 60
10-5-84	0	202	Unstable		468 VAB	465 VBC	467 VCA	Unstable	Instability Fixed	
10-5-84	20	194	Unstable		468 VAB	464 VBC	466 VCA	Unstable		
10-8-84	0	211	43.2	9.12 kW	266	265	265	8.6a	8.6a	8.5a
10-8-84	25	219	156	34.2 kW	266	265	265	36.9a	36.0	39.0
10-8-84	50	216	283	61.1 kW	266	266	265	67.0a	66.6a	67.2a
10-8-84	75	222	398	88.4 kW	267	266	265	96.0	96.0	93.0
10-9-84	50	219	278	60.9 kW	270	269	269	60.0a	66.0a	60.0a
10-12-84	0	220	40.8	8.98 kW	265	264	263	11.4	11.1	10.9
10-15-84	100	213	532.8	113.5 kW	269	268	267	126	132	126

* Efficiency calculations not valid here

TABLE 3-11. BRASSBOARD INVERTER PROBLEMS AND ANOMALIES

	PROBLEM	CONDITION	CAUSE	ACTION
1	Line parallel in automatic mode	After interrupt gate signals stay off, "at load" panel light stays on. Systems must be reset. condition.	BCU's interrupt enable signals resetting too soon. Interrupt signals should be in latched	Changed interrupt signals in both BCU's to latched condition.
2	Check out BCU #1 interrupt signal.	Interrupt signal from MCU controls uC was at 3V level.	MCU PC3 uC V19 had a resistor network pack on output instead of buffer.	Changed V19 from IC 7408 to and/or buffer gate 7432.
3	Line parallel operation in auto mode.	Interrupts due to pole u/c.		Instrumented pole currents to ascertain whether overcurrent is real.
4	Line parallel operation in automatic mode	Cleared fuse in pole 1A.	Extension cable connector to PC3 in CCU B1 connected backward.	Operator error
5	Energizing logic	MCU screen monitor failed	IC chip failed inside monitor (charred).	Returned to manufacturer for repair.
6	Line parallel operation in check-out mode.	Unstable operation at certain input voltages, phase angles and load	Harmonic distortion at zone crossing of line sync signal	Added an active filter for line sync signal.
7	Line parallel operation in check-out mode	Cleared fuse in pole 2C	Gate drive step change during off time.	
8	Line parallel operation in check-out mode	Unstable operation at Vdc 205 volts.	Waveform pattern error in transition from 560 to 420 Hertz.	Changed proms with correct waveforms.
9	Energizing logic	Screen monitor displays logic "not clear" when logic is cleared.		
10	Operated bridges with pole outputs disconnected.	Percent initialization fundamental was not at correct condition.	Failed in MCU-PC2 IC chip U23 pin 5.	U23 failed due to operator error during previous debugging. Changed U23, now ok.

Line Parallel Operation Characterization

The brassboard inverter has been operated in line parallel at loads up to 150 kW ac into the line. Attempts to operate at loads above about 150 kW ac revealed a mismatch between the laboratory test facility 200 kW dc power supply and the inverter minimum voltage rating of 190 Vdc. A power variac was installed in the ac feed to the dc supply to raise the ac input voltage so that its output would not drop below 190 volts. The high ac line volts produced the desired effect on the dc volts output, but also exceeded the voltage regulation limit of the brassboard inverter control, so the output limitation was not significantly improved.

The inverter selective commutation function was activated. Selective commutation is a feature that improves efficiency by eliminating unnecessary thyristor commutations. Since every commutation produces an energy loss, the more commutations that can be eliminated, the better. Selective commutation tests at several load points showed non-optimum operation of selective commutation. Not as many commutations were eliminated as had been predicted. Figure 3-19 shows a graph of predicted efficiency versus actual efficiency with selective commutation active. The part power efficiency was lower than predicted, even when known elements such as an oversized commutation circuit were accounted for. Optimum efficiency with selective commutation was then calculated based on the non-optimum operation of the selective commutation function. The difference between that and predicted efficiency has not been explained. Investigation as to why the selective commutation function is non-optimum is in process.

Line parallel operation was characterized at several load points. Operation was stable and generally met design requirements. Table 3-12 shows line parallel operation characterization data. Figures 3-20 and 3-21 show real versus simulated harmonic voltage and output voltage waveform, respectively. Figure 3-20 shows an output waveform. Figure 3-21 shows the harmonic spectrum of the output waveform shown in Figure 3-20.

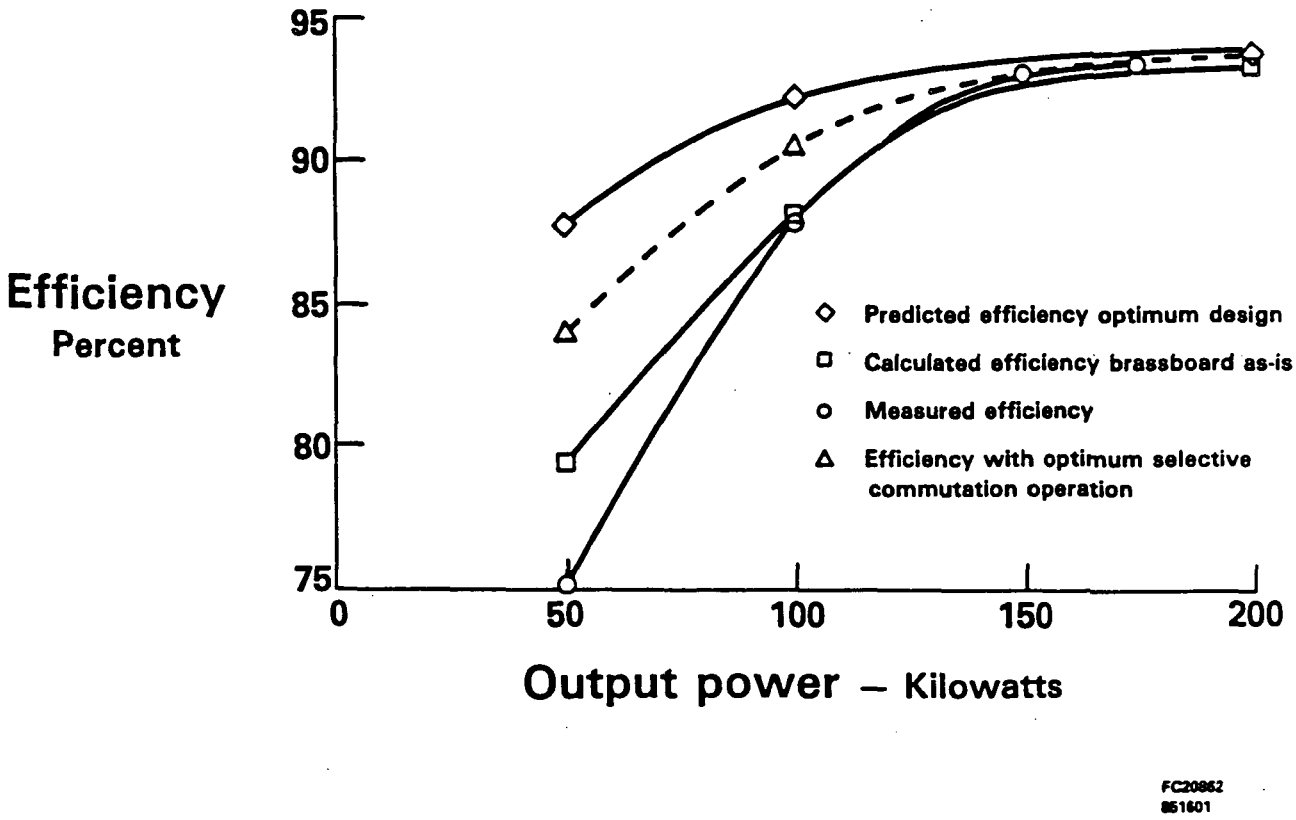

Figure 3-19. 200-kW On-Site Brassboard Inverter System Efficiency vs. Ouput Power

TABLE 3-12. Line Parallel Operation Characterization Data

KVAA	KVAB	KVAC	PA × 60 kW	PB × 60 kW	PC × 60 kW	P Total* kW	KVA	P.F.
2.29	2.28	2.25					6.82	
9.82	9.54	10.33					29.69	
17.8	17.7	17.8	16.2	17.5	16.5	50.2	53.3	.94
25.6	25.5	24.6	24.6	25.8	24.6	75.0	75.7	.99
16.2	17.7	16.2	16.2	17.4	16.2	49.8	50.1	.99
3.02	2.93	2.87						
33.9	35.4	33.6	33.0	34.8	33.6	101.4	102.9	.99

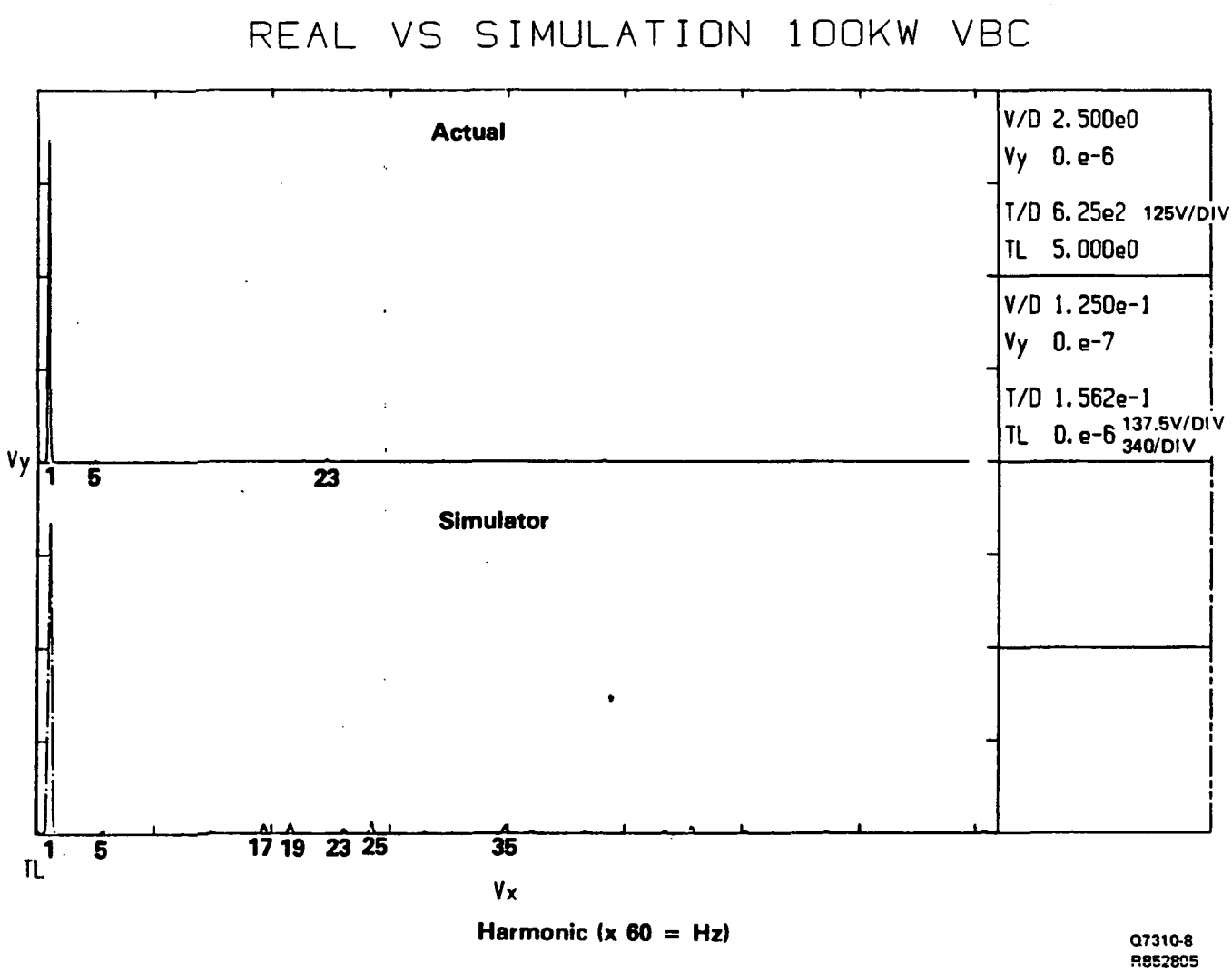

Figure 3-20. 200-kW Inverter Harmonic Voltage Spectrum

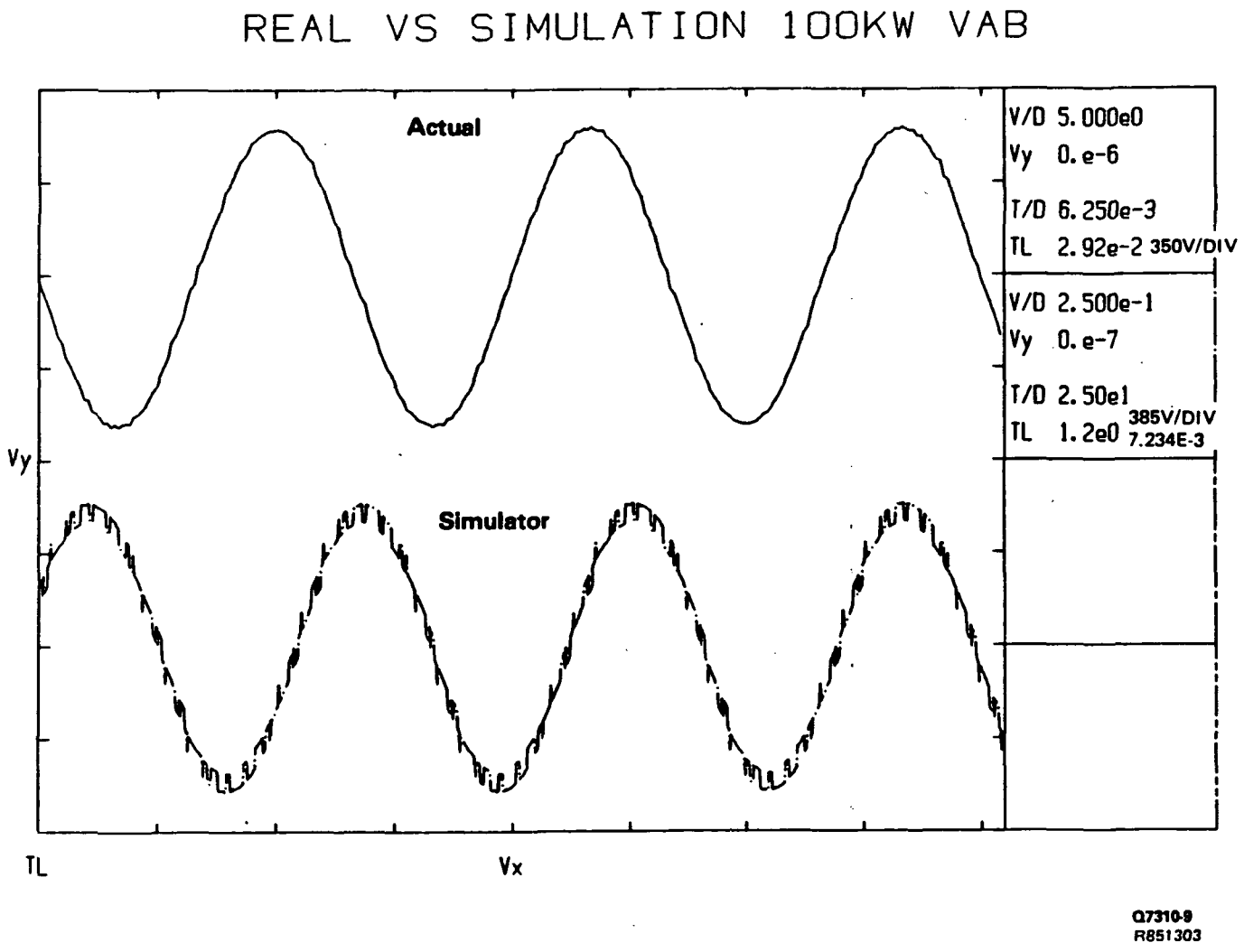

Figure 3-21. 200-kW Inverter Harmonic Voltage

Identified Deficiencies

Deficiencies were identified during brassboard checkout and line parallel operation. Table 3-13 lists samples of the types of deficiencies. Some have been resolved, others require follow-up on subsequent brassboard tests.

Table 3-13. Brassboard Inverter Deficiencies

Item	Cause	Action
o Unstable operation at certain input voltages, phase angles and load	Harmonic distortion at zero crossing of line sync. signal	Added active filter for line sync. signal
o Unstable operation at Vdc 205 volts	Waveform pattern error in transition from 560 to 420 hertz	Changed PROMS with correct waveform patterns
o Screen monitor displays "Logic Not Clear" when logic is cleared	Error in power up diagnostic software	TBD
o Cannot reach rated 200 kW output	Test stand configuration. Incorrect ac service to dc power supply, excessive power supply droop	TBD
o Lower than expected part power load efficiency	Non-optimum selective commutation operation and other unknown causes	Investigation in process

The brassboard power processor has been tested from the initial subsystem/component level through on-line system operation, including evaluation of inverter control logic. Off-limits testing, diagnostics verification, dc unbalance control verification, low part power efficiency, and some unresolved deficiencies remain.

Effort in 1985 will concentrate on resolving the low part power efficiency, completion of off-limits testing, diagnostics and dc unbalance control verification, resolution of deficiencies and test verification of their resolution, and evaluation of improved control and operating approaches. Control and protection studies should identify simplification or elimination of functions and, where practical, the brassboard controls should be modified to test those approaches.

TASK 4

HEAT EXCHANGER DEVELOPMENT

TASK 4 - HEAT EXCHANGER DEVELOPMENT

Objective

The objective of this task is to identify lower cost designs for the technically critical heat exchangers and to evaluate their manufacturability, performance, and reliability.

Summary

There are a number of heat exchangers in a fuel cell power plant. Three of them are high cost units because of the requirement for low pressure drop or corrosive conditions. These heat exchangers (the air preheater, acid condenser, and water condenser) are being evaluated in this program.

Four candidate heat exchangers for the air preheater application were selected for experimental evaluation and procurement was initiated. In selecting these units, an attempt was made to provide a variety of heat exchanger types and geometries that would offer options for packaging. The units selected included tube arrays, ripple plate and compact formed plate designs. These configurations represent a significant reduction in cost relative to the baseline shell and tube unit. An initial prototype ripple plate air preheater had a projected cost of approximately 50% of the baseline. Evaluation testing of this initial unit showed it was well within pressure drop and effectiveness requirements.

Corrosion assessment samples representing Heresite® coated low grade/exhaust condensers and uncoated stainless steel plate type acid condensers were removed from test. Metallographic examination of these samples revealed attack of less than 1 mil and 3 mils, respectively.

An integrated packaging arrangement for the fuel processing heat exchangers was selected for further study. This arrangement is based on a low-cost fin tube core design. Cost estimates will be included in this effort.

Highlights

- Evaluation of an initial low-cost air preheater candidate was successfully completed. Air preheater performance met or exceeded performance requirements.

- Corrosion testing to support the uncoated phosphoric acid condenser and the Heresite® coated low grade/exhaust condenser concepts was completed.

- Candidate fuel processing heat exchangers were identified and an integrated packaging arrangement was studied.

Discussion

Development activity in this area included experimental evaluation of air preheater designs and corrosion testing to support the evaluation of an uncoated stainless steel, phosphoric acid condenser and the Heresite® coated low grade/exhaust condenser.

Program History - Work was conducted under the GRI On-Site Technology Development Program to identify alternative reduced cost designs to the baseline shell and tube air preheater. The results of the GRI work served as the basis for selection of designs that will be evaluated experimentally in this task.

Studies under the GRI On-Site Program also investigated alternative acid management concepts. Work conducted in 1983 identified a Teflon® covered metal heat exchanger as the preferred acid removal device for the baseline 200-kW power plant. The potential for reducing the cost of this design by incorporating a multi-pass flow on the gas side was studied. A significant reduction in core size was realized, along with elimination of water removal during low power operation. Based on preliminary assessments, a design and vendor study was undertaken to determine the full cost reduction and operational potential.

Heat Exchanger Development - The objective of the heat exchanger development effort is to define a more functional and less costly design than that presently being used in the 40-kW power plant. Work conducted in this phase of the program included the assessment of the corrosion tolerance materials and coatings for heat exchangers used in an acid vapor environment, the performance and durability testing of low-cost air preheaters, and the identification and packaging of low-cost fuel processing heat exchangers.

Subscale Corrosion Testing - In addition to the Teflon® covered metal heat exchanger, consideration was given to the use of an acid condenser device using uncoated stainless steel. This device would be designed to maintain moderate to low metal temperatures. These temperatures would result in lower corrosion rates.

Corrosion tests relevant to this concept have been underway since early 1983. In these tests an uncoated stainless steel plate type heat exchanger element was partially immersed in phosphoric acid of approximately 250°F. This element was removed from test after 12,576 hours. Post-test pressure check of this element showed no leaks. Metallographic examination showed an overall corrosion rate of approximately 3 mils per year. There was also some evidence of preferential corrosion of the weld regions caused by incipient cracks. This preferential corrosion was anticipated and could be reduced or eliminated by improved weld procedures. Overall, the surfaces appeared to be relatively free from corrosion products. A post-test photograph of the corrosion test element is presented in Figure 4-1.

The low grade/exhaust condenser is another area where corrosion testing was initiated to support a reduced cost design. These heat exchanger applications require a material that is compatible with city water/coolant on the cold side and low pH condensate water on the hot side. One low-cost approach for the condensers is a Heresite® coated metal unit. This is a standard combination for many fin tube heat exchanger manufacturers. The Heresite® coating is compatible with the low pH condensate. The test program was planned to determine if the coating is suitable in the fin-to-tube joint area. Any corrosion of this joint would severely

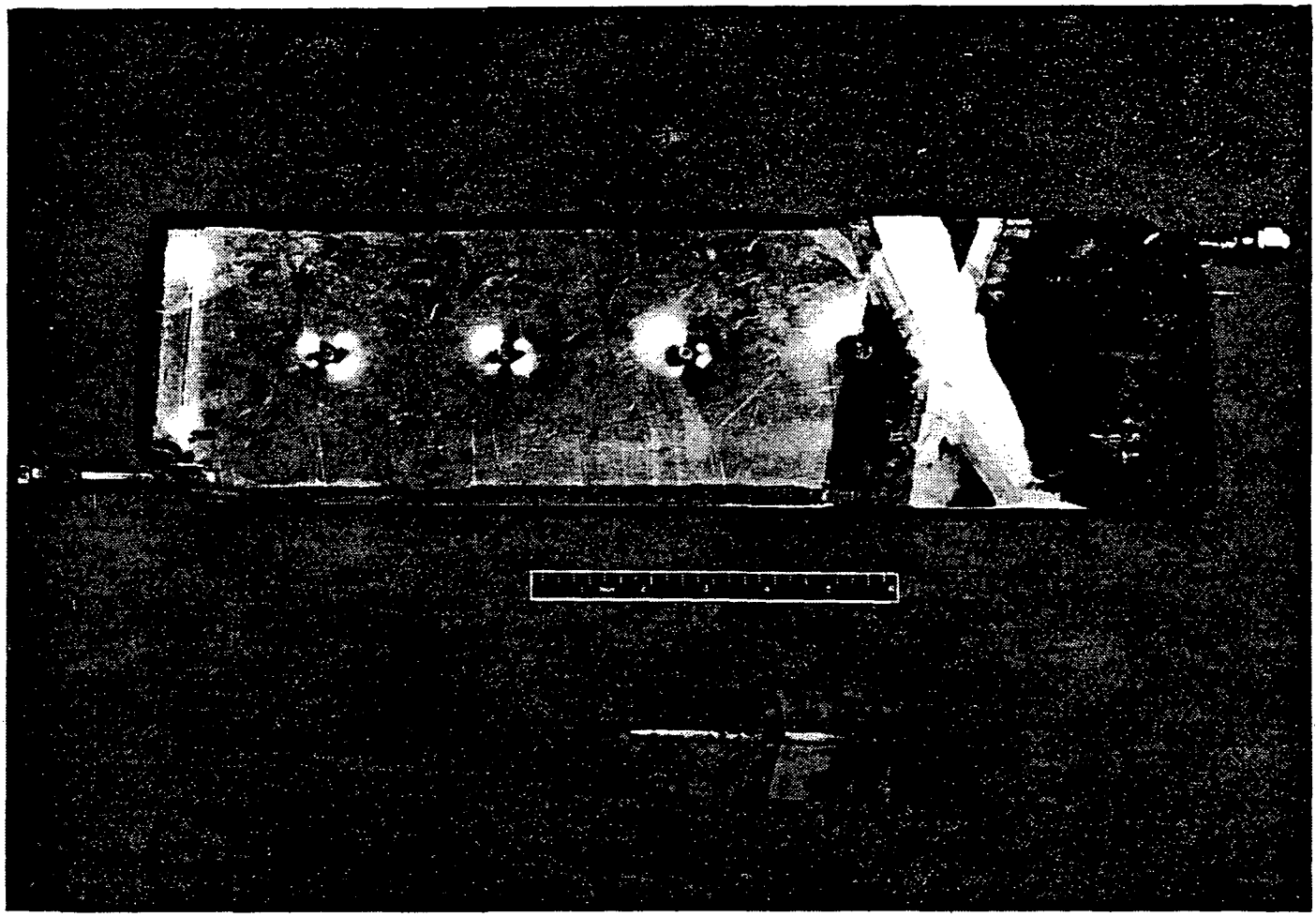

WCN-10928

Figure 4-1. Uncoated Acid Condenser Element - Post-Test

reduce the unit's heat transfer performance. The core sample, shown in Figure 4-2, was thermally cycled at simulated power plant conditions prior to being exposed to a low pH hot water bath. This sample accumulated 5500 hours exposure to 135°F carbonic acid. Metallographic examination of selected regions of this low grade/exhaust condenser sample showed some coating cracks and separations, which allowed corrosion of the base metal. This corrosion amounted to less than 1 mil, which might be significant to heat transfer if it resulted in deterioration of the fin-to-tube bond. This deterioration did not appear to be that extensive. In addition, there is some evidence that the fin/tube separation observed was probably the result of the method of fabrication. Other available methods of attaching the fins to the tube will be explored.

Air Preheater Testing - Four of the candidate heat exchangers for the air preheater application identified in the GRI program were selected for experimental evaluation under this task. In selecting these units an attempt was made to provide a variety of reduced cost heat exchanger types and geometries. This selection provided various options for packaging this unit. The units selected represent tube array, ripple plate, and compact formed plate configurations.

The first candidate air preheater procured for experimental evaluation was the ripple plate unit (Figure 4-3). A test facility for this evaluation was prepared and testing initiated in the third quarter. A schematic of this test facility is shown in Figure 4-4.

Prior to conducting the hot flow performance tests, curing of the ceramic seals used in the concept was performed. This curing cycle involved soaking the unit at incremental temperature steps up to the proposed operating temperature. Initial hot flow testing showed a discrepancy between hot and cold stream heat transfer. This was resolved by relocating the gas temperature sensing thermocouples to an improved mixed point.

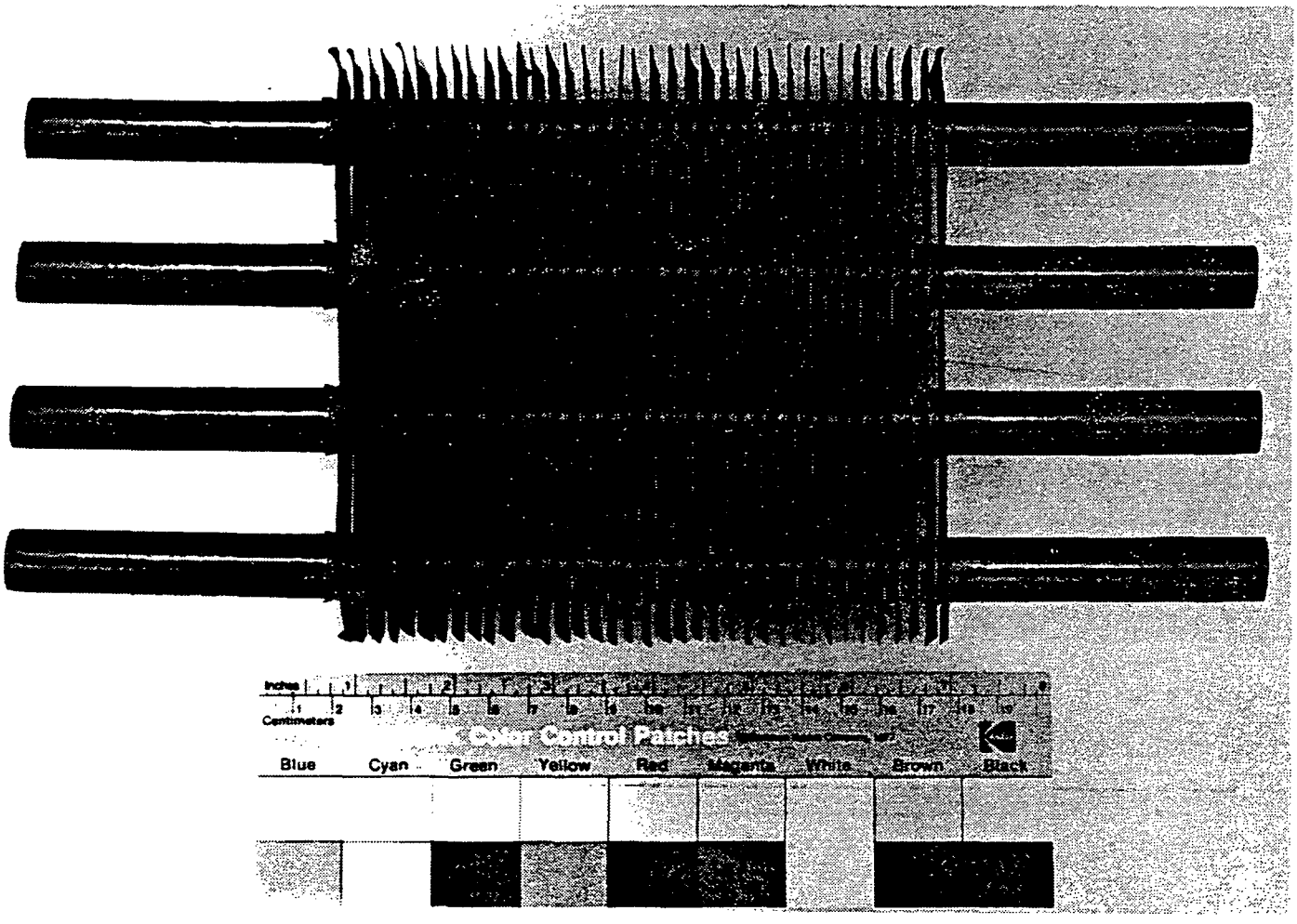

WCN-10051

Figure 4-2. Heresite® Coated Condenser Sample Core

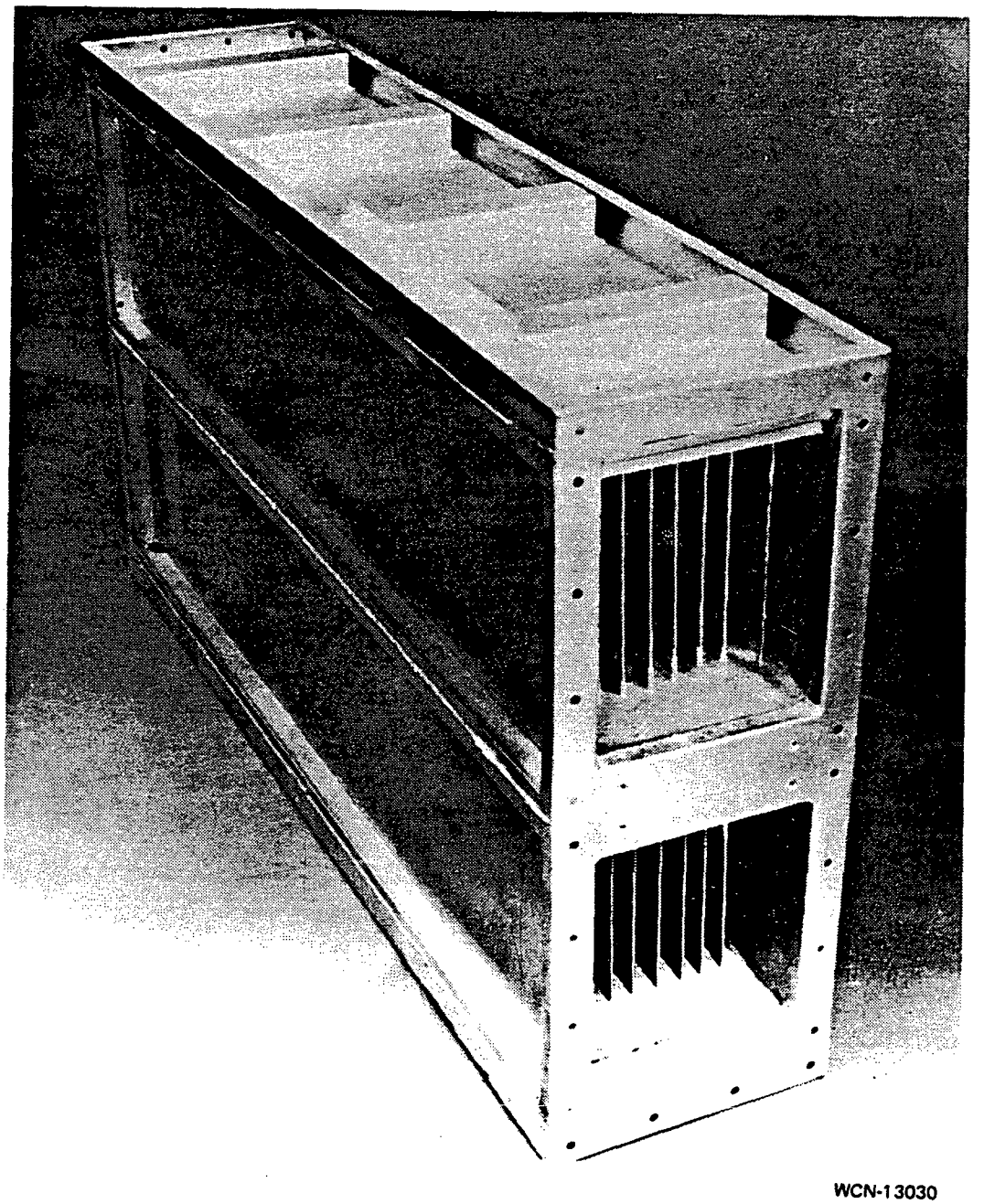

Figure 4-3. Candidate Ripple Plate Air Preheater

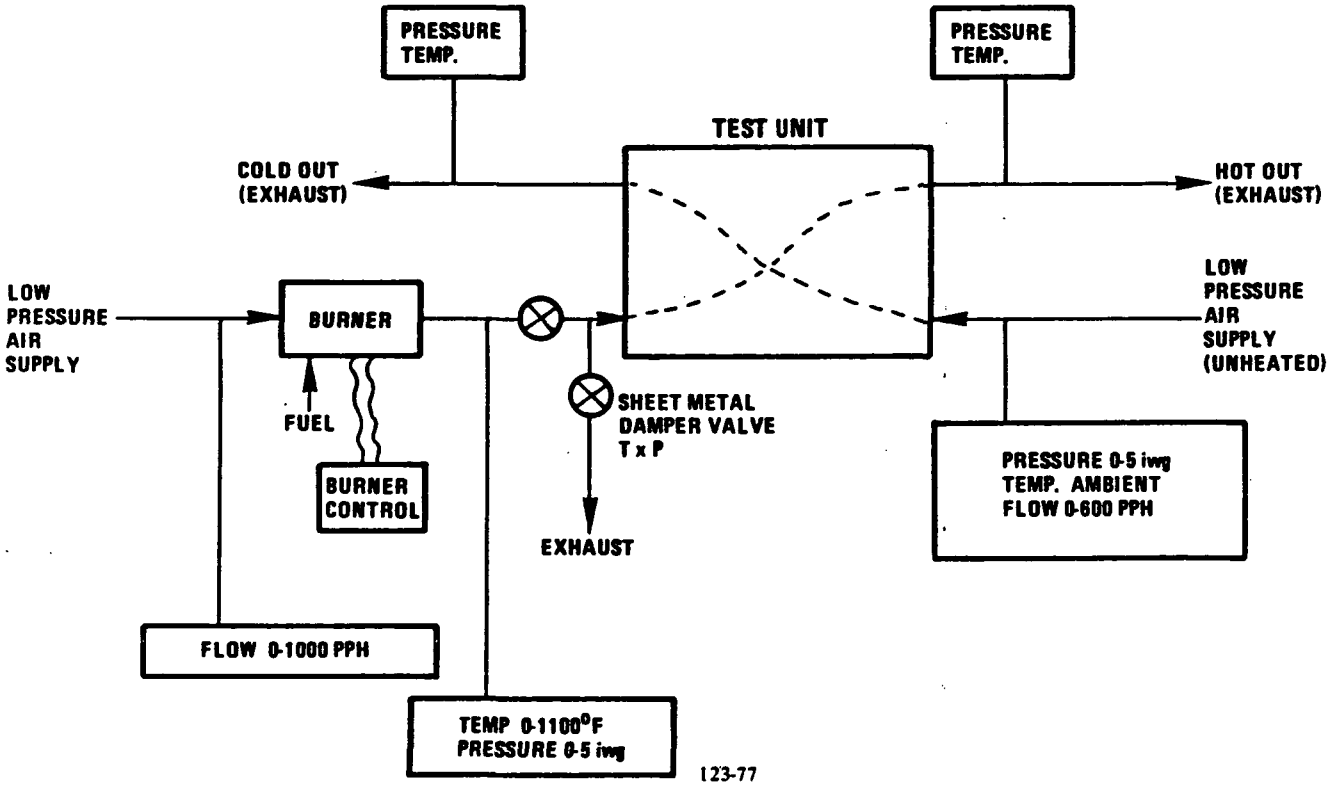

Figure 4-4. Air Preheater Test Set-Up

The experimental evaluation program involved start-up, design and off-design performance, 100-hour endurance and 100-cycle tests. The 100-hour steady state and 100-cycle tests were performed to provide assessment of the integrity of the ceramic seal concept. Post-test inspection revealed some hairline cracks in the sealing material and sealing material debris in the flow passage. Cross and overboard leakage increased relative to "as received". Both these leakages were relatively small and appeared to have little impact on performance. A summary of the test program results is presented in Table 4-1. Post-test photographs of this heat exchanger are shown in Figure 4-5.

A second candidate air preheater configuration was received for experimental evaluation. This unit is representative of the compact formed plate designs: an all-welded heat exchanger that measures only 6" x 21" x 15.5". Photographs of this heat exchanger are shown in Figure 4-6. A size comparison of this unit and the ripple plate unit is shown in the photograph in Figure 4-7. This compact formed plate unit is scheduled for test early in 1985.

Manufacturing drawings for the in-house air preheater were completed and fabrication was initiated. This unit is representative of the tube array designs.

Integrated Fuel Processing Hexs - Low-cost heat exchanger candidates for the fuel processing system were identified. The heat exchangers of interest are the HDS preheater, the shift converter precooler, and the steam superheater. Fin-tube units are proposed for these applications because they provide a better match for the cost, heat transfer, operating pressure, and pressure drop requirements. A sample fin-tube core typical of these units is being built and will be assessed. These units lend themselves to an integrated packaging arrangement. Building on commercially available units, a design approach has been proposed that provides a leak-tight, integrated packaging arrangement. Potential fabricators identified in earlier surveys have been asked to quote on the concept.

Table 4-1. Air Preheater Test Results

	Heat Exchange Effectiveness	
o At Test Conditions	73.4 to 75.5%	
o Projected to Power Plant Conditions	75.0 to 77.5%	
o 200-kW Air Preheater Requirement	70%	
	Heat Exchange Pressure Drop	
o Projected to Power Plant Conditions	0.44 iwg	0.1 iwg
o Allowable, 200-W Air Preheater	1.3 iwg	0.42 iwg

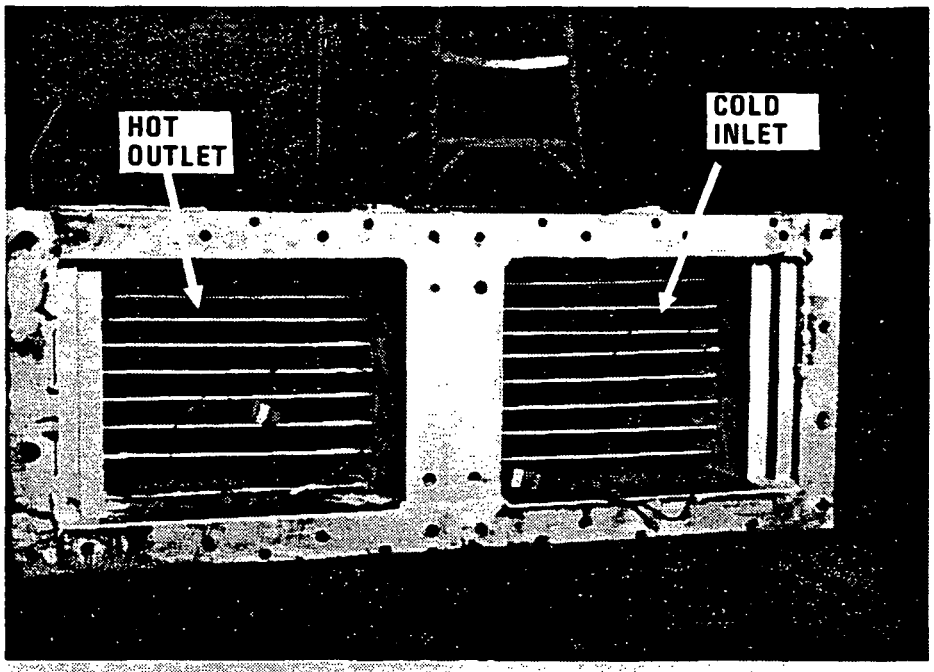

WCN-13170

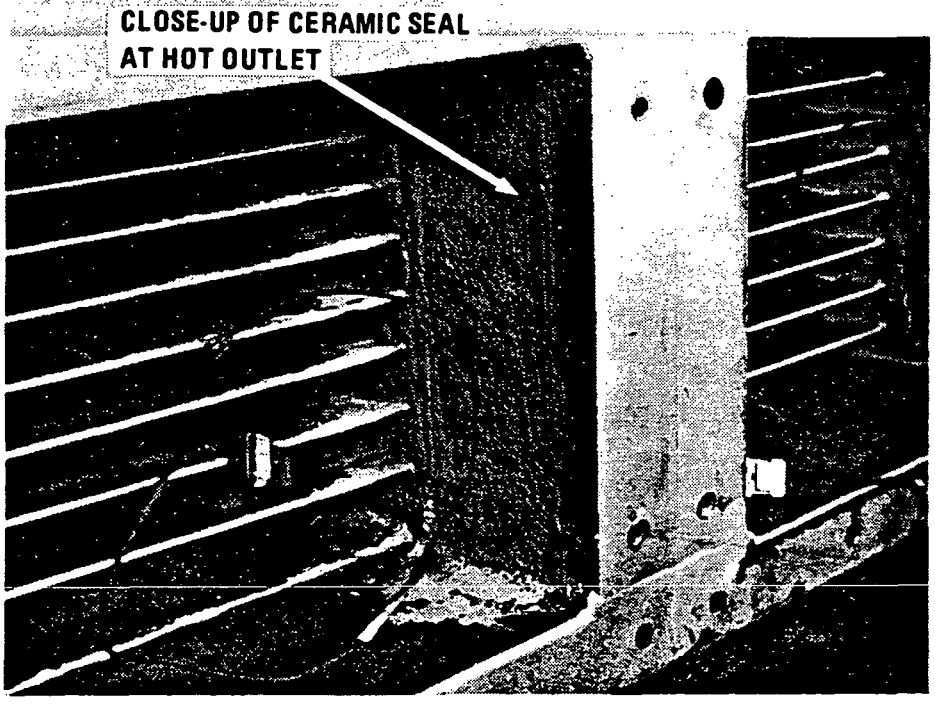

WCN-13169

Figure 4-5. Candidate Ripple Plate Air Preheater - Post-Test

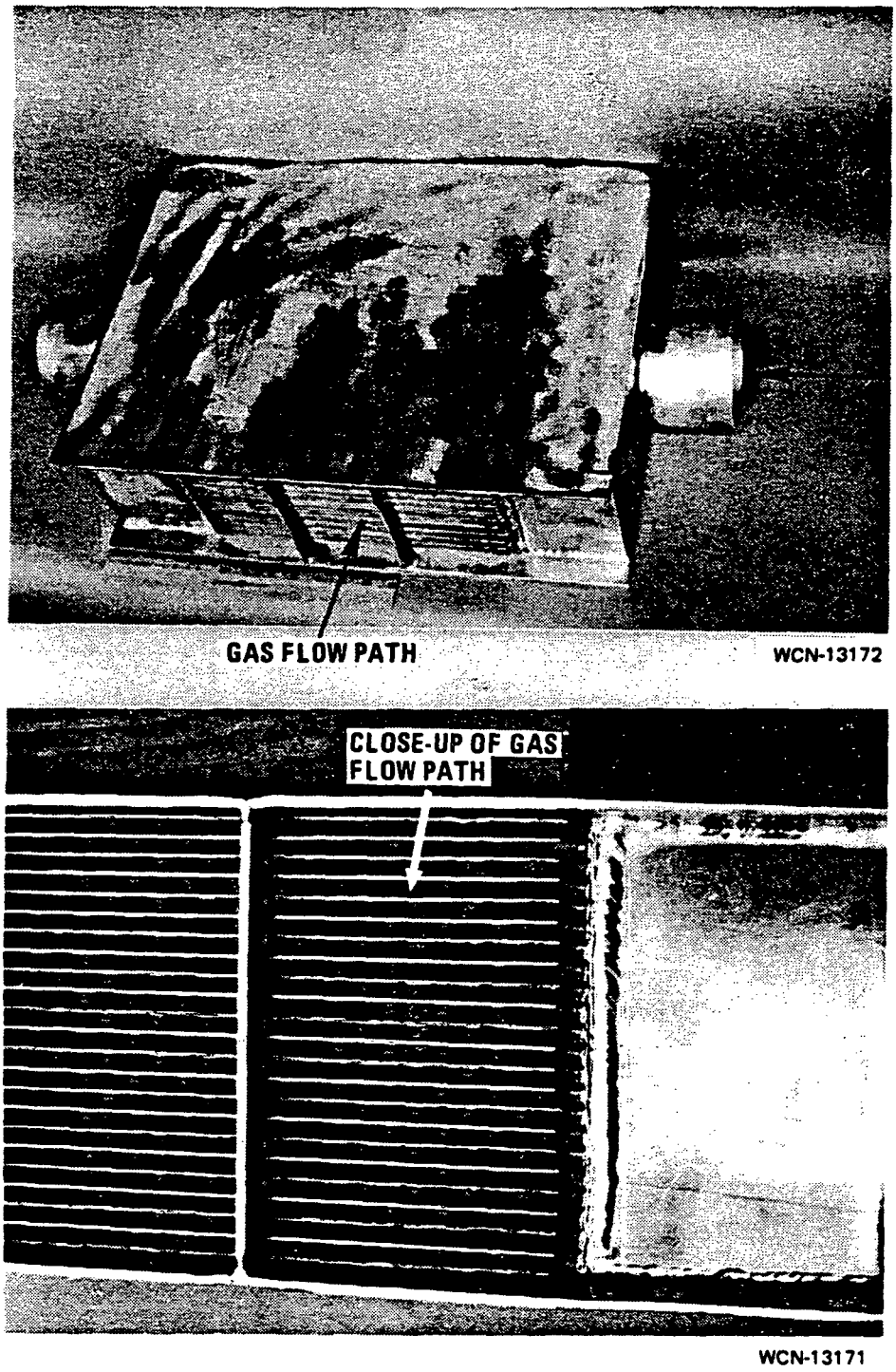

Figure 4-6. Compact Formed Plate Air Preheater Candidate

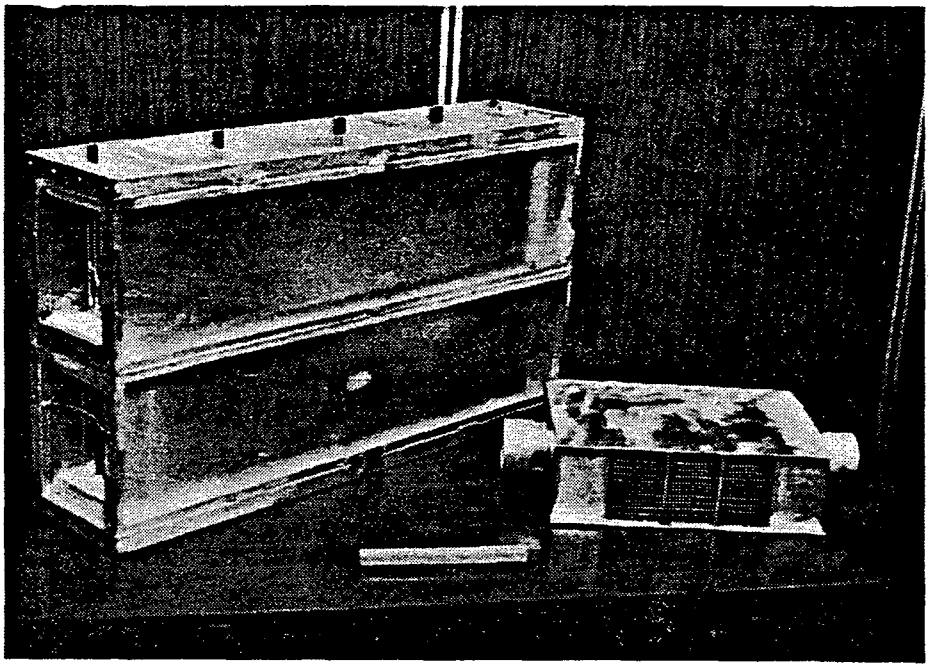

WCN-13207

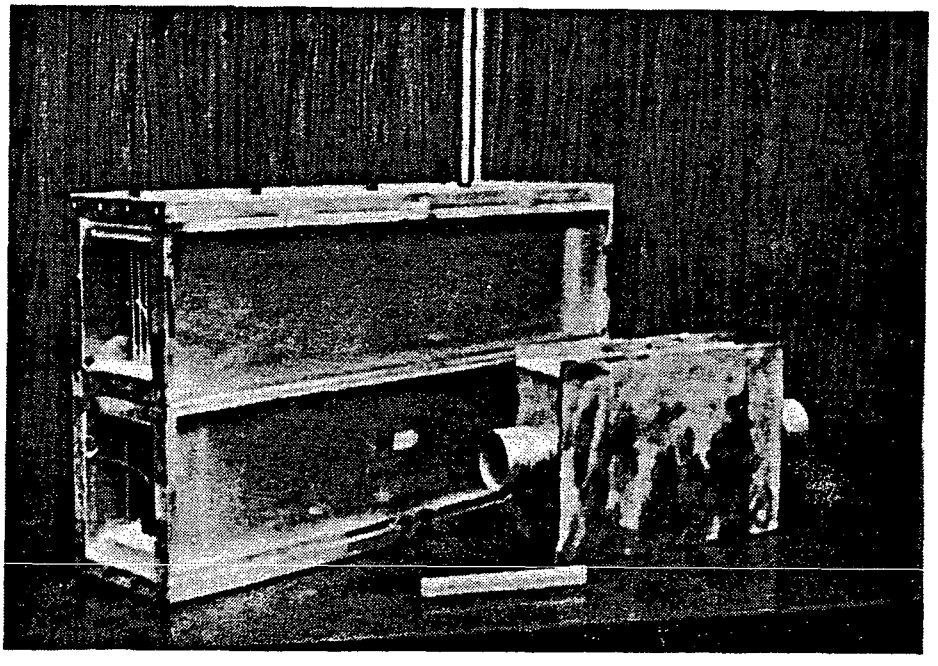

WCN-13208

Figure 4-7. Compact Formed Plate (Right) and Ripple Plate (Left) Air Preheater Heat Exchangers

TASK 5

FUEL PROCESSOR DEVELOPMENT

TASK 5 - FUEL PROCESSOR DEVELOPMENT

Subtask 5.2 - Fuel Processor Catalyst Endurance Testing

Objective

The objective of this subtask is to complete the verification testing of the hydrodesulfurization catalyst started in a previous work period, and to complete a 2000-hour endurance test of the catalyst types selected during this work period. Electrically heated subscale reactors will be used to test hydrodesulfurization, reforming, and low temperature shift catalysts for at least 2000 hours on a representative pipeline quality natural gas. The throughput will be varied over the anticipated range of the power plant, and gas compositions will be monitored at periodic intervals at selected locations in each of the reactors.

Summary

Conventional hydrodesulfurization catalysts require presulfiding prior to becoming active, and are normally operated at several hundred pounds of pressure in order to obtain adequate activity and endurance to completely desulfurize fuel for several years. The desulfurizer previously designed for the On-Site power plant was capable of completely desulfurizing natural gas; however, it was quite large, had a limited life, and because of the requirement of presulfiding was rather expensive. Tests run during a previous work period identified a hydrodesulfurization catalyst that does not require presulfiding, and is potentially smaller and less expensive than the baseline catalyst. Several other catalysts with even greater potential were identified; one was tested and a second was prepared for testing.

Fabrication of the fuel processor catalyst endurance test stand was completed, systems were checked, and over 2000 hours of endurance obtained in an electrically tested fuel processor train consisting of PSD-12 hydrodesulfurizer catalyst, zinc oxide absorbent, HGC-4014 reformer catalyst, and HGC-4015 shift catalyst.

Conditions were varied over the anticipated range of the power plant, and gas compositions were monitored periodically at selected locations in each of the reactors. The hydrodesulfurizer protected the reformer and shift converter for over 2000 hours. Each of the catalysts tested was found to be stable throughout the test.

Highlights

- The fuel processor catalyst train successfully completed over 2000 hours of endurance on pipeline quality natural gas.
- A hydrodesulfurization catalyst requiring no presulfiding and only half the volume of baseline hydrodesulfurization catalyst was qualified for power plant use.
- The stability of a low pressure drop reformer catalyst was verified for power plant use.
- An alternative low temperature shift catalyst was qualified for power plant use. Its activity was found to be 40% greater than the baseline catalyst.

Discussion

Hydrodesulfurizer Testing

Two noble metal hydrodesulfurizer catalysts were evaluated in electrically heated subscale reactors capable of testing catalysts under controlled temperature and pressure conditions. In order to simulate power plant conditions, the hydrodesulfurizer must be operated under vacuum conditions of -1 to -4 psig. A controlled vacuum was obtained by exhausting the hydrodesulfurizer into the suction side of a nitrogen pumped ejector. Catalyst performance was determined by injecting a known quantity of thiophane, a stable sulfur compound used as an odorant, and

measuring the conversion of thiophane to hydrogen sulfide at various sample taps along the length of the reactor. Thiophane was added to the reactor by bubbling a small quantity of reactant gas through a container of thiophane (sulfurizer). A diagram of the test apparatus is shown in Figure 5-1.

It can be seen from this diagram that the sulfur level in the gas stream was maintained constant by controlling the sulfurizer at a temperature of 35°F, and at a constant pressure of about 60 psig. The sulfur level was determined by withdrawing and analyzing a gas sample from the sample tap (shown directly after the sulfurizer back-pressure regulator) but before the simulated shift converter recycle was mixed with the methane. The many heaters and thermocouples shown on the rig allowed control of the catalyst temperature in each of the three catalyst test beds.

The first catalyst tested was a noble metal on alumina catalyst manufactured at United Technologies and designated PSD-12.

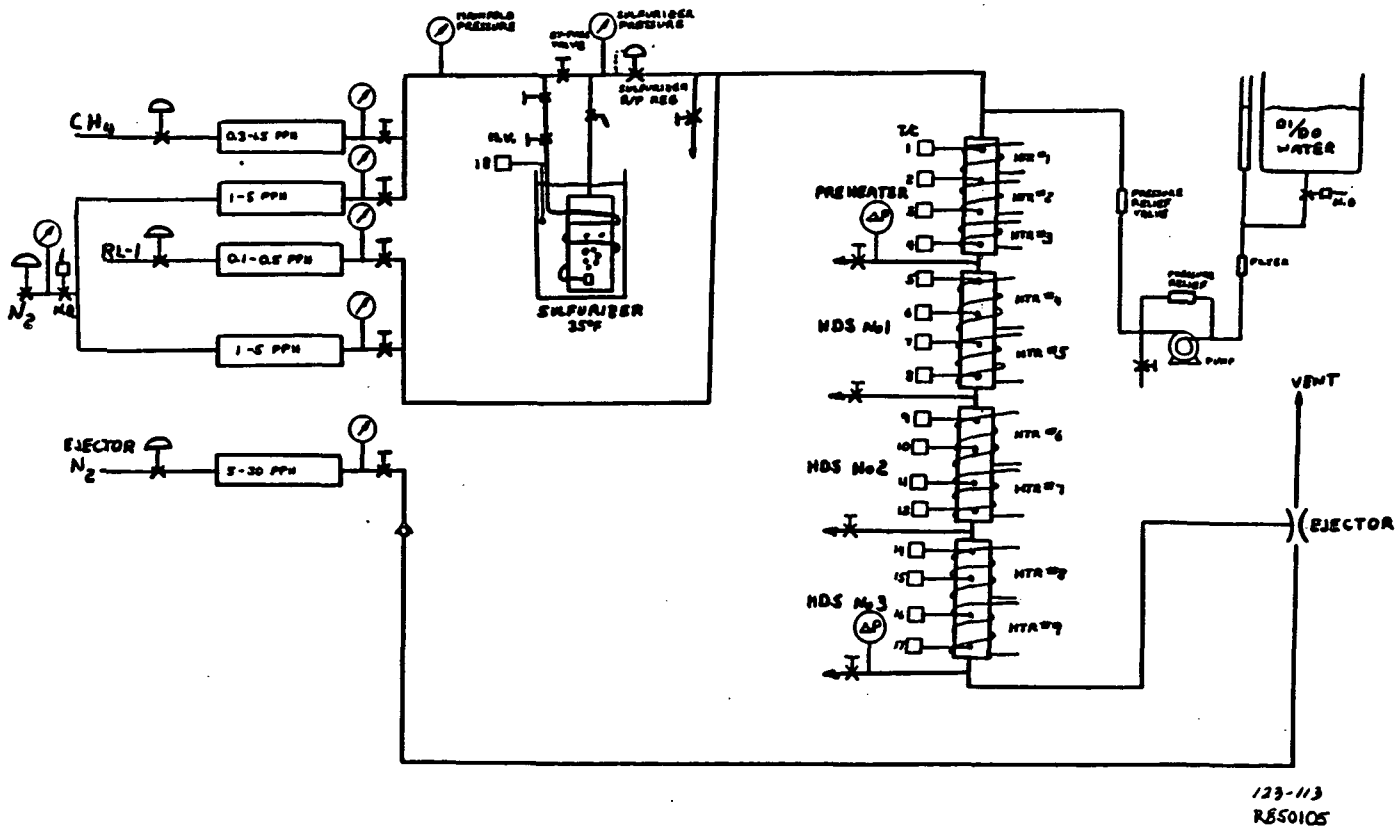

Figure 5-1. On-Site Subambient Hydrodesulfurizer

Much of the initial testing was used to verify the analytical procedure and insure reproducibility of sulfur analysis at very low sulfur concentrations. Subsequent tests were run to verify performance for use in the endurance test. Results from this test, shown in Table 5-1, verified that PSD-12 was capable of operating in the endurance train. No catalyst decay was observed over 500 hours of operation, and less than 0.05 parts per million of sulfur was detected exiting the reactor over the range of conditions expected in the power plant. The required catalyst represents 2.5 times less weight and 2 times less volume than the baseline catalyst. Since PSD-12 was used in the endurance train, a more extensive discussion of its performance will be included in that section.

Table 5-1. Hydrodesulfurizer Test Results of PSD-12 Catalyst

Catalyst Weight	0.542 lbs
Fuel Flow	0.81 lbs/hr
Recycle Flow	12%
HDS Pressure	1 psig

	Sulfur Analysis			
Temp.	Into HDS	Exit HDS No.1	Exit HDS No.2	Exit HDS No.3
450°F	28.5 PPM	8.8 PPM	1.2 PPM	0.3 PPM
500°F	28.4 PPM	2.5 PPM	<0.05 PPM	-
550°F	31.8 PPM	1.3 PPM	<0.05 PPM	-

The second hydrodesulfurizer catalyst tested, PCB-9269, has the potential to further minimize desulfurizer cost and volume. Temperatures of 500°F and 575°F were run while simulated recycle gas was varied from 2.5% to 12% during the over 3000 hours of testing.

Figure 5-2 shows that initially, as the recycle decreased, catalyst activity increased; but after 800 hours of testing, the catalyst slowly decayed. None of the changes in pressure or in recycle rate eliminated the decay, therefore testing was discontinued.

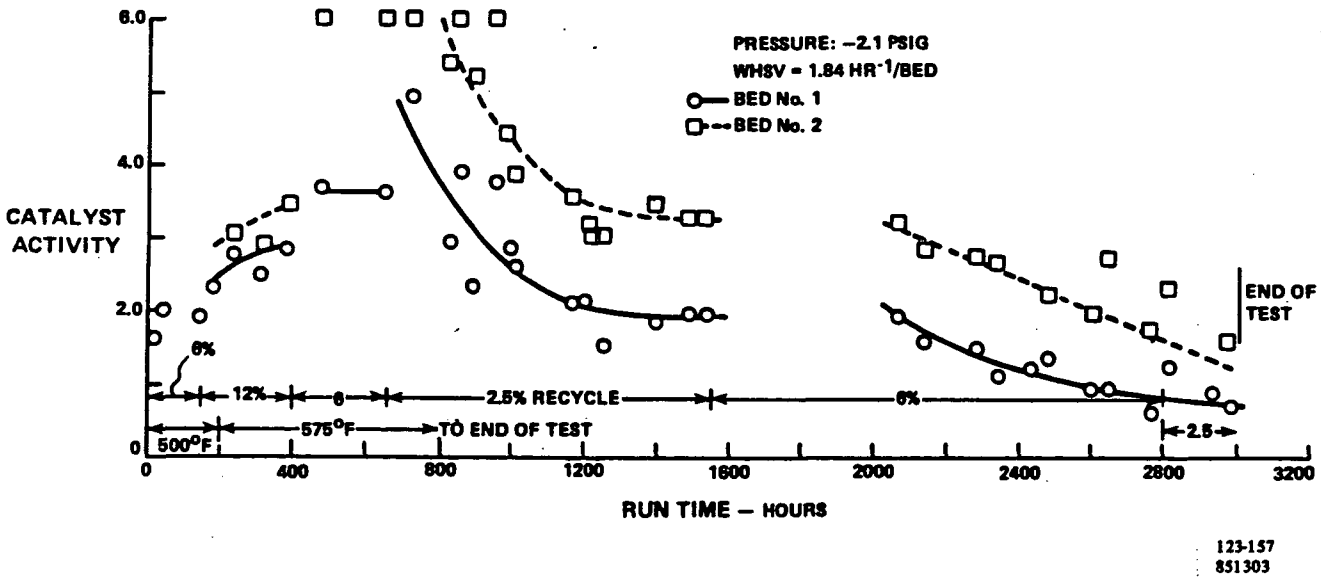

Figure 5-2. Performance of PCB-9269 Desulfurization Catalyst

Test results are summarized in Table 5-2. It is possible that this catalyst could be reformulated and optimized so that decay becomes insignificant; however, at the present time it does not appear to offer a significant enough advantage over PSD-12 to warrant a development effort.

A similar, commercially available catalyst (PCB-9506) has recently been found which would offer a cost advantage over the catalysts previously tested. The hardware for testing this catalyst will be assembled in December, and testing will begin in January 1985.

TABLE 5-2. SUMMARY OF PCB-9269 HYDRODESULFURIZER CATALYST TEST RESULTS

Point No.	1	2	3	4	5	6	7	8
Date	6-20-84	6-21-84	6-25-84	6-27-84	6-29-84	7-2-84	7-5-84	7-9-84
Time on Fuel	21 Hours	47 Hours	144 Hours	190 Hours	238 Hours	312 Hours	384 Hours	479 Hours
Flows								
CH4	.81 pph	.81 pph	.81 pph	.81 pph	.81 pph	.81 pph	0.81 pph	0.81 pph
Recycle	.177 pph	.177 pph	.177 pph	.351 pph	.351 pph	.351 pph	0.351 pph	0.177 pph
Percent Recycle	6%	6%	6%	12%	12%	12%	12%	6%
Bed Temperatures								
HDS #1 T/C #5	501°F	500°F	501°F	499°F	573°F	573°F	574°F	569°F
T/C #6	502°F	502°F	521°F	502°F	573°F	573°F	574°F	571°F
HDS #2 T/C #9	475°F	494°F	493°F	491°F	575°F	575°F	575°F	571°F
T/C #10	510°F	504°F	505°F	501°F	575°F	576°F	574°F	571°F
HDS #3 T/C #14	455°F	493°F	492°F	492°F	574°F	573°F	573°F	567°F
T/C #15	496°F	504°F	504°F	502°F	576°F	576°F	576°F	574°F
Pressures								
HDS In	-2.0 psig	-2.0 psig	-2.05 psig	-2.0 psig	-2.0 psig	-2.1 psig	-2.0 psig	-2.0 psig
HDS Out	-2.0 psig	-2.02 psig	-2.1 psig	-2.12 psig	-2.12 psig	-2.14 psig	-2.1 psig	-2.1 psig
Sulfur Concentration								
Out of Sulfurizer	31.7 ppm	32.7 ppm	34.2 ppm	36.7 ppm	34.4 ppm	37.2 ppm	32.0 ppm	37.0 ppm
In Bed 1	22.7 ppm	23.7 ppm	27.0 ppm	25.0 ppm	23.0 ppm	27.0 ppm	18.6 ppm	24.6 ppm
Exit Bed 1	9.5 ppm	8.0 ppm	9.6 ppm	7.1 ppm	5.1 ppm	7.0 ppm	4.0 ppm	3.3 ppm
Bed 2	4.9 ppm	4.0 ppm	5.3 ppm	7.3 ppm	1.0 ppm	1.5 ppm	0.63 ppm	0.05 ppm
Bed 3	-	1.8 ppm	2.7 ppm	5.2 ppm	.05 ppm	.05 ppm	0.05 ppm	-

TABLE 5-2. SUMMARY OF PCB-9269 HYDRODESULFURIZER CATALYST TEST RESULTS (CONT'D)

Point No.	9	10	11	12	13	14	15	16
Date	7-16-84	7-19-84	7-24-84	7-25-84	7-27-84	8-18-84	8-20-84	8-21-84
Time on Fuel	650 Hours	722 Hours	826 Hours	856 Hours	898 Hours	954 Hours	988 Hours	1010 Hours
Flows								
CH4	0.81 pph	0.81 pph	0.81 pph	.81 pph	.81 pph	.81 pph	.81 pph	.81 pph
Recycle	0.177 pph	.0922 pph	.0924 pph	.0924 pph	.0924 pph	.107 pph	.107 pph	.0922 pph
Percent Recycle	6%	2.5%	2.5%	2.5%	2.5%	2.5%	2.5%	2.5%
Bed Temperatures								
HDS #1 T/C #5	570°F	570°F	569°F	566°F	568°F	566°F	565°F	561°F
T/C #6	573°F	574°F	589°F	573°F	576°F	573°F	571°F	570°F
HDS #2 T/C #9	572°F	569°F	570°F	566°F	564°F	565°F	566°F	565°F
T/C #10	573°F	570°F	572°F	577°F	575°F	573°F	576°F	578°F
HDS #3 T/C #14	568°F	566°F	566°F	567°F	564°F	566°F	563°F	566°F
T/C #15	575°F	574°F	574°F	578°F	577°F	573°F	571°F	573°F
Pressures								
HDS In	-2.1 psig	-2.0 psig	-2.0 psig	-2.0 psig	-2.0 psig	-2.0 psig	-2.0 psig	-2.1 psig
HDS Out	-2.2 psig	-2.1 psig	-2.0 psig	-2.0 psig	-2.0 psig	-2.0 psig	-2.1 psig	-2.1 psig
Sulfur Concentration								
Out of Sulfurizer	28.1 ppm	26.0 ppm	33.0 ppm	29.4 ppm	30.4 ppm	28.1 ppm	30.2 ppm	28.0 ppm
In Bed 1	21.5 ppm	22.0 ppm	29.0 ppm	25.0 ppm	26.4 ppm	24.0 ppm	25.3 ppm	24.5 ppm
Exit Bed 1	3.0 ppm	1.5 ppm	6.0 ppm	3.0 ppm	7.5 ppm	3.1 ppm	5.4 ppm	6.1 ppm
Bed 2	0.05 ppm	.05 ppm	.32 ppm	.05 ppm	0.44 ppm	.05 ppm	.55 ppm	.75 ppm
Bed 3	-	-	.05 ppm	-	.05 ppm	-	.05 ppm	.05 ppm

TABLE 5-2. SUMMARY OF PCB-9269 HYDRODESULFURIZER CATALYST TEST RESULTS (CONT'D)

Point No.	17	18	19	20	21	22	23	24	25	26
Date	8-28-84	8-29-84	8-30-84	9-6-84	9-10-84	9-12-84	10-8-84	10-11-94	10-17-84	10-19-84
Time on Fuel	1170 Hours	1201 Hours	1225 Hours	1394 Hours	1488 Hours	1537 Hours	2070 Hours	2142 Hours	2287 Hours	2336 Hours
Flows										
CH	0.81 pph	0.81 pph	0.81 pph	0.81 pph	0.81 pph	0.81 pph	0.81 pph	0.81 pph	0.81 pph	0.81 pph
Recycle	0.922 pph	.0922 pph	.0922 pph	.0922 pph	.0922 pph	0.922 pph	0.177 pph	0.177 pph	0.177 pph	0.177 pph
Percent Recycle	2.5%	2.5%	2.5%	2.5%	2.5%	2.5%	5%	5%	5%	5%
Bed Temperatures										
HDS #1 T/C #5	564°F	564°F	565°F	562°F	565°F	565°F	566°F	567°F	566°F	566°F
T/C #6	574°F	575°F	575°F	573°F	574°F	574°F	574°F	575°F	575°F	575°F
HDS #2 T/C #9	566°F	563°F	566°F	561°F	565°F	565°F	563°F	568°F	563°F	566°F
T/C #10	575°F	578°F	581°F	577°F	579°F	579°F	572°F	575°F	572°F	574°F
HDS #3 T/C #14	565°F	563°F	561°F	562°F	565°F	565°F	561°F	569°F	568°F	569°F
T/C #15	577°F	574°F	574°F	575°F	576°F	576°F	573°F	576°F	577°F	578°F
Pressures										
HDS In	-2.1 psig	-2.1 psig	-2.1 psig	-2.1 psig	-2.1 psig	-2.1 psig	-2.0 psig	-2.0 psig	-2.0 psig	-2.0 psig
HDS Out	-2.1 psig	-2.1 psig	-2.1 psig	-2.1 psig	-2.1 psig	-2.1 psig	-2.0 psig	-2.0 psig	-2.0 psig	-2.0 psig
Sulfur Concentration										
Out of Sulfurizer	28.0 ppm	28.0 ppm	27.0 ppm	26.5 ppm	27.2 ppm	28.2 ppm	28.5 ppm	27.1 ppm	28.2 ppm	29.2 ppm
In Bed 1	24.0 ppm	24.8 ppm	23.1 ppm	22.5 ppm	23.6 ppm	23.8 ppm	22.8 ppm	21.0 ppm	21.5 ppm	22.8 ppm
Exit Bed 1	7.6 ppm	7.8 ppm	10.2 ppm	8.5 ppm	8.3 ppm	8.3 ppm	8.1 ppm	9.0 ppm	9.6 ppm	12.5 ppm
Bed 2	1.1 ppm	1.4 ppm	2.0 ppm	1.3 ppm	1.4 ppm	1.4 ppm	1.1 ppm	2.0 ppm	2.2 ppm	3.0 ppm
Bed 3	.05 ppm	.05 ppm	.41 ppm	.44 ppm	.26 ppm	.26 ppm	0.13 ppm	0.44 ppm	0.57 ppm	0.45 ppm

TABLE 5-2. SUMMARY OF PCB-9269 HYDRODESULFURIZER CATALYST TEST RESULTS (CONT'D)

Point No.	27	28	29	30	31	32	33	34
Date	10-23-84	10-25-84	10-30-84	11-1-84	11-6-84	11-8-84	11-13-84	11-15-84
Time on Fuel	2432 Hours	2480 Hours	2599 Hours	2648 Hours	2767 Hours	2815 Hours	2932 Hours	2982 Hours
Flows								
CH	0.81 pph	0.81 pph	0.81 pph	0.81 pph	0.81 pph	0.81 pph	0.81 pph	0.81 pph
Recycle	0.177 pph	0.177 pph	0.177 pph	0.177 pph	0.177 pph	0.092 pph	0.092 pph	0.092 pph
Percent Recycle	5%	5%	5%	5%	5%	2.5%	2.5%	2.5%
Bed Temperatures								
HDS #1 T/C #5	566°F	568°F	566°F	566°F	566°F	565°F	565°F	565°F
T/C #6	574°F	577°F	575°F	575°F	577°F	575°F	575°F	575°F
HDS #2 T/C #9	564°F	566°F	566°F	564°F	564°F	561°F	560°F	560°F
T/C #10	573°F	571°F	572°F	573°F	572°F	571°F	569°F	569°F
HDS #3 T/C #14	567°F	567°F	567°F	569°F	565°F	564°F	564°F	563°F
T/C #15	577°F	577°F	576°F	577°F	575°F	575°F	575°F	575°F
Pressures								
HDS In	-2.0 psig	-2.0 psig	-2.0 psig	-2.0 psig	-2.0 psig	-2.0 psig	-2.1 psig	-2.0 psig
HDS Out	-2.0 psig	-2.0 psig	-2.0 psig	-2.0 psig	-2.0 psig	-2.0 psig	-2.1 psig	-2.0 psig
Sulfur Concentration								
Out of Sulfurizer	29.0 ppm	29.8 ppm	30.7 ppm	30.1 ppm	30.2 ppm	30.7 ppm	29.4 ppm	27.7 ppm
In Bed 1	18.4 ppm	23.4 ppm	18.2 ppm	19.3 ppm	15.4 ppm	25.4 ppm	17.8 ppm	23.6 ppm
Exit Bed 1	9.6 ppm	11.2 ppm	11.1 ppm	11.7 ppm	11.4 ppm	13.1 ppm	11.0 ppm	16.3 ppm
Bed 2	-	3.4 ppm	3.8 ppm	2.7 ppm	4.5 ppm	3.8 ppm	7.6 ppm	7.0 ppm
Bed 3	-	0.75 ppm	0.83 ppm	1.1 ppm	1.77 ppm	1.25 ppm	1.8 ppm	1.1 ppm

Subscale Fuel Processor Catalyst Train

A fuel processor catalyst train consisting of each of the catalyst types used in the fuel processor was constructed and operated for over 2000 hours. It was constructed from standard tubing and pipe sections, instrumented for temperature and gas sampling, filled with catalyst, and connected in series. Electrical heaters maintained temperatures similar to those expected in a power plant, and a steam ejector was used to reduce the hydrodesulfurizer pressure to the power plant level expected. A schematic of the endurance train is shown in Figure 5-3, and a photograph showing the actual hardware in Figure 5-4.

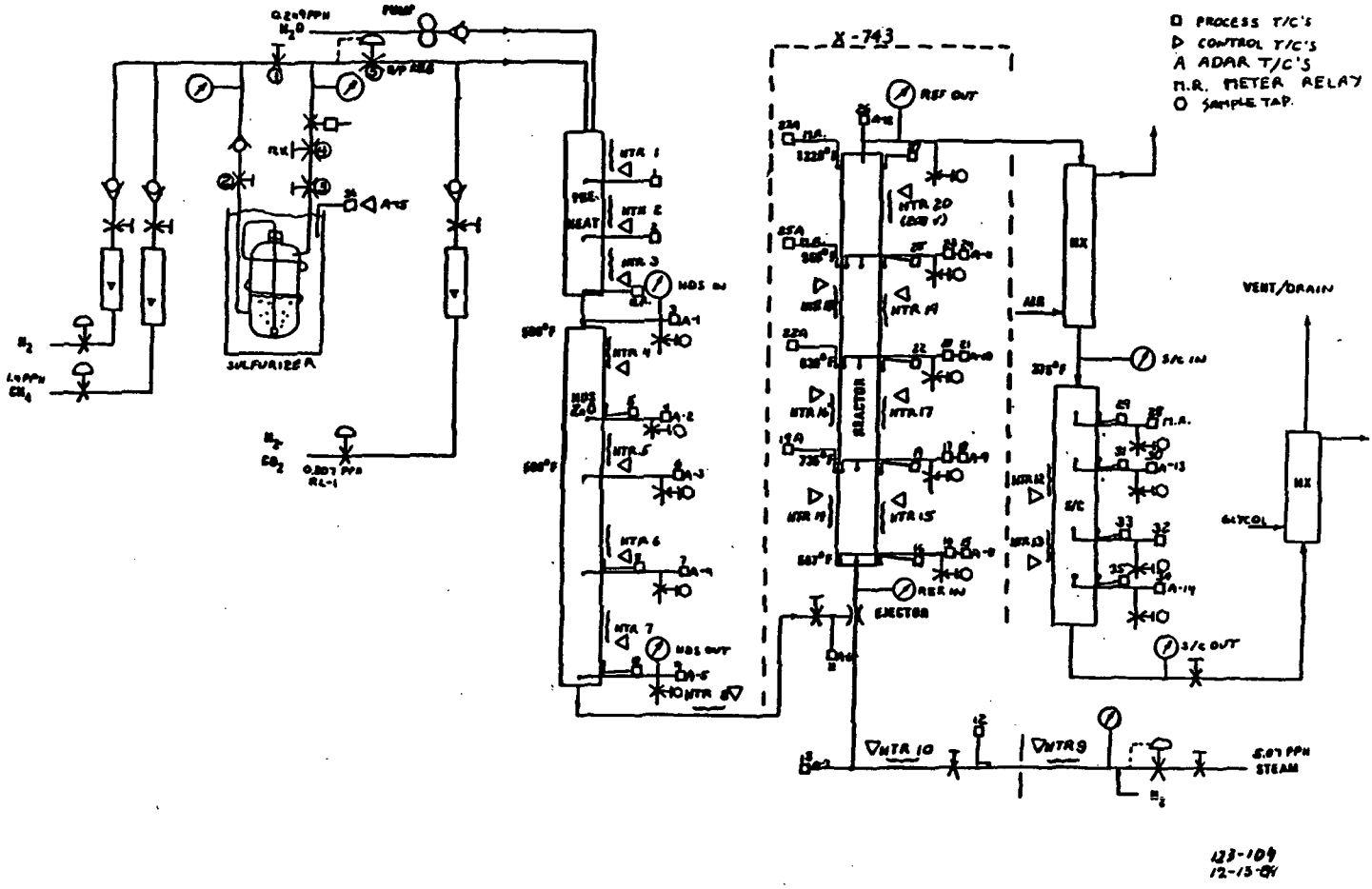

Figure 5-3. On-Site Fuel Processor Catalyst Endurance Rig

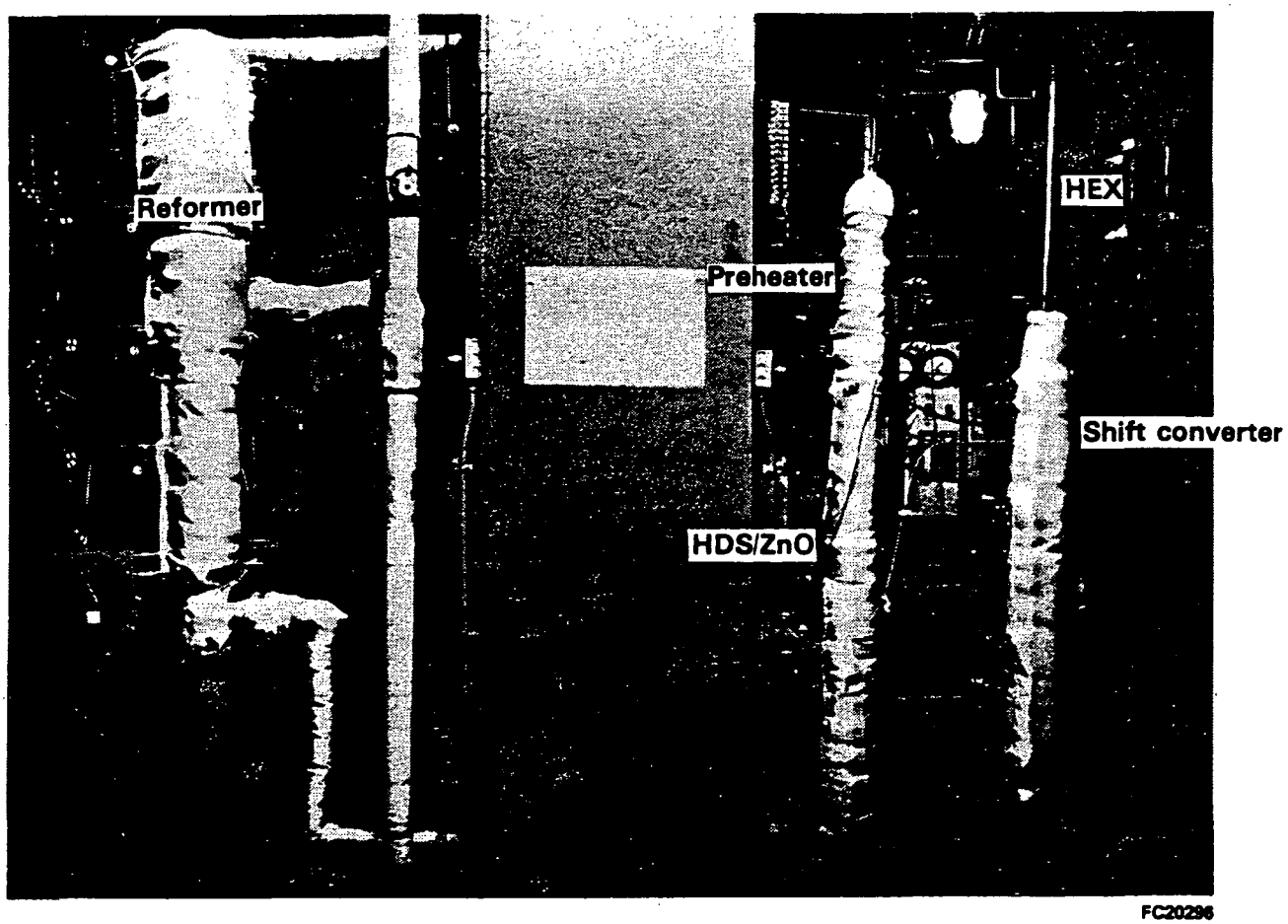

Figure 5-4. Fuel Processor Catalyst Test Hardware

During the over 2000 hours of endurance, the rig shut down a total of ten times. The first three shutdowns were to modify the heat exchanger and ejector in order to more closely match power plant conditions. Subsequent shutdowns were largely the result of facility malfunctions. A shutdown history is shown in Table 5-3.

This test qualified the hydrodesulfurizer and low pressure drop reformer catalysts selected in the previous work period, as well as an alternative shift catalyst, for use in an on-site power plant. All of the catalysts tested were stable throughout the test and demonstrated the expected activity.

The hydrodesulfurizer catalyst operation was verified at baseline conditions and at reduced recycle conditions, which would permit the use of a lower cost control system. The shift catalyst demonstrated 40% more activity at 1600 hours than the baseline catalyst at beginning of life.

Figure 5-5 shows shift conversion, reformer conversion, and hydrodesulfurizer exit sulfur concentration versus run time. Performance of all three reactors is steady with time, with undetectable sulfur exiting the desulfurizer for the entire period.

Reformer performance at 125 hours was very similar to the reformer results from catalyst screening tests completed in a previous test period (Figure 5-6). At 1958 hours, the endurance train reformer bed temperatures were adjusted to exactly match those used in a previous catalyst screening test at 120 hours. Figure 5-7 shows that the endurance test catalyst provided slightly higher fuel conversion than the previous catalyst test after 120 hours, indicating very stable reformer performance. A summary of the points run is provided in Table 5-4. Detailed gas analysis data are provided in Tables 5-5 to 5-7.

Table 5-3. Shutdown History of the Fuel Processing Endurance Test

Shutdown	Time	Date	Time on Fuel (Hrs)	Reason
1	16:45	03/23	25.5	Normal weekend S/D. Heat exchanger capacity increased during this S/D.
2	18:15	03/30	82.0	Weekend. Ejector changed.
3	18:00	04/04	91.0	Changed shift converter catalyst and replaced commercial ejector with PSD-made ejector.
			100.0	Hot hold. Decreased primary of ejector to 0.0292" diameter.
	07:00	04/16	233	Hot hold. Increased mixer of ejector to 0.12" diameter.
4	04:30	04/18	250	Auto S/D by vent system malfunction.
5	18:00	04/30	312	Auto S/D by vent system malfunction.
6	11:30	05/20	885	Auto S/D caused by loss of CH_4.
7	03:45	05/24	950	Auto S/D caused by loss of CH_4. Found loose electrical connection for CH_4 solenoid.
8	09:30	05/25	964	Manual S/D because of loss of steam.
9	08:00	06/01	984	Manual S/D because of loss of steam.
	19:00	06/26	1497	Put stand on hot hold to check faulty controller.
10	13:40	07/21	2077	Auto S/D because of loss of steam. Faulty check valve in sulfurizer resulted in ingestion of sulfur into rig.

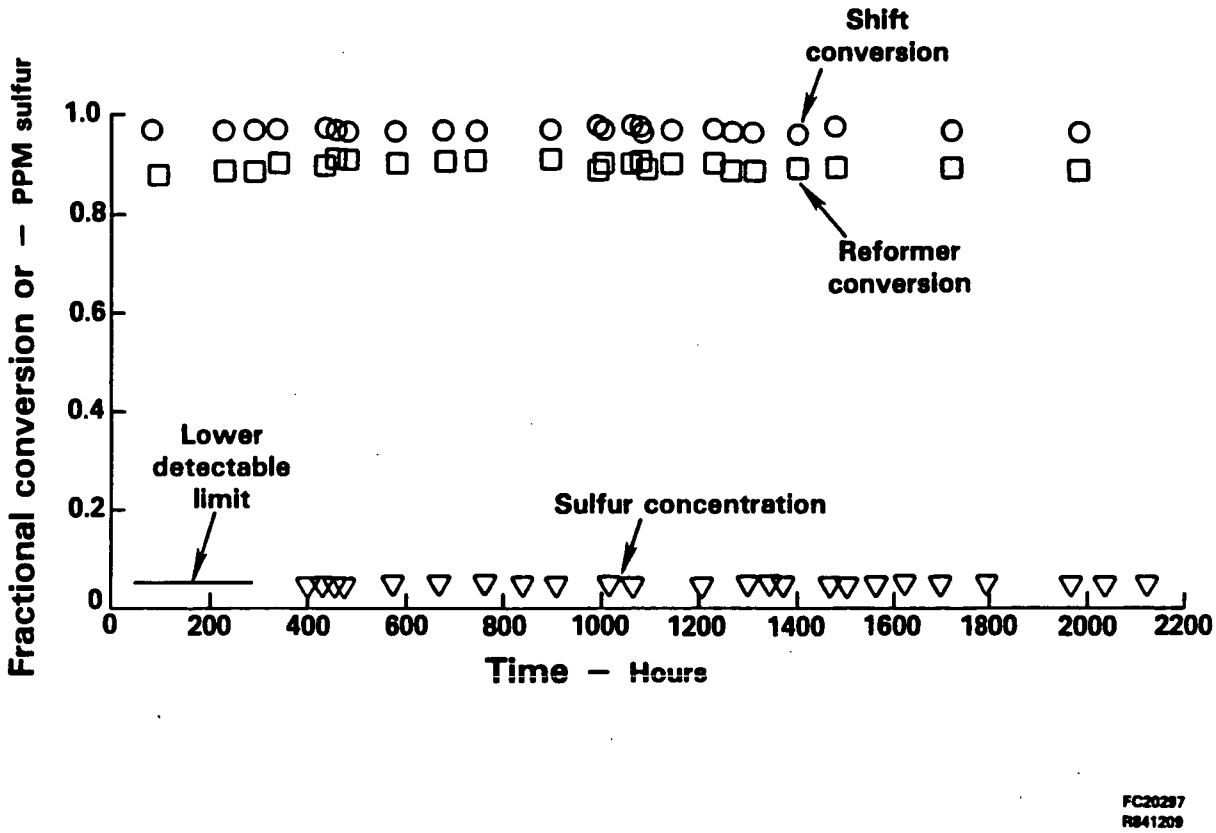

Figure 5-5. Fuel Processing Catalyst Train Performance

C-3

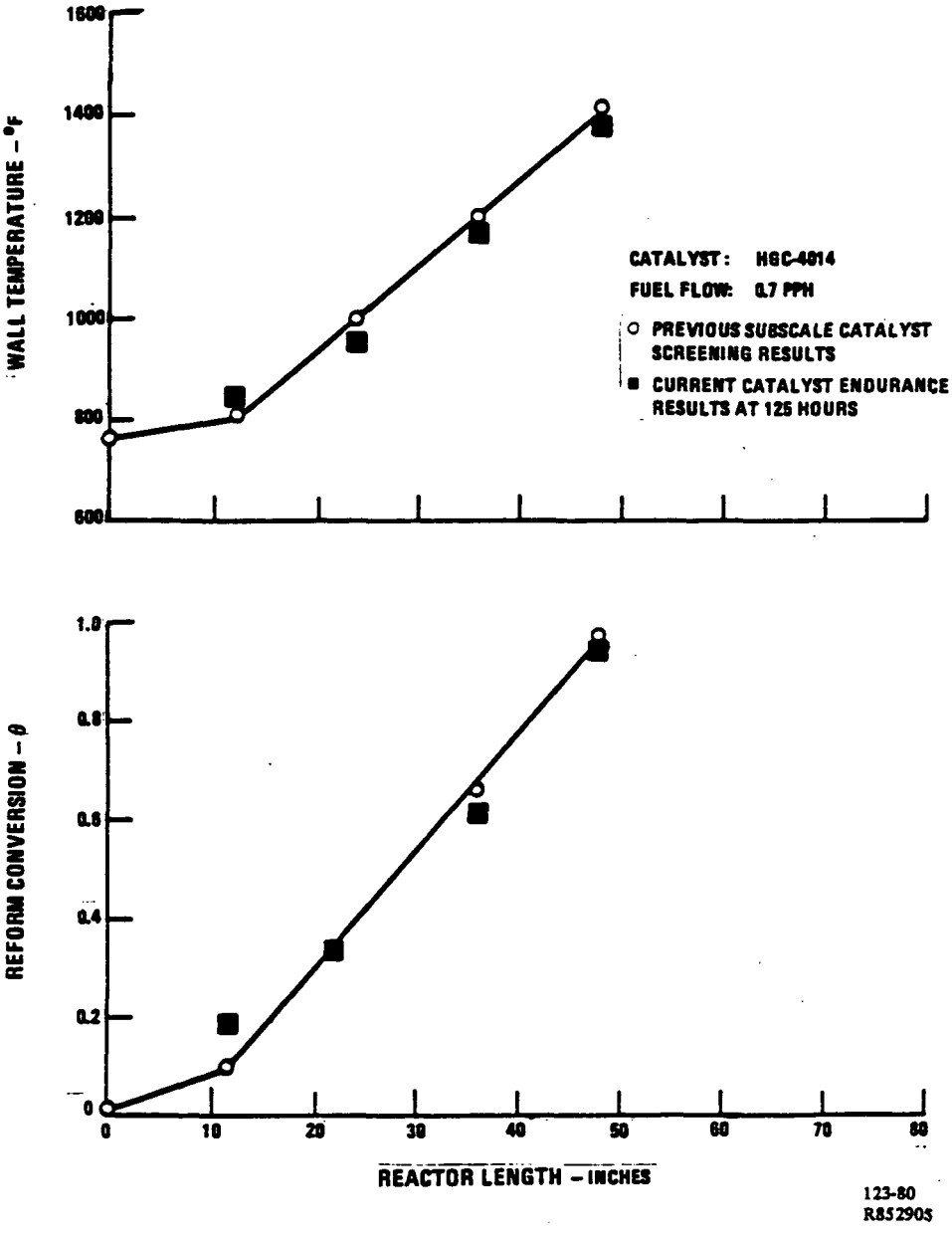

Figure 5-6. Comparison of Present and Previous Reformer Results

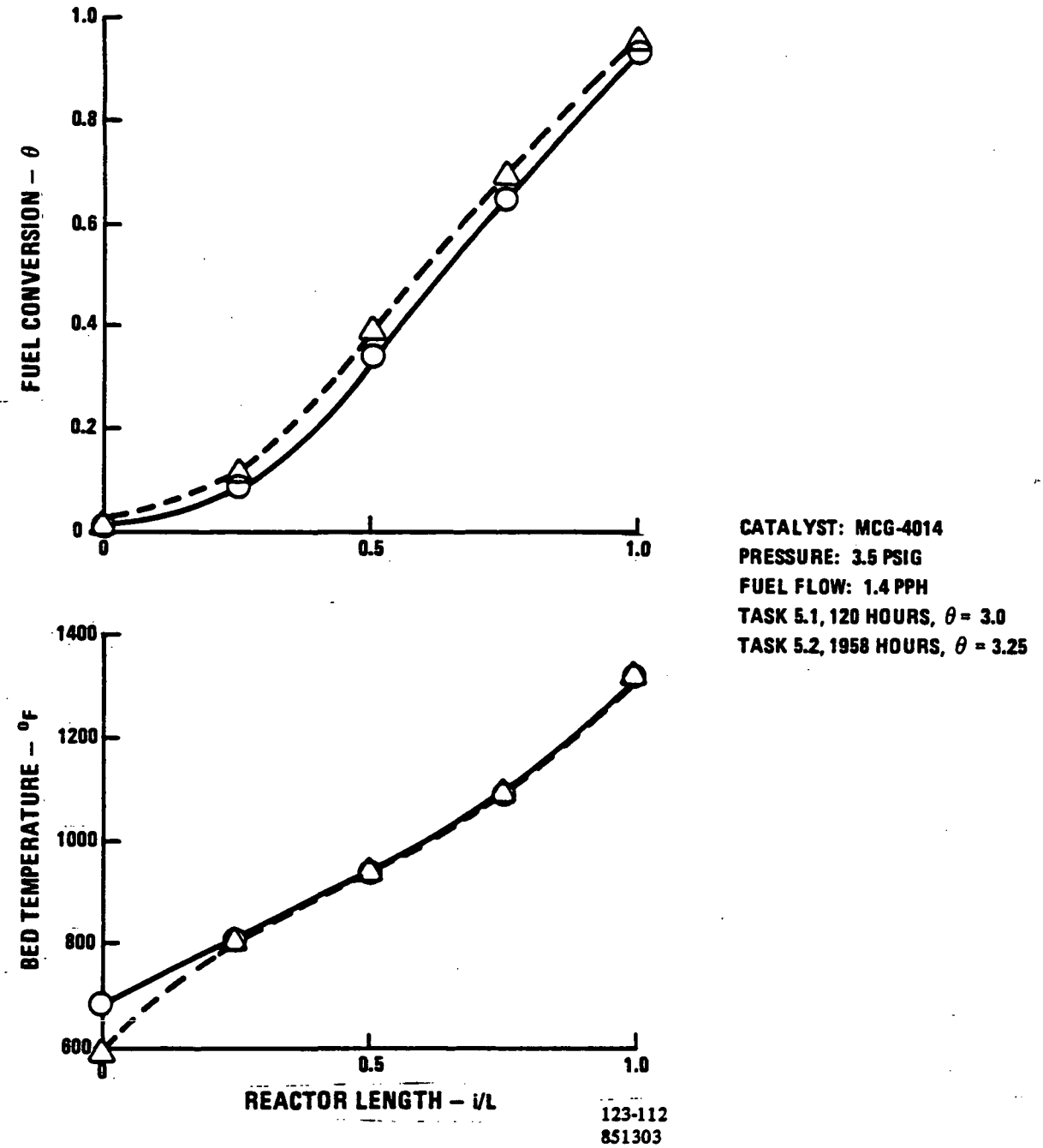

Figure 5-7. Comparison of Data from Catalyst Screening and Endurance Testing

TABLE 5-4. FUEL PROCESSOR CATALYST TRAIN OPERATING DATA

Point No.	1	2	3	4	5	6	7	8
Flows								
CH4	1.0 pph	1.4 pph	1.4 pph	1.4 pph	1.4 pph	0.7 pph	1.4 pph	1.4 pph
Steam	3.7 pph	5.1 pph	5.1 pph	5.1 pph	2.55 pph	2.55 pph	5.1 pph	5.1 pph
Recycle	0.67 pph	1.06 pph	0.73 pph	0.73 pph	0.37 pph	0.37 pph	0.73 pph	0.73 pph
Temperatures								
HDS/ZnO								
T/C 3	498°F	458°F	461°F	503°F	493°F	473°F	490°F	488°F
4	487°F	472°F	482°F	500°F	491°F	491°F	496°F	494°F
6	469°F	478°F	473°F	504°F	495°F	496°F	504°F	504°F
7	486°F	480°F	466°F	494°F	487°F	487°F	494°F	493°F
9	493°F	494°F	477°F	488°F	490°F	490°F	492°F	491°F
Reformer Beds								
T/C 15	625°F	614°F	511°F	651°F	655°F	666°F	533°F	528°F
18	735°F	747°F	747°F	749°F	754°F	751°F	752°F	753°F
21	821°F	840°F	846°F	846°F	847°F	849°F	842°F	842°F
24	903°F	982°F	1000°F	993°F	994°F	996°F	992°F	997°F
26	1216°F	1221°F	1225°F	1214°F	1212°F	1223°F	1212°F	1218°F
Reformer Walls								
T/C 16	681°F	665°F	612°F	706°F	709°F	704°F	648°F	649°F
19	846°F	818°F	855°F	835°F	822°F	814°F	870°F	877°F
22	899°F	974°F	980°F	1001°F	951°F	954°F	986°F	996°F
25	1070°F	1254°F	1246°F	1260°F	1164°F	1168°F	1265°F	1265°F
27	1500°F	1530°F	1474°F	1440°F	1347°F	1361°F	1475°F	1495°F
Shift Converter								
T/C 28	386°F	381°F	369°F	377°F	376°F	370°F	369°F	372°F
30	492°F	488°F	495°F	490°F	474°F	474°F	474°F	480°F
32	467°F	477°F	485°F	496°F	452°F	454°F	470°F	474°F
34	461°F	486°F	486°F	469°F	460°F	461°F	469°F	466°F
Pressures								
HDS In	+1.15				-1.0	-1.0	-0.9	-1.1
HDS Out	+1.13	10.0	7.2	5.0	-1.0	-1.1	-1.0	-1.2
Reformer In	5.6	9.9	13.5	5.2	1.6	1.6	5.1	5.7
Reformer Out	4.8	8.2	12.5	3.1	0.9	0.9	3.1	3.2
Shift Converter In	3.4	6.1	11.7	1.8	0.7	0.7	2.0	2.0
Run Time								
Hours	23	30	90	98	125	170	245	287
Date	3-23-84	3-28-84	4-4-84	4-9-84	4-11-84	4-13-84	4-17-84	4-19-84

TABLE 5-4. FUEL PROCESSOR CATALYST TRAIN OPERATING DATA (CONT'D)

Point No.	9	10	11	12	13	14	15	16	17
Flows									
CH4	1.4 pph	1.4 pph	1.4 pph	1.4 pph	1.4 pph	1.4 pph	1.4 pph	1.4 pph	1.4 pph
Steam	5.1 pph	5.1 pph	5.1 pph	5.1 pph	5.1 pph	5.1 pph	5.1 pph	5.1 pph	5.1 pph
Recycle	0.73 pph	0.73 pph	0.46 pph	0.31 pph	0.31 pph	0.31 pph	0.31 pph	0.31 pph	0.31 pph
Temperatures									
HDS/ZnO									
T/C 3	492°F	493°F	494°F	493°F	495°F	492°F	493°F	493°F	493°F
4	468°F	467°F	466°F	465°F	466°F	464°F	466°F	465°F	465°F
6	491°F	491°F	490°F	492°F	490°F	487°F	490°F	488°F	489°F
7	486°F	486°F	485°F	485°F	486°F	483°F	485°F	484°F	484°F
9	484°F	484°F	483°F	483°F	483°F	482°F	484°F	486°F	486°F
Reformer Beds									
T/C 15	540°F	538°F	537°F	537°F	539°F	536°F	538°F	540°F	540°F
18	750°F	754°F	750°F	750°F	750°F	753°F	753°F	750°F	750°F
21	852°F	855°F	850°F	848°F	849°F	850°F	851°F	851°F	846°F
24	994°F	991°F	995°F	997°F	997°F	995°F	997°F	998°F	997°F
26	1217°F	1218°F	1221°F	1213°F	1221°F	1220°F	1218°F	1227°F	1225°F
Reformer Walls									
T/C 16	650	648°F	650°F	659°F	657°F	658°F	659°F	659°F	658°F
19	864	867°F	867°F	874°F	872°F	877°F	875°F	872°F	872°F
22	1015°F	1016°F	1016°F	1016°F	1017°F	1016°F	1017°F	1028°F	1022°F
25	1260°F	1257°F	1262°F	1262°F	1263°F	1261°F	1263°F	1253°F	1256°F
27	1495°F	1506°F	1494°F	1484°F	1490°F	1493°F	1484°F	1485°F	1476°F
Shift Converter									
T/C 28	374°F	377°F	376°F	376°F	376°F	370°F	373°F	375°F	378°F
30	480°F	483°F	482°F	479°F	484°F	477°F	480°F	483°F	482°F
32	476°F	478°F	476°F	472°F	477°F	473°F	475°F	475°F	474°F
34	467°F	469°F	468°F	465°F	467°F	465°F	466°F	465°F	466°F
Pressures									
HDS In	-1.0	-1.0	-1.1	-1.0	-1.0	-1.0	-1.0	-1.0	-1.1
HDS Out	-1.15	-1.1	-1.2	-1.1	-1.1	-1.1	-1.1	-1.1	-1.2
Reformer In	5.3	5.4	5.0	4.9	4.9	5.2	4.9	5.2	5.1
Reformer Out	3.2	3.2	3.0	2.9	2.9	3.2	2.9	2.9	2.9
Shift Converter In	1.9	1.9	1.8	1.7	1.7	1.7	1.7	1.7	1.7
Run Time									
Hours	340	430	455	479	578	643	787	890	914
Date	4-27-84	5-1-84	5-2-84	5-3-84	5-7-84	5-10-84	5-16-84	5-21-84	5-22-84

TABLE 5-4. FUEL PROCESSOR CATALYST TRAIN OPERATING DATA (CONT'D)

Point No.	18	19	20	21	22	23	24	25	26
Flows									
CH4	1.4 pph	1.4 pph	1.4 pph	1.4 pph	1.4 pph	1.4 pph	1.4 pph	1.4 pph	1.4 pph
Steam	5.1 pph	5.1 pph	5.1 pph	5.1 pph	5.1 pph	5.1 pph	5.1 pph	5.1 pph	5.1 pph
Recycle	0.31 pph	0.31 pph	0.31 pph	0.31 pph	0.31 pph	0.31 pph	0.31 pph	0.31 pph	0.31 pph
Temperatures									
HDS/ZnO									
T/C 3	491°F	472°F	488°F	489°F	488°F	490°F	490°F	485°F	488°F
4	464°F	464°F	463°F	464°F	463°F	464°F	464°F	463°F	463°F
6	486°F	482°F	487°F	486°F	486°F	487°F	488°F	483°F	487°F
7	483°F	486°F	485°F	486°F	486°F	487°F	487°F	484°F	487°F
9	486°F	484°F	487°F	488°F	488°F	489°F	490°F	489°F	490°F
Reformer Beds									
T/C 15	538°F	539°F	537°F	539°F	540°F	539°F	541°F	539°F	540°F
18	750°F	751°F	748°F	748°F	751°F	783°F	752°F	753°F	751°F
21	850°F	852°F	848°F	851°F	853°F	849°F	851°F	849°F	849°F
24	996°F	997°F	992°F	994°F	996°F	991°F	997°F	997°F	999°F
26	1218°F	1217°F	1217°F	1223°F	1220°F	1221°F	1225°F	1223°F	1225°F
Reformer Walls									
T/C 16	654°F	654°F	653°F	656°F	658°F	656°F	658°F	658°F	658°F
19	867°F	872°F	868°F	869°F	869°F	870°F	874°F	873°F	869°F
22	1029°F	1036°F	1026°F	1028°F	1030°F	1025°F	1026°F	1025°F	1025°F
25	1253°F	1252°F	1242°F	1241°F	1241°F	1241°F	1246°F	1252°F	1239°F
27	1474°F	1473°F	1470°F	1473°F	1467°F	1471°F	1471°F	1475°F	1467°F
Shift Converter									
T/C 28	374°F	376°F	378°F	377°F	374°F	377°F	380°F	376°F	380°F
30	477°F	481°F	485°F	485°F	481°F	484°F	507°F	507°F	509°F
32	471°F	475°F	478°F	478°F	475°F	478°F	514°F	516°F	519°F
34	464°F	471°F	472°F	472°F	471°F	470°F	505°F	506°F	507°F
Pressures									
HDS In	-1.0	-1.1	-1.0	-1.0	-1.0	-1.0	-1.1	-2.76	-2.88
HDS Out	-1.1	-1.3	-1.1	-1.1	-1.1	-1.1	-1.2	-2.80	-2.98
Reformer In	5.2	4.8	4.6	4.6	4.6	4.6	4.7	4.8	4.7
Reformer Out	2.9	2.9	2.8	2.8	2.8	2.8	2.85	2.9	2.8
Shift Converter In	1.75	1.75	1.65	1.7	1.7	1.7	1.7	1.7	1.7
Run Time									
Hours	963	970	991	1039	1128	1162	1209	1306	1351
Date	5-24-84	5-31-84	6-5-84	6-7-84	6-11-84	6-12-84	6-14-84	6-18-84	6-20-84

TABLE 5-4. FUEL PROCESSOR CATALYST TRAIN OPERATING DATA (CONT'D)

Point No.	27	28	29	30	31	32	33	34
Flows								
CH4	1.4 pph	1.4 pph	1.4 pph	1.4 pph	1.4 pph	1.4 pph	1.4 pph	1.4 pph
Steam	5.1 pph	5.1 pph	5.1 pph	5.1 pph	5.1 pph	5.1 pph	5.1 pph	5.1 pph
Recycle	0.15 pph	0.15 pph	0.15 pph	0.15 pph	0.15 pph	0.15 pph	0.15 pph	0.15 pph
Temperatures								
HDS/ZnO								
T/C 3	486°F	486°F	486°F	503°F	503°F	502°F	490°F	489°F
4	461°F	462°F	461°F	499°F	499°F	498°F	465°F	463°F
6	487°F	486°F	485°F	519°F	518°F	517°F	492°F	450°F
7	487°F	486°F	486°F	499°F	498°F	498°F	487°F	486°F
9	490°F	489°F	489°F	490°F	490°F	490°F	487°F	486°F
Reformer Beds								
T/C 15	540°F	540°F	540°F	540°F	539°F	538°F	539°F	537°F
18	750°F	750°F	752°F	749°F	750°F	750°F	750°F	751°F
21	849°F	849°F	849°F	850°F	851°F	851°F	849°F	849°F
24	999°F	999°F	998°F	994°F	994°F	994°F	996°F	998°F
26	1222°F	1223°F	1221°F	1222°F	1220°F	1221°F	1220°F	1221°F
Reformer Walls								
T/C 16	659°F	660°F	660°F	658°F	657°F	656°F	656°F	656°F
19	871°F	871°F	872°F	869°F	870°F	868°F	868°F	870°F
22	1030°F	1031°F	1031°F	1034°F	1034°F	1033°F	1032°F	1031°F
25	1253°F	1253°F	1252°F	1245°F	1245°F	1248°F	1248°F	1252°F
27	1461°F	1462°F	1462°F	1478°F	1469°F	1472°F	1466°F	1470°F
Shift Converter								
T/C 28	376°F	385°F	326°F	324°F	331°F	325°F	275°F	275°F
30	484°F	493°F	416°F	420°F	440°F	424°F	301°F	300°F
32	478°F	484°F	434°F	444°F	447°F	447°F	342°F	339°F
34	467°F	469°F	419°F	429°F	437°F	437°F	398°F	396°F
Pressures								
HDS In	-3.18	-3.1	-3.14	-3.14	-3.23	-3.16	-3.14	-3.09
HDS Out	-3.25	-3.2	-3.23	-3.2	-3.3	-3.25	-3.23	-3.18
Reformer In	4.5	4.5	4.5	4.5	4.5	4.5	4.5	4.5
Reformer Out	2.7	2.7	2.7	2.8	2.7	2.75	2.75	2.7
Shift Converter In	1.6	1.6	1.6	1.7	1.7	1.65	1.65	1.6
Run Time								
Hours	1399	1472	1492	1508	1560	1621	1650	1690
Date	6-22-84	6-25-84	6-26-84	6-27-84	6-29-84	7-2-84	7-3-84	7-5-84

TABLE 5-4. FUEL PROCESSOR CATALYST TRAIN OPERATING DATA (CONT'D)

Point No.	35	36	37	38	39	40	41
Flows							
CH4	1.4 pph	1.4 pph	1.4 pph	1.4 pph	1.4 pph	1.4 pph	1.4 pph
Steam	5.1 pph	5.1 pph	5.1 pph	5.1 pph	5.1 pph	5.1 pph	5.1 pph
Recycle	0.15 pph	0.15 pph	0.15 pph	0.15 pph	0.15 pph	0.15 pph	C.15 pph
Temperatures							
HDS/ZnO							
T/C 3	488°F	489°F	489°F	488°F	488°F	488°F	489°F
4	463°F	463°F	463°F	464°F	463°F	464°F	464°F
6	490°F	491°F	491°F	490°F	490°F	491°F	491°F
7	486°F	486°F	486°F	486°F	486°F	486°F	486°F
9	486°F	486°F	486°F	487°F	486°F	487°F	487°F
Reformer Beds							
T/C 15	537°F	539°F	573°F	574°F	572°F	574°F	575°F
18	752°F	752°F	766°F	768°F	767°F	762°F	800°F
21	849°F	850°F	867°F	870°F	874°F	922°F	940°F
24	996°F	998°F	1025°F	1022°F	1030°F	1093°F	1091°F
26	1220°F	1223°F	1250°F	1249°F	1266°F	1272°F	1323°F
Reformer Walls							
T/C 16	655°F	656°F	688°F	689°F	686°F	680°F	724°F
19	872°F	871°F	888°F	890°F	888°F	889°F	957°F
22	1030°F	1033°F	1065°F	1064°F	1073°F	1181°F	1184°F
25	1252°F	1252°F	1282°F	1275°F	1287°F	1331°F	1321°F
27	1481°F	1481°F	1492°F	1499°F	1509°F	1444°F	1509°F
Shift Converter							
T/C 28	375°F	376°F	373°F	374°F	376°F	375°F	375°F
30	500°F	501°F	506°F	508°F	511°F	512°F	522°F
32	506°F	508°F	512°F	512°F	514°F	516°F	524°F
34	511°F	513°F	515°F	514°F	508°F	516°F	520°F
Pressures							
HDS In	-3.0 psig	-3.0 psig	-2.9 psig	-2.8 psig	-2.8 psig	-2.8 psig	-2.7 psig
HDS Out	-3.1 psig	-3.1 psig	-3.0 psig	-2.9 psig	-2.9 psig	-2.9 psig	-2.8 psig
Reformer In	4.6 psig	4.6 psig	4.6 psig	4.7 psig	4.7 psig	4.7 psig	4.8 psig
Reformer Out	2.9 psig	2.9 psig	2.9 psig	2.9 psig	2.9 psig	2.9 psig	2.9 psig
Shift Converter In	1.7 psig	1.7 psig	1.7 psig	1.7 psig	1.7 psig	1.7 psig	1.8 psig
Run Time							
Hours	1714	1791	1814	1833	1859	1882	1955
Date	7-6-84	7-9-84	7-10-84	7-11-84	7-12-84	7-13-84	7-16-84

TABLE 5-4. FUEL PROCESSOR CATALYST TRAIN OPERATING DATA (CONT'D)

Point No.	42	43	44	45
Flows				
CH4	1.4 pph	1.4 pph	1.4 pph	0.7 pph
Steam	5.1 pph	5.5 pph	4.33 pph	2.08 pph
Recycle	0.15 pph	0.15 pph	0.15 pph	0.15 pph
Temperatures				
HDS/ZnO				
T/C 3	489°F	488°F	488°F	486°F
4	463°F	463°F	462°F	450°F
6	490°F	490°F	488°F	485°F
7	486°F	486°F	484°F	482°F
9	486°F	487°F	486°F	483°F
Reformer Beds				
T/C 15	545°F	543°F	540°F	504°F
18	752°F	750°F	751°F	753°F
21	850°F	849°F	848°F	851°F
24	997°F	995°F	994°F	992°F
26	1220°F	1219°F	1221°F	1217°F
Reformer Walls				
T/C 16	656°F	656°F	648°F	599°F
19	867°F	867°F	861°F	838°F
22	1031°F	1036°F	1019°F	959°F
25	1247°F	1252°F	1242°F	1142°F
27	1484°F	1484°F	1505°F	1375°F
Shift Converter				
T/C 28	376°F	374°F	375°F	377°F
30	501°F	494°F	519°F	525°F
32	507°F	503°F	520°F	511°F
34	513°F	510°F	519°F	511°F
Pressures				
HDS In	-3.05 psig	-3.05 psig	-2.7 psig	-2.65 psig
HDS Out	-3.15 psig	-3.15 psig	-2.8 psig	-2.7 psig
Reformer In	4.6 psig	5.0 psig	3.75 psig	1.2 psig
Reformer Out	2.9 psig	3.1 psig	2.3 psig	0.6 psig
Shift Converter In	1.7 psig	1.8 psig	1.4 psig	0.5 psig
Run Time				
Hours	1980	2004	2026	2053
Date	7-17-84	7-18-84	7-19-84	7-20-84

Table 5-5. Fuel Processor Catalyst Train Gas Analysis Results 4/4/84

POINT NO: 3
DATE: 4-4-84
TIME ON FUEL: 90 HOURS

FUEL FLOW: 1.4 PPH
STEAM FLOW: 5.1 PPH
RECYCLE FLOW: 0.73 PPH

GAS ANALYSIS (MOLE FRACTION DRY)

Reformer	Bed Temp.	CO	CO2	CH4	θ	ψ
Tap 1	747°F	-	-	-		
Tap 2	846°F	-	-	-		
Tap 3	1000°F	-	-	-		
Tap 4	1225°F	-	-	-		
Shift Converter						
Tap 1	369°F	0.112	0.118	0.0420	0.846	0.513
Tap 2	495°F	0.0244	0.187	0.0410	0.838	0.885
Tap 3	485°F	0.0076	0.201	0.0402	0.838	0.964
Tap 4	486°F	-	-	-		

$$\theta = \frac{CO + CO2}{CO + CO2 + CH4}$$

$$\psi = \frac{CO2}{CO + CO2}$$

Table 5-6. Fuel Processor Catalyst Train Gas Analysis Results 4/9/84

POINT NO: 4
DATE: 4-9-84
TIME ON FUEL: 98 HOURS

FUEL FLOW: 1.4 PPH
STEAM FLOW: 5.1 PPH
RECYCLE FLOW:0.73 PPH

GAS ANALYSIS (MOLE FRACTION DRY)

Reformer	Bed Temp.	CO	CO2	CH4	θ	ψ
Tap 1	749°F	0.0011	0.111	0.572	0.164	0.990
Tap 2	846°F	0.0054	0.144	0.384	0.280	0.964
Tap 3	993°F	0.0309	0.136	0.0312	0.881	0.588
Tap 4	1214°F	0.0952	0.136	0.0312	0.881	0.588
Shift Converter						
Tap 1	377°F	0.0946	0.136	0.0316	0.879	0.590
Tap 2	490°F	0.0116	0.202	0.0296	0.878	0.946
Tap 3	496°F	0.00507	0.208	0.0295	0.878	0.976
Tap 4	469°F	0.00405	0.208	0.0294	0.878	0.981

$$\theta = \frac{CO + CO2}{CO + CO2 + CH4}$$

$$\psi = \frac{CO2}{CO + CO2}$$

Table 5-7. Fuel Processor Catalyst Train Gas Analysis Results 4/11/84

POINT NO: 5
DATE: 4-11-84
TIME ON FUEL: 125 HOURS

FUEL FLOW: 0.7 PPH
STEAM FLOW: 2.55 PPH
RECYCLE FLOW: 0.37 PPH

GAS ANALYSIS (MOLE FRACTION DRY)

Reformer	Bed Temp.	CO	CO2	CH4	θ	ψ
Tap 1	754°F	0.0015	0.118	0.505	0.191	0.987
Tap 2	847°F	0.0068	0.150	0.320	0.330	0.957
Tap 3	994°F	0.0333	0.169	0.128	0.612	0.835
Tap 4	1212°F	0.0997	0.132	0.0165	0.934	0.570
Shift Converter						
Tap 1	376°F	0.100	0.133	0.0162	0.935	0.571
Tap 2	474°F	0.00672	0.214	0.0141	0.940	0.970
Tap 3	452°F	0.00353	0.217	0.0144	0.939	0.984
Tap 4	460°F	0.00414	0.200	0.0133	0.939	0.980

$$\theta = \frac{CO + CO2}{CO + CO2 + CH4}$$

$$\psi = \frac{CO2}{CO + CO2}$$

Results of low temperature shift converter catalyst tests indicate that the HGC-4015 shift catalyst is more active than the baseline catalyst. Figure 5-8 compares the measured performance obtained at the different shift converter inlet temperatures with the calculated performance computed for an adiabatic bed containing catalyst 1.4 times as active as fresh baseline shift converter catalyst. The measured data follow the calculated curves very closely, indicating that the HGC-4015 catalyst is about 40% more active than the baseline catalyst, and is more than adequate as an alternative catalyst for the power plant.

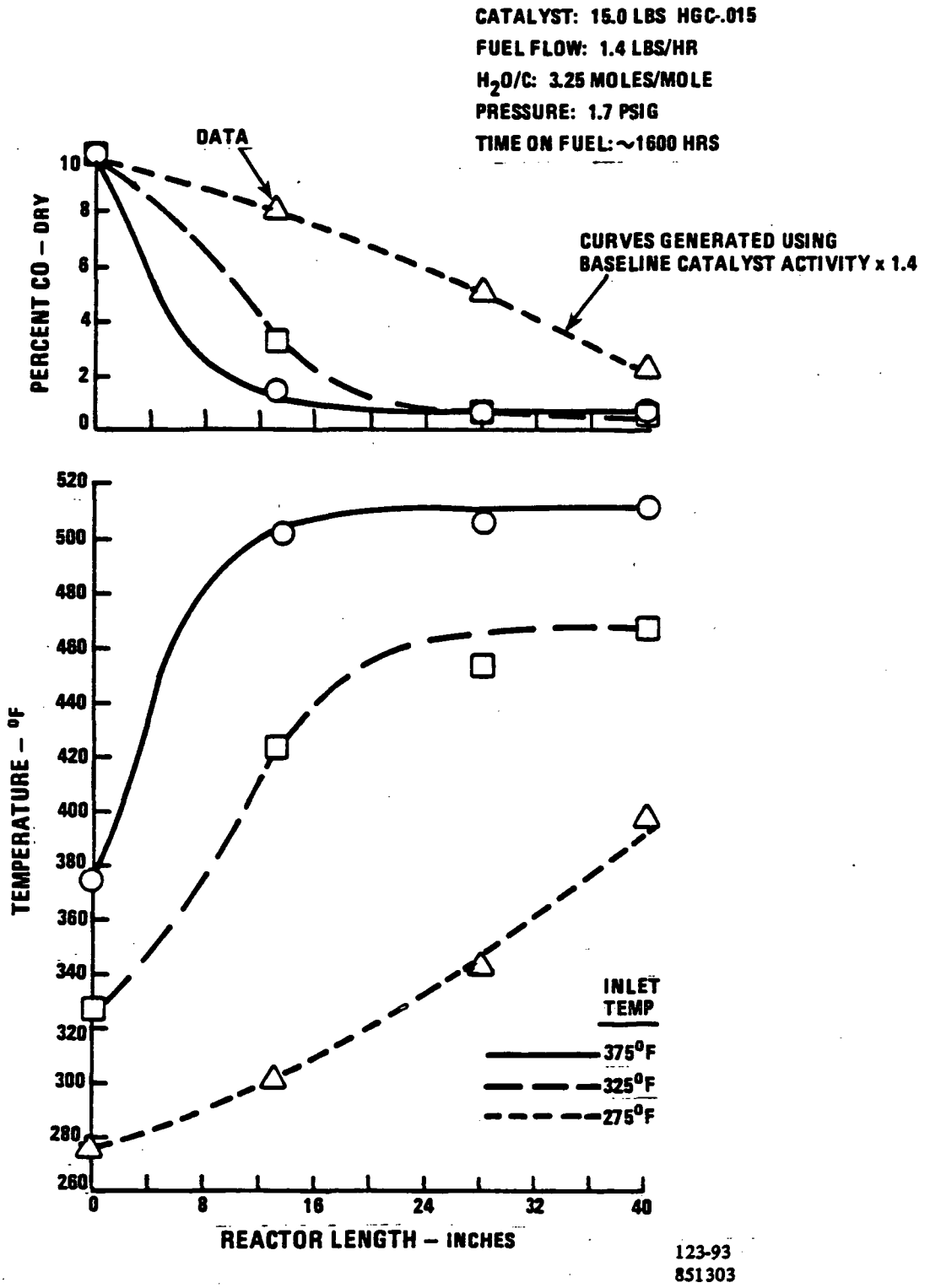

Figure 5-8. Shift Converter Performance

The PSD-12 desulfurizer catalyst showed no decay throughout the initial 2077 hours of the endurance test. Changing recycle and reactor pressure had a slight effect on catalyst activity; however, a major upset in performance occurred at 2077 hours when the rig shut down automatically because of loss of steam. Subsequently, an N_2 flow loss depressurized the sulfurizer and a faulty check valve on the sulfurizer (see Figure 5-3) leaked liquid thiophane onto the catalyst. This resulted in poisoning of the reformer and shift converter as well as the hydrodesulfurizer catalyst. Both reformer and shift converter catalysts were poisoned to the extent that they could no longer perform their function; however, the hydrodesulfurizer was still capable of desulfurizing the fuel to less than detectable sulfur levels (less than 0.05 parts per million).

Catalyst activity for the first section of catalyst is plotted in Figure 5-9. The present test conditions at 600°F, 2% recycle and -4.0 PSIG are the most severe conditions expected to be encountered in a standard power plant. This test is continuing in order to obtain performance data over a broader range of operating conditions. A summary of the test results obtained with PSD-12 is tabulated in Table 5-8, including the extended points (marked "E") from the continuation of the test after the endurance train shutdown. The points listed in this table correspond to an equivalent gas analysis point; therefore, some points appear to be missing while in other cases they appear to be listed more than once. This test will continue into 1985.

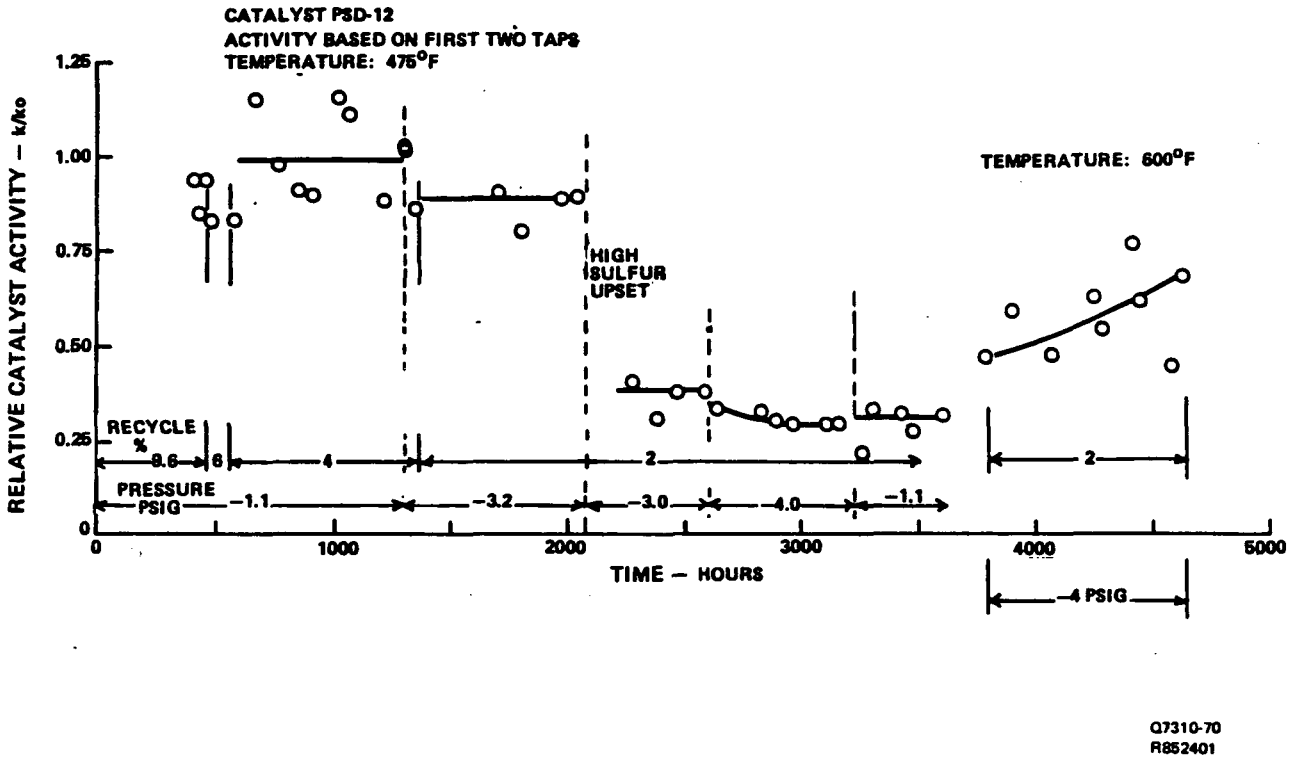

Figure 5-9. PSD-12 Hydrodesulfurizer Performance

TABLE 5-8. PSD-12 FUEL PROCESSOR CATALYST TRAIN DESULFURIZER RESULTS

Point No.	9	10	10	11	13	14	15	15
Date	4-30-84	5-1-84	5-2-84	5-3-84	5-7-84	5-11-84	5-18-84	5-18-84
Time on Fuel	405 Hours	427 Hours	452 Hours	477 Hours	572 Hours	667 Hours	765 Hours	839 Hours
Bed Temperatures								
T/C #3	492°F	495°F	494°F	497°F	493°F	496°F	493°F	498°F
T/C #4	467°F	467°F	466°F	465°F	464°F	464°F	466°F	465°F
T/C #6	491°F	490°F	491°F	488°F	488°F	488°F	490°F	488°F
T/C #7	486°F	486°F	484°F	484°F	484°F	484°F	483°F	484°F
T/C #9	483°F	483°F	483°F	483°F	483°F	483°F	484°F	483°F
Pressures								
HDS In	-1.1 psig	-1.0 psig	-1.2 psig	-1.0 psig	-1.0 psig	-0.9 psig	-1.05 psig	-1.0 psig
HDS Out	-1.2 psig	-1.1 psig	-1.3 psig	-1.1 psig	-1.1 psig	-1.0 psig	-1.15 psig	-1.1 psig
Flows								
CH	1.4 pph	1.4 pph	1.4 pph	1.4 pph	1.4 pph	1.4 pph	1.4 pph	1.4 pph
Recycle	0.73 pph	0.73 pph	0.73 pph	0.46 pph	0.31 pph	0.31 pph	0.31 pph	0.31 pph
Percent Recycle	9.6%	9.6%	9.6%	6.0%	4.0%	4.0%	4%	4%
Sulfur Concentration								
In CH	25.8 ppm	27.8 ppm	28.3 ppm	27.0 ppm	27.3 ppm	34.0 ppm	26.7 ppm	25.2 ppm
Tap #1	17.0 ppm	18.5 ppm	19.9 ppm	22.4 ppm	22.1 ppm	23.1 ppm	20.9 ppm	21.0 ppm
Tap #2	0.31 ppm	0.49 ppm	0.36 ppm	0.64 ppm	0.64 ppm	0.17 ppm	0.32 ppm	0.43 ppm
Tap #3	0.05 ppm	0.05 ppm	0.05 ppm	0.05 ppm	0.05 ppm	0.05 ppm	0.05 ppm	0.05 ppm
Tap #4	-	-	-	-	-	-	-	-
Tap #5	-	-	-	-	-	-	-	-

TABLE 5-8. PSD-12 FUEL PROCESSOR CATALYST TRAIN DESULFURIZER RESULTS (CONT'D)

Point No.	17	20	21	23	24	25	26	26
Date	5-22-84	6-6-84	6-8-84	6-13-84	6-14-84	6-19-84	6-20-84	6-21-84
Time on Fuel	910 Hours	1012	1062	1203	1296	1298	1343	1372
Bed Temperatures								
T/C #3	492°F	488°F	489°F	488°F	486°F	486°F	485°F	486°F
T/C #4	464°F	463°F	463°F	463°F	463°F	463°F	462°F	461°F
T/C #6	487°F	489°F	488°F	488°F	485°F	483°F	483°F	484°F
T/C #7	483°F	484°F	486°F	485°F	485°F	484°F	484°F	485°F
T/C #9	486°F	488°F	488°F	488°F	489°F	489°F	489°F	489°F
Pressures								
HDS In	-1.05 psig	-1.2 psig	-1.05 psig	-1.23 psig	-1.16 psig	-2.8 psig	-2.81 psig	-3.18 psig
HDS Out	-1.15 psig	-1.3 psig	-1.15 psig	-1.31 psig	-1.24 psig	-2.9 psig	-2.91 psig	-3.26 psig
Flows								
CH	1.4 pph	1.4 pph	1.4 pph	1.4 pph	1.4 pph	1.4 pph	1.4 pph	1.4 pph
Recycle	0.31 pph	0.31 pph	0.31 pph	0.31 pph	0.31 pph	0.31 pph	0.31 pph	~15 pph
Percent Recycle	4%	4%	4%	4%	4%	4%	4%	2%
Sulfur Concentration								
In CH	31.0 ppm	28.1 ppm	25.3 ppm	25.3 ppm	27.3 ppm	27.3 ppm	25.5 ppm	-
Tap #1	23.5 ppm	23.3 ppm	19.6 ppm	20.6 ppm	22.0 ppm	22.0 ppm	20.6 ppm	-
Tap #2	0.51 ppm	0.17 ppm	0.17 ppm	0.48 ppm	0.28 ppm	0.29 ppm	0.53 ppm	0.92 pph
Tap #3	0.05 ppm	0.05 ppm	0.05 ppm	0.05 ppm	-	0.05 ppm	0.05 ppm	-
Tap #4	-	-	-	-	-	-	-	-
Tap #5	-	-	-	-	-	-	-	-

TABLE 5-8. PSD-12 FUEL PROCESSOR CATALYST TRAIN DESULFURIZER RESULTS (CONT'D)

Point No.	28	30	31	32	34	36	42	44	45
Date	6-25-84	6-27-84	6-29-84	7-2-84	7-5-84	7-9-84	7-16-84	7-19-84	7-26-84
Time on Fuel	1470	1504	1564	1628	1700	1797 Hours	1968 Hours	2038 Hours	2125 Hours
Bed Temperatures									
T/C #3	462°F	504°F	503°F	504°F	490°F	489°F	490°F	489°F	480°F
T/C #4	449°F	499°F	499°F	500°F	464°F	463°F	464°F	464°F	460°F
T/C #6	486°F	517°F	518°F	519°F	491°F	490°F	491°F	490°F	480°F
T/C #7	486°F	498°F	498°F	499°F	487°F	486°F	487°F	486°F	488°F
T/C #9	489°F	490°F	490°F	490°F	487°F	486°F	487°F	487°F	492°F
Pressures									
HDS In	-3.1 psig	-3.14 psig	-3.18 psig	-3.15 psig	-3.05 psig	-3.07 psig	-3.02 psig	-2.8 psig	-3.15 psig
HDS Out	-3.2 psig	-3.21 psig	-3.25 psig	-3.25 psig	-3.15 psig	-3.15 psig	-3.12 psig	-2.9 psig	-3.2 psig
Flows									
CH	1.4 pph	1.4 pph	1.4 pph	1.4 pph	1.4 pph	1.4 pph	1.4 pph	1.4 pph	0.7 pph
Recycle	.15 pph	.15 pph	.15 pph	.15 pph	.15 pph	0.15 pph	0.15 pph	0.15 pph	0.15 pph
Percent Recycle	2%	2%	2%	2%	2%	2%	2%	2%	4%
Sulfur Concentration									
In CH	30.4 ppm	30.0 ppm	29.2 ppm	26.0 ppm	22.0 ppm	28.3 ppm	25.4 ppm	26.7 ppm	131.1 ppm
Tap #1	-	22.7 ppm	22.3 ppm	21.0 ppm	17.3 ppm	22.7 ppm	17.6 ppm	23.9 ppm	-
Tap #2	1.4 ppm	.05 ppm	.05 ppm	.05 ppm	.37 ppm	0.75 ppm	0.40 ppm	0.53 ppm	-
Tap #3	0.16 ppm	-	-	-	.05 ppm	0.05 ppm	0.05 ppm	0.05 ppm	-
Tap #4	.05 ppm	-	-	-	-	-	-	-	-
Tap #5	-	-	-	-	-	-	-	-	0.05 ppm

TABLE 5-8. PSD-12 FUEL PROCESSOR CATALYST TRAIN DESULFURIZER RESULTS (CONT'D)

Point No.	1E	2E	3E	4E	5E	6E	7E
Date	09-12-84	09-17-84	9-20-84	9-25-84	9-27-84	10-5-84	10-8-84
Time on Fuel	2272 Hours	2393 Hours	2484 Hours	2585 Hours	2633 Hours	2824 Hours	2893 Hours
Bed Temperatures							
T/C #3	478°F	488°F	488°F	488°F	488°F	490°F	486°F
T/C #4	476°F	463°F	463°F	462°F	461°F	461°F	461°F
T/C #6	471°F	484°F	487°F	490°F	484°F	486°F	487°F
T/C #7	478°F	484°F	487°F	486°F	485°F	484°F	487°F
T/C #9	474°F	483°F	484°F	484°F	483°F	484°F	484°F
Pressures							
HDS In	-2.9	-2.95	-2.42	-2.9	-3.9	-3.9	-3.9
HDS Out	-3.0	-3.05	-2.55	-3.0	-4.0	-3.95	-4.0
Flows (PPH)							
CH4	1.4	1.4	1.4	1.4	1.4	1.4	1.4
Recycle	0.15	0.15	0.15	0.15	0.15	0.15	0.15
Percent Recycle	2%	2%	2%	2%	2%	2%	2%
Sulfur Concentration (PPM)							
In CH4	29.4	29.0	29.6	30.8	28.1	32.0	27.0
Tap #1	28.3	30.1	24.3	26.8	20.4	20.4	17.1
Tap #2	4.4	8.2	4.9	5.4	5.0	5.1	4.8
Tap #3	0.71	1.6	1.1	0.86	1.0	1.4	1.0
Tap #4	$\leq$ 0.05	$\leq$ 0.05	$\leq$ 0.05	$\leq$ 0.05	$\leq$ 0.05	$\leq$ 0.05	$\leq$ 0.05
Tap #5	-	-	-	-	-	-	-

TABLE 5-8. PSD-12 FUEL PROCESSOR CATALYST TRAIN DESULFURIZER RESULTS (CONT'D)

Point No.	8E	9E	10E	11E	12E	13E
Date	10-11-84	10-17-84	10-19-84	10-23-84	10-25-84	10-30-84
Time on Fuel	2967 Hours	3110 Hours	3159 Hours	3255 Hours	3303 Hours	3427 Hours
Bed Temperatures						
T/C #3	485°F	486°F	486°F	490°F	486°F	486°F
T/C #4	460°F	460°F	460°F	460°F	460°F	460°F
T/C #6	486°F	487°F	487°F	486°F	488°F	491°F
T/C #7	486°F	487°F	486°F	486°F	487°F	486°F
T/C #9	483°F	489°F	483°F	483°F	484°F	484°F
Pressures						
HDS In	-3.9	-4.0	-3.9	-1.0	-0.95	-1.0
HDS Out	-3.95	-4.1	-4.0	-1.1	-1.05	-1.1
Flows (PPH)						
CH4	1.4	1.4	1.4	1.4	1.4	1.4
Recycle	0.15	0.15	0.15	0.15	0.15	0.15
Percent Recycle	2%	2%	2%	2%	2%	2%
Sulfur Concentration (PPM)						
In CH4	27.0	28.0	27.6	36.0	30.4	30.4
Tap #1	17.5	15.8	15.1	27.6	22.6	24.6
Tap #2	5.1	4.5	4.3	11.1	5.5	6.3
Tap #3	1.7	1.4	1.4	2.5	0.63	0.5
Tap #4	< 0.05	0.30	< 0.05	< 0.05	< 0.05	< 0.05
Tap #5	-	< 0.05	-	-	-	-

TABLE 5-8. PSD-12 FUEL PROCESSOR CATALYST TRAIN DESULFURIZER RESULTS (CONT'D)

Point No.	14E	15E	16E	17E	18E	19E	20E	21E
Date	11-1-84	11-6-84	11-8-84	11-15-84	11-20-84	11-27-84	12-4-84	12-6-84
Time on Fuel	3472 Hours	3571 Hours	3619 Hours	3785 Hours	3901 Hours	4071 Hours	4241 Hours	4285 Hours
Bed Temperatures								
T/C #3	485°F	483°F	486°F	602°F	601°F	600°F	600°F	599°F
T/C #4	459°F	457°F	457°F	601°F	599°F	598°F	600°F	598°F
T/C #6	487°F	488°F	488°F	600°F	598°F	600°F	597°F	599°F
T/C #7	486°F	486°F	486°F	603°F	604°F	604°F	604°F	604°F
T/C #9	483°F	481°F	482°F	601°F	602°F	602°F	602°F	602°F
Pressures								
HDS In	-1.0	-1.0	-1.0	-4.0 psig	-4.0 psig	-4.0 psig	-4.0 psig	-4.0 psig
HDS Out	-1.1	-1.1	-1.1	-4.1 psig	-4.1 psig	-4.1 psig	-4.1 psig	-4.1 psig
Flows (PPH)								
CH4	1.4	1.4	1.4	1.4	1.4	1.4	1.4	1.4
Recycle	0.15	0.15	0.15	0.15	0.15	0.15	0.15	0.15
Percent Recycle	2%	2%	2%	2%	2%	2%	2%	2%
Sulfur Concentration (PPM)								
In CH4	27.0	27.2	30.0	30.6	28.2	27.5	30.5	30.5
Tap #1	20.1	17.3	22.4	16.3	18.7	17.7	23.4	22.0
Tap #2	5.9	5.3	5.5	2.2	2.3	2.4	1.6	2.2
Tap #3	0.79	0.70	0.8	0.05	0.4	0.7	1.1	0.8
Tap #4	< 0.05	< 0.05	< 0.05	-	-	0.05	0.05	0.05
Tap #5	-	-	-	-	-	-	-	-

TABLE 5-8. PSD-12 FUEL PROCESSOR CATALYST TRAIN DESULFURIZER RESULTS (CONT'D)

Point No.	22E	23E	24E	25E
Date	12/11/84	12-13-84	12-18-84	12-20-84
Time on Fuel	4407 Hours	4455 Hours	4579 Hours	4623 Hours
Bed Temperatures				
T/C #3	602°F	600°F	599°F	598°F
T/C #4	598°F	598°F	598°F	598°F
T/C #6	599°F	600°F	599°F	601°F
T/C #7	604°F	605°F	604°F	604°F
T/C #9	602°F	602°F	602°F	602°F
Pressures				
HDS In	-4.0	-4.0	-4.0	-4.0 psig
HDS Out	-4.1	-4.1	-4.1	-4.1 psig
Flows (PPH)				
CH4	1.4	1.4	1.4	1.4
Recycle	0.15	0.15	0.15	0.15
Percent Recycle	2%	2%	2%	2%
Sulfur Concentration (PPM)				
In CH4	30.3	29.3	30.5	29.4
Tap #1	21.0	22.2	24.4	25.6
Tap #2	0.80	1.6	3.7	1.4
Tap #3	0.5	0.6	1.8	0.7
Tap #4	$\leq$ 0.05	$\leq$ 0.05	$\leq$ 0.05	$\leq$ 0.05
Tap #5	-	-	-	-

Subtask 5.3 Verify Reformer Technology

Objective

The objective of this subtask is to demonstrate the operational capabilities of the on-site reformer configuration and generate performance data for system integration. A development reformer will be fabricated, taking into account the low pressure drop characteristics of the reforming catalyst chosen in a screening test completed in a previous work period. A low-cost industrial burner will be selected and modified as required to meet the reformer requirements. The reformer configuration will duplicate material selections, heat transfer, and pressure drop required for the baseline system. A test facility will be modified to accept the development reformer.

Highlights

- An industrial burner was selected for the development reformer and verification testing was completed.
- Design of the development reformer was completed; the selected configuration has six tubes with an upfired burner.
- Fabrication of the development reformer has been completed.
- Modifications were made to an existing UTC facility in preparation for development reformer testing.

Summary

An industrial burner was selected for the development reformer and was verification tested. Modifications were made as a result of this testing to insure compliance with pressure drop and combustion efficiency requirements.

Visual flow testing was conducted using a two-dimensional model of the development reformer burner cavity. The objective of these tests was to define an acceptable burner gas flow path geometry within the reformer burner cavity that would provide uniform burner gas flow and therefore maintain uniform reformer tube temperatures. Based on these tests, the initial development reformer design was modified slightly to improve temperature uniformity.

Design and fabrication of the development reformer was completed. The selected configuration has six reformer tubes and utilizes the low pressure drop catalyst selected in a catalyst screening test completed in a previous work period. Process heat is supplied by a single up-fired industrial burner. The completed reformer is 56" in diameter by 10' high.

The development reformer test facility was designed, and construction was completed. Final stand checkouts, installation of piping insulation, plus hookup and checkout of the automatic data acquisition and retrieval (ADAR) system remain to be completed prior to test startup.

A test plan was completed and reviewed with NASA. The test plan details the test sequence and conditions required to verify that the development reformer meets design requirements over the complete range of power plant operating conditions. Specific performance objectives to be addressed include:

(1) Establish reformer heat-up characteristics
(2) Verify that fuel conversion/efficiency performance goals are met at rated power
(3) Map performance characteristics from 0% to 100% rated net power
(4) Determine allowable variations in burner air flow and steam to carbon ratio
(5) Verify that the reformer can supply sufficient hydrogen for the cell stack during an up-transient from standby to rated power
(6) Verify performance stability in a 250-hour endurance test.

The development reformer testing will start in early 1985.

Discussion

Burner Evaluation

Initial testing of an off-the-shelf industrial burner was undertaken to identify any problem areas that might require modification prior to conducting more comprehensive performance tests. The burner was operated on both natural gas and a low Btu fuel gas composition to simulate depleted anode exhaust gas. A preliminary assessment of burner ignition, heat release, turndown ratio, flame length, and temperature pattern did not reveal any major problem areas on either natural gas or low Btu fuel. Burner pressure drop was unacceptably high when burning low Btu fuel gas, however, as a result of the larger volumetric flow when operating with this fuel. Based on these test results, it was determined that this burner could not be modified sufficiently to reduce the pressure drop to acceptable levels. After consultation with the burner manufacturer, a larger burner model was selected that projects to meeting the goal pressure drops. The design of the development reformer was modified at this time to accept the larger industrial burner.

The available industrial burner, somewhat smaller than needed for the development reformer, was modified to reduce fuel pressure drop. It was also tested to verify the effectiveness of the burner modification for reducing pressure drop and to determine if the modification would compromise any other aspects of performance. The test data were obtained in an atmospheric pressure test rig.

The burner modification reduced the fuel pressure drop substantially, while other performance parameters remained acceptable. At the 200-kW flow conditions the fuel side pressure drop was 12.5 inches water compared to three psi for the as-received burner, and the air side pressure drop was 7.5 inches water, up slightly from the as-received level. Axial temperature profiles measured at the 200, 140, and

70-kW operating points, and the radial profiles at the 200-kW point, were acceptable. The turndown ratio of the burner was not affected by the reduction in the fuel side pressure drop. This was demonstrated by the stable performance observed as the air flow was increased over a range of three to one. Operation on natural gas fuel was also demonstrated to be stable over at least a three to one fuel turndown ratio.

The larger commercial burner selected for the development reformer was then procured and installed in the test stand. Modifications were made to the stand to accommodate the larger burner dimensions. In addition, a traverse system was installed to allow rapid measurement of radial and axial temperature profiles. A schematic of the test rig showing the traverse system is shown in Figure 5-10 and photographs of the larger burner installed in the stand are shown in Figure 5-11. The new traverse system consists of two traverse pusher actuators, each driving five thermocouples.

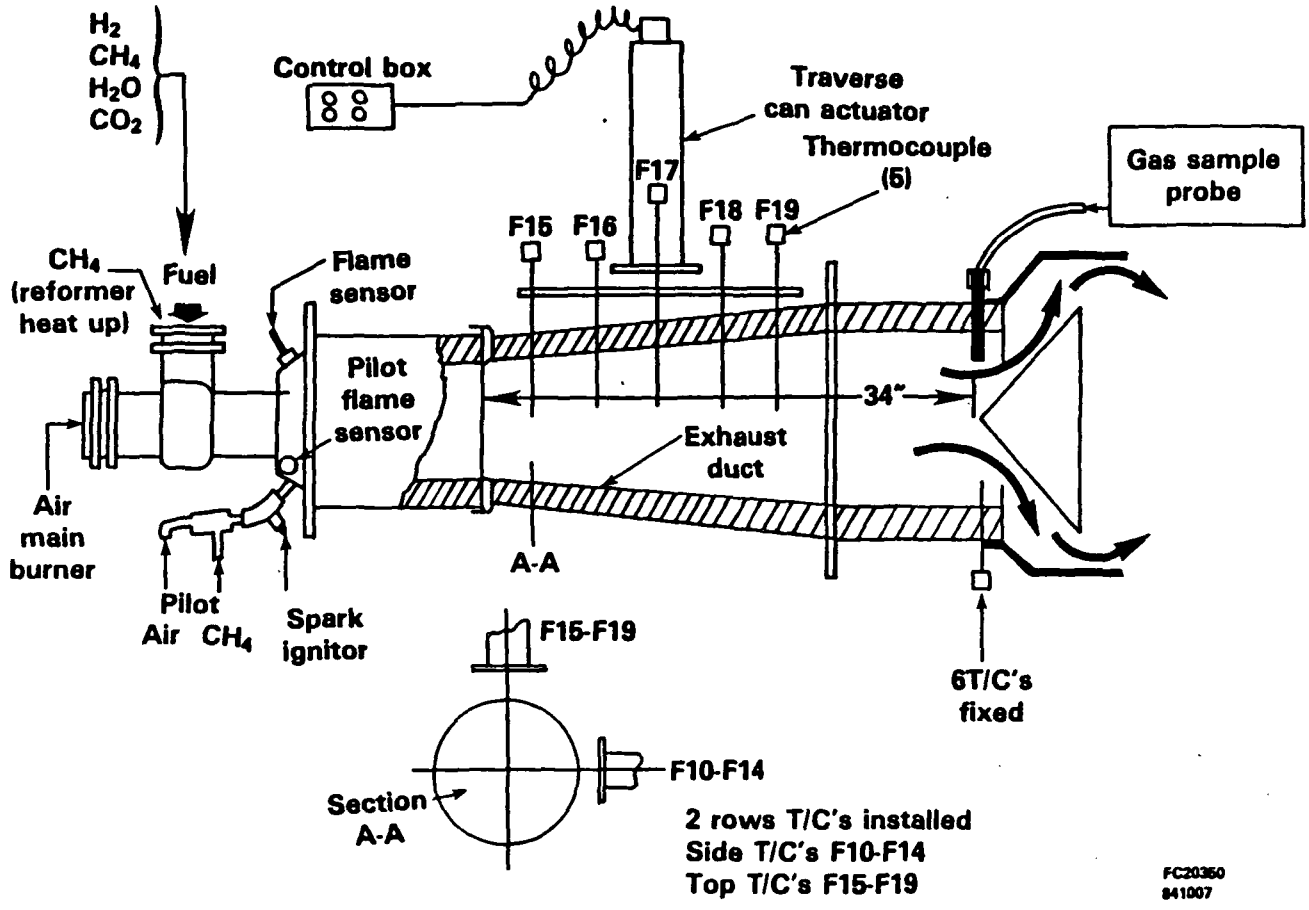

Figure 5-10. Burner Test Rig

ORIGINAL PAGE IS
OF POOR QUALITY

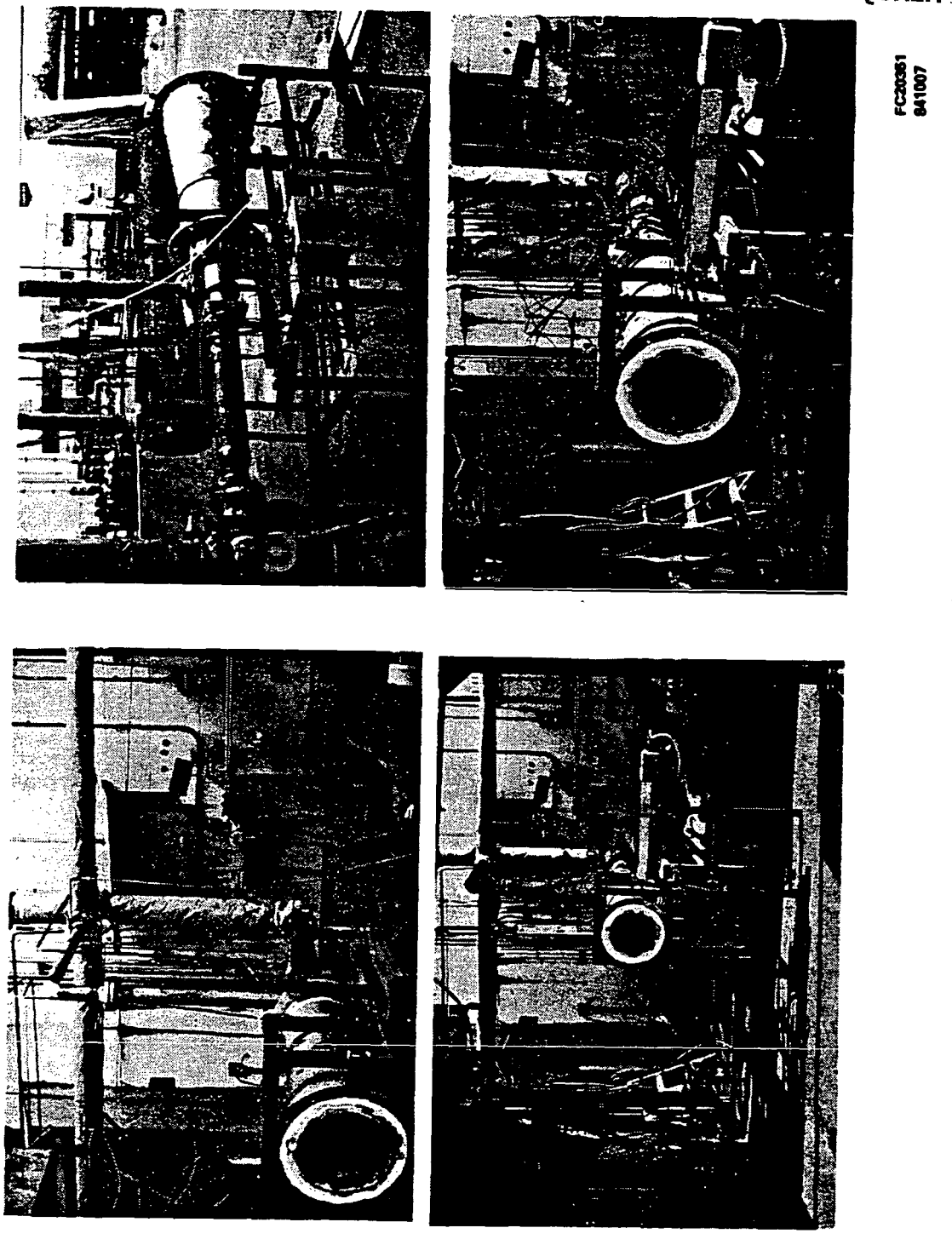

Figure 5-11. Development Reformer Burner Installed in X-704 Stand

The test results using the larger commercial burner for the development reformer are presented in Figures 5-12 through 5-19.

Burner air and fuel side pressure drop versus power level are shown compared to the modified smaller burners in Figures 5-12 and 5-13. At the 100% power point, the air side ΔP was 0.45" H_2O and the fuel side ΔP was 0.45" H_2O. Pressure drop data was obtained at both hot and cold flow conditions to assure the validity of the measurements because of the very low pressure drop involved. The data scatter for the burner air side, shown in Figure 5-12, is minimal and follows a 2 to 1 slope as expected, except for the lowest flows. The fuel side exhibited more scatter, as shown in Figure 5-13. The curve shown on the plot in Figure 5-13 is based on both the hot test data and nitrogen data point, which was corrected for the molecular weight difference.

Radial and axial temperatures provided at the 200-kW power flows are shown in Figure 5-14 for the side thermocouple traverse and in Figure 5-15 for the vertical thermocouple traverse. (Refer to Figure 5-10 for burner rig test set-up.) The profiles are similar to those obtained from the smaller commercial burner. Audio and visual characteristics observed at the maximum flow point were excellent. No discernible flame structure was visible, the exhaust being clear and clean. The burner exhibited no combustion noise, such as rumble or oscillations, and the flow appeared to be smooth and steady.

The radial and axial temperature profiles obtained on natural gas are shown in Figures 5-16 and 5-17. The radial temperature profiles graphically show the location of the flame interface and the axial distance required for complete mixing.

Testing was also conducted to establish the range of operation of the gas torch. The results obtained are shown in Figures 5-18 and 5-19. The tests were conducted at two main burner air flow settings, 482 and 300 PPH, and at various torch air and fuel settings. The figures also show the torch air and fuel pressure drops, and the flame sensor readings at each setting.

ORIGINAL PAGE IS
OF POOR QUALITY

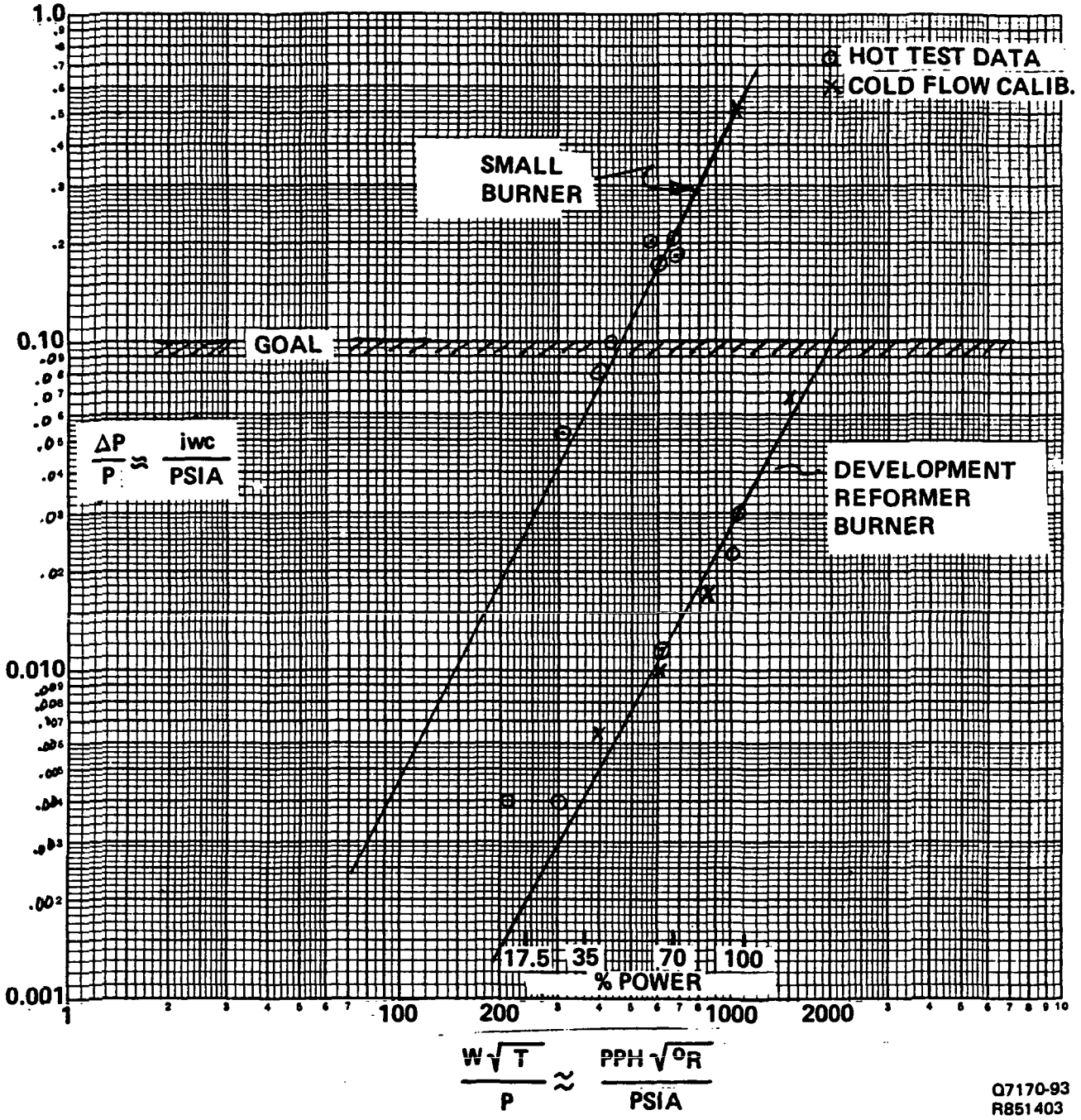

Figure 5-12. Burner Air Side Pressure Drop

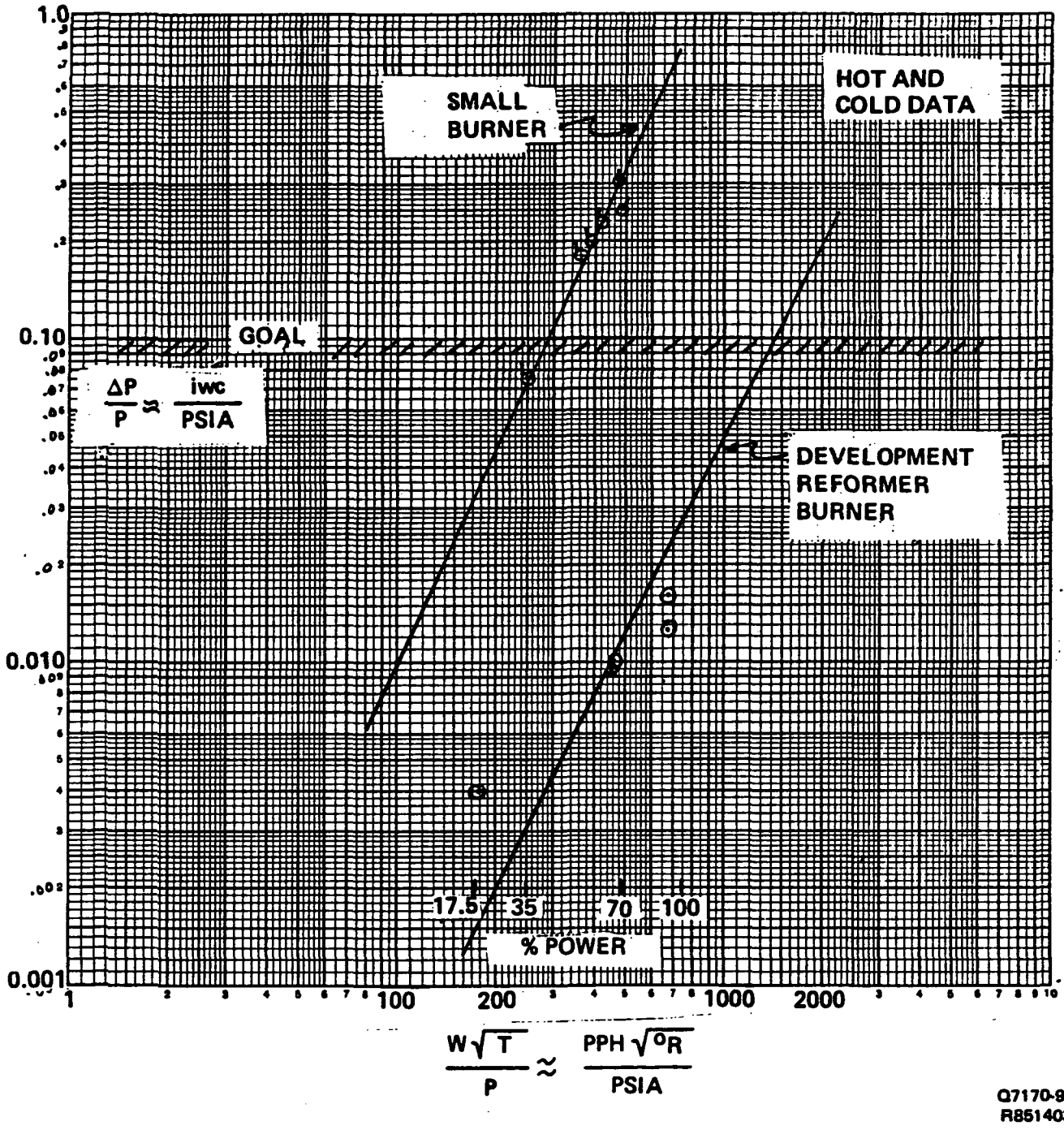

Figure 5-13. Burner Fuel Side

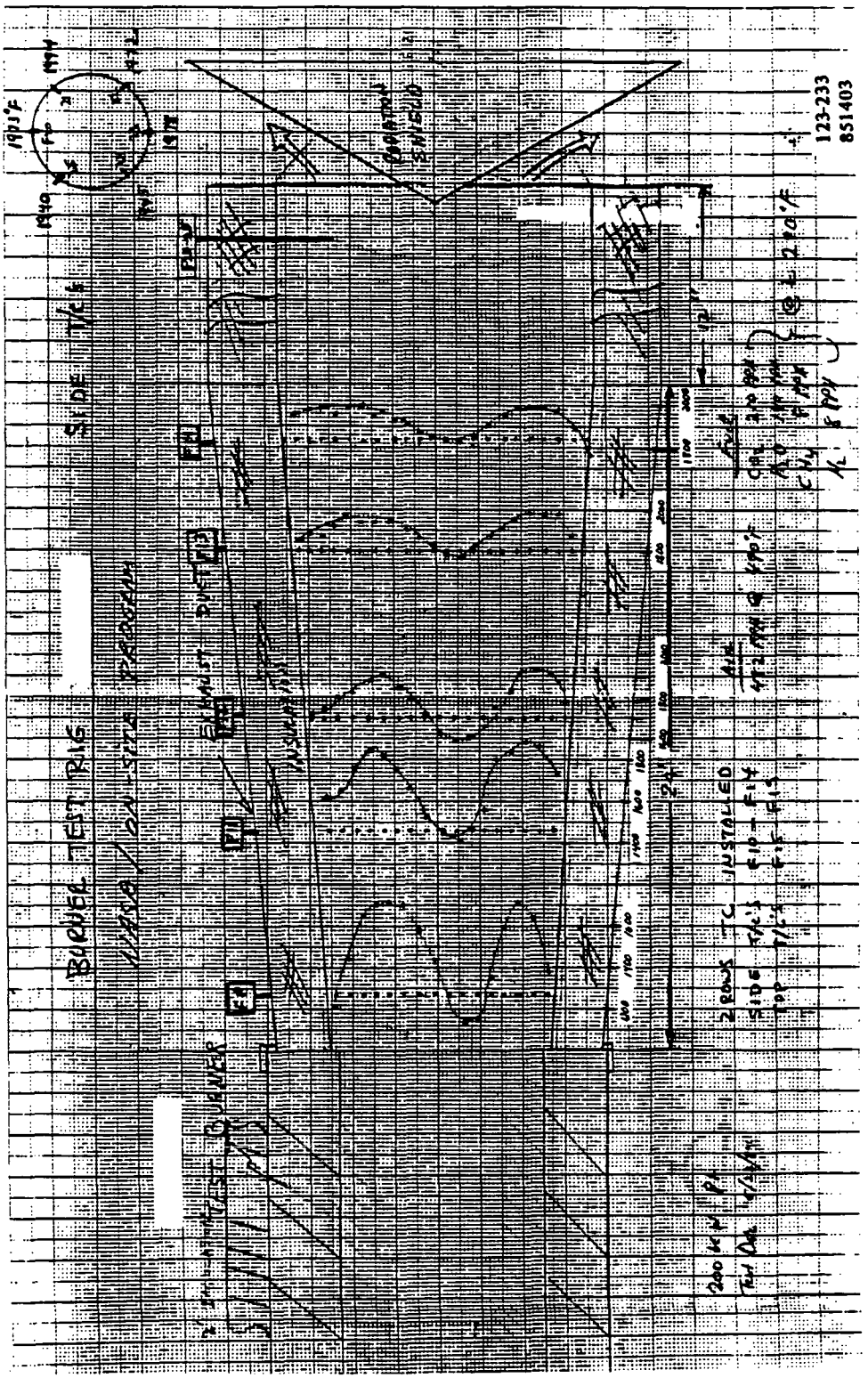

Figure 5-14. Development Reformer Burner Radial and Axial Temperature Profiles at 200 kW Flows (Side Thermocouple Traverse)

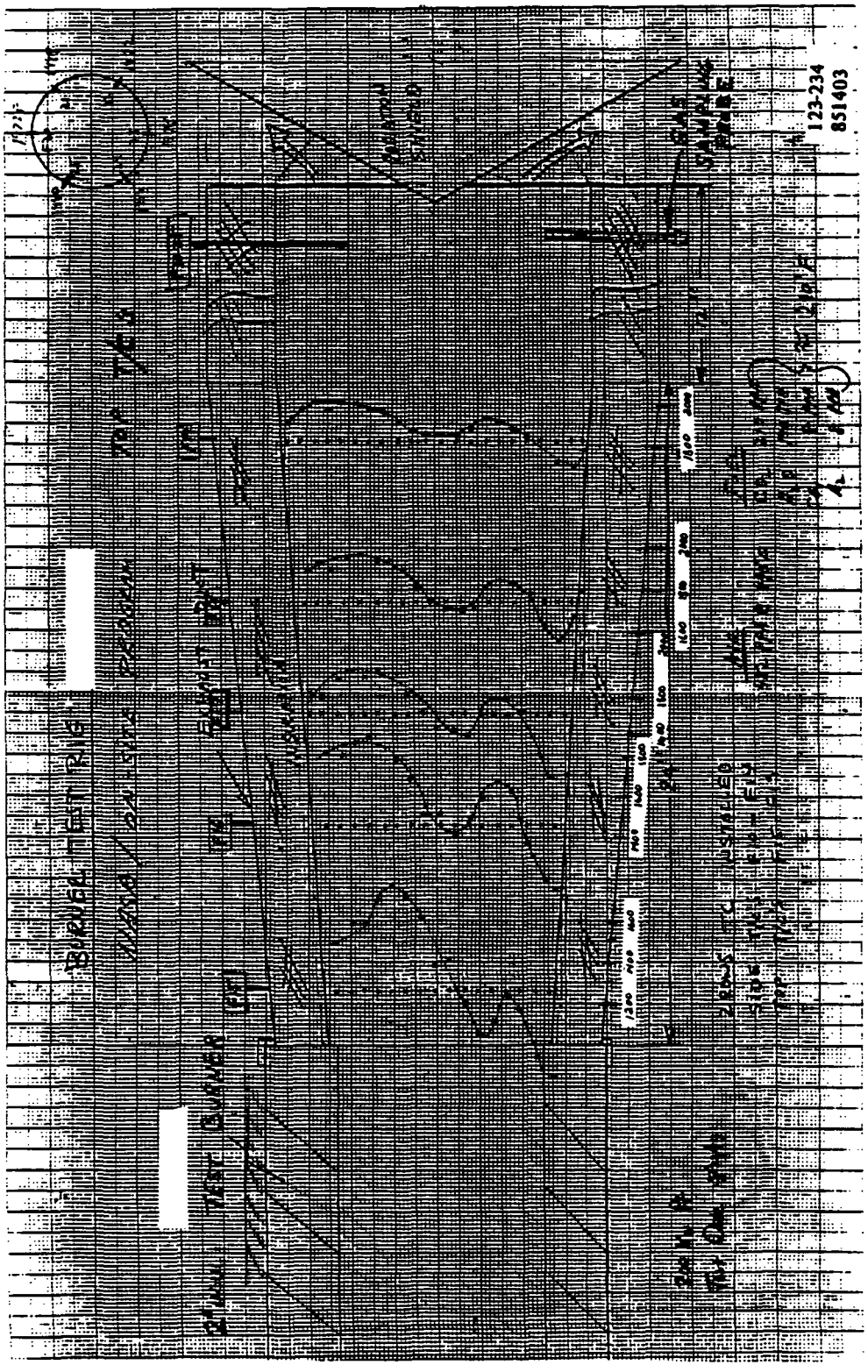

Figure 5-15. Development Reformer Burner Radial and Axial Temperature Profiles at 200 kW Flows (Vertical Thermocouple Traverse)

ORIGINAL PAGE IS
OF POOR QUALITY

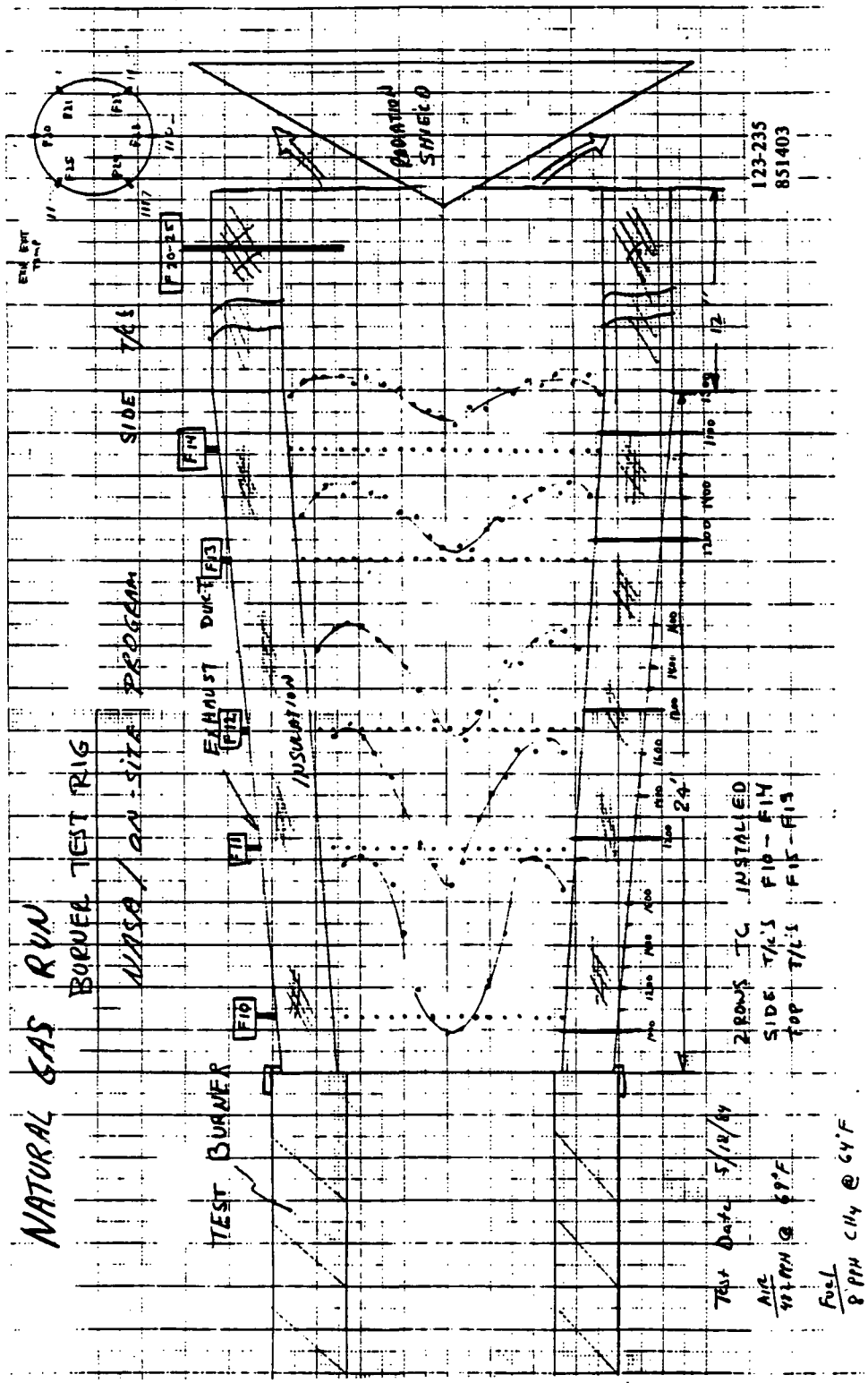

Figure 5-16. Development Reformer Burner Temperature Profiles on Natural Gas Fuel

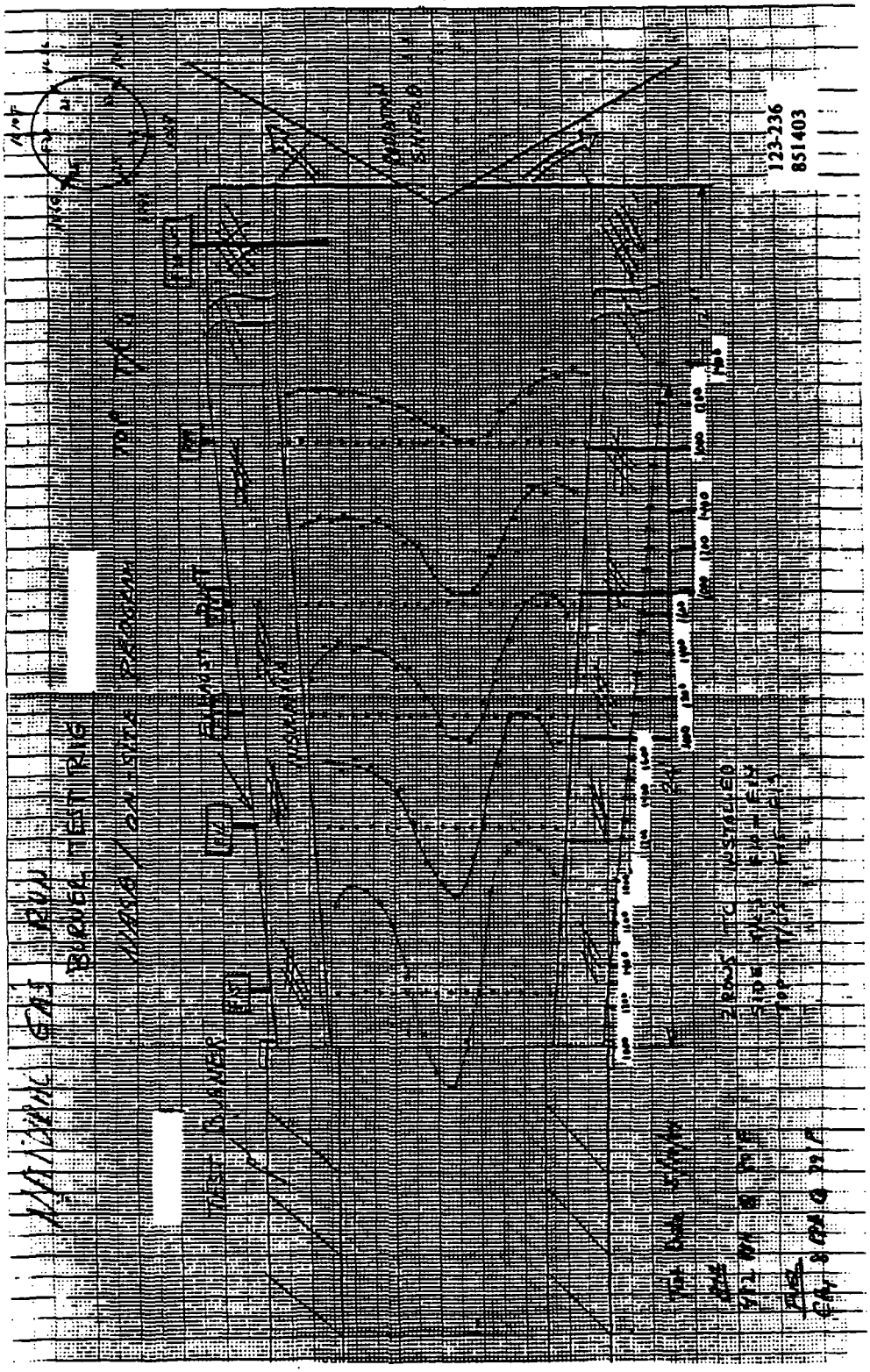

Figure 5-17. Development Reformer Burner Temperature Profiles on Natural Gas Fuel

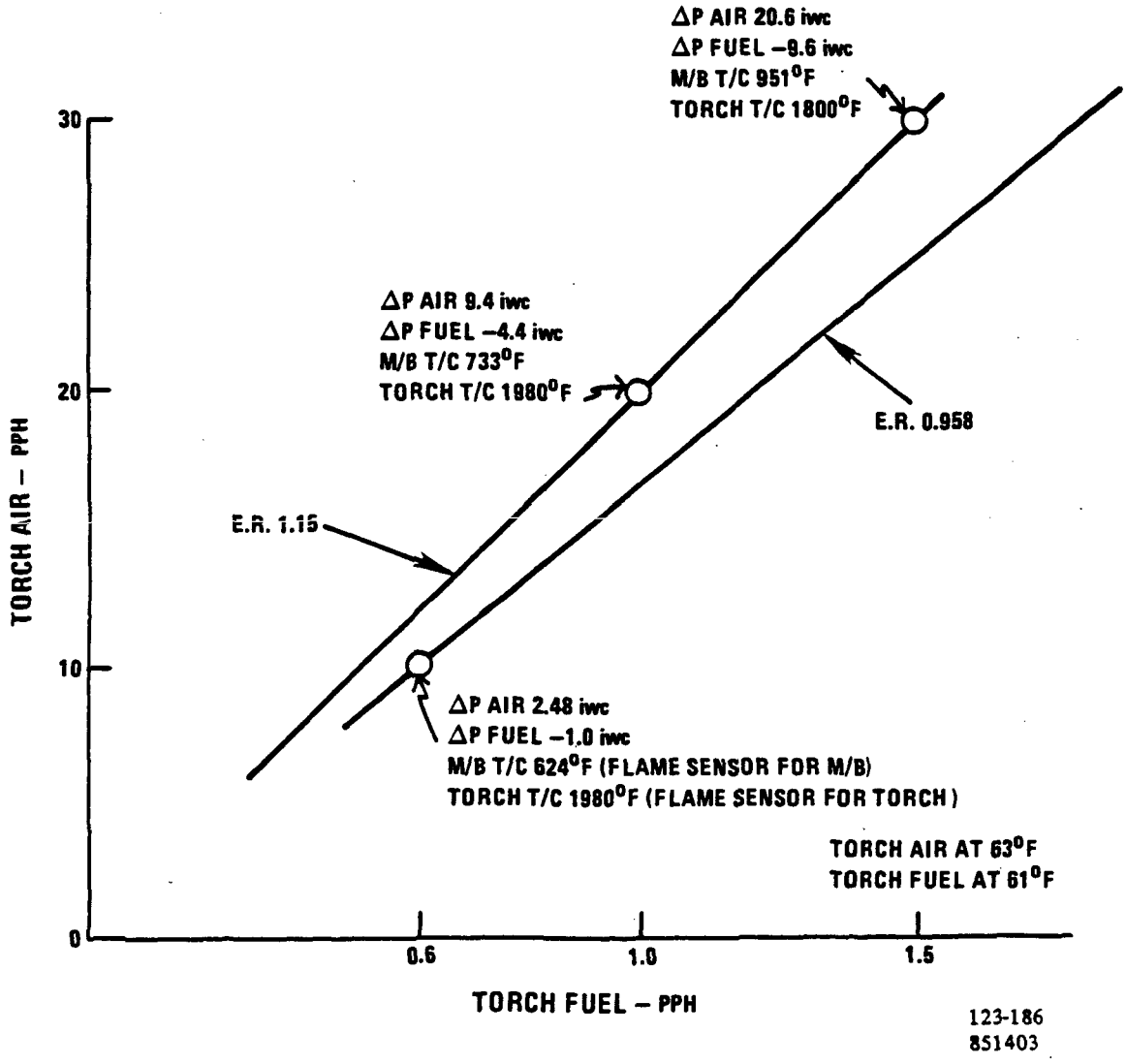

Figure 5-18. Torch Test with Main Burner Air Flow 482 PPH @ 64°F

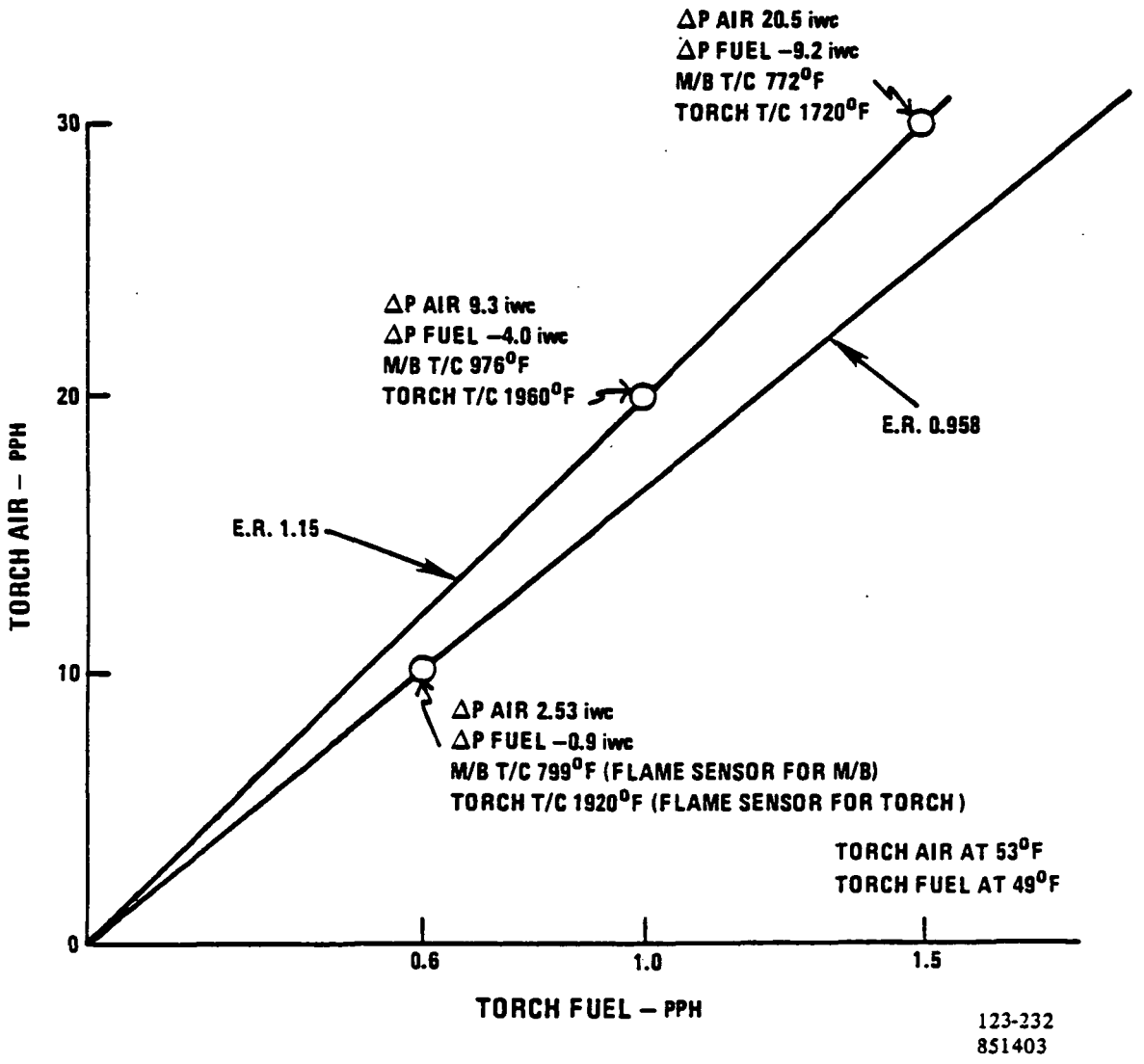

Figure 5-19. Torch Test with Main Burner Air 300 PPH @ 69°F

A gas sampling probe was located 34 inches from the burner discharge (shown in Figure 5-10) to obtain gas analysis samples to measure burner combustion efficiency. Gas analysis equipment was installed to measure CO using a non-dispersive infrared (NDIR) analyzer and total hydrocarbon as CH_4 using a flame ionization detector. Measurements of these two products (CO and CH_4) were made at flow conditions equivalent to 200, 140, 70, and 35 kW operation. In addition, axial and radial temperature traverses were obtained at each flow condition.

The burner gas flows and gas analysis results are shown in Table 5-9 and in Figures 5-20 and 5-21 as a function of power level and equivalence ratio. The axial and radial temperature profiles for the 70 kW tests are shown in Figures 5-22 and 5-23. The observed temperatures are lower than those from the previously tested, smaller burner.

The high concentrations of CO and CH_4 required further testing to determine whether burner modifications would be required. The first step was to test the burner in a test rig that more closely matched the development reformer dimensions and heat loss. A schematic of the revised test rig is shown in Figure 5-24. The exhaust duct is internally insulated, has a 9" diameter, and is 72" long, duplicating the geometry of the burner gas path in the burner sleeve of the 200-kW development reformer. A radiation shield and deflector assembly was installed at the back end of the duct to reduce thermocouple radiation losses. The presence of high levels of unburned CO and CH_4 in the exhaust was re-established with the new long duct, and a test program was conducted to reduce the unburned CO and CH_4 concentrations to acceptable levels. A modification (Mod 3) was developed that reduced the concentrations to 70 PPM CO and 0 PPM CH_4.

The first test conducted was a rerun of the burner configuration (Mod 1), which previously had produced excessive levels of unburned CH_4 and CO with the old exhaust duct (36" long diverging duct).

Table 5-9. Development Reformer Burner Gas Analysis Test Results for Combustion Products

Test Date	Power Setting	Burner Air Flow Lbs/Hr	Burner Air Temp. °F	Fuel Flow[2] Lbs/Hr	Fuel Temp. °F	CO PPM[1]	CH_4 PPM[1]
6/1/84	200 kW	482	580	369	316	350-600	40-110
6/1/84	140 kW	300	536	238	324	270	25
6/4/84	70 kW	152	564	127	306	340	90
6/4/84	35 kW	107	397	91	294	310	130

Notes: (1) Parts per million by volume on dry gas basis

(2) Fuel composition

H_2 = 23.20%

CH_4 = 02.90%

H_2O = 46.14%

CO_2 = 27.70%

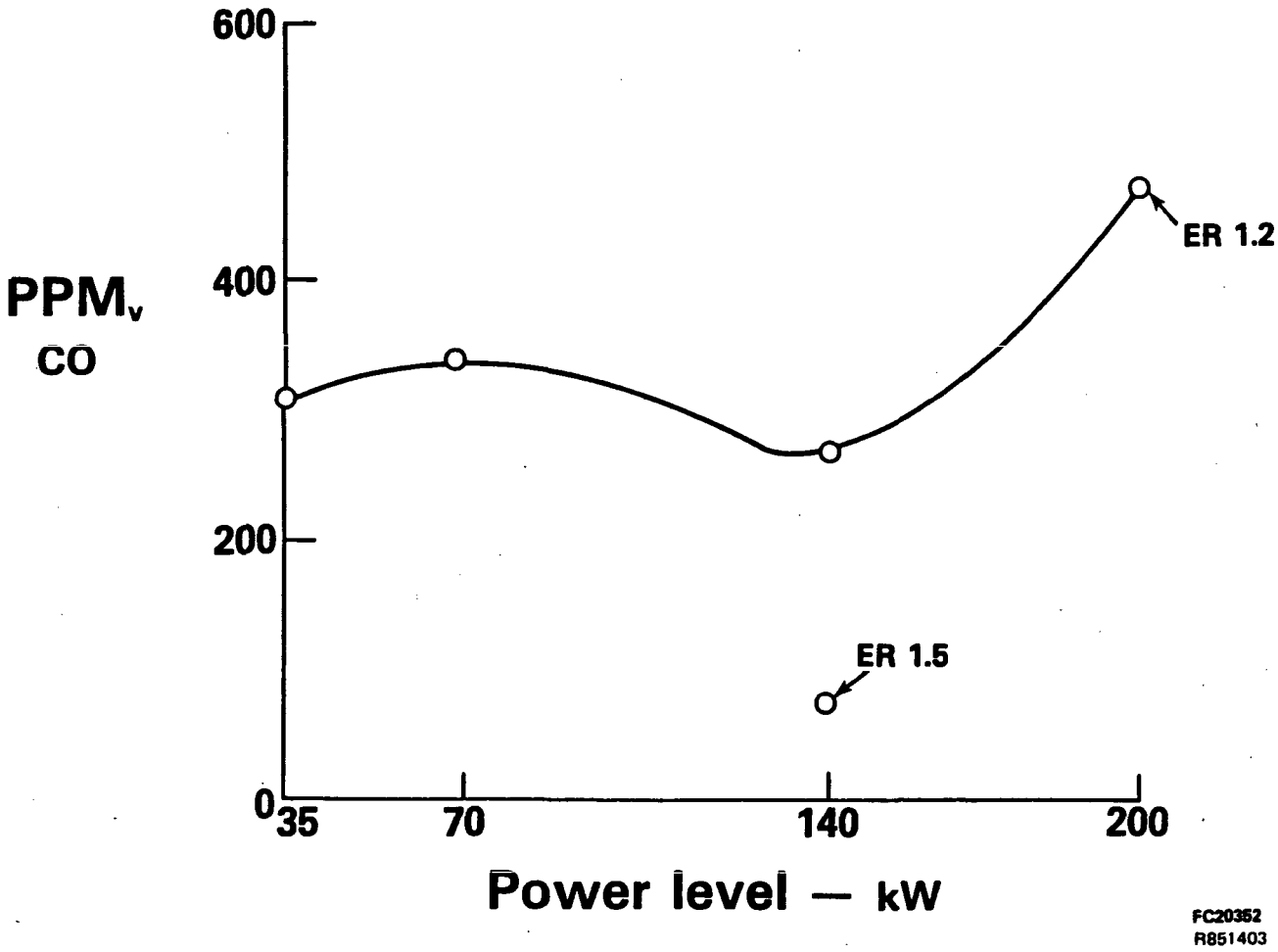

Figure 5-20. Exit CO Concentration vs. Power Level and Burner Equivalent Ratio for Development Reformer Burner

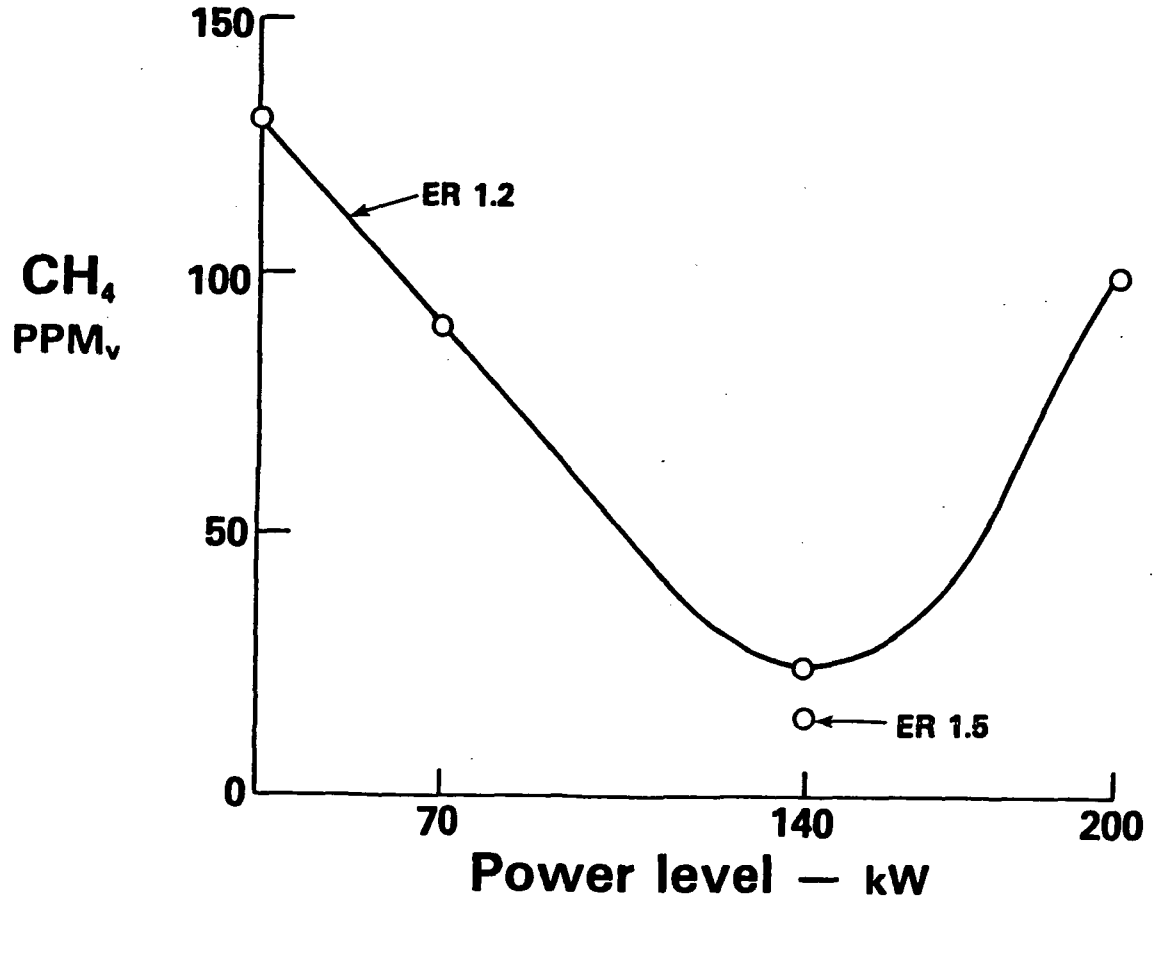

Figure 5-21. Exit Methane Concentration vs. Power Level and Burner Equivalent Ratio for Development Reformer Burner

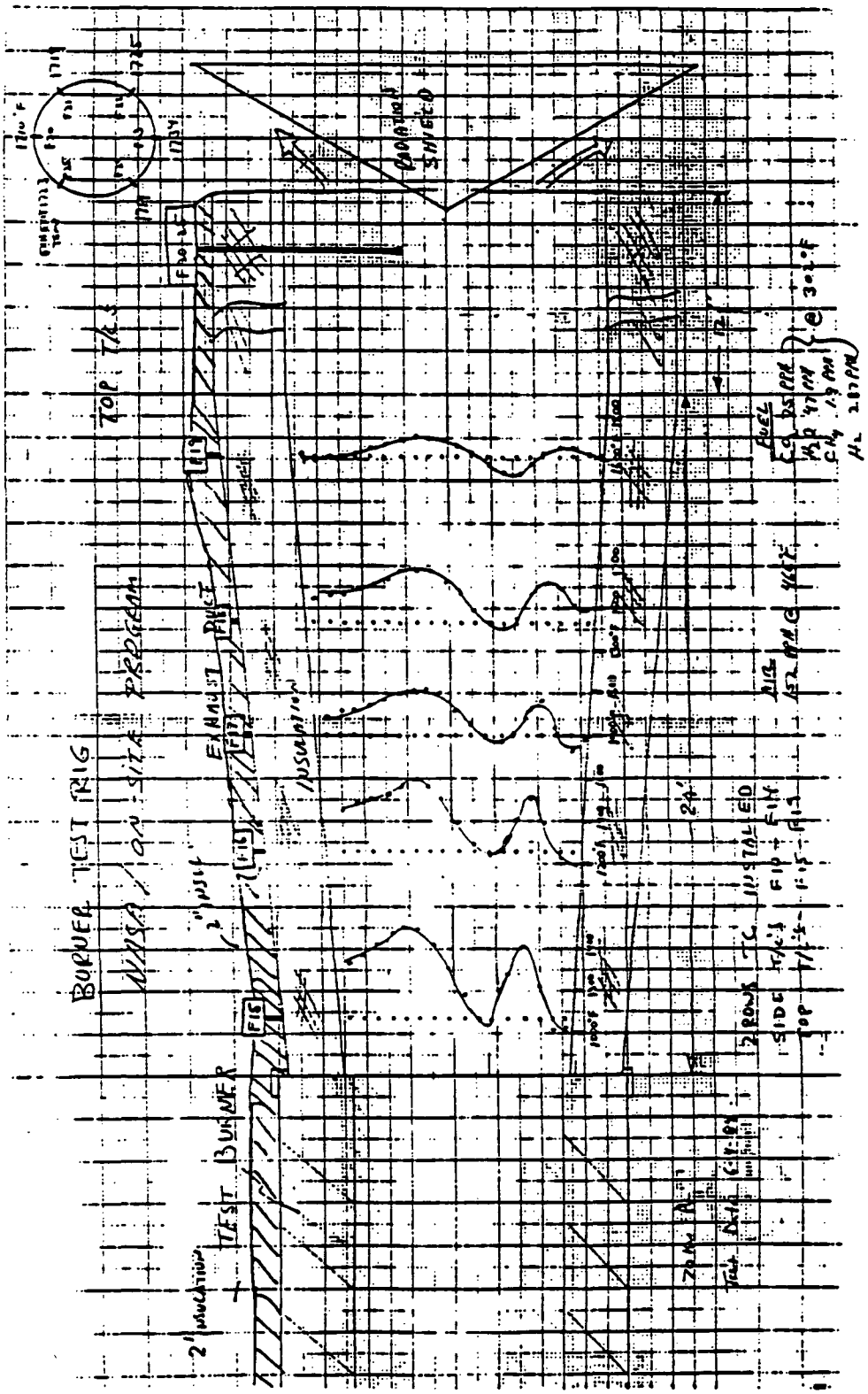

Figure 5-22. Development Reformer Burner Temperatures at 70 kW Flows (Top Thermocouple Traverse)

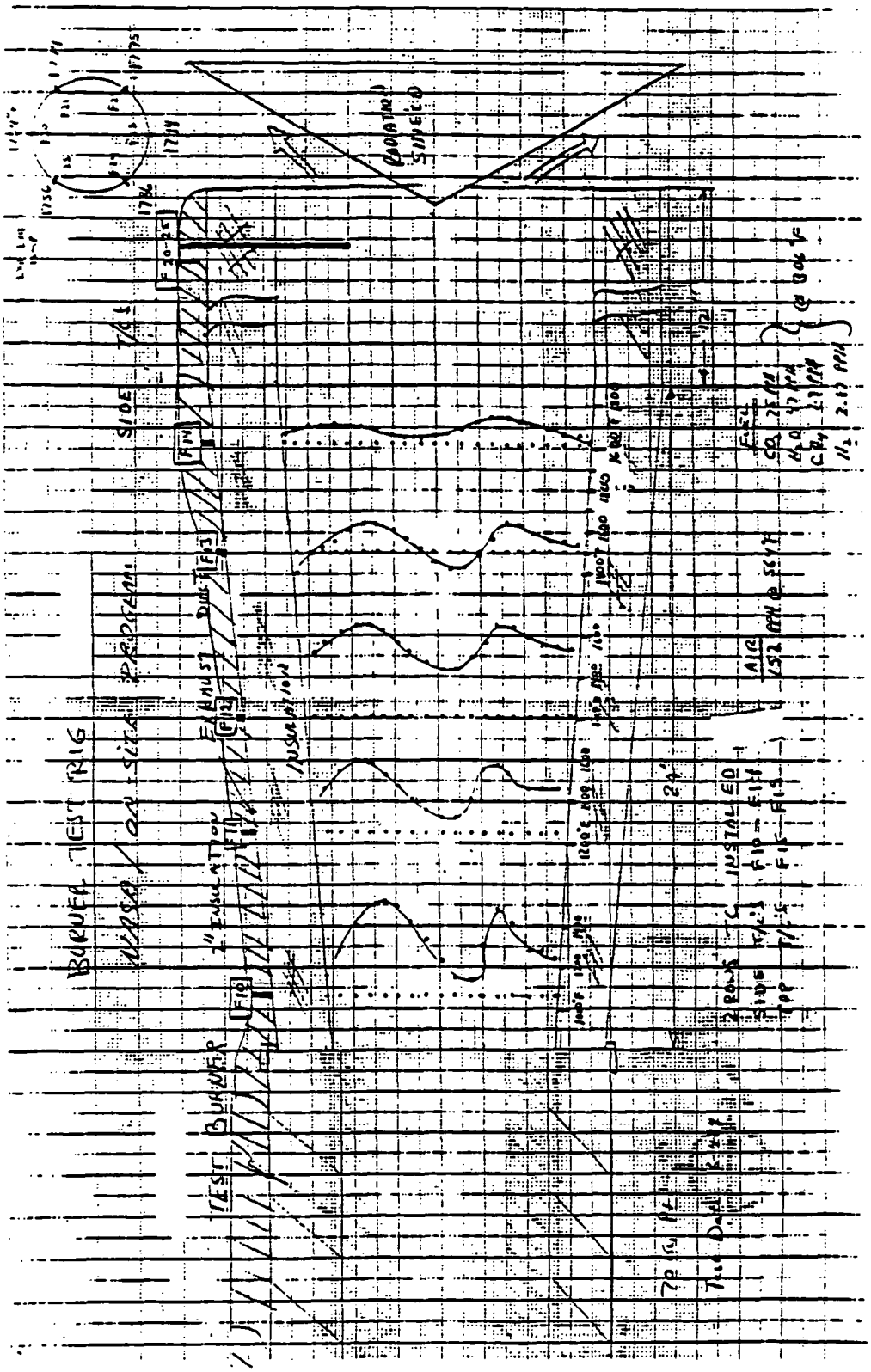

Figure 5-23. Development Reformer Burner Temperatures at 70 kW Flows (Side Thermocouple Traverse)

ORIGINAL PAGE IS
OF POOR QUALITY

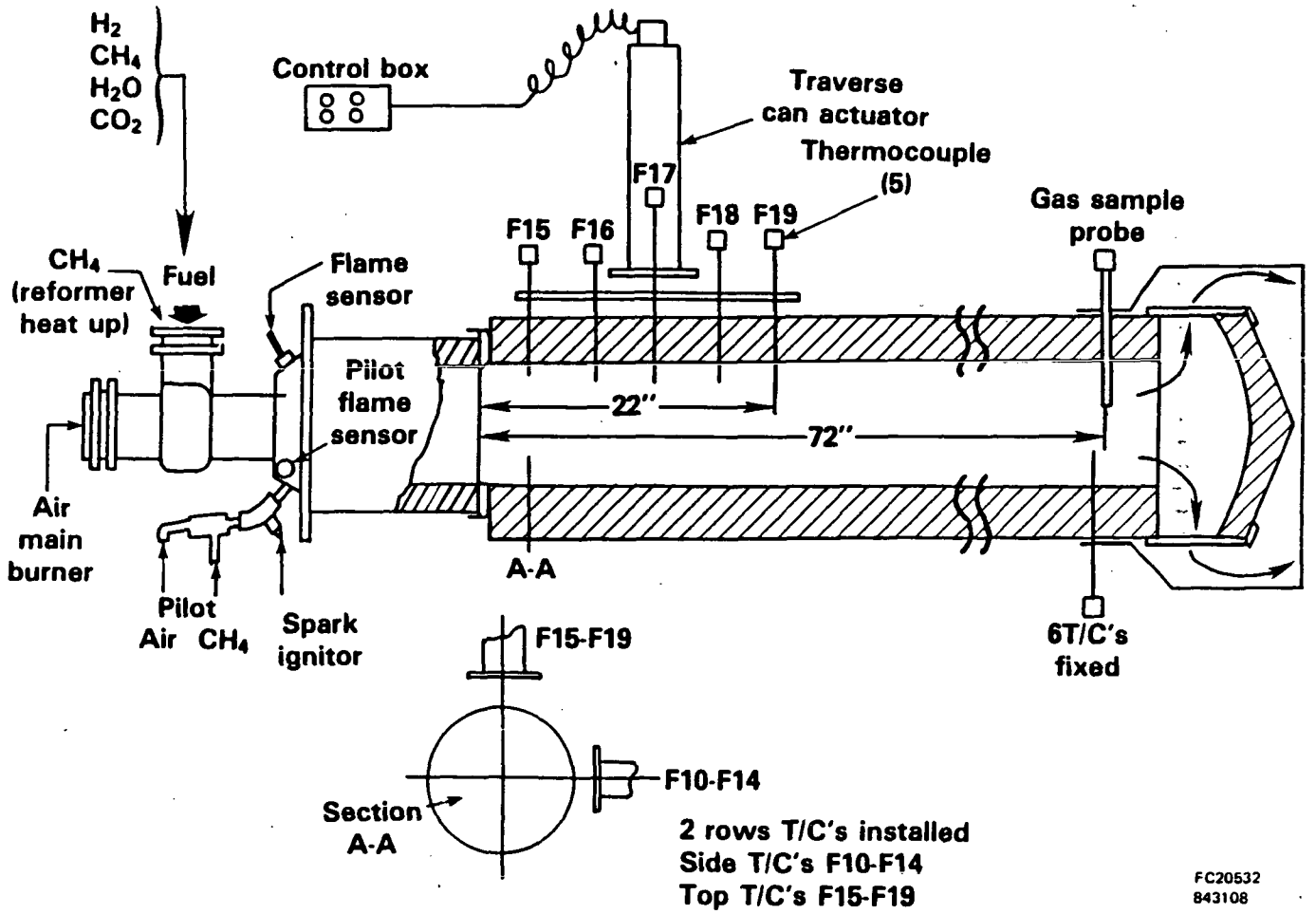

Figure 5-24. Modified Burner Test Rig Showing Details of New Exhaust Duct Which Duplicates Geometry of Development Reformer Gas Path

The next series of tests evaluated the effect of a burner modification (Mod 2) upon overall burner performance. Gas analyses from these tests are shown in Figure 5-25. The results of a further burner modification (Mod 3) are presented in Figure 5-25 (gas analyses) and Figures 5-26 and 5-27 (temperature profiles).

As shown in Figure 5-25, a substantial reduction in CO was realized using the Mod 3 burner design. Measurements taken at three points in the exhaust duct (from center line to near outer wall) showed no more than 70 PPM CO concentration. No measurable amount of CH_4 was found.

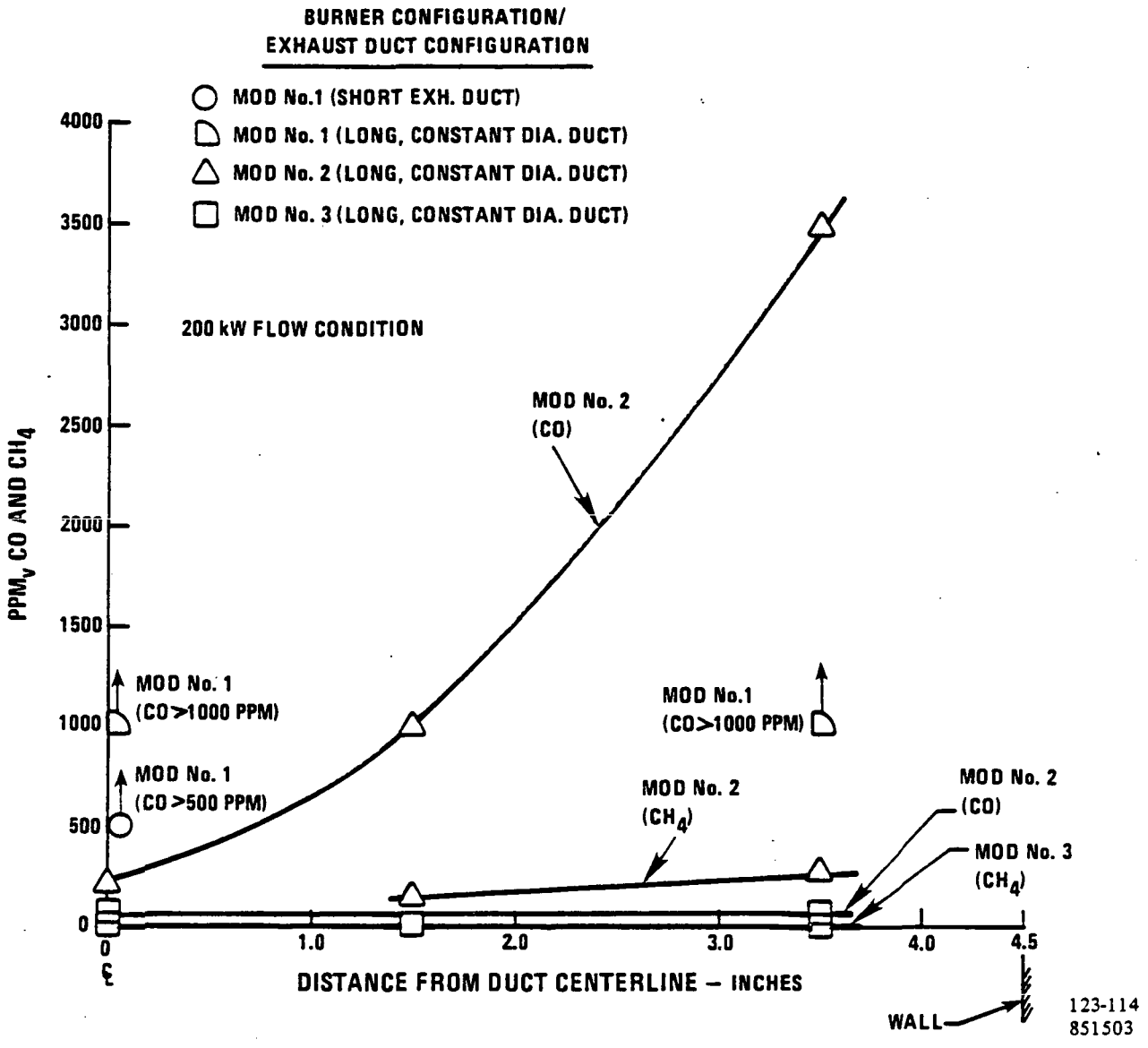

Figure 5-25. CH_4 and CO Concentration Measured Across Exhaust Duct, Center Line to Wall, Showing Successful Reduction in CO and CH_4 with the Mod 3 Design

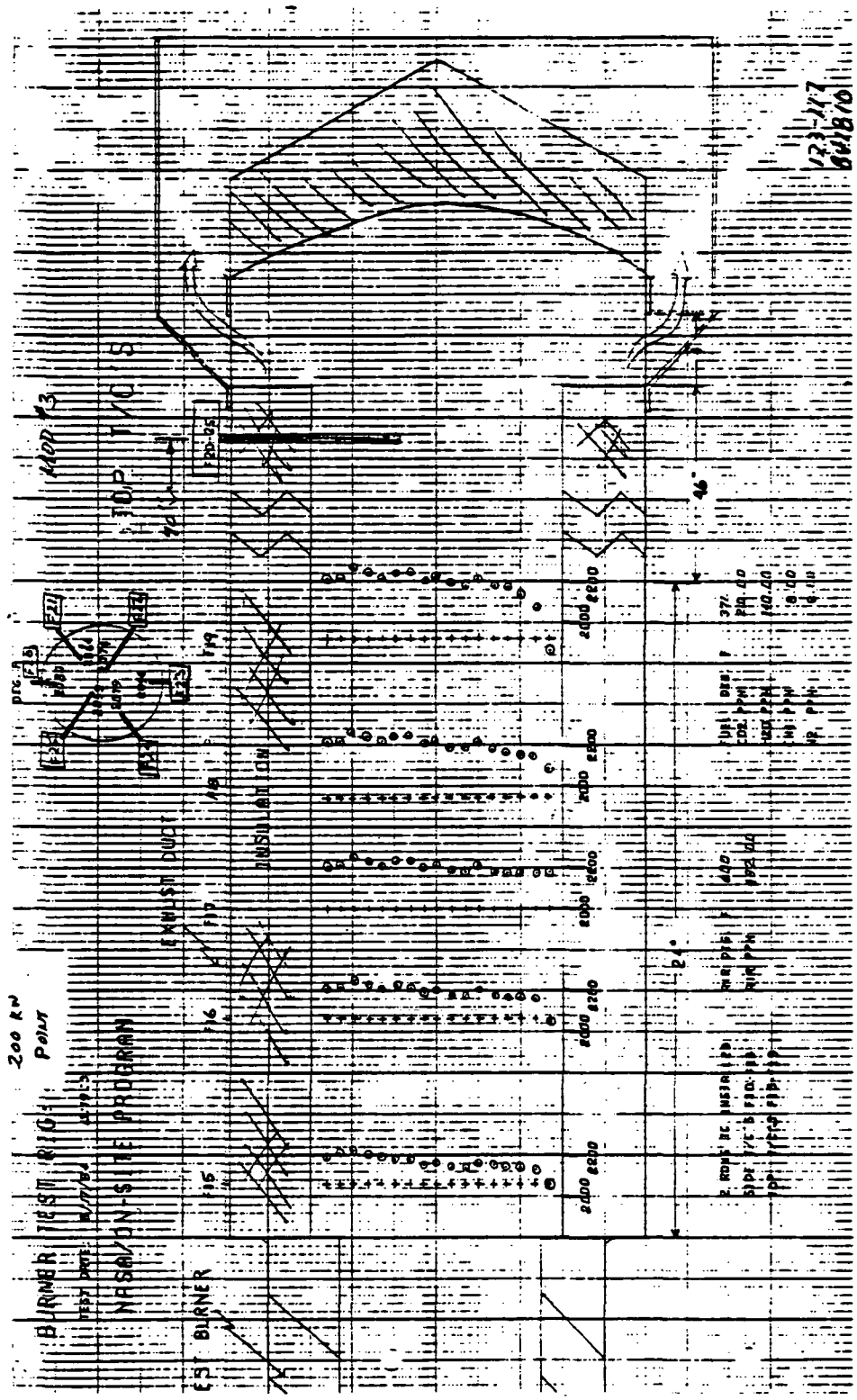

Figure 5-26. Development Reformer Burner Mod 3 Horizontal Temperature Profiles at 200 kW Flows (Long Exhaust Duct)

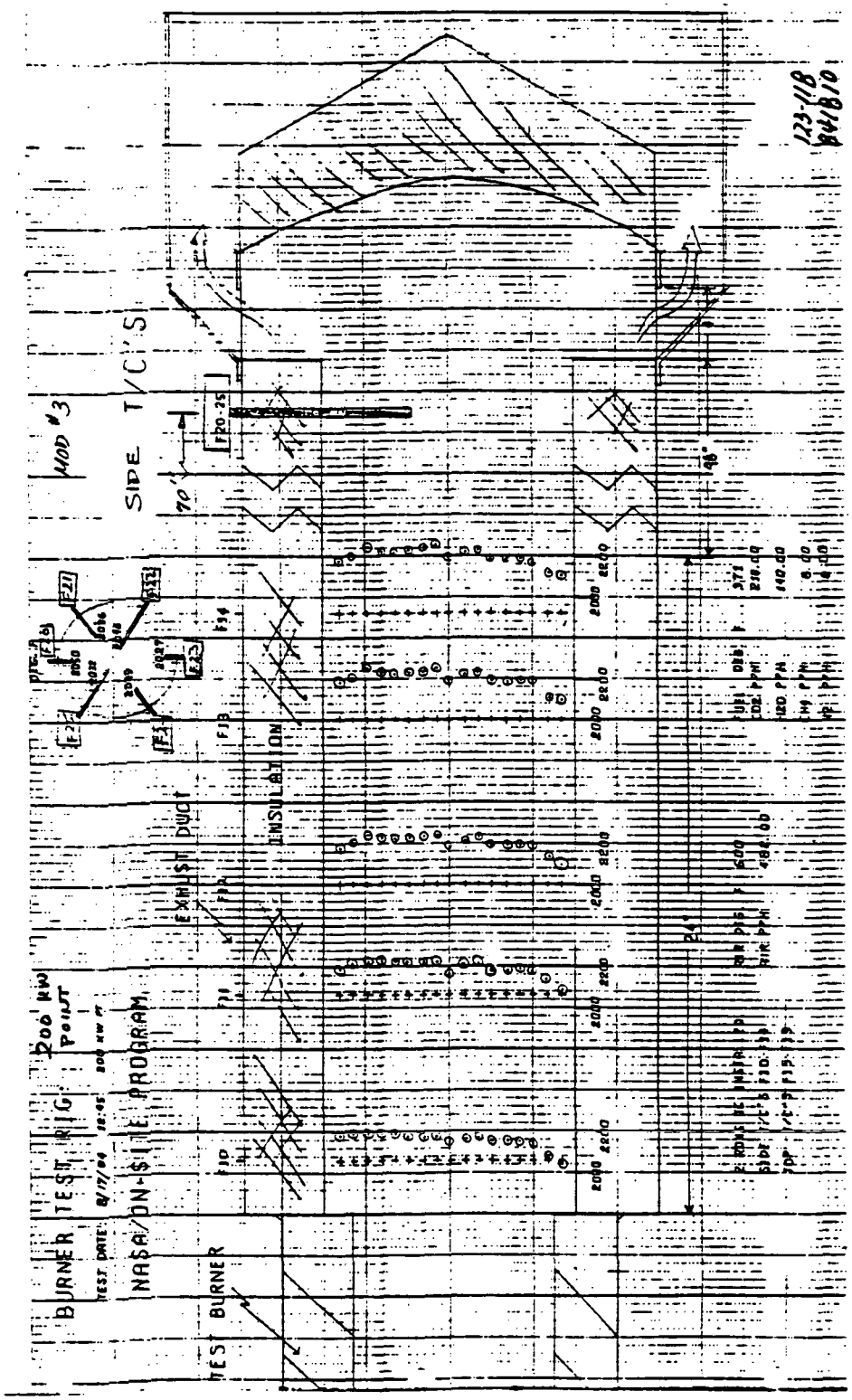

Figure 5-27. Development Reformer Burner Mod 3 Vertical Temperature Profiles at 200 kW Flows (Long Exhaust Duct)

A duplicate burner for the development reformer was procured and modified to the Mod 3 design. To save time, the modified burner was installed directly in the development reformer, where it will be tested with the industrial burner control system as a part of the development reformer testing.

Water Table Testing - Visual flow testing was initiated on the water table using a two-dimensional model representation of the 200-kW development reformer burner configuration. The objective of these tests was to define an acceptable burner gas flow path geometry within the burner cavity to provide uniform burner gas flow and therefore maintain uniform reformer tube temperatures. Visual flow observation on the water table was conducted with a two-dimensional model representation of the 200-kW development reformer configuration.

Water table testing of a two-dimensional model of an early version of the development reformer burner cavity (Mod 3C) indicated that more flow was going to the outer diameter than the inner diameter. The flow pattern obtained on the Mod 3C model is shown in Figure 5-28 using talcum powder.

Modifications to the burner gas path were tested to improve the balance between the inner and outer flow paths. Two test approaches were tried. The results of this testing are shown in Figures 5-28 through 5-30. Both approaches improve the uniformity of the observed flow. The development reformer design was modified to permit easy adjustment of the burner riser height to facilitate fine-tuning required to obtain acceptable tube temperature uniformity.

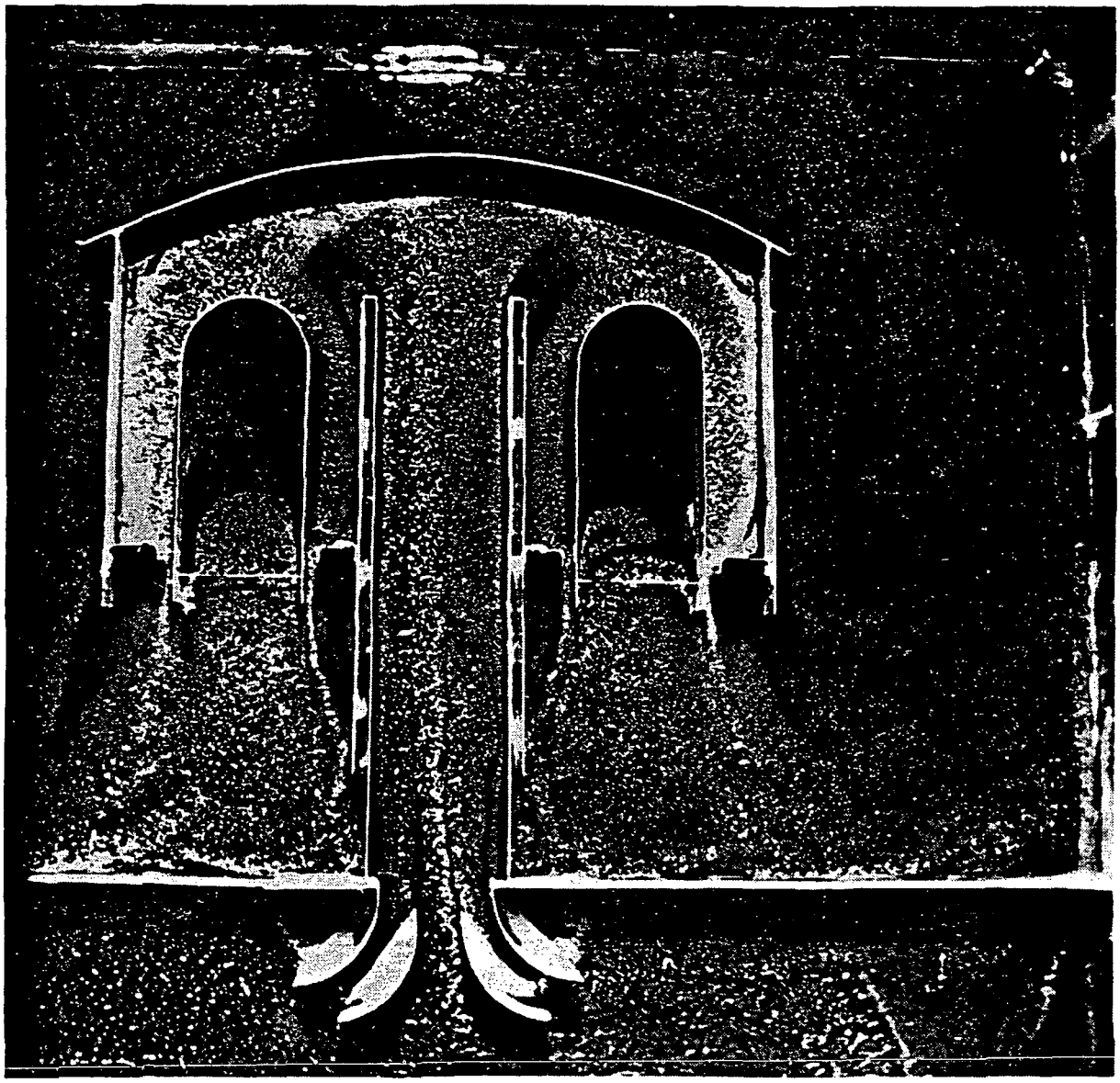

W5170-16

Figure 5-28. Mod 3C Talcum Reveals Non-Uniform Flow Over Reformer Tubes

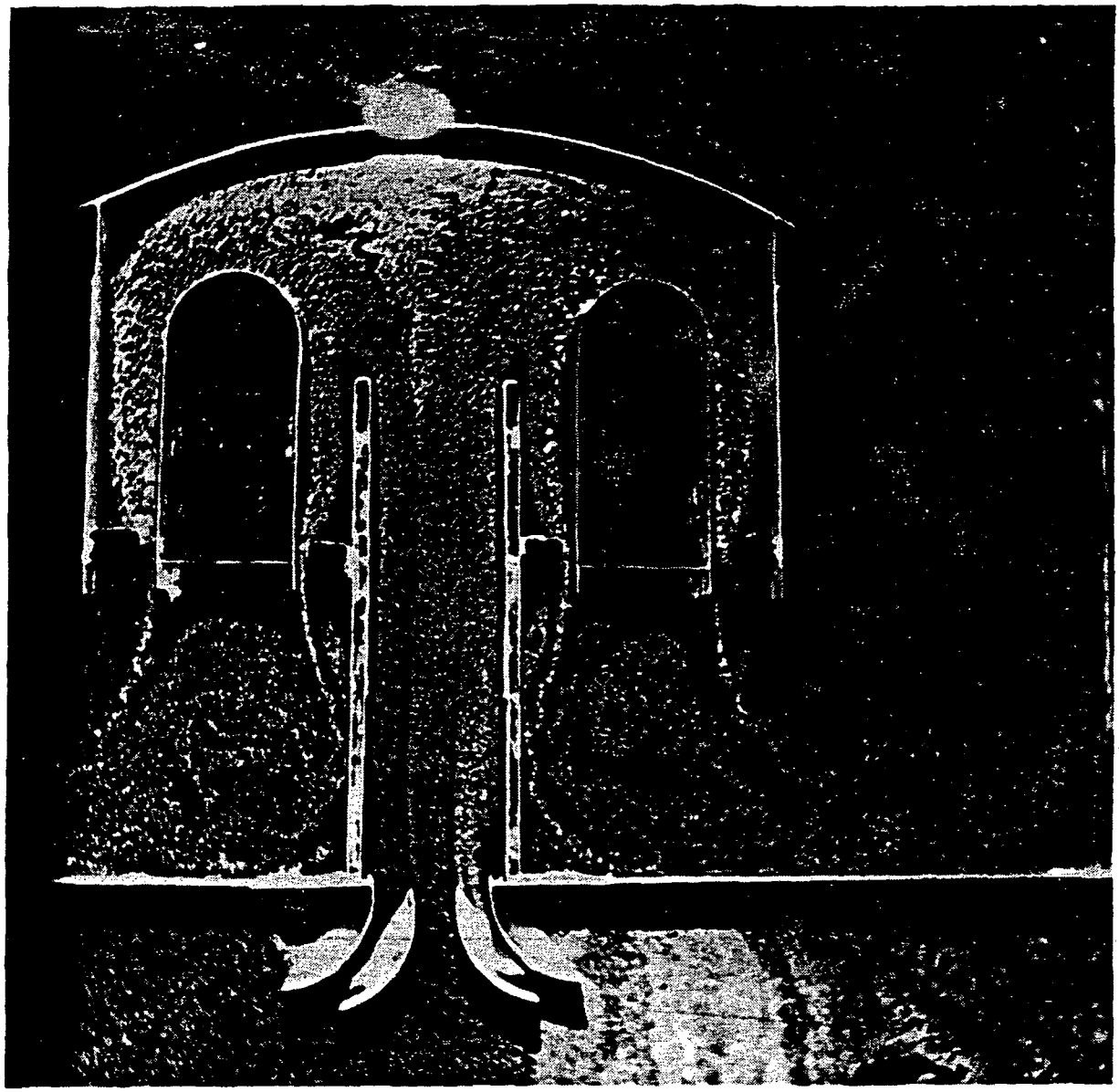

WO-1298

Figure 5-29. Talcum Powder Visualization with Shorter Riser Improves Flow Uniformity

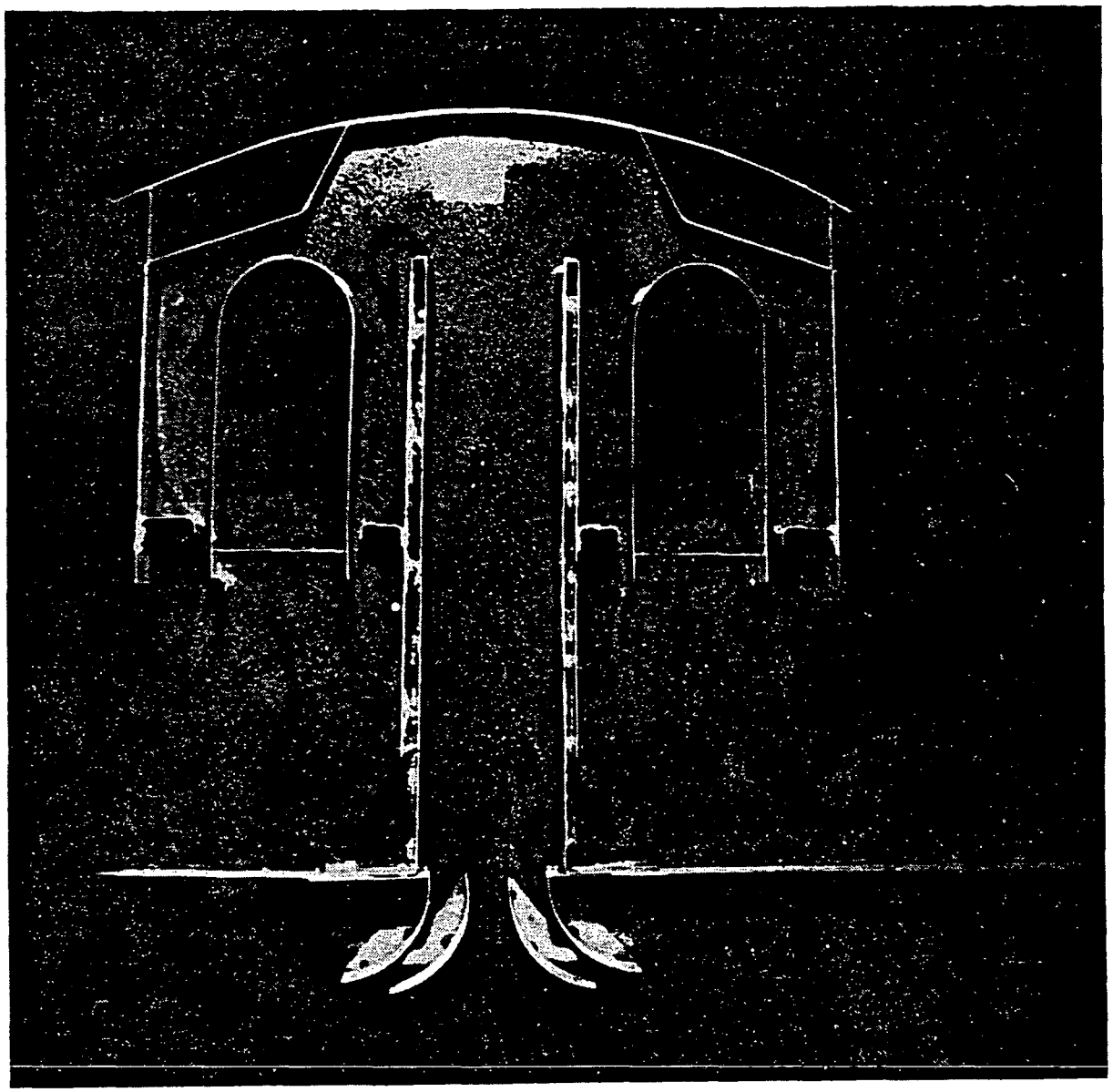

WO 1306

Figure 5-30. Talcum Powder Visualization with Modified Dome Showing Improved Flow Uniformity

A water table model of a down-fired configuration was evaluated. A sketch of the model is shown in Figure 5-31. The model is a two-dimensional representation of a conical dome with a diverging half angle of 30°. The flow patterns observed at two different water surface velocities are shown in Figures 5-32 and 5-33. In both cases the water stream expanded very little and persisted as a jet flow all the way to the top of the middle tube, which then acted as a flow deflector. The flow pattern also showed two large recirculation zones on either side of the center tube. Modifications to improve the flow distribution would require either a much shallower dome angle (probably 10°) resulting in an undesirable reformer height or physical flow deflectors, which would present durability problems in the hot exhaust stream. No further effort is planned on this configuration.

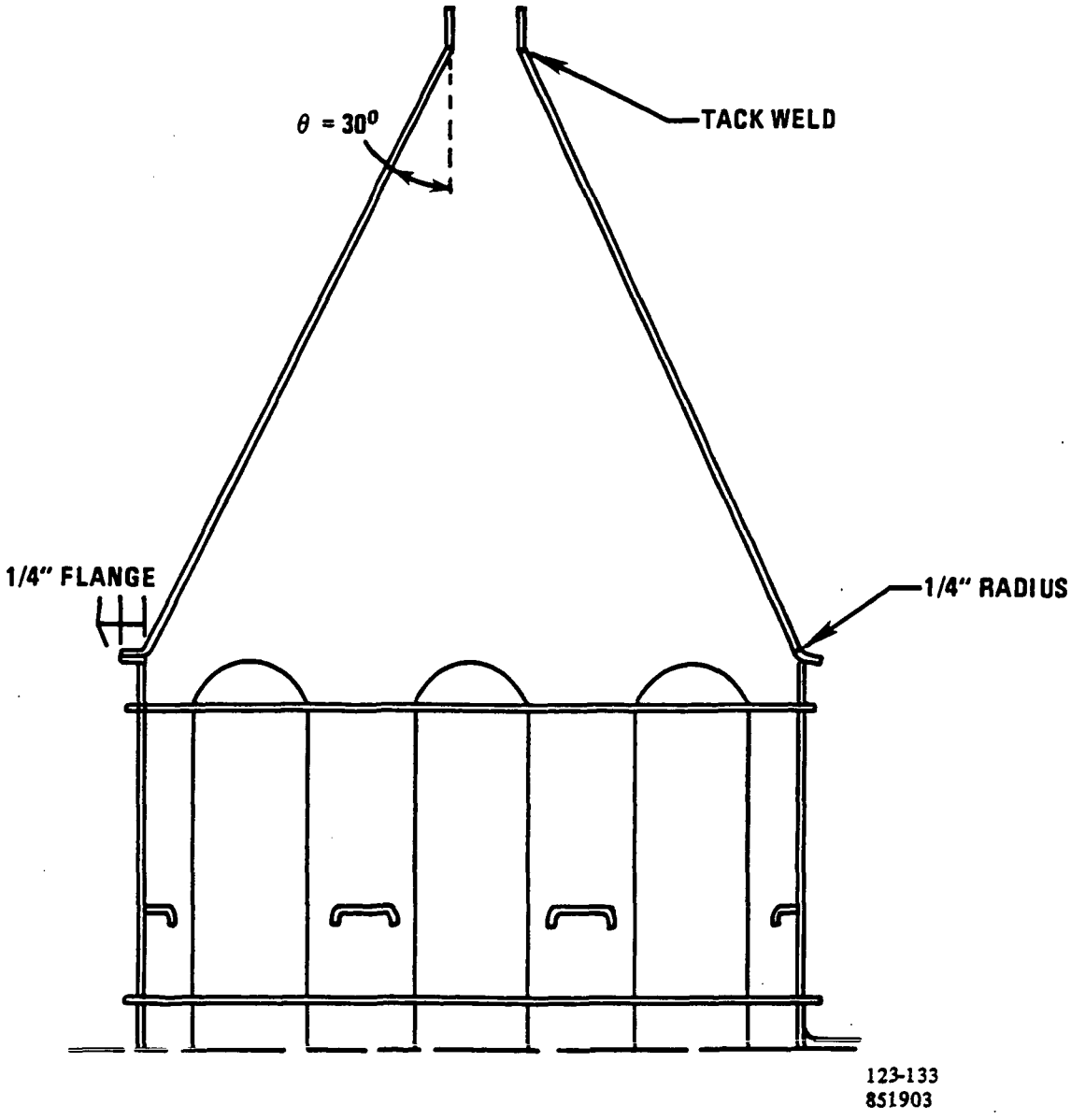

Figure 5-31. Down-Fired Reformer Burner Water Table Model

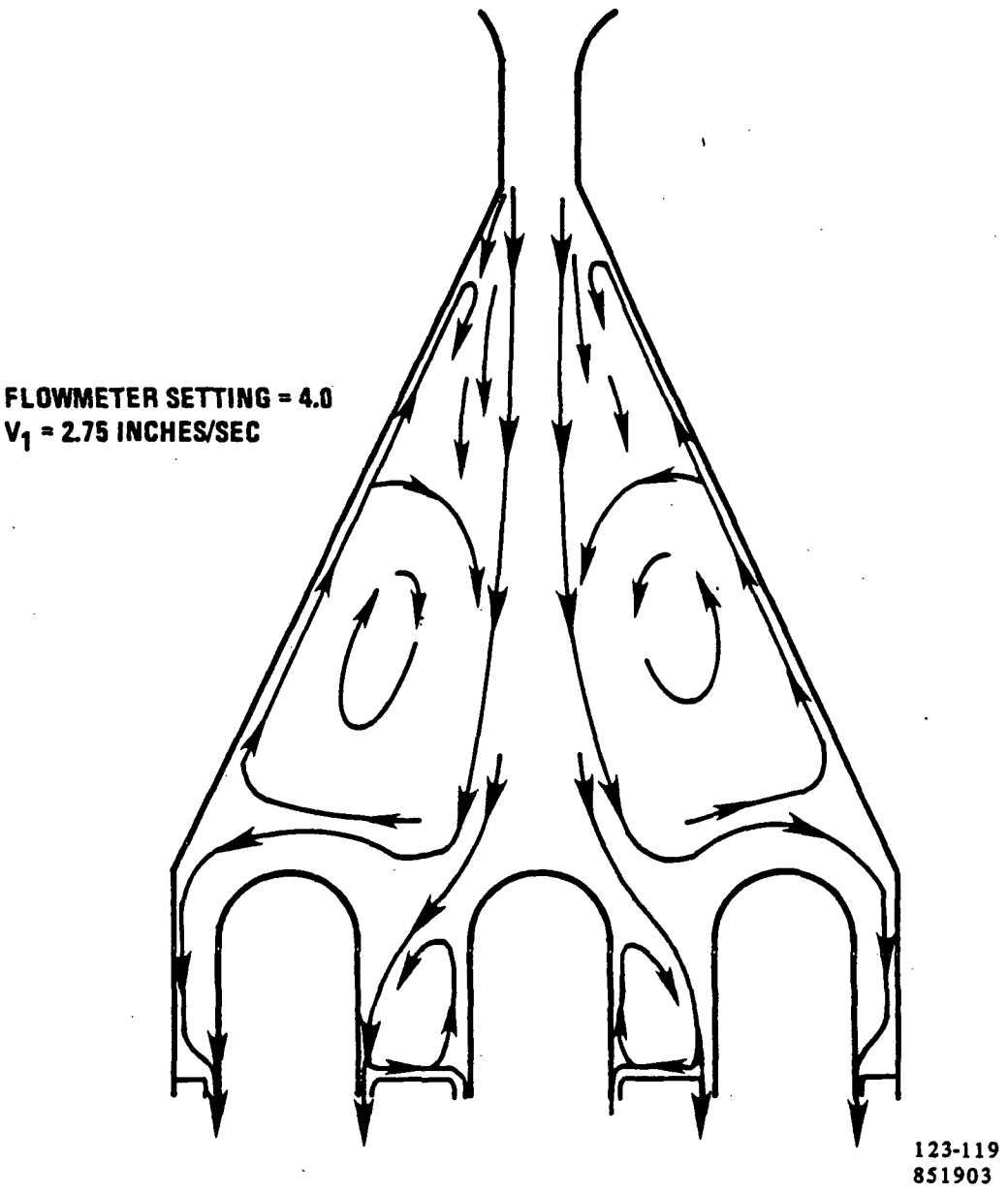

Figure 5-32. Down-Flow Burner Configuration - Water Table Flow Visualization Test

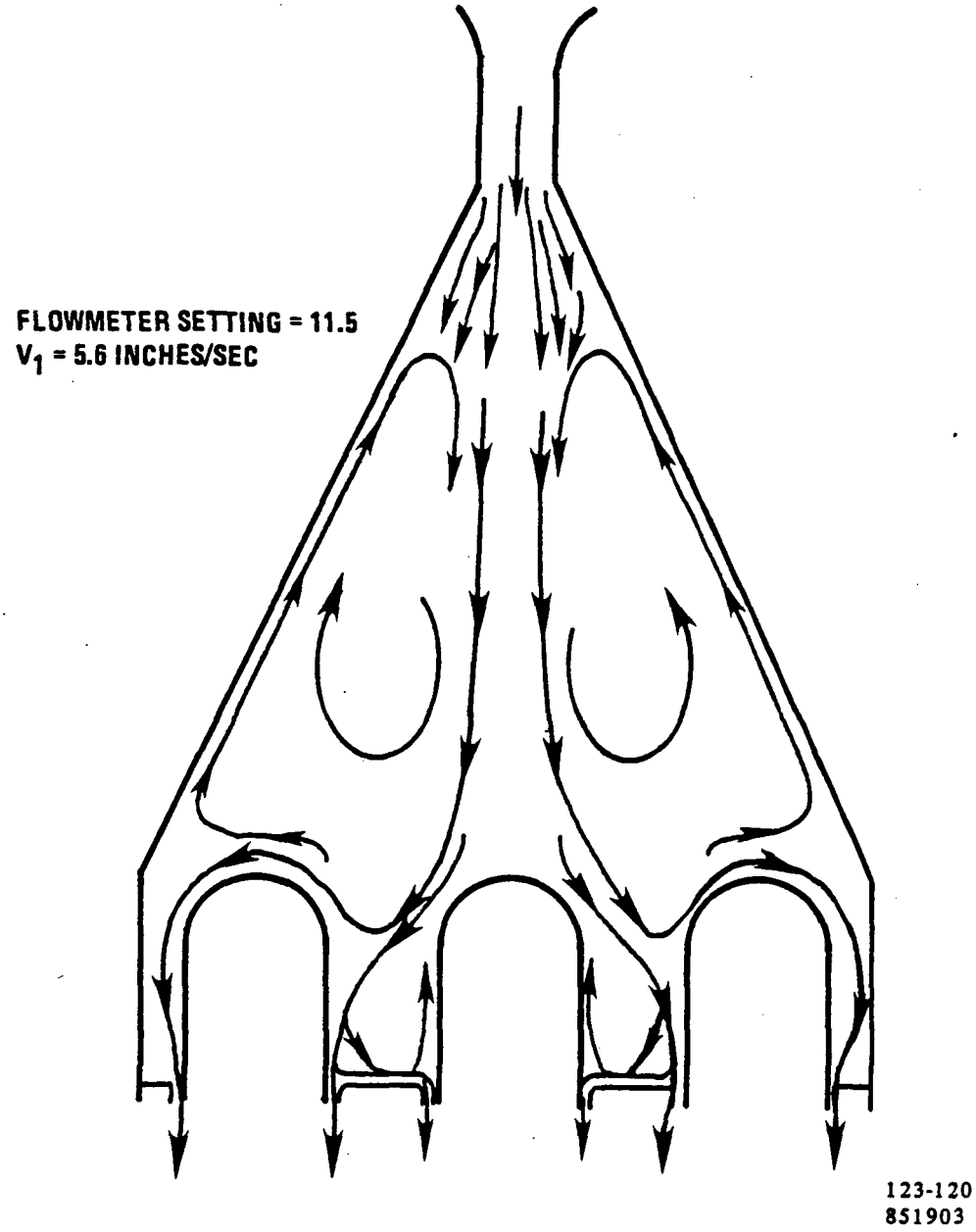

Figure 5-33. Down-Flow Burner Configuration - Water Table Flow Visualization Test

Development Reformer Fabrication

The 200-kW development reformer fabrication was undertaken and completed during the past year. The design of this reformer was provided under a parallel GRI-sponsored contract. The selected design consists of six 8 5/8-inch diameter tubes, each with a 60-inch long catalyst bed. The tubes are heated by a single industrial burner. A summary of the 200-kW development reformer design is compared to the 40-kW power plant reformer in Table 5-10. The completed development reformer is shown next to the test facility in Figure 5-34.

Table 5-10. Summary of Development Reformer Design

Tube Geometry	40-kW Reformer (For Comparison)	Development Reformer
Number of Tubes	4	6
PPH Fuel Processed/Tube	4.5	15
Tube Diameter	5.6"	8.6"
Tube Length	31"	60"
Tube-Tube Spacing	4"	5"
PPH Natural Gas Processed Per Square Foot Tube Surface	1.0	1.2
Tube Material	Wrought 310 S. Stl	310 S. Stl Pipe
Catalyst Size	0.7" Dia. x .14" Long	.31" D x .31" L .13" Hole
Burner Type	6 Fuel/Air Nozzles Per Reformer Tube, Separate Natural Gas Start Nozzles	Single Burner For Start And Steady State
Heat Transfer Enhancement	Lower Metal Sleeves With 1" Ceramic Balls in the 1.75" Gap	Ceramic Sleeves
Package Dimensions	36" Diameter x 49" High	56" Diameter x 10' High

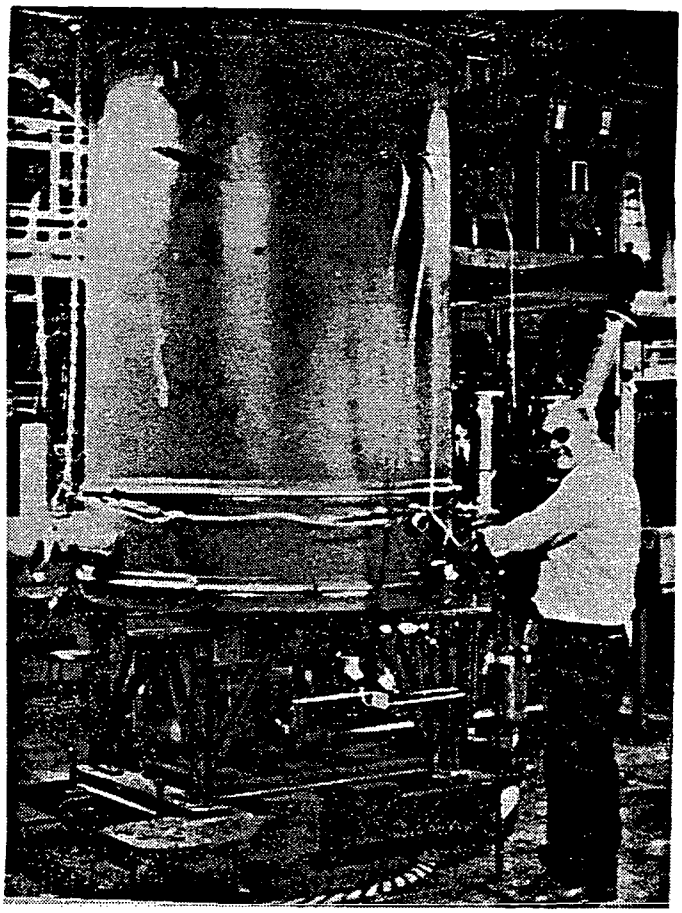

WCN-13152

Figure 5-34. Completed 200-kW Development Reformer

The major sheet metal parts of the reformer (tubes, dome, cylinder, and skirt) are shown during fabrication in Figure 5-35. The reformer tube subassemblies, process inlet and exhaust manifolds, and pigtails were welded together and heat treated to relieve weld stresses. The fixtured assembly is shown after heat treatment in Figure 5-36. The reformer dome, cylinder, and skirt are shown fully prepared for insulating in Figure 5-37, and the cylinder is shown as it was being insulated in Figure 5-38.

The low pressure drop catalyst was loaded into the reformer tubes, and the tubes were individually flow checked using nitrogen to assure uniform process gas flow distribution. The caps were welded to the reformer tubes, and the entire process side of the reformer was successfully pressure checked for leaks.

The completed tube-manifold assembly was mounted on the reformer support structure and transporter cart, and the lower tube thermocouples and skirt were installed (see Figure 5-39).

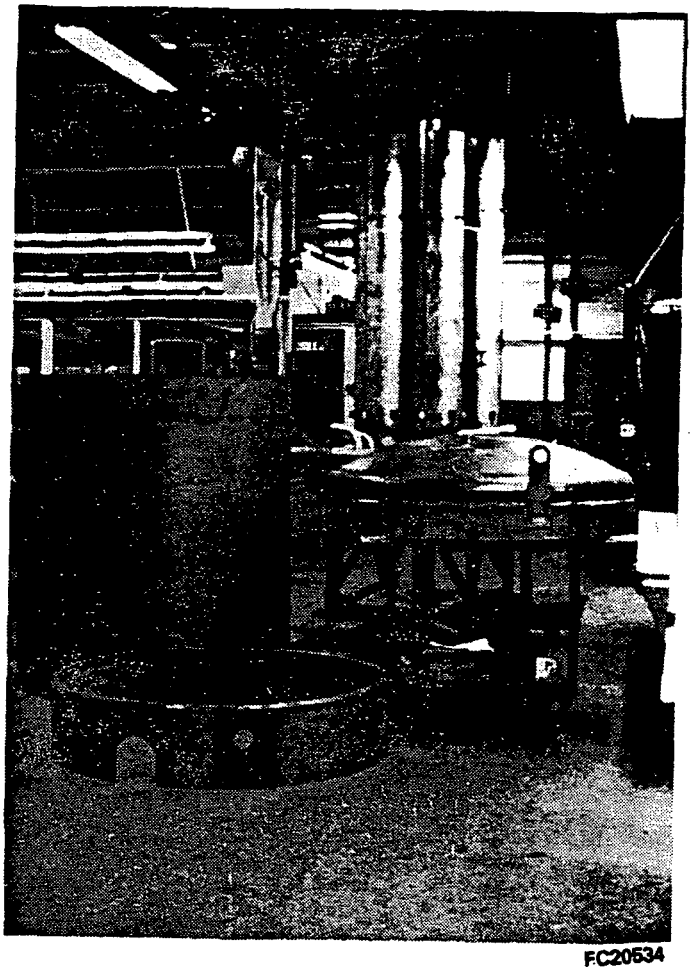

FC20534
840709

Figure 5-35. 200-kW Development Reformer During Fabrication

(WCN-13102)

Figure 5-36. Development Reformer Tube and Manifold Assembly After Heat Treatment

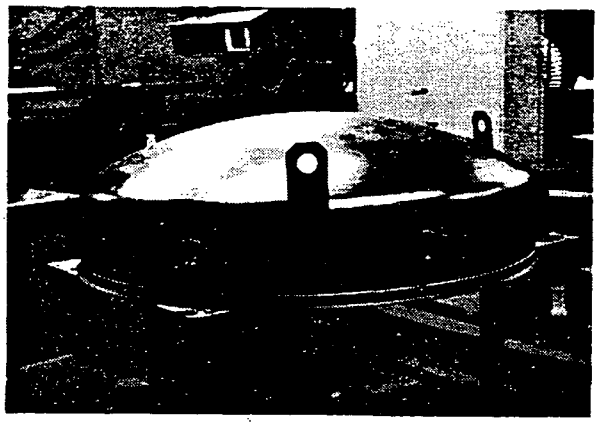

DOME

(WCN-13103)

CYLINDER

(WCN-13104)

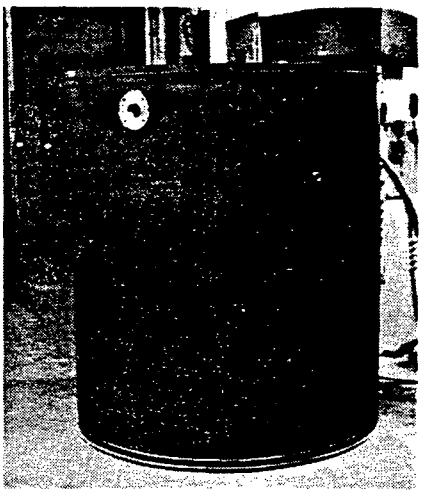

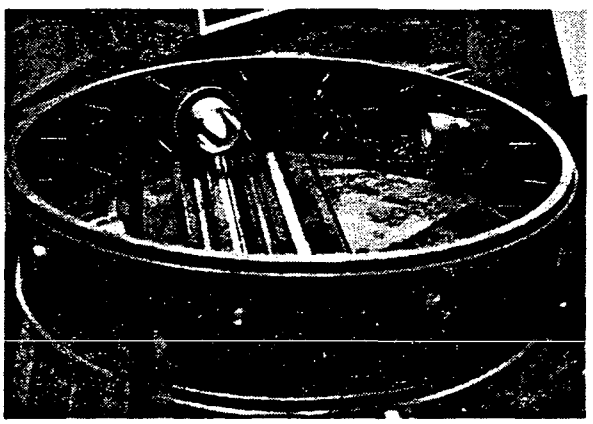

SKIRT

(WCN-13105)

Figure 5-37. Development Reformer Vessel Pieces Ready for Insulating

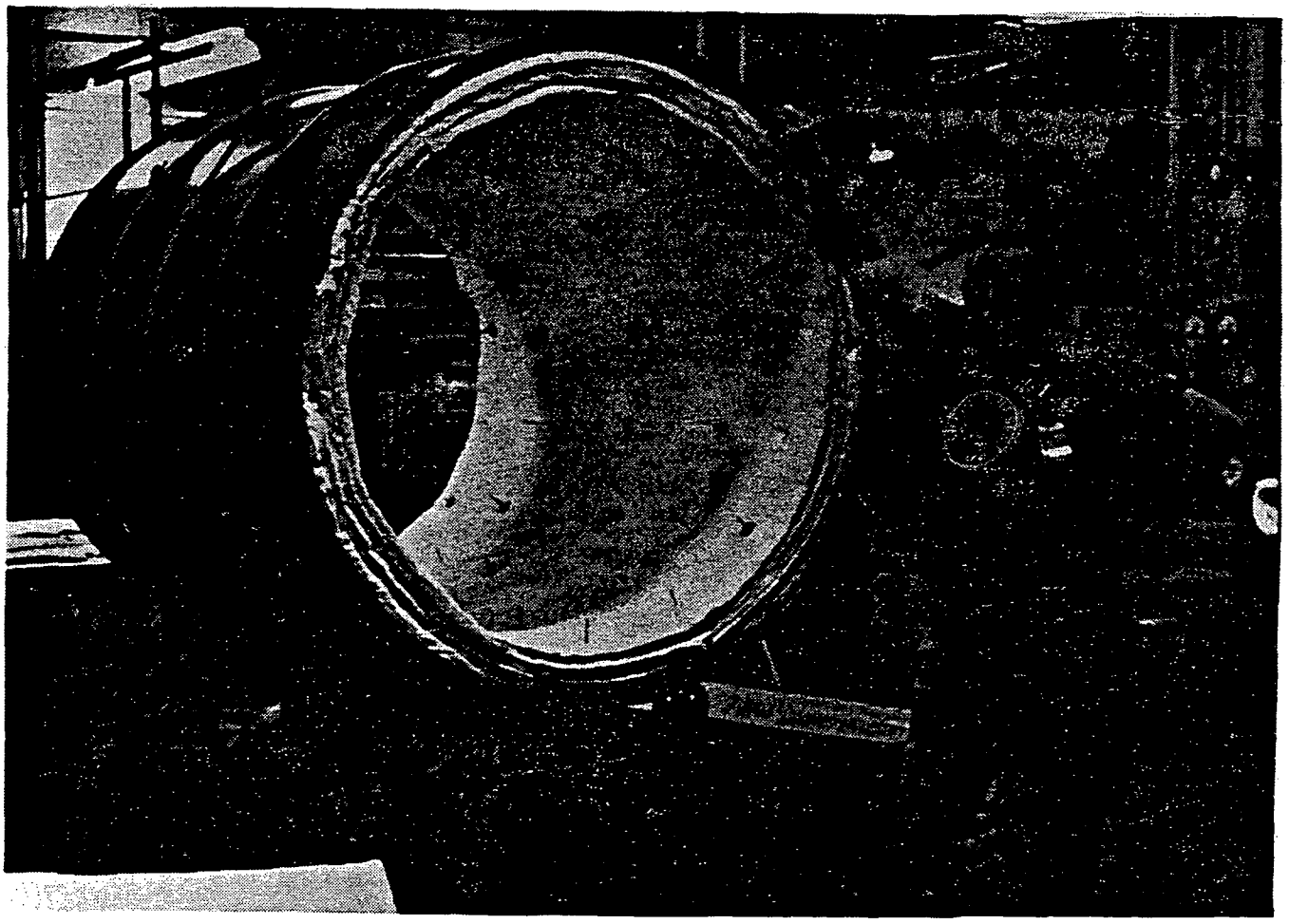

WCN-13156

Figure 5-38. Development Reformer Cylinder During Application of Interal Blanket Insulation

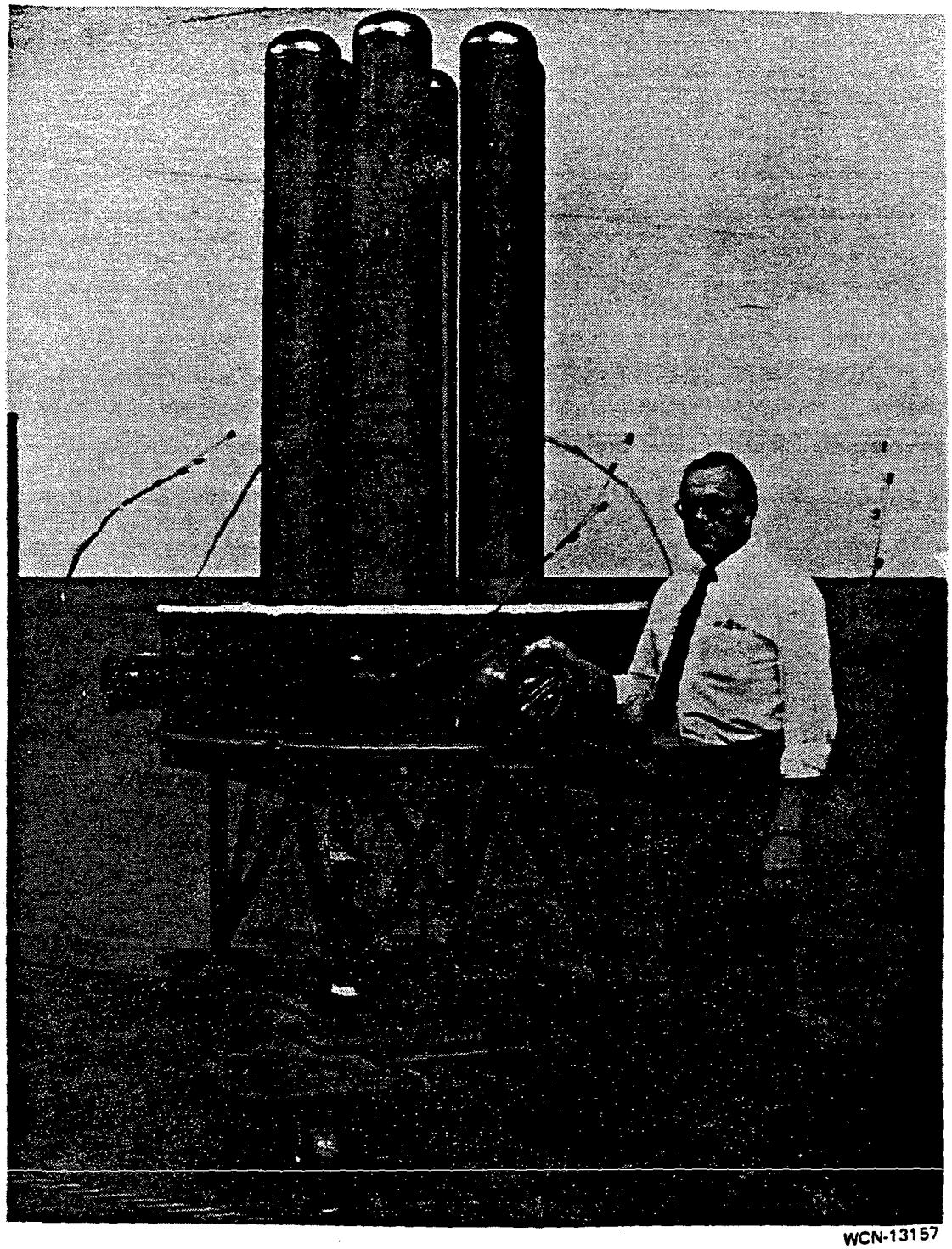

Figure 5-39. Completed Development Reformer Tube-Manifold Assembly Mounted on Support Structure with Skirt Installed

Facility Modification

During the past year the 200-kW development reformer test facility was designed and construction was completed. All gas delivery systems, piping, heaters, controls, and thermocouples were installed. Final stand checkouts of these items, installation of piping insulation, plus hookup and checkout of the automatic data acquisition and retrieval (ADAR) system remain prior to test startup, which is expected to begin early next year. A schematic showing the development reformer test facility requirements is shown in Figure 5-40. Plan view and elevation drawings of the test facility are shown in Figures 5-41 and 5-42.

Fabrication of the control panel and installation of all process gas piping from the control panel to the rig and from the rig to the exhaust is complete. Figure 5-43 shows the back side of the control panel during fabrication. Installation of thermocouple cables from the control panel to the rig is also completed. The back of the test facility, with heaters installed, is shown in Figure 5-44.

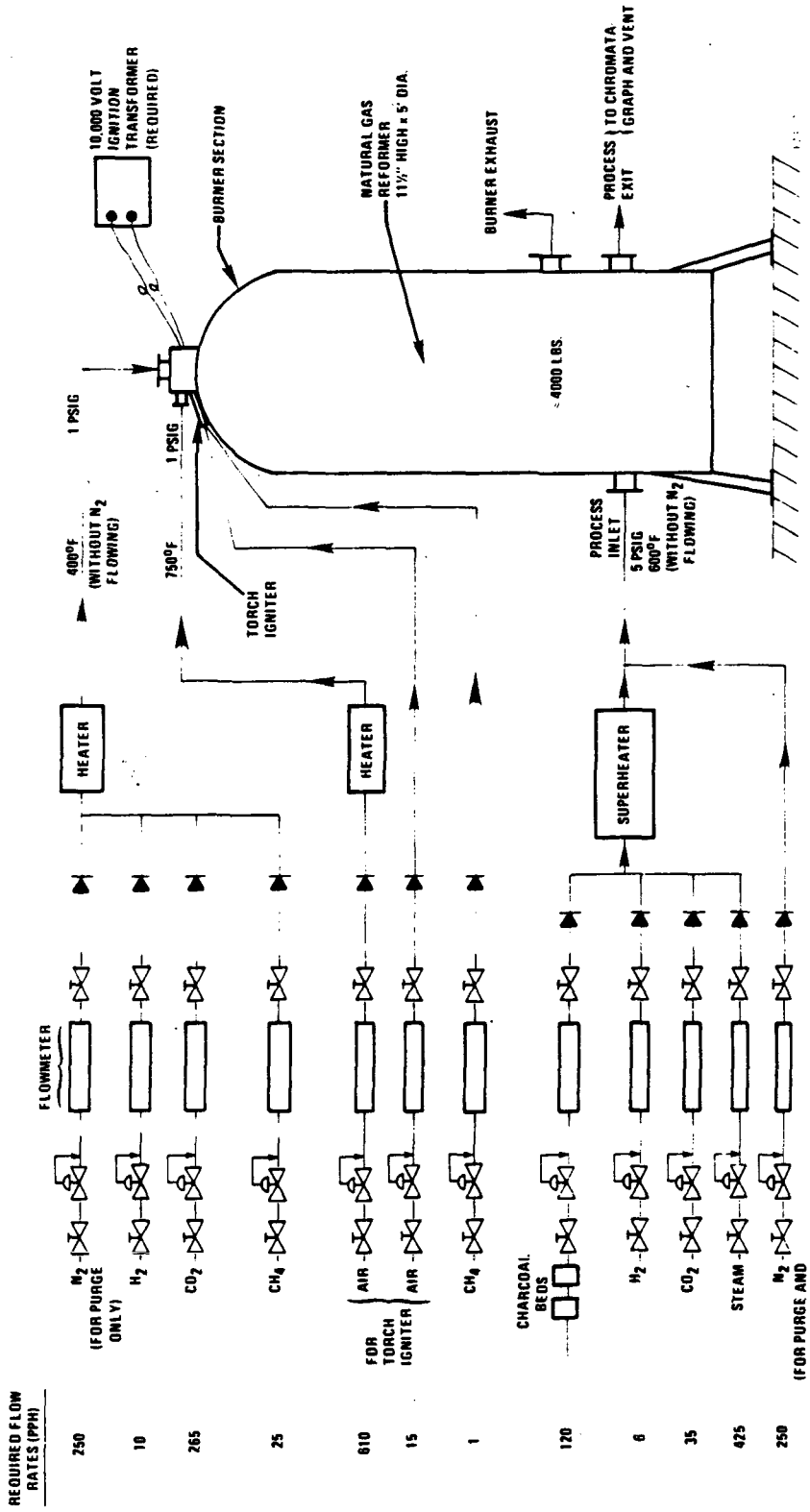

Figure 5-40. 200-kW Natural Gas Development Reformer Test Rig

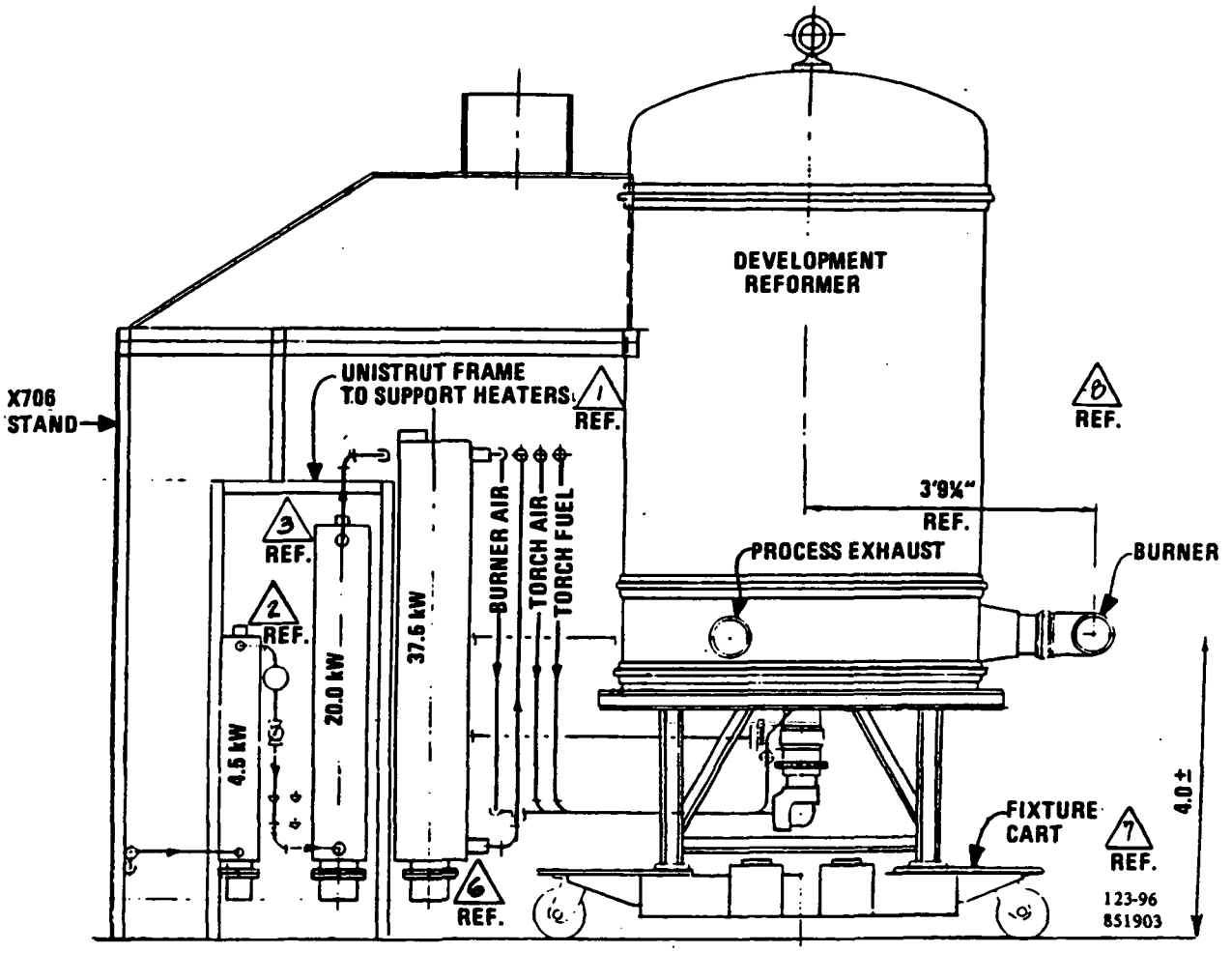

Figure 5-41. Elevation View of Development Reformer and Test Stand

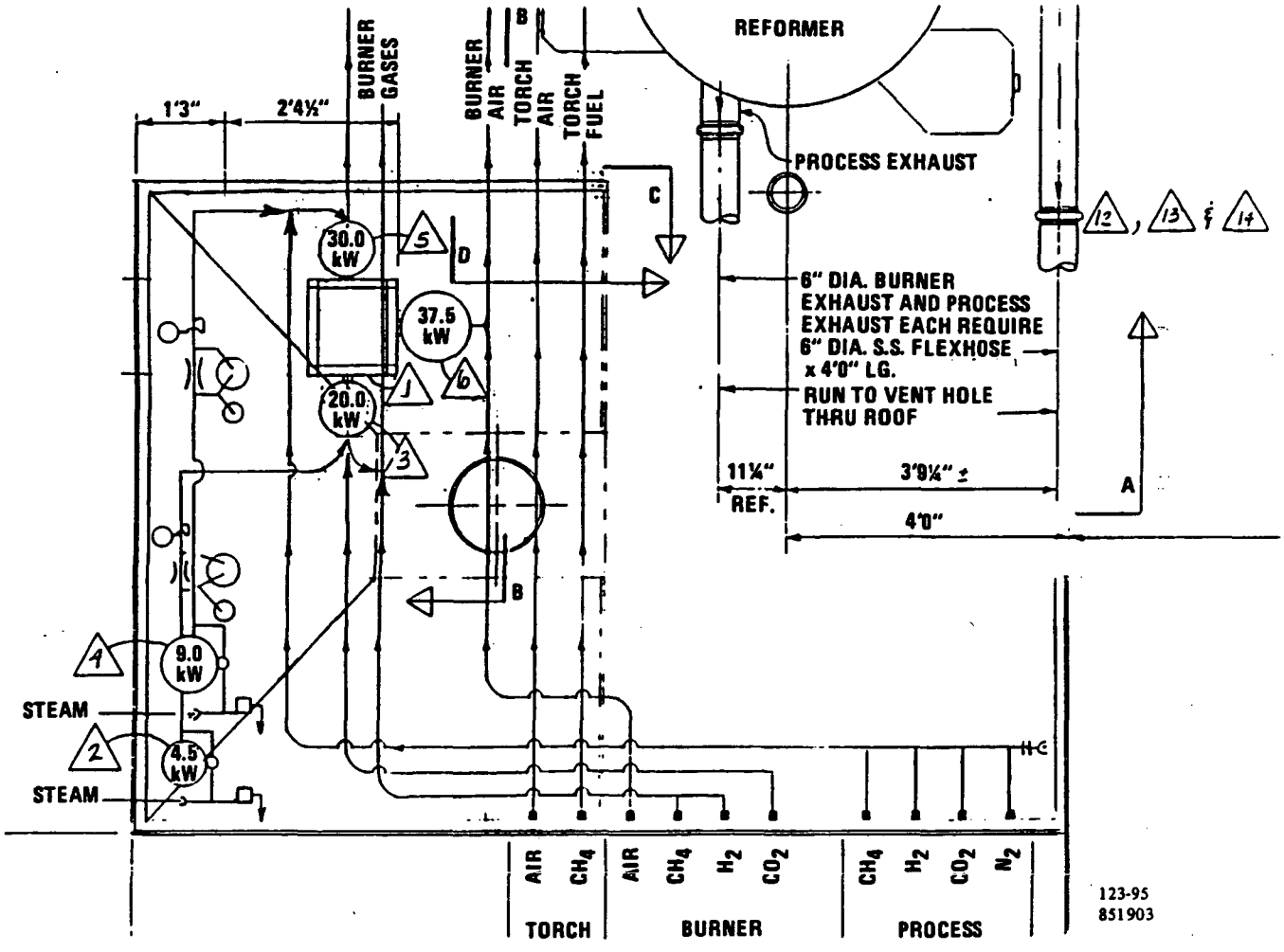

Figure 5-42. Plan View of Development Reformer Facility

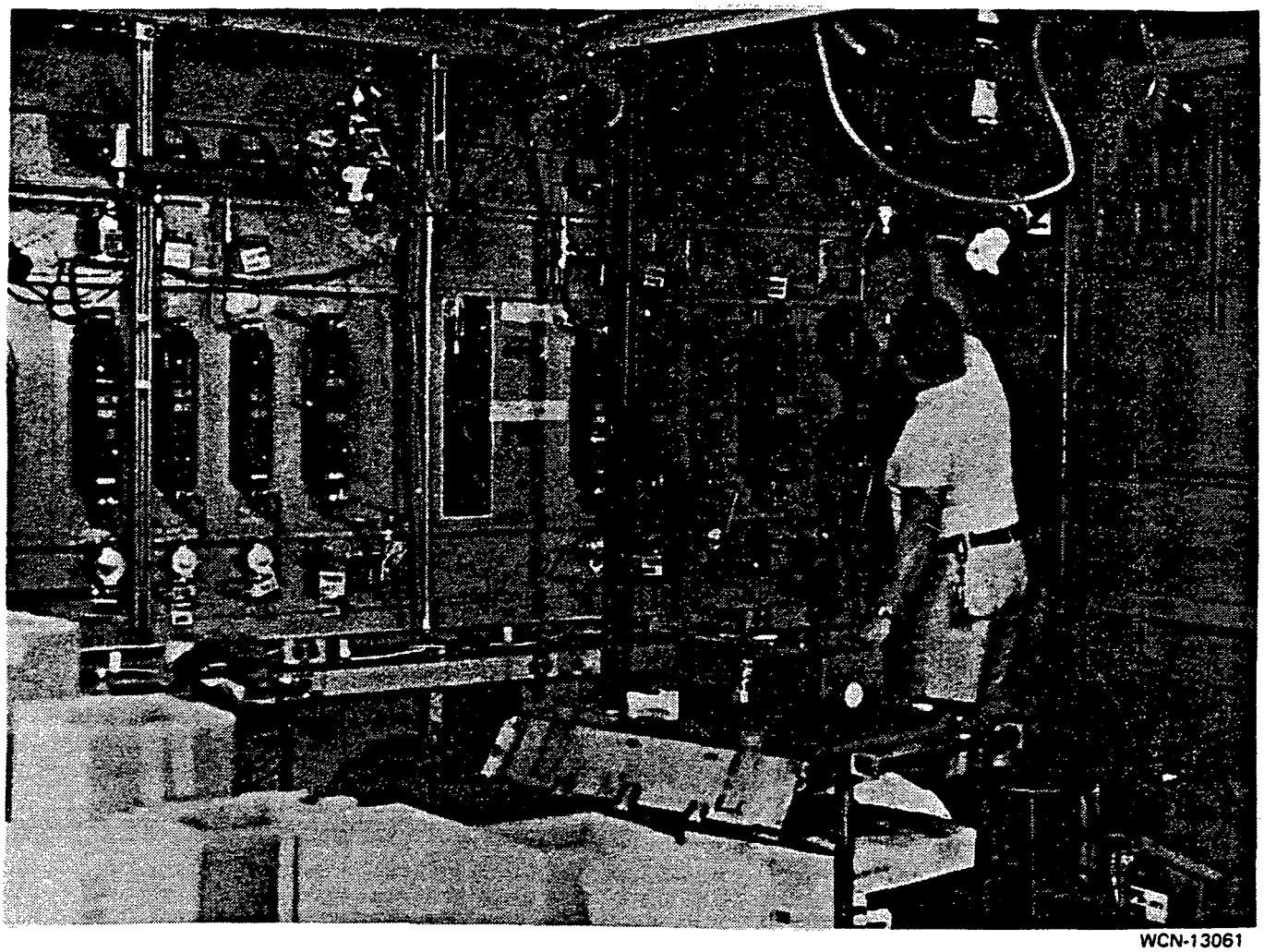

WCN-13061

Figure 5-43. Development Reformer Facility During Fabrication

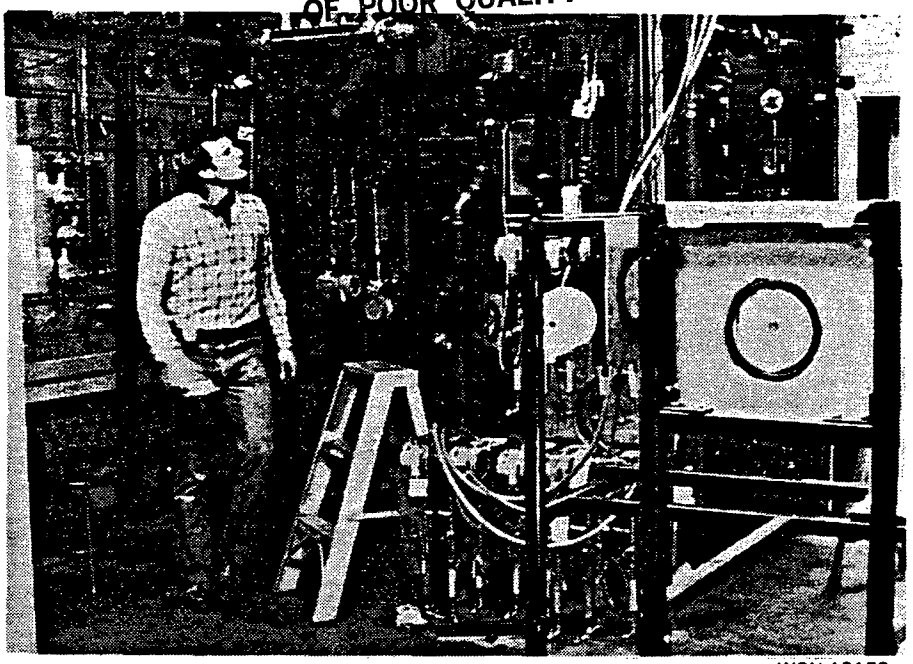

WCN-13158

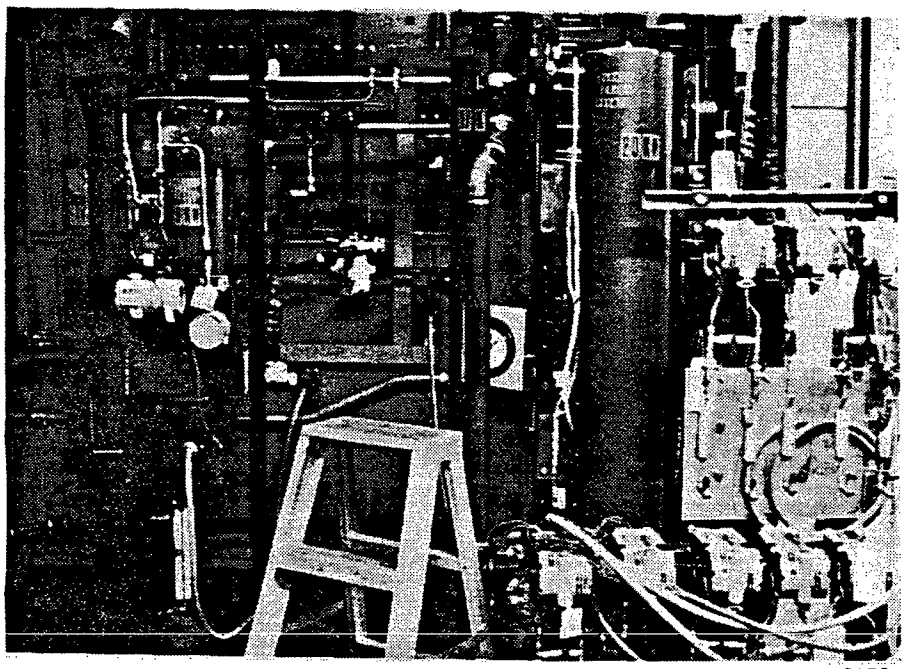

WCN-13159

Figure 5-44. Development Reformer Facility
After Installation of Heaters

TASK 7

VERIFICATION TESTING

TASK 7 - VERIFICATION TESTING

Subtask 7.1 - Define Test Plan

Objective

The NASA/DOE focus for the end of this program is a verification test article which incorporates major system components in a single test to evaluate their operation and interaction under simulated power plant conditions. The objective of the 1984 effort is to develop a plan for this test.

Summary

A test plan was established which included a 200 kW stack, a stack cooling and water treatment system, and a full scale fuel processor as the major elements of the verification test article. A more complete test plan and definition of the test article will be provided in 1986. In order to provide early assessment of the water treatment issue, a subscale water treatment system will be operated with a short stack for several thousand hours during 1985.

Highlights

- A preliminary test plan for the verification test article was written which includes a 200-kW stack, a stack cooling and water treatment system, and a full-scale fuel processor.
- This test plan was reviewed with NASA and approval to proceed was obtained.
- A subscale water treatment system will be operated with a short stack during 1985.

Discussion

The NASA/DOE focus for the end of this program is a verification test article which incorporates the major system components in a single test to evaluate power plant scale components at simulated system conditions and to evaluate interactions between these components. Work under this task during 1984 involved an assessment of technical issues related to the on-site power plant and definition of a test plan to resolve significant issues.

A review of the power plant design showed that the most significant unresolved issues involved interaction of the cell starts, water treatment system, and fuel processor. Therefore, it was proposed that the verification test be primarily test of a 200-kW stack with a stack cooling and water recovery system and a full scale fuel processor.

A review of these plans with NASA resulted in a final definition of the verification test article, which included these three components. It was also decided to provide an early evaluation of the water recovery and water treatment issues by operating a subscale water treatment system with a short stack in 1985.

Subtask 7.1 (Milestones shown in Figure 7-1) of the 1985 NASA On-Site Technology Program will provide a more complete plan to verify the critical aspects of the power plant design. The testing will include a full-scale fuel cell stack, stack cooling and water treatment systems, a fuel processor, and necessary controls and components. This task will define the test article and the design of the verification test facility. Verification testing is expected to begin in 1986 with the integrated operation of the full-scale water treatment system fabricated under a 1985 GRI program and a full height cell stack fabricated under Subtask 2.4 of the 1985 NASA Work Plan. Late in 1986, it is planned to add the fuel processor from Subtask 5.4 of the 1986 NASA Program. Full-scale verification testing is planned to be conducted during early 1987.

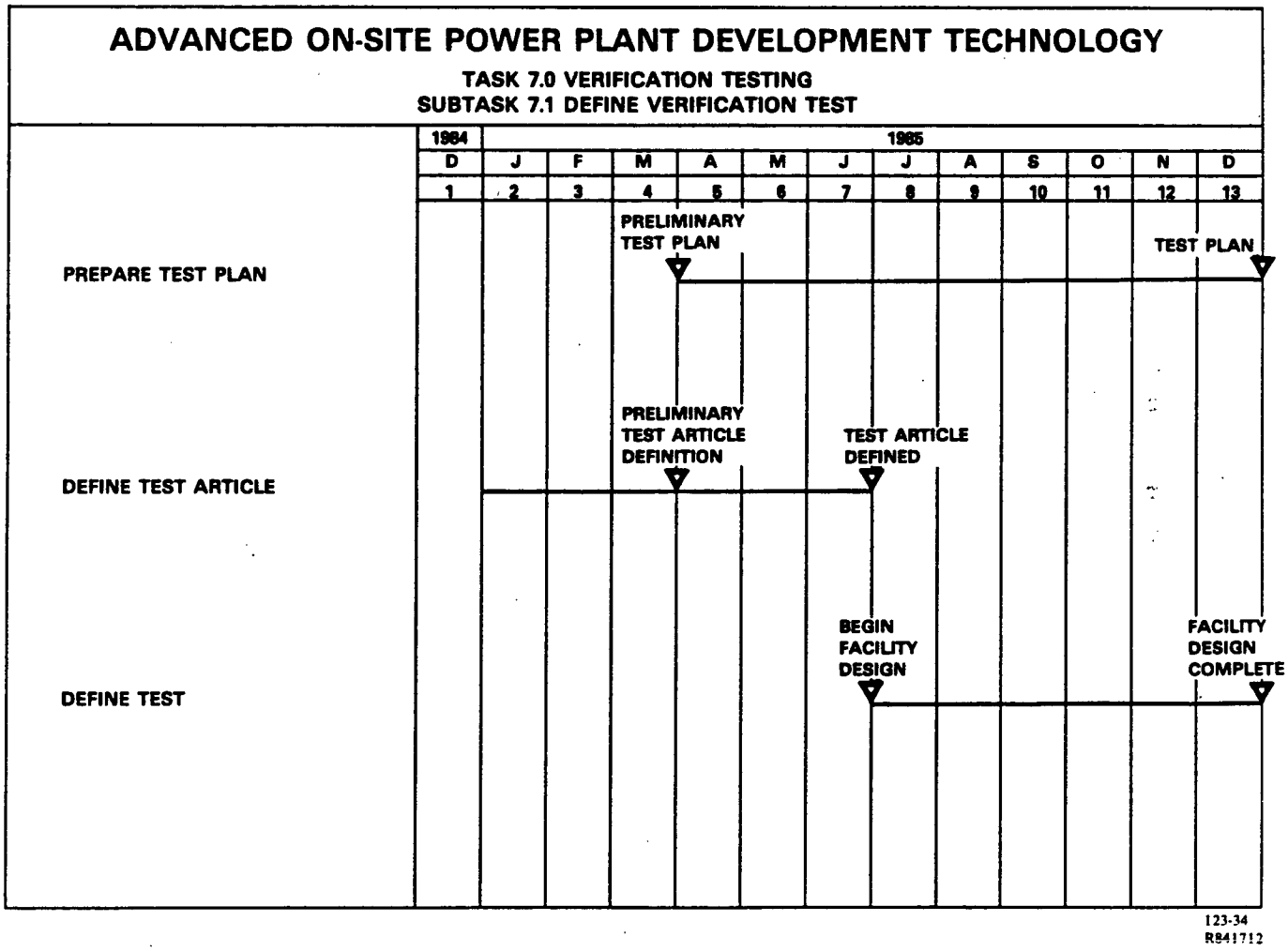

Figure 7-1. Milestone Schedule for Verification Test Definition

Task 7.2 (Milestones shown in Figure 7-2) of the 1985 NASA On-Site Technology Development Program will integrate a short cell stack with a subscale water treatment system from a parallel GRI program. The combined test rig will be configured to operate with cell stack condensate being returned to the water treatment system. The testing will confirm key features of the water treatment system and provide an early evaluation of the overall design concept.

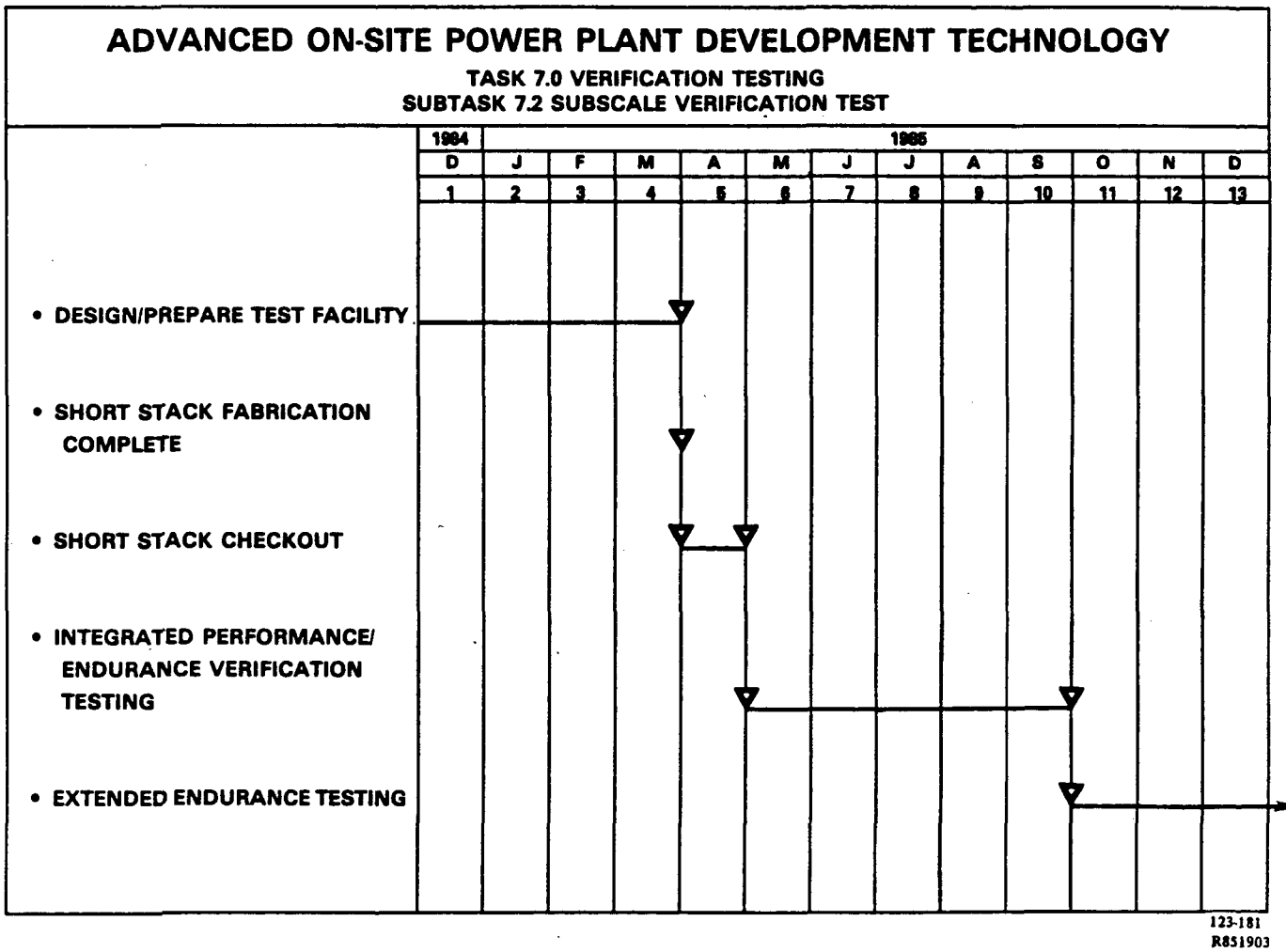

Figure 7-2. Milestone Schedule for Subscale Verification Test

CONCLUSIONS

CONCLUSIONS

Subscale endurance cells containing the Configuration "B" cell design were run for 1500 hours. This cell design meets the performance goal for the program. The increased acid capacity of the Configuration "B" cell allows for an increased refill interval of 150%. This cell design has been incorporated into the second short stack of the program.

The encapsulated serpentine cooler design was verified in the first short stack test. After 5000 hours of testing, a cooler was disassembled and found to have no acid in the holder and no corrosion of the metal cooler arrays. Larger diameter stainless steel coolers have been incorporated in the second short stack.

A successful acid spray refill was conducted on the first short stack after 6000 hours of testing. No performance decay was noted during this refill operation.

The first short stack was tested for a total of 7,200 hours. The encapsulated serpentine cooler design functioned properly. The stack refilled with acid without performance loss. The electrodes performed stably at about E-10 millivolts until the cell was disassembled at about 5000 hours for diagnostics.

A 200-kW brassboard inverter was designed and fabricated using a two-bridge ASCR circuit design. Initial testing indicated the design to be sound and analytical predictions of performance to be correct. The testing of the brassboard will continue into the next reporting period to evaluate the full power range capability and off design limitations.

Candidate full-scale critical heat exchangers were evaluated. Selected candidates will be incorporated in the full-scale verification test system for evaluation in 1985-87. Also, an approach to the integrated low temperature heat exchanger for the full-scale fuel processing system was selected.

Fuel processing catalysts were verified in a 2000-hour catalyst train endurance test for use in the development reformer and full-scale fuel processor tests. The development reformer was designed and fabricated for testing in 1985. A six-tube design containing low pressure drop reforming catalyst was selected. It is fired by a commercial, single-nozzle, upfired burner.

The initial test plan for the verification test was developed; it calls for a subscale water treatment system/short stack in 1985. This is followed by a 200-kW water treatment system/stack test in 1986 and a full-scale water treatment system/stack/fuel processor in 1987.

1. Report No.	2. Government Accession No.	3. Recipient's Catalog No.
NASA CR-175007		

4. Title and Subtitle	5. Report Date
Advanced On-Site Power Plant Development Technology Program 1984 Annual Report	February 1985
	6. Performing Organization Code
7. Author(s)	8. Performing Organization Report No.
Fred S. Kemp	FCR 6848
	10. Work Unit No.
9. Performing Organization Name and Address	11. Contract or Grant No.
UNITED TECHNOLOGIES CORPORATION Power Systems Division P.O. Box 109 South Windsor, Ct. 06074	DEN 3-289
	13. Type of Report and Period Covered
12. Sponsoring Agency Name and Address	Contractor Report
U.S. Department Morgantown Energy Technology Center Morgantown, VA. 26505	14. Sponsoring Agency Code
	Report No. DOE/NASA/0289-3

15. Supplementary Notes

Annual Report. Prepared under Interagency Agreement DE-A121-80 ET 17088. Project Manager S. Simons, Energy Technology Division, NASA Lewis Research Center, Cleveland, Ohio.

16. Abstract

A 30-cell stack was tested for 7200 hours. At 6000 hours the stack was successfully refilled with acid with no loss of performance. A second stack containing the advanced Configuration "B" cell package was fabricated and assembled for testing in 1985. A 200-kW brassboard inverter was successfully evaluated, verifying the design of the two-bridge ASCR circuit design. A fuel processing catalyst train was tested for 2000 hours verifying the catalyst for use in a 200-kW development reformer. The development reformer was fabricated for evaluation in 1985. The initial test plan was prepared for a 200-kW verification test article.

17. Key Words (Suggested by Author(s))	18. Distribution Statement
On-Site Fuel Cells and Technology Development	Unclassified - Unlimited Star Category - 44 DOE Category - UC - 97D

19. Security Classif. (of this report)	20. Security Classif. (of this page)	21. No. of Pages	22. Price*
Unclassified	Unclassified	269	

* For sale by the National Technical Information Service, Springfield, Virginia 22161